NEW DIRECTIONS IN THE MANAGEMENT OF STATUS EPILEPTICUS

EDITED BY: Batool F. Kirmani, Ashok K. Shetty and Lee A. Shapiro
PUBLISHED IN: Frontiers in Neurology and Frontiers in Pharmacology

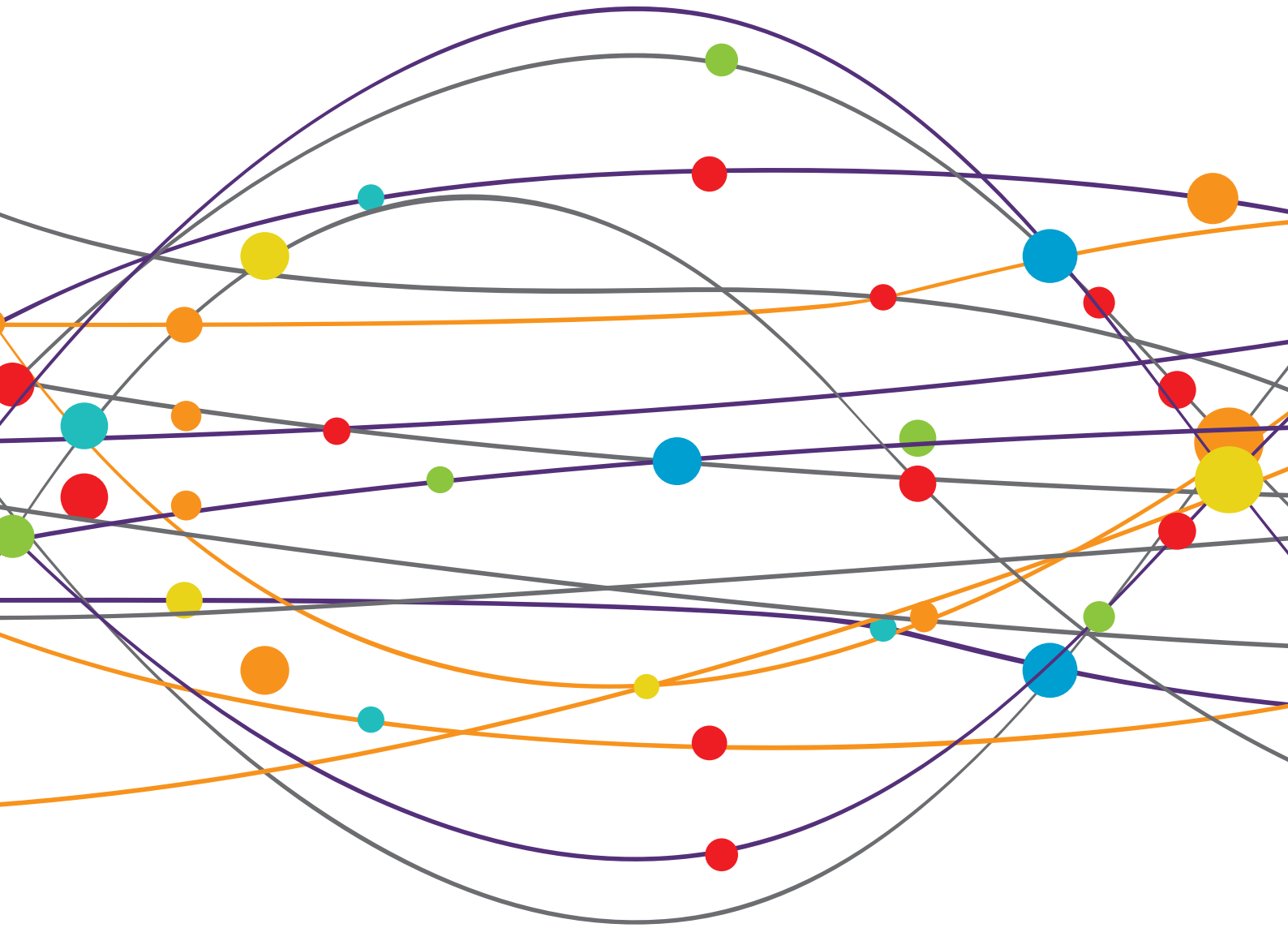

frontiers Research Topics

ISSN 1664-8714
ISBN 978-2-88945-727-4
DOI 10.3389/978-2-88945-727-4

About Frontiers

Frontiers is more than just an open-access publisher of scholarly articles: it is a pioneering approach to the world of academia, radically improving the way scholarly research is managed. The grand vision of Frontiers is a world where all people have an equal opportunity to seek, share and generate knowledge. Frontiers provides immediate and permanent online open access to all its publications, but this alone is not enough to realize our grand goals.

Frontiers Journal Series

The Frontiers Journal Series is a multi-tier and interdisciplinary set of open-access, online journals, promising a paradigm shift from the current review, selection and dissemination processes in academic publishing. All Frontiers journals are driven by researchers for researchers; therefore, they constitute a service to the scholarly community. At the same time, the Frontiers Journal Series operates on a revolutionary invention, the tiered publishing system, initially addressing specific communities of scholars, and gradually climbing up to broader public understanding, thus serving the interests of the lay society, too.

Dedication to Quality

Each Frontiers article is a landmark of the highest quality, thanks to genuinely collaborative interactions between authors and review editors, who include some of the world's best academicians. Research must be certified by peers before entering a stream of knowledge that may eventually reach the public - and shape society; therefore, Frontiers only applies the most rigorous and unbiased reviews.
Frontiers revolutionizes research publishing by freely delivering the most outstanding research, evaluated with no bias from both the academic and social point of view. By applying the most advanced information technologies, Frontiers is catapulting scholarly publishing into a new generation.

What are Frontiers Research Topics?

Frontiers Research Topics are very popular trademarks of the Frontiers Journals Series: they are collections of at least ten articles, all centered on a particular subject. With their unique mix of varied contributions from Original Research to Review Articles, Frontiers Research Topics unify the most influential researchers, the latest key findings and historical advances in a hot research area! Find out more on how to host your own Frontiers Research Topic or contribute to one as an author by contacting the Frontiers Editorial Office: researchtopics@frontiersin.org

NEW DIRECTIONS IN THE MANAGEMENT OF STATUS EPILEPTICUS

Topic Editors:
Batool F. Kirmani, Centra Health Epilepsy Center, Centra Neurosciences, United States
Ashok K. Shetty, Texas A&M University College of Medicine, United States
Lee A. Shapiro, Texas A&M University College of Medicine, United States

Status Epilepticus (SE) is a neurological emergency and has high morbidity and mortality. The International League Against Epilepsy (ILAE) recently updated their definition to specify that, "SE is a condition resulting either from the failure of the mechanisms responsible for seizure termination or from the initiation of mechanisms, which lead to abnormally, prolonged seizures." Such phenomena can lead to long-term neurological complications due to neuronal death, glia, neurological injury, aberrant neuroplasticity, oxidative stress and inflammation, and alteration of neuronal networks. Depending upon the type and duration of SE, these mechanisms are quite variable. Therefore, in response to the updated definition of SE, novel avenues of research are required to address the specified involvement of the underlying mechanisms and pathophysiology resulting in the development of and outcomes from SE.

Improving the basic science understanding of SE will facilitate essential clinical trials. One can envision such experiments to include device and compound-based technological interventions directed at aborting the seizure activity and improving clinical outcomes. Benzodiazepines remain one of the cornerstones of treatment, and studies are underway to study new delivery options, including intranasal, buccal, and intramuscular midazolam, in addition to rectal diazepam, with the goal of aborting the seizure activity outside the hospitals, as rapidly as possible. Approved and off-label anticonvulsants, such as phenytoin, phenobarbital, valproate, topiramate, levetiracetam, lacosamide, steroids, immunosuppressants, and neuroprotective compounds, have also shown some efficacy at treating SE. However, substantial challenges remain in optimally managing SE and minimizing the short- and long-term complications. Such difficulties can be overcome by innovative approaches targeting the underlying mechanisms of neuronal excitability, glia, neuronal death, neuroplasticity, oxidative stress, inflammation, and neuroinflammation.

Citation: Kirmani, B. F., Shetty, A. K., Shapiro, L. A., eds. (2019). New Directions in the Management of Status Epilepticus. Lausanne: Frontiers Media. doi: 10.3389/978-2-88945-727-4

Table of Contents

frontiers in Neurology

EDITORIAL
published: 23 November 2018
doi: 10.3389/fneur.2018.00994

Editorial: New Directions in the Management of Status Epilepticus

Batool F. Kirmani[1]*, *Ashok K. Shetty*[2] and *Lee A. Shapiro*[3]

[1] Epilepsy Center, Centra Neurosciences, CMG Neurology Center, Lynchburg, VA, United States, [2] Institute for Regenerative Medicine, Department of Molecular and Cellular Medicine, Texas A&M University College of Medicine, College Station, TX, United States, [3] Department of Neuroscience and Experimental Therapeutics, Texas A&M University College of Medicine, Bryan, TX, United States

Keywords: epilepsy, staustus epilepticus, seizures, anticonvulsants, autoimmune epilepsy

Editorial on the Research Topic

New Directions in the Management of Status Epilepticus

Status Epilepticus (SE) is a neurological emergency and has high morbidity and mortality. The International League Against Epilepsy (ILAE) recently updated their definition to specify that, "SE is a condition resulting either from the failure of the mechanisms responsible for seizure termination or from the initiation of mechanisms, which lead to abnormally, prolonged seizures." Such phenomena can lead to long-term neurological complications due to neuronal death, glia, neurological injury, aberrant neuroplasticity, oxidative stress and inflammation, and alteration of neuronal networks. Depending upon the type and duration of SE, these mechanisms are quite variable. Therefore, in response to the updated definition of SE, novel avenues of research are required to address the specified involvement of the underlying mechanisms and pathophysiology resulting in the development of and outcomes from SE.

Improving the basic science understanding of SE will facilitate essential clinical trials. One can envision such experiments to include device and compound-based technological interventions directed at aborting the seizure activity and improving clinical outcomes. Benzodiazepines remain one of the cornerstones of treatment, and studies are underway to study new delivery options, including intranasal, buccal, and intramuscular midazolam, in addition to rectal diazepam, with the goal of aborting the seizure activity outside the hospitals, as rapidly as possible. Approved and off-label anticonvulsants, such as phenytoin, phenobarbital, valproate, topiramate, levetiracetam, lacosamide, steroids, immunosuppressants, and neuroprotective compounds, have also shown some efficacy at treating SE. However, substantial challenges remain in optimally managing SE and minimizing the short- and long-term complications. Such difficulties can be overcome by innovative approaches targeting the underlying mechanisms of neuronal excitability, glia, neuronal death, neuroplasticity, oxidative stress, inflammation, and neuroinflammation.

The book comprises six original research articles and four reviews. Collectively, the materials provide insights into the pathophysiology, clinical presentation, treatment, recent advances and future directions in the management of SE, with the goal of providing an in-depth view and advancing the field to improve management of SE.

The book opens with an original research article by Kristin Phillips et al. which showed the role of hypothermia as a neuroprotective agent for preventing the development of calcium plateau against SE-induced delayed hippocampal injury. Hypothermia-mediated neuroprotection after pilocarpine-induced SE was evident from decreased Fluoro-Jade C+ neurons in the hippocampus. The second original article by Matos et al. described SE-induced changes in spontaneous locomotor activity and the temporal expression of genes related to circadian rhythms (Clock, Bmal1, Cry1, Cry2, Per1, Per2, and Per3) in the hippocampus at both early post-SE and chronic epilepsy phases. Authors propose that seizures can act as a non-photic cue and altered temporal expression of clock genes likely contributes to the pathogenesis of mesial temporal lobe epilepsy.

OPEN ACCESS

Edited and reviewed by:
Fernando Cendes, Universidade Estadual de Campinas, Brazil

***Correspondence:**
Batool F. Kirmani
Fkirmani@msn.com

Specialty section:
This article was submitted to Epilepsy, a section of the journal Frontiers in Neurology

Received: *18 October 2018*
Accepted: *05 November 2018*
Published: *23 November 2018*

Citation:
Kirmani BF, Shetty AK and Shapiro LA (2018) Editorial: New Directions in the Management of Status Epilepticus. Front. Neurol. 9:994. doi: 10.3389/fneur.2018.00994

The third original article by Hutson et al. presented an interesting case study which showed evidence of brain dynamics resetting after successful anticonvulsant treatment following SE utilizing stereo encephalography (SEEG) data.

A review by Kirmani et al. conferred the current literature about autoimmune SE including therapeutic options and future directions. An original research article by Wyatt-Johnson et al. reported that SE-induced morphological alterations in microglia at different time-points and discussed the role of such changes on epileptogenesis. Another research article by Kortland et al. addressed the socioeconomic outcome and quality of life outcome in adults after status epilepticus in their original article. The authors conducted a multicenter, longitudinal, matched case-control analysis and concluded that relatively favorable outcomes seen in patients with refractory and super refractory SE as compared to non-refractory SE cases underlying the need of effective therapeutic choices.

An original research article by Bertoglio et al. compared the effects of two different protocols of kainate-induced SE in two strains of rats on neurodegeneration and chronic epilepsy development. The findings revealed that severe neuron loss after SE does not necessarily correlate with a higher seizure rate in the chronic phase after SE. In a review article, Castro et al. discussed the efficacy and promise of resveratrol, a phytoalexin found in the skin of red grapes, for easing SE-induced neurodegeneration, neuroinflammation, aberrant neurogenesis and for restraining the evolution of SE-induced brain injury into a chronic epileptic state. Sharma et al. by reviewing methods of induction and characterization of behavioral SE and EEG correlates in mice and rats, highlighted the advantages of a repeated low dose of kainate protocol for minimizing the variability in the initial SE severity and reducing the mortality rate. The last original article by Lucchi et al. described the role peroxisome proliferator-activated receptor gamma in the anticonvulsant properties of EP-80317, a Ghrelin receptor antagonist in pilocarpine-induced SE rat model and repeated 6 Hz corneal stimulation model in mice.

AUTHOR CONTRIBUTIONS

All authors listed have made a substantial, direct and intellectual contribution to the work, and approved it for publication.

Conflict of Interest Statement: The authors declare that the research was conducted in the absence of any commercial or financial relationships that could be construed as a potential conflict of interest.

frontiers in Neurology

ORIGINAL RESEARCH
published: 11 June 2018
doi: 10.3389/fneur.2018.00438

Hypothermia Reduces Mortality, Prevents the Calcium Plateau, and Is Neuroprotective Following Status Epilepticus in Rats

Kristin F. Phillips[1], *Laxmikant S. Deshpande*[1,2] *and Robert J. DeLorenzo*[1,2]*

[1] Department of Neurology, Virginia Commonwealth University, Richmond, VA, United States, [2] Department of Pharmacology and Toxicology, Virginia Commonwealth University, Richmond, VA, United States

OPEN ACCESS

Edited by:
Batool F. Kirmani,
Epilepsy Center, Baylor Scott and White Health Neuroscience Institute, United States

Reviewed by:
Ashok K. Shetty,
Institute for Regenerative Medicine, Texas A&M University College of Medicine, United States
Dinesh Upadhya,
Manipal Academy of Higher Education, India
Olagide Wagner Castro,
Federal University of Alagoas, Brazil

***Correspondence:**
Robert J. DeLorenzo
robert.delorenzo@vcuhealth.org

Specialty section:
This article was submitted to Epilepsy, a section of the journal Frontiers in Neurology

Received: 01 March 2018
Accepted: 24 May 2018
Published: 11 June 2018

Citation:
Phillips KF, Deshpande LS and DeLorenzo RJ (2018) Hypothermia Reduces Mortality, Prevents the Calcium Plateau, and Is Neuroprotective Following Status Epilepticus in Rats. Front. Neurol. 9:438. doi: 10.3389/fneur.2018.00438

Status Epilepticus (SE) is a major neurological emergency and is considered a leading cause of Acquired Epilepsy (AE). We have shown that SE produces neuronal injury and prolonged alterations in hippocampal calcium levels ($[Ca^{2+}]_i$) that may underlie the development of AE. Interventions preventing the SE-induced Ca^{2+} plateau could therefore prove to be beneficial in lowering the development of AE after SE. Hypothermia is used clinically to prevent neurological complications associated with Traumatic Brain Injury, cardiac arrest, and stroke. Here, we investigated whether hypothermia prevented the development of Ca^{2+} plateau following SE. SE was induced in hippocampal neuronal cultures (HNC) by exposing them to no added $MgCl_2$ solution for 3 h. To terminate SE, low Mg^{2+} solution was washed off with 31°C (hypothermic) or 37°C (normothermic) physiological recording solution. $[Ca^{2+}]_i$ was estimated with ratiometric Fura-2 imaging. HNCs washed with hypothermic solution exhibited $[Ca^{2+}]_i$ ratios, which were significantly lower than ratios obtained from HNCs washed with normothermic solution. For *in vivo* SE, the rat pilocarpine (PILO) model was used. Moderate hypothermia (30–33°C) in rats was induced at 30-min post-SE using chilled ethanol spray in a cold room. Hypothermia following PILO-SE significantly reduced mortality. Hippocampal neurons isolated from hypothermia-treated PILO SE rats exhibited $[Ca^{2+}]_i$ ratios which were significantly lower than ratios obtained from PILO SE rats. Hypothermia also provided significant neuroprotection against SE-induced delayed hippocampal injury as characterized by decreased FluoroJade C labeling in hypothermia-treated PILO SE rats. We previously demonstrated that hypothermia reduced Ca^{2+} entry via N-methyl-D-aspartate and ryanodine receptors in HNC. Together, our studies indicate that by targeting these two receptor systems hypothermia could interfere with epileptogenesis and prove to be an effective therapeutic intervention for reducing SE-induced AE.

Keywords: status epilepticus, pilocarpine, hypothermia, intra neuronal calcium levels, mortality, neuroprotection, Sprague-Dawley rats

INTRODUCTION

Status Epilepticus (SE) is a major clinical emergency associated with significant mortality and severe neurological morbidities amongst the survivors (1, 2). One of the major morbidities associated with survival from SE is the development of acquired epilepsy (AE) (3, 4). Epilepsy is a common neurological condition characterized by recurring spontaneous seizures. It affects approximately 1–2% of the population worldwide (1, 4). Acquired epilepsy (AE) results from a previous neurological insult such as a SE or a stroke, or a traumatic brain injury (TBI) and accounts for at least 40% of all epilepsy cases (1–4). In AE, a known cause or injury damages the brain and produces a plasticity change that leads to the development of epilepsy (5, 6). The transformation of normal brain tissue into a hyperexcitable neuronal population manifesting spontaneous recurrent epileptic discharges, or seizures, is called epileptogenesis (5–7).

It has been demonstrated in both *in vivo* and *in vitro* models of SE, stroke, and TBI that neuronal calcium (Ca^{2+}) dynamics are severely altered following injury (8–10). One such alteration relevant to this study is a persistent elevation in intracellular calcium concentrations ($[Ca^{2+}]_i$) following SE, termed the "Ca^{2+} plateau" (8, 11, 12). The formation of the Ca^{2+} plateau has been implicated in playing a major role in the development of AE (13). Ca^{2+} is responsible for an array of cellular effects (14, 15), and alterations in a neuron's ability to regulate Ca^{2+} could substantially contribute to neuronal plasticity changes (16) that lead to epileptogenesis and subsequently AE (5, 13, 15). Therefore, preventing the rise in $[Ca^{2+}]_i$ immediately after SE may prevent the Ca^{2+}-mediated signaling effects that lead to the development of AE. Targeting the molecular alterations observed in epileptogenesis such as elevated $[Ca^{2+}]_i$ may therefore offer new avenues to developing anti-epileptogenic approaches (5, 13, 15).

One such possible intervention is hypothermia. Hypothermia is used clinically to reduce neurological injury following a variety of insults including cardiac arrest (17–19), TBI (20, 21) and stroke (22, 23). Hypothermia exerts its neuroprotective effects through a variety of mechanisms including a reduction in cerebral metabolism, apoptosis, and inflammation (24, 25). One particular mechanism of interest is its ability to modulate neuronal Ca^{2+}entry (26). Evidence has shown that the N-methyl-D-aspartate (NMDA) receptor mediates the majority of Ca^{2+} influx during SE (8, 11). Inhibition of the NMDA receptors during SE blocks the formation of the Ca^{2+} plateau and prevents the development of AE (5, 8). The excessive entry of Ca^{2+} into the cell during SE stimulates Ca^{2+}-induced Ca^{2+} release via activation of ryanodine receptors. Evidence has suggested ryanodine receptors may be responsible for maintaining the Ca^{2+} plateau following SE (27, 28). Our lab has demonstrated in hippocampal neuronal cultures that hypothermia reduces neuronal Ca^{2+} entry through NMDA and ryanodine receptors following a high-potassium or glutamate stimulation (26). Therefore, hypothermia may prevent the formation of the Ca^{2+} plateau following SE and thus may serve as a valuable therapeutic option in preventing epileptogenesis.

This study was initiated to investigate whether hypothermia prevents the formation of the Ca^{2+} plateau following SE and decreases neuronal injury and mortality. We utilized two widely used *in vivo* (29) and *in vitro* (27) models of SE in this study. The results of this study demonstrate that hypothermia prevents the development of the Ca^{2+} plateau when administered following SE. Based on previous studies showing that blocking the Ca^{2+} plateau prevents the development of AE, the results of this study offer promising evidence that hypothermia induced following SE prevents the long lasting rise in $[Ca^{2+}]_i$, neuronal loss and decreases mortality and may prevent the development of AE.

MATERIALS AND METHODS

All reagents were purchase from Sigma Chemical Co. (St. Louis, MO) unless otherwise specified. Cell culture media was purchased from Invitrogen (Carlsbad, CA). All animal use procedures were in strict accordance with the National Institutes of Health Guide for the Care and Use of Laboratory Animals and approved by Virginia Commonwealth University's Institutional Animal Care and Use Committee.

Hippocampal Neuronal Culture Preparation

Studies were conducted on primary mixed hippocampal neuronal cultures (HNC) prepared as described previously (27, 30, 31). In brief, hippocampal cells were obtained from 2-day post-natal Sprague-Dawley rats (Harlan, Frederick, MD) and plated at a density of 2.0×10^4 cells/cm^2 onto a glial support layer previously plated onto poly-L-lysine coated (0.05 mg/ml) Lab-Tek® two-well cover glass chambers (Nunc, Naperville, IL). Cultures were maintained at 37°C in a 5% CO2/95% air atmosphere and fed twice weekly with MEM enriched with N3 supplement containing 25 mM HEPES buffer (pH 7.4), 2 mM L-glutamine, 3 mM glucose, 100 μg/ml transferrin, 5 μg/ml insulin, 100 μM putrescine, 3 nM sodium selenite, 200 nM progesterone, 1 mM sodium pyruvate, 0.1% ovalbumin, 0.2 ng/ml triiodothyroxine, 0.4 ng/ml corticosterone and supplemented with a glial bed-condition media (20%). These mixed cultures were used for experiments between 15 and 21 days *in vitro* following neuronal plating.

In Vitro SE in Hippocampal Neuronal Cultures and Hypothermia Induction

In vitro SE was generated using a low Mg^{2+}-containing solution (27, 30, 32). Hippocampal neuronal culture media was replaced with physiological basal recording solution (pBRS) containing (in mm): 145 NaCl, 2.5 KCl, 10 HEPES, 2 CaCl2, 10 glucose, 1 MgCl2 and 0.002 glycine, pH 7.3, and osmolarity adjusted to 325 ± 5 mOsm with sucrose or pBRS without any added $MgCl_2$ (referred to hereafter as low Mg^{2+}). The cells were then incubated at 37°C under 5% CO2 / 95% O2 atmosphere for 3 h. During this time, neurons in low Mg^{2+} demonstrate high-frequency spiking, characterized as *in vitro* SE. Neurons treated with pBRS for 3 h served as sham-controls.

SE was terminated by replacing the low Mg^{2+} solution with either 31°C (moderate hypothermia) or 37°C (physiological

temperature) pBRS. $[Ca^{2+}]_i$ was measured at the end of the 3 h treatment every 30 s for 20 min to get a measurement of $[Ca^{2+}]_i$.

Pilocarpine Model of SE and Induction of Moderate Hypothermia *in Vivo*

Sprague-Dawley male rats (Envigo, formerly Harlan) weighing 200–250 g were administered methyl scopolamine nitrate (1 mg/kg, i.p.) followed by pilocarpine nitrate (PILO) (375 mg/kg, i.p.) 30 min later. Sixty minutes after the onset of SE, rats were administered diazepam (5 mg/kg, i.p.) followed by additional diazepam injections at 3 and 5 h after the onset of SE to control seizure activity (8, 29, 33).

Moderate hypothermia was rapidly induced at 30 min post-SE onset by gently spraying rats with chilled ethanol (17°C) to speed the process of cooling. Rats were then placed in a cold room (5–8°C) for 8–10 min. Surface cooling methods were used because they are non-invasive and cost-effective. Core body temperature was determined every 2–3 min using a rectal probe (2100 Tele-thermometer; YSI, Inc., Yellow Springs, OH USA). Once core temperatures reached a 32-33°C, the rats were returned to their home cages in a room temperature environment. Core temperatures were continuously monitored and maintained between 30 and 33°C (moderate hypothermia range) with the intermittent use of ice packs and heating pads. Moderate hypothermia was maintained for 4 h at which point all the active cooling procedures were stopped and the animal was allowed to naturally rewarm to physiological temperature at room temperatures (see **Figures 1**, **3A**).

At 24 h post-SE, gross behavior was noted to assess recovery from SE. Rats were assigned a score of 0 or 1 on three parameters: mobility, posture, and alertness. For mobility, a score of 1 indicated rat being ambulatory, while a score of 0 indicated rat sitting in the cage, lethargic, and not moving about. For posture, a score of 1 indicated normal posture while 0 indicated a hunched posture. Alertness as indicated by being responsive to handling and approach was scored as 1 while 0 score indicated being non-responsive to handle and approach. Sum of all the scores gave the gross behavioral score and was indicative of physical recovery following SE.

Acute Isolation of Hippocampal Neurons

Hippocampal CA1 neurons were acutely isolated by a modification of the methods described previously (8, 10–12). The brain was rapidly dissected and placed in a 4°C chilled oxygenated (95% O_2-5% CO_2) artificial cerebrospinal fluid solution (aCSF) composed of (in mM) 201 sucrose, 3 KCl, 1.25 $NaHPO_4$, 6 $MgCl_2$, 0.2 $CaCl_2$, 26 $NaHCO_3$, MK-801 (1 μM) and 10 glucose (solution A). Hippocampal slices of 450 μm were cut with a vibratome sectioning system (Series 3000, Technical Products International, St. Louis, MO) and incubated for 10 min in an oxygenated medium at 34°C containing (in mM) 120 NaCl, 5 KCl, 6 $MgCl_2$, 0.2 $CaCl_2$, 25 glucose, and 20 PIPES, pH adjusted to 7.2 with NaOH (solution B). Slices were then treated with 8 mg/ml of Protease XXIII (Sigma Chemical Co.) in solution B for 6–8 min and then thoroughly rinsed with solution B. The CA1 region was visualized in a dark background with the help of a dissecting microscope and tissue chunks were excised. These tissue preparations were then triturated in solution B with a series of Pasteur pipettes of decreasing diameter at 4°C in the presence of acetoxymethyl (AM) form of high affinity Ca^{2+} indicator Fura-2AM (1 μM) in order to load the cells prior to $[Ca^{2+}]$i measurements. The resulting cell suspension was then placed in the center of poly-L-lysine coated Lab-Tek² two-well cover glass chambers (Nalge-Nunc International, Naperville, IL) and immediately placed in a humidified oxygenated dark chamber at 37°C for 45 min. Fura-2 was washed off with solution B and the loaded cells were allowed to equilibrate for 15 min allowing the cellular esterase to cleave the dyes from their AM forms.

Calcium Microfluorimetry

Fura-2AM was loaded in the neurons as described above and then transferred to a heated stage (37°C) of an Olympus IX-70 inverted microscope coupled to an ultra-high-speed fluorescence imaging system (Olympus/ Perkin-Elmer). Ratio images were acquired by using alternating excitation wavelengths (340/380 nm) with a filter wheel (Sutter Instruments, Novato, CA) and Fura filter cube at 510/540 nm emissions with a dichroic mirror at 400 nm. Image pairs were captured and digitized every 15 s, and the images at each wavelength were averaged over four frames and corrected for background fluorescence by imaging a non-indicator loaded field.

In neuronal cultures, ratio measurements for individual neurons were taken at 30 s intervals for 20 min. For acutely isolated neurons, ratio measurements for individual neurons were taken at 5 s intervals for 30 s. The resulting 340/380 ratios correspond directly to the total concentration of Ca^{2+} inside the cell (8, 10–12).

Fluoro-Jade Staining

Rats were sacrificed 48 h following SE. Briefly, deep anesthesia was induced in rats with ketamine/xylazine (75 mg/kg/7.5 mg/kg i.p.) mixture. Anesthetized animals were flushed transcardially with saline and perfused with 4% paraformaldehyde in a 100 mM sodium phosphate buffer (pH 7.4). Fixed brains were removed and post-fixed in 4% paraformaldehyde/phosphate buffer overnight, cryoprotected in 30% sucrose/phosphate buffer (pH 7.4) (48 h), flash frozen in isopentane and stored at −80°C until used for sectioning. Coronal sections (40 μm) were cut on a cryostat (Leica Microsystems, Wetzlar, Germany) and mounted onto microscope slides (Trubond 380; Tru Scientific LLC, Bellingham, WA). Slides were dried in a desiccant chamber at 55°C for 30 min prior to staining. Slides were first incubated in a solution of 1% NaOH in 80% ethanol for 5 min followed by hydration in a 70% ethanol and then ddH_2O for 2 min each. Slides were then incubated in a 0.06% $KMnO_4$ solution for 10 min followed by washing in ddH_2O for 2 min. Slides were then stained in a 0.0004% Fluoro-Jade C (FJC) solution in 0.1% acetic acid for 20 min (12, 28, 34). Stained slides underwent 3x washes in ddH_2O for 2 min each and then dried in a desiccant chamber at 55°C for 30 min. Stained slides were then cleared with xylene for 5 min and cover slipped with DPX mounting agent. Stained sections were evaluated with a fluorescent inverted microscope with a 20X (UApo 340, 0.7 n.a., water) objective and

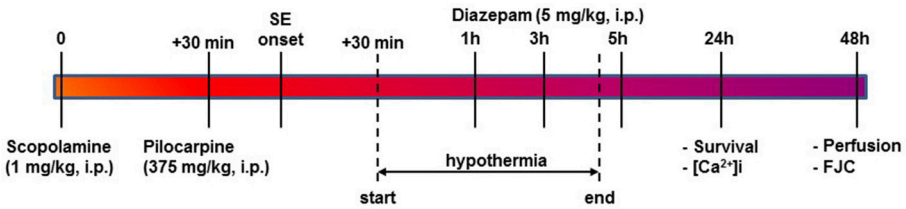

FIGURE 1 | Timeline for PILO SE, induction of HYPO, and experimental endpoints. SE was induced using PILO injection and terminated with diazepam injections as per established procedures. At 30-mins into SE, moderate HYPO was induced and then maintained for 4 h using procedures described in the Materials and Methods section. At 24 h post-SE, survival and ratiometric Ca^{2+} imaging studies were conducted. At 48 h post-SE, rats were perfused and brain sections from these rats were labeled with FJC for assessing neuronal injury as described.

excitation/emission filters for visualization of FITC. Grayscale digital images (1,324 × 1,024, 16-bit, 1X1 binning) of FJC staining for select brain regions were acquired.

Data Analyses

For experiments performed in cell cultures, a sample size (n) of at least 6 plates per treatment group was used. Experiments in cultures were performed over several weeks so that results were representative of multiple cultures. For experiments performed in whole animal, a sample size of $n = 15$ rats per treatment group were used. For each rat, 20–30 hippocampal neurons were isolated and imaged. Individual neurons from multiple experiments were pooled to calculate average and standard error of the mean (SEM). Data is presented as mean ± SEM. To determine statistical significance between treatment groups, student's *t*-test or one-way analysis of variance (ANOVA) were used followed by Tukey *post-hoc* analysis when appropriate. A *p*-value of less than 0.05 ($p < 0.05$) was considered statistically significant. Analysis of digital images to count FJC positive cell staining was carried out with Image-J (NIH, Bethesda, MD) by thresholding for specific stain and obtaining positive cell counts using the particle analysis component (size range in pixel: 25–1,000). Digital acquisition and staining analysis parameters remained constant throughout. Statistical analysis and graphs were drawn using SigmaPlot 13 (Systat Software, San Jose, CA).

RESULTS

Hypothermia Blocked the Development of the Ca^{2+} Plateau in the HNC Model of SE

Figure 2A depicts ratiometric pseudocolor images of hippocampal neurons from the cultures under different temperature conditions. Fura-2 ratios were measured at 20-min following 3 h of low Mg^{2+} treatment. As illustrated in **Figure 2B**, hippocampal neurons washed with physiological 37°C buffer solution exhibited 340/380 ratios of 0.49 ± 0.03 compared to control ratios of 0.26 ± 0.02, indicating that $[Ca^{2+}]_i$ was elevated after *in vitro* SE under physiological temperature. In contrast, hypothermia treated hippocampal neurons (31°C pBRS) quickly recovered the low Mg^{2+} SE induced elevated $[Ca^{2+}]_i$ to baseline levels and exhibited 340/380 ratios of 0.25 ± 0.01 which were significantly lower than SE-only ratios but not significantly different from 340/380 ratios in control neurons (one-way ANOVA, $p < 0.05$).

To evaluate the dynamics of this $[Ca^{2+}]_i$ decay, at the end of 3 h of low Mg^{2+} treatment, $[Ca^{2+}]_i$ of neurons washed with either 31 or 37°C pBRS was measured over the course of 20 min. The ratio values for 31°C (hypothermia) and 37°C (normothermia) wash groups were normalized to the peak ratio (**Figure 2C**). After 5 min post-treatment, neurons washed with 37°C pBRS showed a slight decay in 340/380 ratios. However, cells exposed to hypothermic treatment exhibited a larger decrease in 340/380 ratios that were 62% of the peak observed at the end of *in vitro* SE. At 10 min post-treatment, the 340/380 ratio values reduced by 41 and 26% of the post-SE peak in cells washed with 31 and 37°C pBRS, respectively. At 15 min post-treatment, the ratio values fell by 44% of the post-SE peak for cells washed with 31°C pBRS and 30% of the peak for cells washed with 37°C solution. After 20 min, in the cells treated with hypothermia ratio values fell by 42% of the peak. These reductions were significantly higher than the cells washed with 37°C solution whose 340/380 ratio values fell by only 29% of the peak. Within 20 min of hypothermia treatment, $[Ca^{2+}]_i$ had returned to baseline ratio values of 0.25 ± 0.01 which were not significantly different from values observed in control neurons (0.26 ± 0.02). In comparison, $[Ca^{2+}]_i$ remained significantly elevated in cells washed with 37°C pBRS with values of 0.36 ± 0.02 (**Figure 2B**). There was a significant difference in the 340/380 ratio values between the two groups at each time point after 5 min of treatment (Student's *t*-test, $p < 0.05$).

Hypothermia Reduces Mortality and Improves Recovery From SE

PILO administration induced SE in 14 out of 15 rats, with an average seizure onset latency of 17 ± 3 min. Seizure severity as indicated by Racine score was 4.0 ± 0.2. There were no deaths during the first hour of SE, at which point diazepam regime was initiated to terminate the seizures. At 24 h post-SE, 3 out of 14 rats died giving a mortality rate of 21%. The surviving rats displayed hunched posture, were less ambulatory, and were not responsive to handling or approach. Their average gross physical recovery score was 0.72 ± 0.2 (see section Materials and Methods).

In separate group of 15-rats PILO was used to induce SE using established procedures. Moderate hypothermia (31–33°C)

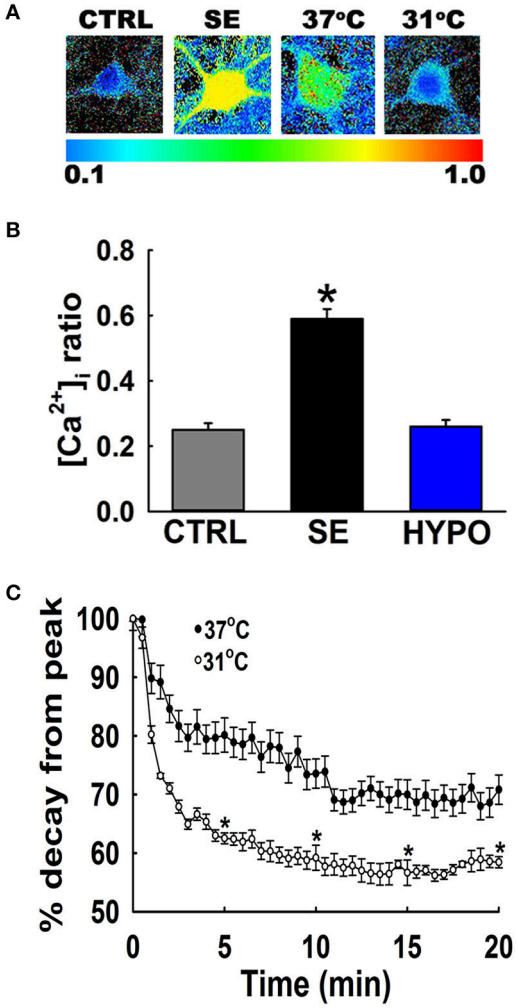

FIGURE 2 | Hypothermia blocked the Ca^{2+} plateau after *in vitro* SE. **(A)** Pseudocolor ratiometric images of representative hippocampal neurons in culture from control, low Mg^{2+} SE, 37°C pBRS, and 31°C pBRS. All the ratiometric images are at the 20-min time point following respective treatments. **(B)** Fura-2 340/380 ratiometric values at the end of 20-min of treatment with hypothermic solution (31°C pBRS). **(C)** Ca^{2+} decay curves in the presence and absence of hypothermic intervention. Following 3 h of *in vitro* SE (time = 0), cells were washed with either 31°C pBRS or 37°C pBRS. 340/380 ratios were recorded every 30 s for 20 min and normalized to percent of the peak ratio observed at time = 0. $n = 6$ plates per treatment group with 40–60 neurons imaged per group. *$p < 0.05$, Student's *t*-test for all time points after 5 min.

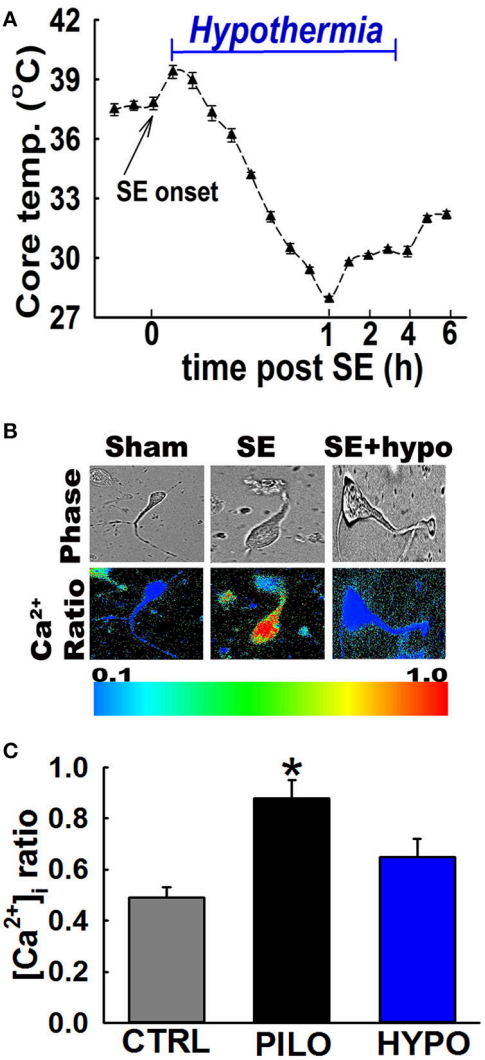

FIGURE 3 | Hypothermia blocked the Ca^{2+} plateau after *in vivo* SE. **(A)** Hypothermia in rats was induced using surface cooling methods. Core body temperatures at various time points depicts rapid induction and steady maintenance of moderate hypothermia in the therapeutic range. **(B)** Pseudocolor ratiometric images of representative acutely isolated hippocampal neurons from control, PILO and hypothermia (HYPO) treated SE rats. Control and HYPO neurons had bluish color that corresponds to lower Fura-2 ratio while SE neurons had orange-red color that corresponds to higher Fura-2 ratio. **(C)** Elevated $[Ca^{2+}]_i$ in hippocampal neurons acutely isolated from animals at 24 h following 1 h of PILO induced SE compared to neurons from control and hypothermia (HYPO) treated rats. (*$p < 0.001$, *t*-test, $n = 6$ and 5 animals respectively). Data are represented as mean ± SEM.

was induced in 14-rats 30 min after PILO SE and maintained for 4 h (**Figure 3A**. Also see materials and methods). No differences were observed in the severity of seizures during the remainder of 30 min of SE. However, mortality rate assessed at 24 h post-SE was only 7% in hypothermia treated group. Surviving rats in the hypothermia group ($n = 13$) were alert, mobile, displayed normal posture, and were responsive to handing and approach. Fifty-percent of the hypothermia-SE survivors exhibited a complete behavioral recovery score of 3.0. Their mean gross recovery score was 2.53 ± 0.3, which was significantly higher than PILO-SE group ($n = 13$, *t*-test, $p < 0.05$).

Hypothermia Blocked the Development of the Ca^{2+} Plateau Following SE

In order to investigate whether hypothermia was able to lower hippocampal neuronal $[Ca^{2+}]_i$, *in vivo*, moderate hypothermia (31–33°C) was induced in rats 30 min after PILO SE and

maintained for 4 h (**Figure 3A**. Also see materials and methods). Hippocampal neurons were acutely isolated 24 h after SE to evaluate $[Ca^{2+}]_i$ using established procedures.

Figure 3B depicts ratiometric pseudocolor images of CA1 hippocampal neurons acutely isolated from rats treated with and without therapeutic hypothermia. As illustrated in **Figure 3C**, hippocampal neurons isolated 24 h after PILO-induced SE exhibited significant elevations in $[Ca^{2+}]_i$ compared to naïve controls. The average Fura-2 ratio values increased from 0.49 $\pm$ 0.04 in controls neurons to 0.88 $\pm$ 0.07 in neurons isolated from PILO-SE rats (n = 8 rats, t-test, $p < 0.05$). Thus, these results confirm our previous findings that PILO-SE results causes significant elevations in $[Ca^{2+}]_i$ 24 h after SE. In contrast, neurons isolated from rats treated with 4 h moderate hypothermia exhibit an average ratio value of 0.65 $\pm$ 0.07, which was significantly lower than ratios obtained from PILO-SE only rats ($n = 12$ rats, one-way ANOVA, $p < 0.05$).

Hypothermia Reduces Neuronal Injury Following SE

To assess neuronal injury in rats surviving SE, brain sections from SE animals treated with and without hypothermia were labeled with Fluoro-Jade C (FJC), which is an early marker of neurodegeneration (12, 28, 34). We focused on dentate-gyrus and CA1 region of the hippocampus since neurons in these regions are sensitive to SE-induced neuronal injury. Across brain regions examined, there was negligible FJC labeling in sections obtained from control rats. In contrast, after PILO-SE, within the hippocampus, FJC-positive staining was observed in the polymorphic layer and along the hilus/granule cell border of the dentate gyrus and CA1 region. An average of 8.4 $\pm$ 2.4 and 10.6 $\pm$ 3.2 FJC positive cells/ 100 μM^2 were quantified in dentate gyrus and CA1 region respectively. Brain sections from hypothermia-treated SE rats exhibited minimal FJC staining within these regions. The quantification of the neuronal injury expressed as FJC positive cells revealed approximately a 60% reduction in FJC labeling in the dentate gyrus and CA1 region of hypothermia-SE slices with an average of 3.0 $\pm$ 1.2 and 4.4 $\pm$ 0.8 FJC positive cells/ 100 μM^2 respectively (**Figures 4A,B**).

DISCUSSION

The results of this study demonstrate that hypothermia administered following SE not only reduces mortality but improves the recovery from SE. Hypothermia was effective at blocking the development of the Ca^{2+} plateau, and also reduced the hippocampal neuronal injury following SE.

In both the *in vivo* and *in vitro* models of SE, $[Ca^{2+}]_i$ remains elevated following injury, and this persistent elevation in $[Ca^{2+}]_i$ is believed to contribute to the pathological consequences associated with epileptogenesis. Blocking the development of the plateau has been shown to prevent the development of epilepsy in both *in vivo* and *in vitro* models of SE-induced AE (5, 8, 13, 27). The novel finding that hypothermia not only reduces mortality but also reduces elevated $[Ca^{2+}]_i$ and prevent the formation of the Ca^{2+} plateau offers additional information about the neuroprotective mechanisms of hypothermia as well as evidence that it could serve as an alternative intervention to pharmacological agents in preventing epileptogenesis after SE. This study has enormous translational potential for clinical application since hypothermia is already used in hospitals and ambulances settings to provide neuroprotection following cardiac arrest and hypoxia (18, 19, 23, 35, 36).

It has been demonstrated in the PILO model of SE-induced AE that SE causes a significant rise in $[Ca^{2+}]_i$ and these elevations persist in animals that eventually develop epilepsy (8, 37), which suggests that the Ca^{2+} plateau is involved the progression of epileptogenesis to the epileptic phenotype (5, 13). Ca^{2+} is a ubiquitous second messenger involved in a variety of cellular processes including neurotransmitter release and protein transcription, as well as long-term potentiation (14, 16, 38). Excessive elevations in $[Ca^{2+}]_i$ activate several downstream effectors leading to plasticity changes and eventually activation neuronal death pathways (38–41). Therefore, modulating the rise in $[Ca^{2+}]_i$ may be effective in blocking the Ca^{2+}-mediated cascade that leads to plasticity changes associated with epileptogenesis, thus preventing epilepsy.

Blocking the formation of the Ca^{2+} plateau with the use of NMDA receptor antagonists prior to and during SE prevents the development of AE (8, 11, 27), further suggesting that elevations in $[Ca^{2+}]_i$ are involved in the pathophysiology associated with epileptogenesis. However, NMDA antagonists are ineffective at preventing AE if administered after the injury (8, 11, 27). Currently, there are no anti-epileptogenic drugs that can be administered following a neurological insult (42). Thus, it is important to develop a therapy that can block epileptogenesis when administered post-SE injury (6).

There are several postulated mechanisms for neuroprotective actions of hypothermic interventions (24, 25). Hypothermia is known to reduce cerebral metabolism and improve post-ischemic glucose utilization (43). Studies have reported beneficial effects of hypothermia on cellular redox regulation. For example, under ischemia/reperfusion conditions, therapeutic hypothermia suppresses enhanced oxidative stress and enhances anti-oxidative potency (44). Hypothermia is also reported to inhibit several aspects of apoptosis including increased production of anti-apoptotic protein Bcl2 (45) and inhibition of cytochrome C (46). In addition, hypothermia has been shown to produce an anti-inflammatory effect in the brain. Amongst other mechanisms, hypothermia suppresses microglial activation (47) and inhibits inflammatory transcription factor nuclear factor kappa B (48). Hypothermia also reduces excitotoxic insult by attenuating glutamate release following ischemia (49). NMDA receptor-mediated Ca^{2+} entry has been shown to play a major role in excitotoxic neuronal injury and cell death (11, 12, 50). We have shown that hypothermia reduces Ca^{2+} entry through NMDA receptors (26), and this could be an important mechanism for the strong neuroprotective effects observed after SE following hypothermia. Thus, the mechanisms underlying the neuroprotective effects of hypothermia are multifactorial. Although they have different inciting injuries, stroke, TBI, and SE share the common pathology of elevated $[Ca^{2+}]_i$, and subsequent neuronal loss (5). Therefore, it stands to reason that

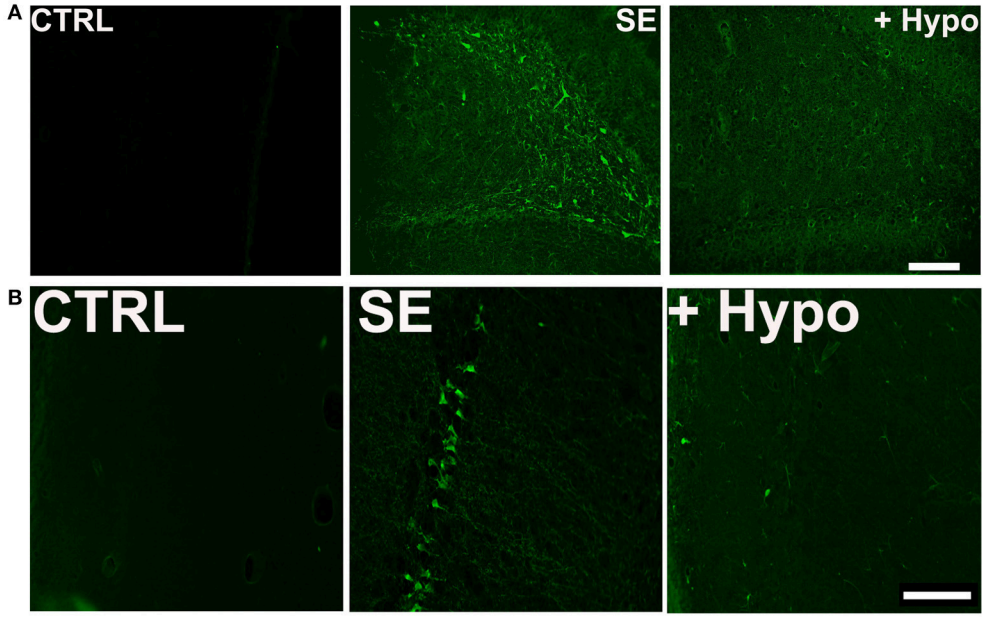

FIGURE 4 | Neuroprotective effect of hypothermia. Representative photomicrographs of Fluoro-Jade C (FJC) staining in the **(A)** dentate gyrus hilus and **(B)** CA1 region of a control (CTRL), pilocarpine-SE (SE), and hypothermia (+HYPO) treated rats. Scale bars, 100 μm.

hypothermia would provide similar neuroprotection after SE as it does with stroke and TBI. Indeed, hypothermia has been shown to reduce neurological injuries associated with out-of-hospital cardiac arrests (17–19), stroke (22, 23), and TBI (20, 21).

Hypothermia could be a promising therapeutic alternative for modifying epileptogenesis and AE outcomes after SE. It has been shown to have anticonvulsant properties and has been used to treat refractory SE (51, 52). The mechanism by which hypothermia prevents the persistent rise in $[Ca^{2+}]_i$ is most likely mediated by its ability to modulate Ca^{2+} influx into the cell via NMDA and ryanodine receptors. However, NMDA receptor activation is not responsible for Ca^{2+} influx post-SE. At this point, the influx of Ca^{2+} following SE recruits ryanodine receptors, resulting in enhanced Ca^{2+}-induced Ca^{2+} release. Ryanodine receptor activation is believed to be involved in maintaining the Ca^{2+} plateau in SE (12, 27, 28). Interestingly, hypothermia is also effective at reducing Ca^{2+} entry via ryanodine receptors (26), thus preventing the formation of the Ca^{2+} plateau. Indeed, as shown in this study, hypothermia administered 30 min post-SE blocked the protracted hippocampal Ca^{2+} elevations, and extended significant neuroprotection in hippocampus following SE.

The results of this study have important clinical implications. The neuroprotective mechanisms of hypothermia are complex and not completely understood. These findings offer additional insight into how hypothermia protects against neurological injury. In addition, the results suggest that hypothermia may prevent epileptogenesis by blocking the formation of the Ca^{2+} plateau. Further research to investigate the long-term effects of hypothermia following SE are necessary to evaluate the therapeutic potential of hypothermia as an anti-epileptogenic intervention.

AUTHOR CONTRIBUTIONS

RD conceptualized the study. KP and LD designed and conducted the experiments. KP, LD, and RD analyzed the data and drafted the manuscript the paper.

ACKNOWLEDGMENTS

This research was supported by the National Institute of Neurological Disorders and Stroke (NINDS), Grant Number R56NS092494-01 to RD.

REFERENCES

1. Hauser WA, Hesdorffer DC. *Epilepsy: Frequency, Causes and Consequences.* New York, NY: Demos (1990).
2. DeLorenzo RJ, Hauser WA, Towne AR, Boggs JG, Pellock JM, Penberthy L, et al. A prospective, population-based epidemiologic study of status epilepticus in Richmond, Virginia. *Neurology* (1996) **46**:1029–35. doi: 10.1212/WNL.46.4.1029
3. Hesdorffer DC, Logroscino G, Cascino G, Annegers JF, Hauser WA. Risk of unprovoked seizure after acute symptomatic seizure: effect of status epilepticus. *Ann Neurol.* (1998) **44**:908–12. doi: 10.1002/ana.410440609

4. Thurman DJ, Beghi E, Begley CE, Berg AT, Buchhalter JR, Ding D, et al. Standards for epidemiologic studies and surveillance of epilepsy. *Epilepsia* (2011) **52**(Suppl. **7**):2–26. doi: 10.1111/j.1528-1167.2011.03121.x
5. DeLorenzo RJ, Sun DA, Deshpande LS. Cellular mechanisms underlying acquired epilepsy: the calcium hypothesis of the induction and maintainance of epilepsy. *Pharmacol Ther.* (2005) **105**:229–66. doi: 10.1016/j.pharmthera.2004.10.004
6. Pitkanen A, Lukasiuk K, Dudek FE, Staley KJ. Epileptogenesis. *Cold Spring Harb Perspect Med.* (2015) **5**:a022822. doi: 10.1101/cshperspect.a022822
7. McNamara JO, Huang YZ, Leonard AS. Molecular signaling mechanisms underlying epileptogenesis. *Sci STKE* (2006) **2006**:re12. doi: 10.1126/stke.3562006re12
8. Raza M, Blair RE, Sombati S, Carter DS, Deshpande LS, DeLorenzo RJ. Evidence that injury-induced changes in hippocampal neuronal calcium dynamics during epileptogenesis cause acquired epilepsy. *Proc Natl Acad Sci USA.* (2004) **101**:17522–7. doi: 10.1073/pnas.0408155101
9. DeLorenzo RJ, Sun DA, Blair RE, Sombati S. An *in vitro* model of stroke-induced epilepsy: elucidation of the roles of glutamate and calcium in the induction and maintenance of stroke-induced epileptogenesis. *Int Rev Neurobiol.* (2007) **81**:59–84. doi: 10.1016/S0074-7742(06)81005-6
10. Sun DA, Deshpande LS, Sombati S, Baranova A, Wilson MS, Hamm RJ, et al. Traumatic brain injury causes a long-lasting calcium-plateau of elevated intracellular calcium levels and altered calcium homeostatic mechanisms in hippocampal neurons surviving the brain injury. *Eur J Neurosci.* (2008) **27**:1659–72. doi: 10.1111/j.1460-9568.2008.06156.x
11. Deshpande LS, Carter DS, Blair RE, DeLorenzo RJ. Development of a prolonged calcium plateau in hippocampal neurons in rats surviving status epilepticus induced by the organophosphate diisopropylfluorophosphate. *Toxicol Sci.* (2010) **116**:623–31. doi: 10.1093/toxsci/kfq157
12. Deshpande LS, Carter DS, Phillips KF, Blair RE, DeLorenzo RJ. Development of status epilepticus, sustained calcium elevations and neuronal injury in a rat survival model of lethal paraoxon intoxication. *Neurotoxicology* (2014) **44C**:17–26. doi: 10.1016/j.neuro.2014.04.006
13. Nagarkatti N, Deshpande LS, DeLorenzo RJ. Development of the calcium plateau following status epilepticus: role of calcium in epileptogenesis. *Expert Rev Neurother.* (2009) **9**:813–24. doi: 10.1586/ern.09.21
14. Berridge MJ. Neuronal calcium signaling. *Neuron* (1998) **21**:13–26. doi: 10.1016/S0896-6273(00)80510-3
15. Deshpande LS, Blair RE, Phillips KF, DeLorenzo RJ. Role of the calcium plateau in neuronal injury and behavioral morbidities following organophosphate intoxication. *Ann NY Acad Sci.* (2016) **1374**:176–83. doi: 10.1111/nyas.13122
16. Bengtson CP, Bading H. Nuclear calcium signaling. *Adv Exp Med Biol.* (2012) **970**:377–405. doi: 10.1007/978-3-7091-0932-8_17
17. Scholefield B, Duncan H, Davies P, Gao Smith F, Khan K, Perkins GD, et al. Hypothermia for neuroprotection in children after cardiopulmonary arrest. *Cochrane Database Syst Rev.* (2013) **2**:CD009442. doi: 10.1002/14651858.CD009442.pub2
18. Kim HJ, Kim GW, Oh SH, Park SH, Choi JH, Kim KH, et al. Therapeutic hypothermia after cardiac arrest caused by self-inflicted intoxication: a multicenter retrospective cohort study. *Am J Emerg Med.* (2014) **32**:1378–81. doi: 10.1016/j.ajem.2014.08.045
19. Lascarrou JB, Meziani F, Le Gouge A, Boulain T, Bousser J, Belliard G, et al. Therapeutic hypothermia after nonshockable cardiac arrest: the HYPERION multicenter, randomized, controlled, assessor-blinded, superiority trial. *Scand J Trauma Resusc Emerg Med.* (2015) **23**:26. doi: 10.1186/s13049-015-0103-5
20. McIntyre LA, Fergusson DA, Hebert PC, Moher D, Hutchison JS. Prolonged therapeutic hypothermia after traumatic brain injury in adults: a systematic review. *JAMA* (2003) **289**:2992–9. doi: 10.1001/jama.289.22.2992
21. Madden LK, DeVon HA. A systematic review of the effects of body temperature on outcome after adult traumatic brain injury. *J Neurosci Nurs.* (2015) **47**:190–203. doi: 10.1097/JNN.0000000000000142
22. Kuramatsu JB, Kollmar R, Gerner ST, Madzar D, Pisarcikova A, Staykov D, et al. Is hypothermia helpful in severe subarachnoid hemorrhage? An exploratory study on macro vascular spasm, delayed cerebral infarction and functional outcome after prolonged hypothermia. *Cerebrovasc Dis.* (2015) **40**:228–35. doi: 10.1159/000439178
23. Yao Z, You C, He M. Effect and feasibility of therapeutic hypothermia in patients with hemorrhagic stroke: a systematic review and meta-analysis. *World Neurosurg.* (2018) **111**:404–412.e2. doi: 10.1016/j.wneu.2018.01.020
24. Polderman KH. Mechanisms of action, physiological effects, and complications of hypothermia. *Crit Care Med.* (2009) **37**:S186–202. doi: 10.1097/CCM.0b013e3181aa5241
25. Karnatovskaia LV, Wartenberg KE, Freeman WD. Therapeutic hypothermia for neuroprotection: history, mechanisms, risks, and clinical applications. *Neurohospitalist* (2014) **4**:153–63. doi: 10.1177/1941874413519802
26. Phillips KF, Deshpande LS, DeLorenzo RJ. Hypothermia reduces calcium entry via the N-methyl-D-aspartate and ryanodine receptors in cultured hippocampal neurons. *Eur J Pharmacol* (2013) **698**:186–92. doi: 10.1016/j.ejphar.2012.10.010
27. Nagarkatti N, Deshpande LS, Carter DS, DeLorenzo RJ. Dantrolene inhibits the calcium plateau and prevents the development of spontaneous recurrent epileptiform discharges following *in vitro* status epilepticus. *Eur J Neurosci.* (2010) **32**:80–8. doi: 10.1111/j.1460-9568.2010.07262.x
28. Deshpande LS, Blair RE, Huang BA, Phillips KF, DeLorenzo RJ. Pharmacological blockade of the calcium plateau provides neuroprotection following organophosphate paraoxon induced status epilepticus in rats. *Neurotoxicol Teratol.* (2016) **56**:81–6. doi: 10.1016/j.ntt.2016.05.002
29. Falenski KW, Carter DS, Harrison AJ, Martin BR, Blair RE, DeLorenzo RJ. Temporal characterization of changes in hippocampal cannabinoid CB(1) receptor expression following pilocarpine-induced status epilepticus. *Brain Res.* (2009) **1262**:64–72. doi: 10.1016/j.brainres.2009.01.036
30. Deshpande LS, Nagarkatti N, Ziobro JM, Sombati S, Delorenzo RJ. Carisbamate prevents the development and expression of spontaneous recurrent epileptiform discharges and is neuroprotective in cultured hippocampal neurons. *Epilepsia* (2008) **49**:1795–802. doi: 10.1111/j.1528-1167.2008.01667.x
31. Nagarkatti N, Deshpande LS, DeLorenzo RJ. Levetiracetam inhibits both ryanodine and IP3 receptor activated calcium induced calcium release in hippocampal neurons in culture. *Neurosci Lett.* (2008) **436**:289–93. doi: 10.1016/j.neulet.2008.02.076
32. Deshpande LS, Blair RE, Ziobro JM, Sombati S, Martin BR, DeLorenzo RJ. Endocannabinoids block status epilepticus in cultured hippocampal neurons. *Eur J Pharmacol.* (2007) **558**:52–59. doi: 10.1016/j.ejphar.2006.11.030
33. Wallace MJ, Blair RE, Falenski KW, Martin BR, DeLorenzo RJ. The endogenous cannabinoid system regulates seizure frequency and duration in a model of temporal lobe epilepsy. *J Pharmacol Exp Ther.* (2003) **307**:129–37. doi: 10.1124/jpet.103.051920
34. Phillips KF, Deshpande LS. Repeated low-dose organophosphate DFP exposure leads to the development of depression and cognitive impairment in a rat model of Gulf War Illness. *Neurotoxicology* (2016) **52**:127–33. doi: 10.1016/j.neuro.2015.11.014
35. Scholefield BR, Lyttle MD, Berry K, Duncan HP, Morris KP. Survey of the use of therapeutic hypothermia after cardiac arrest in UK paediatric emergency departments. *Emerg Med J.* (2013) **30**:24–7. doi: 10.1136/emermed-2011-200348
36. Sherman AL, Wang MY. Hypothermia as a clinical neuroprotectant. *Phys Med Rehabil Clin N Am.* (2014) **25**:519–29. doi: 10.1016/j.pmr.2014.04.003
37. Raza M, Pal S, Rafiq A, DeLorenzo RJ. Long-term alteration of calcium homeostatic mechanisms in the pilocarpine model of temporal lobe epilepsy. *Brain Res.* (2001) **903**:1–12. doi: 10.1016/S0006-8993(01)02127-8
38. Baker KD, Edwards TM, Rickard NS. The role of intracellular calcium stores in synaptic plasticity and memory consolidation. *Neurosci Biobehav Rev.* (2013) **37**:1211–39. doi: 10.1016/j.neubiorev.2013.04.011
39. Adasme T, Haeger P, Paula-Lima AC, Espinoza I, Casas-Alarcon MM, Carrasco MA, et al. Involvement of ryanodine receptors in neurotrophin-induced hippocampal synaptic plasticity and spatial memory formation. *Proc Natl Acad Sci USA.* (2011) **108**:3029–34. doi: 10.1073/pnas.1013580108
40. Bodalia A, Li H, Jackson MF. Loss of endoplasmic reticulum Ca^{2+} homeostasis: contribution to neuronal cell death during cerebral ischemia. *Acta Pharmacol Sin.* (2013) **34**:49–59. doi: 10.1038/aps.2012.139
41. Chadwick W, Mitchell N, Martin B, Maudsley S. Therapeutic targeting of the endoplasmic reticulum in Alzheimer's disease. *Curr Alzheimer Res.* (2013) **9**:110–9. doi: 10.2174/156720512799015055

42. Pitkanen A, Nehlig A, Brooks-Kayal AR, Dudek FE, Friedman D, Galanopoulou AS, et al. Issues related to development of antiepileptogenic therapies. *Epilepsia* (2013) **54**(Suppl. 4):35–43. doi: 10.1111/epi.12297
43. Lanier WL. Cerebral metabolic rate and hypothermia: their relationship with ischemic neurologic injury. *J Neurosurg Anesthesiol.* (1995) **7**:216–21. doi: 10.1097/00008506-199507000-00021
44. Nosaka N, Okada A, Tsukahara H. Effects of therapeutic hypothermia for neuroprotection from the viewpoint of redox regulation. *Acta Med Okayama* (2017) **71**:1–9. doi: 10.18926/AMO/54819
45. Zhang Z, Sobel RA, Cheng D, Steinberg GK, Yenari MA. Mild hypothermia increases Bcl-2 protein expression following global cerebral ischemia. *Brain Res Mol Brain Res.* (2001) **95**:75–85. doi: 10.1016/S0169-328X(01)00247-9
46. Yenari MA, Iwayama S, Cheng D, Sun GH, Fujimura M, Morita-Fujimura Y, et al. Mild hypothermia attenuates cytochrome c release but does not alter Bcl-2 expression or caspase activation after experimental stroke. *J Cereb Blood Flow Metab.* (2002) **22**:29–38. doi: 10.1097/00004647-200201000-00004
47. Zheng Z, Yenari MA. Post-ischemic inflammation: molecular mechanisms and therapeutic implications. *Neurol Res.* (2004) **26**:884–92. doi: 10.1179/016164104X2357
48. Han HS, Karabiyikoglu M, Kelly S, Sobel RA, Yenari MA. Mild hypothermia inhibits nuclear factor-kappaB translocation in experimental stroke. *J Cereb Blood Flow Metab.* (2003) **24**:589–98. doi: 10.1097/01.WCB.0000059566.39780.8D
49. Busto R, Globus MY, Dietrich WD, Martinez E, Valdes I, Ginsberg MD. Effect of mild hypothermia on ischemia-induced release of neurotransmitters and free fatty acids in rat brain. *Stroke* (1989) **20**:904–10.
50. de Araujo Furtado M, Lumley LA, Robison C, Tong LC, Lichtenstein S, Yourick DL. Spontaneous recurrent seizures after status epilepticus induced by soman in Sprague-Dawley rats. *Epilepsia* (2010) **51**:1503–10. doi: 10.1111/j.1528-1167.2009.02478.x
51. Bennett AE, Hoesch RE, DeWitt LD, Afra P, Ansari SA. Therapeutic hypothermia for status epilepticus: a report, historical perspective, and review. *Clin Neurol Neurosurg.* (2014) **126**:103–9. doi: 10.1016/j.clineuro.2014.08.032
52. Kim DH, Kang HH, Kim M, Yang TW, Kwon OY, Yeom JS, et al. Successful use of therapeutic hypothermia for refractory nonconvulsive status epilepticus. *J Epilepsy Res.* (2017) **7**:109–14. doi: 10.14581/jer.17017

Conflict of Interest Statement: The authors declare that the research was conducted in the absence of any commercial or financial relationships that could be construed as a potential conflict of interest.

frontiers in Neurology

ORIGINAL RESEARCH
published: 02 August 2018
doi: 10.3389/fneur.2018.00632

Rhythms of Core Clock Genes and Spontaneous Locomotor Activity in Post-*Status Epilepticus* Model of Mesial Temporal Lobe Epilepsy

Heloisa de Carvalho Matos[1], *Bruna Del Vechio Koike*[2], *Wanessa dos Santos Pereira*[1], *Tiago G. de Andrade*[2,3], *Olagide W. Castro*[4], *Marcelo Duzzioni*[4], *Maheedhar Kodali*[5], *Joao P. Leite*[6], *Ashok K. Shetty*[5]* *and Daniel L. G. Gitaí*[1,5]*

[1] *Department of Cellular and Molecular Biology, Institute of Biological Sciences and Health, Federal University of Alagoas, Maceio, Brazil,* [2] *Laboratory of Molecular Chronobiology, Federal University of Alagoas, Arapiraca, Brazil,* [3] *Department of Physiology and Pharmacology, Institute of Biological Sciences and Health, Federal University of Alagoas, Maceio, Brazil,* [4] *Institute for Regenerative Medicine, Department of Molecular and Cellular Medicine, Texas A&M Health Science Center College of Medicine, College Station, TX, United States,* [5] *Division of Neurology, Department of Neurosciences and Behavioral Sciences, Ribeirão Preto School of Medicine, University of São Paulo, Ribeirão Preto, Brazil,* [6] *Faculty of Medicine, Federal University of Alagoas, Maceio, Brazil*

OPEN ACCESS

Edited by:
Patrick A. Forcelli, Georgetown University, United States

Reviewed by:
Jana Dimitrova Tchekalarova, Institute of Neurobiology (BAS), Bulgaria
Thomas Nicholas Ferraro, Cooper Medical School of Rowan University, United States

***Correspondence:**
Ashok K. Shetty
shetty@medicine.tamhsc.edu
Daniel L. G. Gitaí
danielgitai@gmail.com

Specialty section:
This article was submitted to Epilepsy, a section of the journal Frontiers in Neurology

Received: *18 December 2017*
Accepted: *12 July 2018*
Published: *02 August 2018*

Citation:
Matos HC, Koike BDV, Pereira WS, de Andrade TG, Castro OW, Duzzioni M, Kodali M, Leite JP, Shetty AK and Gitaí DLG (2018) Rhythms of Core Clock Genes and Spontaneous Locomotor Activity in Post-Status Epilepticus Model of Mesial Temporal Lobe Epilepsy. Front. Neurol. 9:632. doi: 10.3389/fneur.2018.00632

The interaction of Mesial Temporal Lobe Epilepsy (mTLE) with the circadian system control is apparent from an oscillatory pattern of limbic seizures, daytime's effect on seizure onset and the efficacy of antiepileptic drugs. Moreover, seizures *per se* can interfere with the biological rhythm output, including circadian oscillation of body temperature, locomotor activity, EEG pattern as well as the transcriptome. However, the molecular mechanisms underlying this cross-talk remain unclear. In this study, we systematically evaluated the temporal expression of seven core circadian transcripts (*Bmal1, Clock, Cry1, Cry2, Per1, Per2,* and *Per3*) and the spontaneous locomotor activity (SLA) in post-*status epilepticus* (SE) model of mTLE. Twenty-four hour oscillating SLA remained intact in post-SE groups although the circadian phase and the amount and intensity of activity were changed in early post-SE and epileptic phases. The acrophase of the SLA rhythm was delayed during epileptogenesis, a fragmented 24 h rhythmicity and extended active phase length appeared in the epileptic phase. The temporal expression of circadian transcripts *Bmal1, Cry1, Cry2, Per1, Per2,* and *Per3* was also substantially altered. The oscillatory expression of *Bmal1* was maintained in rats imperiled to SE, but with lower amplitude (A = 0.2) and an advanced acrophase in the epileptic phase. The diurnal rhythm of *Cry1* and *Cry2* was absent in the early post-SE but was recovered in the epileptic phase. *Per1* and *Per2* rhythmic expression were disrupted in post-SE groups while *Per3* presented an arrhythmic profile in the epileptic phase, only. The expression of *Clock* did not display rhythmic pattern in any condition. These oscillating patterns of core clock genes may contribute to hippocampal 24 h cycling and, consequently to seizure periodicity. Furthermore, by using a pool of samples collected at 6 different Zeitgeber Times (ZT), we found that all clock transcripts were significantly dysregulated after SE

induction, except *Per3* and *Per2*. Collectively, altered SLA rhythm in early post-SE and epileptic phases implies a possible role for seizure as a nonphotic cue, which is likely linked to activation of hippocampal–accumbens pathway. On the other hand, altered temporal expression of the clock genes after SE suggests their involvement in the MTLE.

Keywords: clock genes, epilepsy, seizure, spontaneous locomotor activity, circadian rhythm

INTRODUCTION

The circadian timing system generates 24 h oscillations of metabolic, physiologic and behavioral functions as an adaptive response to diurnal environmental changes (1, 2). In mammals, this temporal program is systemically regulated by cells in the suprachiasmatic nucleus (SCN) of the hypothalamus. SCN is the master pacemaker, which integrates environmental time cues (e.g., light/dark cycle) for the necessary synchronization of different tissues in the body (peripheral oscillators) (3, 4). These circadian oscillations are driven by a network of transcription/translation-based interlocking feedback loops, involving a CLOCK/BMAL1 and Period (PER1, PER2, and PER3)/Cryptochrome (CRY1 and CRY2) protein complexes (5–7). The CLOCK and BMAL1 form a heterocomplex that induces the transcription of *Per* and *Cry* genes (positive feedback loop). On the other hand, PERs and CRYs form complexes that suppress the activity of CLOCK and BMAL1 and their expression (negative feedback loop), allowing the cycle to repeat (7, 8). This self-oscillating molecular machinery regulates the expression of several clock-controlled genes in different tissues, which is critical for circadian outputs (9, 10). Multiple studies have shown that circadian disruption might be the cause or consequence of various human diseases (11–19).

Mesial Temporal Lobe Epilepsy (mTLE) is a chronic disease characterized by spontaneous and recurrent partial seizures (SRS) elicited by an excessive and overly synchronized neuronal activity in limbic regions of the brain. An intriguing well-documented feature in this condition is the occurrence of seizures. Despite being unpredictable, seizure episodes display a circadian rhythm (20). In fact, it has been shown in mTLE patients, that seizures present a 24 h non-random pattern of distribution with a unimodal or bimodal distribution (20–22). Similarly, experimental models of mTLE exhibit a diurnal oscillation pattern for the occurrence of SRS (23–30), with an exception (31). These data suggest that the limbic seizures are modulated by a circadian regulatory system.

The pathogenesis of mTLE is a complex process having a close relationship with the circadian system. Prior to the onset of SRS, the brain undergoes series of progressive structural and cellular alterations and reorganization elicited by an initial precipitating injury, such as *Status Epilepticus* (SE). The changes, collectively referred to as epileptogenic processes, comprise neuron loss, aberrant neurogenesis, gliosis, axonal damage, dendritic plasticity, altered gene expression, and inflammation. Such changes occur prominently in the hippocampal formation (32–38), a region of the brain identified as an important peripheral oscillator in mammalian (39–44). Nonetheless, the extent to which circadian rhythms and epileptogenesis influence each other remains unclear though studies point to the presence of bidirectional interaction (13, 27, 45–48). On the one hand, some studies imply that the time of the day has an effect on the threshold for seizure induction in different experimental models (49–53). For example, in pilocarpine (PILO) induced SE, both shorter latency to seizures and severe seizures were associated with the induction of SE in daytimes vis-à-vis the dark period. Moreover, circadian disruption through knockdown of *Bmal1* or clock-controlled genes leads to a reduced seizure threshold (54, 55). On the other hand, epileptogenic processes can alter circadian biological rhythms. It has been reported in experimental models of mTLE that changes in the diurnal rhythms of spontaneous locomotor activity (SLA) and temperature body occur a few weeks after SE induction or/and after SRS onset (27, 56–58). Continuous 24/7 video/telemetric hippocampal EEG recordings in a PILO-induced SE have revealed that SE induces a transient suppression of the physiologic circadian EEG pattern, which correlates with less severe seizures during this period. Remarkably, SRS ensue after the stabilization of the circadian rhythm and start to emerge in clusters or a more severe manner (59).

However, molecular mechanisms involved in the interaction between epileptogenesis and the circadian system remains unclear. Partly, this is due to a lack of studies on the rhythmic expression of clock genes in epileptic phases. A recent study, using large-scale approaches, demonstrated a diurnal molecular landscape in the hippocampus of epileptic mice [(60), preprint publication]. However, the potential changes in clock genes across different phases of epileptogenesis have not been investigated. It is also unknown how does circadian gene expression relate to induction of spontaneous seizures and epilepsy. In our previous study, we analyzed the temporal profiling of clock genes mRNA levels in the hippocampus of naïve rats (61). Here, we address this issue by studying these genes in a post-SE model of mTLE, a prototype showing similar epileptogenic and histopathological processes as human mTLE (62). First, we evaluated the effects of SE on diurnal rhythms of SLA in rats during the early post-SE and epileptic periods. Next, we examined the temporal expression of *Clock*, *Bmal1*, *Cry1*, *Cry2, Per1, Per2,* and *Per3* mRNA levels in the hippocampus of naïve rats and rats subjected to SE in early post-SE and epileptic phases. Finally, the gene expression levels were investigated by RT-qPCR in the hippocampus of experimental and control animals.

MATERIALS AND METHODS

Animals and Experimental Groups

Experiments included 100 male adult Wistar rats (300–400 g) from the main breeding stock of the Federal University of Alagoas. Ten rats were designated for SLA experiments, and 90 rats were used for molecular analysis (**Figure 1**). Rats were 192–206 days-old and kept at 22 ± 2°C in groups of five per cage with free access to food and water. The animals were under a 12 h light and 12 h dark regimen, which was divided into 24 h Zeitgeber time units (ZT), where ZT0 is when the light is turned on (6 a.m.) and ZT12 when the light is turned off (6 p.m.). The rats assigned to SLA experiments ($n = 10$) were the same recorded during the baseline. These comprise the naïve control group, the early post-SE group (i.e., 17 days after SE-induction), and the epileptic group (**Figure 1A**). Rats belonging to molecular analyses ($n = 90$) were euthanized every 4 h during a 24 h period (five animals per time point) at the ZT 0, 4, 8, 12, 16 and 20 for each group. These animals were euthanized by decapitation using a guillotine within 20 min of the each ZT. For ZT12, ZT16, and ZT20, the euthanasia was done in dim red light (**Figure 1B**). All animal experiments were performed per a protocol approved by the Research Ethics Committee of the Federal University of Alagoas (Permit number: 12/2014) and were consistent with the International guidelines of the ethical use of animals, such as those from the Society for Neuroscience. Animal health was monitored throughout the experimental period as described previously (61). All efforts were made to reduce the number of animals used and to avoid any unnecessary suffering. No animals presented clinical/behavioral signs of pain or unexpected distress used as humane endpoint criteria for euthanasia. We have followed the standard biosecurity.

Post-SE Model of MTLE

The SE induction and evaluation were performed as detailed elsewhere (63). Briefly, rats were injected intraperitoneally (i.p.) with lithium chloride (127 mg/kg, Sigma) followed by PILO (30 mg/kg, Sigma) after 18 h. To counteract the peripheral cholinergic effects, scopolamine butyl-bromide (1 mg/kg, Sigma) was administered 30 min before the administration of PILO. Animals were kept in SE for 90 min before seizure interruption with an injection of diazepam (5 mg/kg; i.p.). For the molecular analysis, from post-SE day 3, animals were individually placed in acrylic cages, and their behavior was videotaped for ∼8 h per day over 11 weeks. All videos were analyzed by two independent observers, and the severity score of SRS was classified as per Racine scale, which is based on five stages: stage 1 (mouth and facial movement), stage 2 (head nodding), stage 3 (forelimb clonus), stage 4 (rearing with forelimb clonus), and stage 5 (rearing and falling with forelimb clonus) (64). Animals that displayed no SRS were included for analysis in the early post-SE phase, whereas animals that exhibited two or more SRS with severity scores equal or greater than 3 were chosen for analysis in the epileptic phase. Animals were euthanized 7 days after SE for the early post-SE phase analysis, and 11 weeks after SE for the epileptic phase analysis. During the video-recordings, we observed a total of 80 SRS. Of these, 48.5% were classified as stage 5 according to the Racine Scale severity, 26.25% as stage 4, 18.75% as stage 3, 5% as stage 2, and 1.25% as stage 1. The average frequencies of different stages of spontaneous seizures recorded per animal in the epileptic group were 1.3 (stage 5), 0.7 (stage 4), 0.54 (stage 3), and 0.1 (stage 2). Only the animals which presented at least two stage 3 or higher seizures were included in the epileptic group.

SLA

The rats were habituated individually to 37 × 24.2 × 24 cm cages for 14 days, and SLA was then continuously detected over a 10-day period (named as the baseline). The infrared motion sensors detect any movement inside the cage. They were placed 15 cm above the cage lids and automatically recorded the movement time in a computer every 5 min by the SAP System (Dr. Marconi Camara Rodrigues, Universidade Federal do Rio Grande do Norte, Natal, Brazil, 2011). After 240 h of baseline recordings, rats were subjected to SE. SLAs were again recorded from each animal for 10 days, starting both at 7 days post-SE (called early post-SE group) and at 10 weeks post-SE (epileptic group).

RNA Extraction and Reverse Transcription

The entire hippocampus was rapidly dissected, isolated on an ice-chilled plate and immediately frozen and stored in liquid nitrogen until RNA extraction. Total RNA was purified using Trizol reagent (Invitrogen, CA, USA) following the manufacturer's protocol. Total RNA from the left hippocampus of each rat was treated with DNase I (Ambion, TX, USA) for 30 min to avoid amplification of genomic DNA. Total RNA (1 μg) was reverse transcribed to single-stranded cDNA using the High-Capacity cDNA Reverse Transcription Kit (Applied Biosystems, Foster City, CA) according to manufacturer's instructions. Once reverse-transcription was complete, samples were diluted (10X) in TE (Tris 10 mM, pH 7.4; EDTA 0.1 mM, pH 8.0) and stored at −80°C until further analysis.

qPCR

qPCR was carried out on a StepOnePlus PCR System (Applied Biosystems). The clock primer sequences and characteristics are described in previous reports (61, 65). Reactions were performed in a 12 μL volume containing cDNA (2 μL), 0.2 ± 0.6 μM each of specific forward (F) and reverse (R) primers, and 6 μl Power Syber1Green PCR Master Mix (Applied Biosystem, CA, USA). The amplification protocol was as follows: initial 10 min denaturation and 40 cycles of 95°C for 15 s and 60°C for 1 min. To ensure specificity of the PCR amplicon, we performed a melting curve analysis, ranging from 60 to 95°C, with temperature increases in steps of 0.5°C every 10 s. All primers showed an RT-qPCR efficiency ranging from 90 to 110%, as assessed by a standard curve based on a 5 points serial dilution of pooled cDNA (1:20; 1:40; 1:80; 1:160, and 1:320). The absence of contamination was confirmed using a no template control (NTC), with water in place of cDNA in each. Each assay was performed in triplicate, and the mean values were used for further analysis. The target gene expression was normalized to the *Tubb2a/Rplp1* as previously determined in our previous study as the best combination of reference genes for diurnal expression

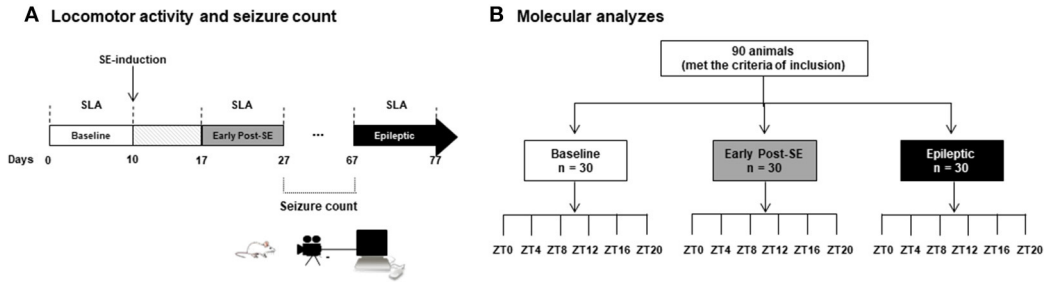

FIGURE 1 | Experimental design. **(A)** Rats assigned to the SLA experiments ($n = 10$) were placed on the rack equipped with sensors in order to record the spontaneous locomotor activity. The basal activity was considered the recording of 10 days in free movement, what we called baseline (white bar). At 10th day, these rats received the pilocarpine injection to promote the status epilepticus (SE). After a week, the animals were in the early post-SE phase, and the SLA was recorded for 10 days (from day 17 to 27, gray bar), and they are considered as early post-SE group. The animals were transferred to the video recording chamber, and the seizure observation was done every day from 10 a.m. to 6 p.m. All animals that presented two or more stage 3 seizures (Racine scale) were considered for the epileptic group. These rats were then re-placed at the SLA recording chamber, and the SLA was recorded for 10 days (black bar). **(B)** Rats belonging to molecular analyses ($n = 90$) were euthanized every 4 h during a 24 h period (five animals per time point) at the ZT 0, 4, 8, 12, 16, and 20 for each group. All these animals were euthanized by decapitation using a guillotine within 20 min of the each ZT. For ZT12, ZT16, and ZT20, the euthanasia was done in the dim red light. SE, *Status Epilepticus;* SLA, Spontaneous Locomotor Activity; ZT, Zeitgeber time units.

analysis in the hippocampus (61). A similar profile was seen with Tubb2a/Rplp1 in the prior study. Relative amounts of transcripts were calculated using the ^{2}-ΔΔCt method (66). Values were expressed in quantities relative to the calibrator, which was run on each PCR plate through the entire experiment.

Statistical Analysis

The serial analysis of the locomotor activity was carried out using the software El Temps (Dr. Antoni Diez-Noguera, University of Barcelona, Barcelona, Spain, 1999). This software calculates all the rhythmic parameters, such as the period, onset, offset, alpha (active phase), acrophase, amplitude, the center of gravity, area under curve, mean waveform, and intracycle variability. The variables' comparisons between conditions were made by repeated measures ANOVA, followed by Bonferroni's *post hoc* tests.

Acrophase software (http://www.circadian.org/softwar.html) was used for the analysis of circadian patterns of clock genes expression. A $p < 0.05$ was taken as indicative of the presence of a rhythm with the 24 h (anticipated) period. Acrophase (ACRO) performs a cosinor regression to fit the time-course data to a cosine function that occurs in a 24 h period. The program detects periodicity and computes the achophase of circadian rhythm with the 95% confidence interval.

For gene expression's rhythm comparisons, the Spearman correlation and the cross-correlations were done using the IBM SPSS Statistics® (version 21). We considered high correlation when coefficient values were above 0.80, moderately correlation when values ranged from 0.50 −0.79, and low correlation when coefficient values were below 0.50. All datasets were assessed for normal distribution by Kolmogorov-Smirnov test. To compare mean gene expression per condition (the mean of all ZTs), we performed the Kruskal-Wallis test with Dunn's *post hoc* tests, once the distribution was found to be not normal according to the Kolmogorov-Smirnov test. Mean differences were considered statistically significant when $p < 0.05$, and the results were presented graphically as the mean and standard error of the mean.

RESULTS

SLA

All animals maintained the circadian rhythmicity of the SLA, with a similar period from the baseline [**Figures 2A,B**; Mean = 1437 ± 6 min; $F_{(2,8)} = 2.869$, $p = 0.115$]. The SLA (area under the curve of the mean waveform) was higher in both early post-SE and epileptic phases. However, during the light period, epileptic animals presented an even more intense activity than the animals in the early post-SE phase [**Figure 2D**; $F_{(2,8)} = 18.954$, $p = 0.001$; *post-hoc* Bonferroni $p = 0.008$ and $p < 0.001$]. Concerning the circadian phase (**Figure 2C**), the activity onset occurred earlier in epileptic rats [$F_{(2,8)} = 23.581$, $p < 0.001$, *post-hoc* Bonferroni $p < 0.001$], compared to other conditions. However, the acrophase was observed later in epileptic animals in comparison to the baseline only. There was no difference in the activity's end time among conditions. The intracycle variabilities were higher in the epileptic phase compared to other conditions, revealing that the circadian rhythm of the locomotor activity is more fragmented in this condition [$F_{(2,8)} = 13.813$, $p = 0.003$; *post-hoc* Bonferroni $p = 0.003$ and $p = 0.005$] (**Figure 2E**).

Temporal Profiling of Clock Transcript Levels in Post-SE Model of MTLE

We systematically evaluated the temporal profiling of *Bmal1*, *Clock*, *Cry1, Cry2, Per1, Per2,* and *Per3* mRNA levels in the hippocampus of naïve rats or rats subjected to SE (early post-SE and epileptic phases) sacrificed every 4 h during a 24 h period. **Figure 3** illustrates the temporal organization and phase relationship of clock genes analyzed. Using the Acrophase software, we observed that only *Clock* did not show a rhythmic expression pattern in all conditions (**Figure 3D**). The oscillatory expression of *Bmal1* was kept in rats subjected to SE. However,

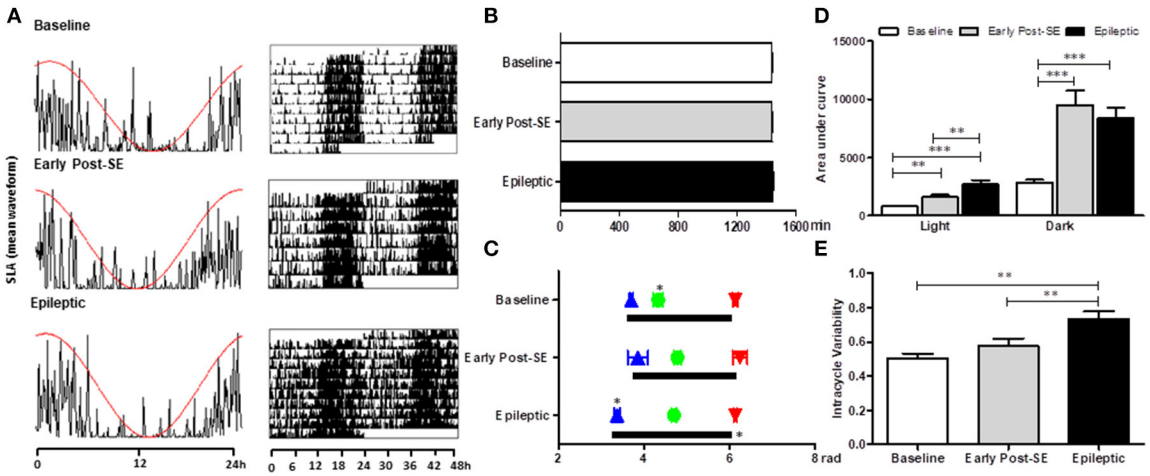

FIGURE 2 | Circadian rhythm analysis of locomotor activity variables in different stages after SE induction. **(A)** Representative graphics of one-day activity waveform (left) with the cosine fit curve (red) and a representative actogram (right) in each condition. All three phases maintained the circadian rhythm of the rest-activity cycle, without alterations in the period **(B)**. **(C)** The activity onset (blue triangles) is similar to baseline rats and the ones in the early post-SE phase. However, the epileptic animals started the activity earlier than the others, meaning that the phase angle between the activity onset and the lights off is shorter in the epileptic condition. The activity's end time is similar for all 3 phases (red triangles). The acrophase (green balls) occurs later in the experimental (early post-SE and epileptic) groups. The duration of the activity phase (alpha, black bars) of epileptic animals is longer. **(D)** The amount of activity measured by the area under the curve of the mean waveform showed that the rats are less active during the light than during the dark in all three conditions. Besides, the experimental animals (early post-SE and epileptic) have higher locomotor activity both during the light and during the darkness. The activity of the epileptic rats is even higher than in the early post-SE condition during the light phase. **(E)** The epileptic condition has a more fragmented rhythm, represented by the higher intra-daily variability values. Statistical test for circadian analysis was done by Acrophase software and El Temps. Comparisons between conditions were done by repeated measures ANOVA, followed by Bonferroni's *post hoc* test. $^{*}p < 0.05$, $^{**}p < 0.01$, and $^{***}p < 0.001$.

the *Bmal1* acrophase was progressively phase advanced over epileptogenesis (ZT 1.2 for early post-SE condition and ZT 0 for epileptics) compared to naïve rats (ZT 2) (**Figure 3C**). Interestingly, the diurnal rhythm of *Cry1* and *Cry2* was lost in the early post-SE period but were restored in the epileptic condition with an earlier acrophase for *Cry1* (ZT16.4) and later for *Cry2* (ZT 9.6) compared to naïve rats (ZT 17.6 and ZT 7.6, respectively) (**Figures 3A,B**). However, by the ANOVA, a significant difference was observed for *Cry2* at a single time point. The *Per1, Per2,* and *Per3* expressions present circadian rhythms on the naïve condition, as expected (40, 67–69). However, the *Per1* and *Per2* rhythmic expressions were disrupted during the epileptogenesis, both during the early post-SE as well as the epileptic condition (**Figures 3E,F**). The *Per3* expression oscillates during the early post-SE, but the rhythm was lost in the epileptic group (**Figure 3F**).

Bmal1 expression was in antiphase to *Per1 and Per3* in naïve (ZT 2 (*Bmal1*) x ZT 16 (*Per1*), rho $= -0.829$, $p = 0.021$ and ZT14.8 (*Per3*), rho $= -0.946$, $p = 0.002$), as well as to *Per3* in early post-SE (ZT 1.2 × 14.4, rho $= -0.886$, $p = 0.009$), and to *Cry2* in epileptic (ZT 0 × ZT 9.6, rho $= -0.771$, $p = 0.036$) rats, which is consistent with the negative temporal correlation found between these genes in these conditions (**Figure 3**). *Cry1, Cry2, Per1,* and *Per2* did not present a rhythmic profile in the cosinor analysis in the early post-SE period, which also showed high correlation with *Clock* [Cry1 rho $= 0.886$, $p = 0.009$ (Cry1); rho $= 0.886$, $p = 0.009$ (Cry2); rho $= 0.943$, $p = 0.002$ (Per1); rho $= 0.886$, $p = 0.009$ (Per2)]. *Cry2* became negatively correlated to *Bmal1* after SE (rho $= -0.771$, $p = 0.036$) probably due to the phase changes observed (**Figures 3B,C**).

We performed the cross-correlation analysis between the SLA and the expression of clock genes at lag 0 (**Figure 4A**). We found higher coefficient indices for *Cry1*, *Per1,* and *Per3* expression (0.95; 0.97, and 0.82, respectively). This pattern suggested that the rhythmic expression of these genes is highly correlated with the SLA rhythm in the naïve condition. This positive correlation is maintained during the early post-SE period for *Per1* and *Per3* (0.83 and 0.86) but decreased during the epileptic phase. On the other hand, *Bmal1* expression presented a moderate negative correlation with the SLA at lag 0. Verifying the cross-correlation at other lags, we found that at lag −1 the cross-correlation coefficient between *Bmal1* and SLA was higher, as shown in **Figure 4B**. At lag −1 the cross-correlation coefficient was −0.95 for naïve and −0.90 for the early post-SE group. The coefficient is reduced for the epileptic condition at lag −1 (−0.78), but increased at lag −2 and decreased at lag 0 when compared with the naïve (from −0.40 to −0.52 at lag −2 and from −0.76 to −0.425 at lag 0), indicating the phase shift observed throughout the epileptogenesis.

Finally, the cross-correlation between all the genes and the SLA are shown for each condition in **Figure 4C**. The naïve rats presented a positive correlation between the SLA and the *Cry1*, *Per1,* and *Per3* expression (0.95; 0.97, and 0.82, respectively). All these 4 components present the acrophase on the dark phase. There is a positive correlation between *Per1* and *Cry1*

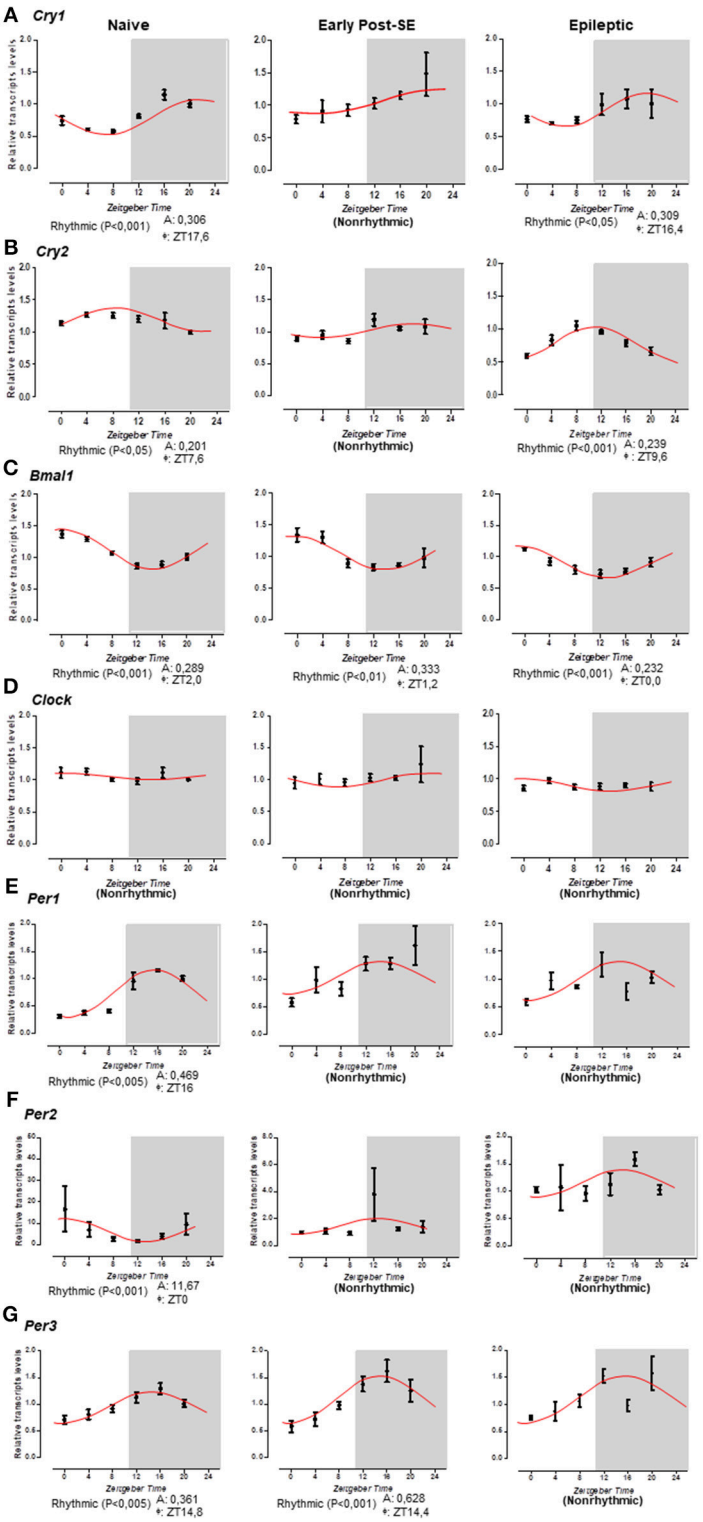

FIGURE 3 | Temporal pattern of gene expression in the rat hippocampus. Relative transcripts levels for 6 time-points (ZT0, ZT4, ZT8, ZT12, ZT16, and ZT20) after normalization with *Tubb2a*/*Rplp1*. **(A)** The cosine curve adjusted for scattering points of *Cry1* relative gene expression revealed the presence of the rhythmicity in naïve (acrophase at ZT17.6, $p < 0.001$) and in epileptic conditions (acrophase at 16.4, $p < 0.05$), but the points in the early post-SE condition do not fit in a cosine curve, indicating no rhythmic expression throughout 24 h. **(B)** The same occurs for the *Cry2* gene; the relative gene expression showed the presence of the rhythmicity in

(Continued)

FIGURE 3 | naïve (acrophase at ZT17.6, $p < 0.05$) and in epileptic conditions (acrophase at 9.6, $p < 0.001$), but during the early post-SE, there is no rhythmic expression throughout 24 h. **(C)** *Bmal1* exhibits rhythmicity for all conditions—naïve, early post-SE and epileptic, although the acrophase phase shifted (acrophase at ZT2.0, $p < 0.001$, ZT1.2, $p < 0.01$, and ZT0, $p < 0.001$, respectively). **(D)** The *Clock* gene does not fit a cosine curve in any condition, revealing no circadian rhythmic expression. **(E)** For *Per1* gene, the relative gene expression showed the presence of the rhythmicity only in naïve (acrophase at ZT16, $p < 0.005$). **(F)** Relative gene expression for *Per2* gene showed the presence of the rhythmicity in naïve (acrophase at ZT0, $p < 0.001$). **(G)** *Per3* exhibit rhythmicity for naïve (acrophase at ZT14.8, $p < 0.005$) and early post-SE conditions (acrophase at ZT14.4, $p < 0.001$). Data are presented as mean ± SE per point. Statistical test for circadian analysis was done by Acrophase software.

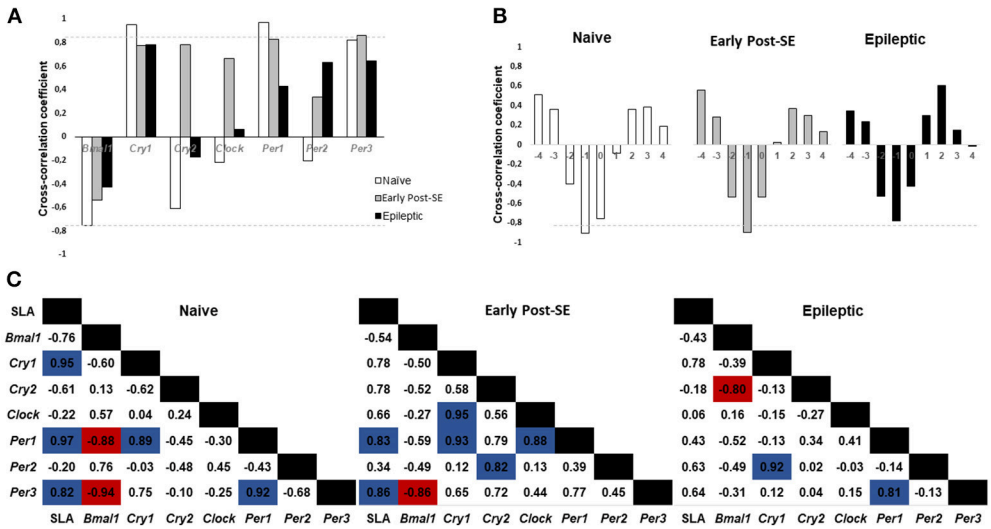

FIGURE 4 | Cross-correlation analysis between SLA and gene expression. **(A)** Histogram of Spontaneous Locomotor Activity (SLA) rhythm cross-correlation coefficient at lag 0 versus gene expression. Coefficients above 0.80 (gray dotted line) are considered highly correlated. The SLA rhythm is highly correlated with *Cry1*, *Per1,* and *Per3* circadian gene expression in naïve rats and with *Per1* and *Per3* during the early post-SE. In epileptic rats, the SLA rhythm does not show high correlation with any gene expression rhythm. **(B)** Cross-correlation analysis between *Bmal1* expression and SLA in different lags. Note that the highest (negative) correlation occurs at lag −1 and it is higher than 0.80 for naïve and early post-SE condition, but not for the epileptic condition. **(C)** Cross-correlation coefficients for the SLA rhythm and all gene expression. The positive correlations are highlighted in blue, and the negative ones are in red.

(0.89) and also between *Per1* and *Per3* (0.92) in this group. The *Bmal1* expression showed a negative correlation with the *Per1* and *Per3* expression (−0.88 and −0.94) since they are in antiphase (acrophases: *Bmal1* = ZT 2; *Per1* = ZT16 and *Per3* = ZT14.8) on the naïve group. In the early post-SE condition, some correlations were maintained, which include the SLA and *Per1* (0.83), SLA and *Per3* (0.86), *Cry1* and *Per1* (0.931), and *Bmal1* and *Per3* (−0.86). Additionally, there were three new correlations: *Cry1* and *Clock* (0.95), *Per1* and *Clock* (0.88) and *Per2* and *Cry2* (0.82). The association with *Clock* expression suggests the weakening of the rhythm, since *Clock* presents no rhythmic expression, as well as *Per2* and *Cry2* in the early post-SE period. Lastly, in the epileptic condition, the correlation between *Per1* and *Per3* returned (0.81). Despite losing the rhythm in this condition, the expression of these two genes presented the same pattern. The correlation between *Bmal1* and *Cry2* expression increased (−0.80), in as much as the *Cry2* rhythm return in antiphase with *Bmal1* expression (acrophases in ZT9.6 x ZT0). No high correlations were identified between gene expression in the hippocampus and SLA in the epileptic phase.

Differential Clock Expression Analysis in Post-SE Model of MTLE

To investigate if the overall expression of clock genes was dysregulated over SE-induced epileptogenesis in the hippocampus, we compared the transcript levels among epileptic, early post-SE and naïve conditions pooled from 6 different ZT (n = 5/ZT). The analysis of the mean gene expression (the mean from all ZTs) is required to verify the total gene expression variation throughout the epileptogenesis process, despite possible differences due to phase shifts. *Bmal1* and *Clock* transcripts were significantly decreased in the hippocampus of epileptic rats [$H_{(3)} = 10.52$, $p = 0.0052$, **Figure 5C** and $H_{(3)} = 18.39$, $p = 0.0001$, **Figure 5D**, respectively]. *Cry2* was progressively decreased over epileptogenesis [$H_{(3)} = 32.39$, $p < 0.0001$, **Figure 5B**], whereas *Cry1* and *Per1* increased in the early post-SE condition, and returned to normal levels in the epileptic condition [$H_{(3)} = 7.808$, $p = 0.0202$, **Figure 5A** and $H_{(3)} = 10.96$, $p = 0.0042$, **Figure 5E**, respectively]. *Per3* and *Per2* did not present significant differences among the groups (**Figure 5**).

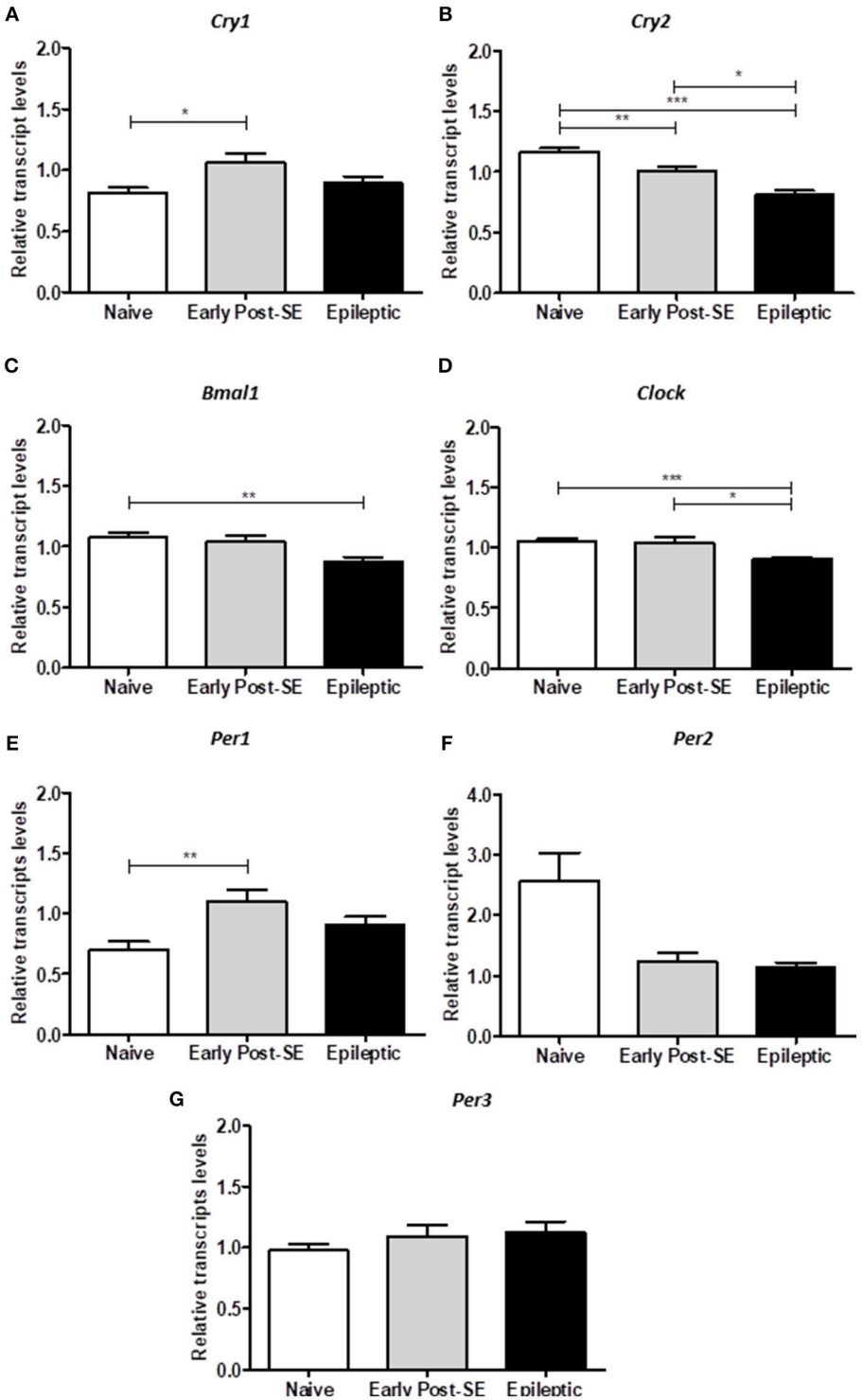

FIGURE 5 | Differential gene expression in the post-SE model. The computed mean ± SE for each condition are represented in these histograms. **(A)** The mean of *Cry1* transcripts are increased in the early post-SE condition, compared to naïve, but returns to basal levels in the epileptic condition. **(B)** The *Cry2* expression is gradually decreased over the epileptogenesis. **(C)** The *Bmal1* relative transcript levels are diminished in the epileptic animals, compared to naïve. **(D)** The total *Clock* expression is similar in naïve and early post-SE phases, but is reduced in the epileptic condition. **(E)** The mean of *Per1* transcripts are increased in the early post-SE condition, compared to naïve, but returns to basal levels in the epileptic condition. No differences were found in *Per2* **(F)** and *Per3* **(G)** expression levels. One way ANOVA, followed by Bonferroni's *post hoc*. $^{*}p < 0.05$, $^{**}p < 0.01$, and $^{***}p < 0.001$.

DISCUSSION

SLA

Considering that a few studies have examined the impact of SE on biological rhythms, our first objective was to evaluate the temporal pattern of SLA during epileptogenesis. Corroborating with the literature (56), we observed that: (i) the 24 h-oscillating SLA remains intact in post-SE groups, although the phase and the activity's amount change in early post-SE and epileptic conditions. (ii) Both light and dark phase SLA were increased after SE and remained elevated in the epileptic condition. (iii) The acrophase of the SLA rhythm was delayed during epileptogenesis. (iv) The SLA onset occurred earlier in epileptic animals. Our current findings complement these data by showing that epileptic rats present a more fragmented 24 h rhythmicity for SLA besides having an extended active phase (alpha) length and higher intracycle variability index, which was evidenced by a significant advance in activity onset followed by no changes on the activity's end time. Since they started the SLA earlier with a delayed acrophase, there was also a change in the phase angle.

It has been well documented that SE or limbic seizures do not abort the diurnal rhythm of SLA (27, 56), body temperature (57), and the EEG pattern (59). The EEG pattern is only transiently suppressed during a few days (2.9 ± 0.5 days) after PILO-induced SE (59). Besides, the phase shift (∼12 h) observed in the hippocampus electrical activity does not alter the 24 h period of the global rhythms in epileptic animals, including the core body temperature and theta state transitions (70). Our observation that both SE and SRS do not abolish the rhythmic oscillation of some core clock genes, such as *Bmal1*, *Cry*1, and *Cry2*, provides molecular support for the maintenance of circadian output during the epileptogenic processes. Indeed, the loss of *Bmal1* in mice results in SLA impairment, reducing the activity level and abolishing the circadian rhythmicity in constant darkness (71).

On the other hand, in TLE, some aspects of the rhythms are altered, as evidenced by the advances and delays in circadian rhythm temperature (CRT) (58) and the long-term changes in the diurnal SLA rhythm. Since the hippocampus is an important peripheral oscillator, it is possible that the remapping in the hippocampus circadian outputs in epileptic rats contribute to modulation of some diurnal rhythms. In fact, the phase advance of SLA may be related to the phase advance observed for *Bmal1* in the hippocampus. Also, astrocytes in conditional *Bmal1* knockout mice showed a significantly advanced SLA onset after constant darkness (72), which may correlate to the reduced levels observed for *Bmal1* in the hippocampus in our study, concomitant to an earlier SLA onset. The disrupted expression of *Per1*, *Per2,* and *Per3* found in the epileptic group and the rearrangements in the correlation patterns during epileptogenesis could also be related to the modifications observed for SLA during this condition, such as a more fragmented activity. In this regard, the lack of significant correlations between SLA and gene expression in the epileptic group may indicate an uncoupling process between peripheral, and the central oscillators in this condition occurred during the neuronal rearrangement of the early post-SE period.

The contribution of alterations in the hippocampus to SLA is likely linked to the activation of hippocampal–accumbens pathway after PILO-SE induction as demonstrated previously (56). Alternatively, the SRS could modulate SCN-related functions (73). Notwithstanding, it has been shown that there is no histological damage at the SCN, in the PILO-model of epilepsy (56), though there is no physiological or molecular rhythm study to provide the evaluation about the temporal cellular activity inside the SCN in this model. The causality of these associations, however, cannot be determined herein. Also, a higher temporal resolution in data series would be necessary to precise changes in phase advance/delay between oscillators.

Clock Genes in Early Post-SE and Epileptic Phases

The current study describes, for the first time, the effect of SE on the temporal transcriptional expression of seven core clock genes in post-*Status Epilepticus*-model of mTLE. A remarkable feature in clinical and experimental TLE is that the SRS follows a 24 h periodicity and the pattern persists in a constant darkness condition (27). However, the molecular mechanism underlying this phenomenon is yet to be uncovered (74). We observed that the 24 h rhythmicity of *Bmal1, Cry1,* and *Cry2* transcripts in the hippocampus is maintained in epileptic animals, although with phase changes. However, we did not identify rhythmic expression for *Per1, Per2,* and *Per3* in epileptic rats. We also confirmed our previous finding that the *Clock* gene expression in the hippocampus of naïve rats does not fit in a cosine curve (61). This noncyclic expression pattern is kept in early post-SE and epileptic conditions. Since rhythmic expression of core clock proteins following the transcription of clock genes is fundamental to sustain the Transcriptional Translational Feedback Loops (TTFLs), it is expected that clock proteins also present rhythmicity in our samples when the mRNAs are rhythmic. The activity of these clock genes in the normal hippocampus may be regulating morphological and physiological circadian changes in this structure, including dendritic patterning and spine density, neurogenesis, and long-term potentiation (75–79). On the other hand, the circadian products oscillation in an epileptic hippocampus may contribute to rhythmic variation in the epilepsy threshold, and generation of SRS in a temporal pattern. In fact, it has been shown that the daytime or dark/light conditions influence the susceptibility for seizure onset and severity (51–53, 80) as well as the anticonvulsant efficacy of antiepileptic drugs (81). Thus, the oscillatory gene can drive a circadian availability of molecular factors that act in the electrical activity of the brain, resulting in rhythmic fluctuation in neuronal excitability (23, 82). Accordingly, a recent study using large-scale approach, demonstrated a diurnal remapping of the circadian molecular landscape in the hippocampus of a mouse model of TLE [(60), preprint publication]. Interestingly, *mTOR* pathway activity which is increased in epileptic animals demonstrates

circadian oscillations (40, 83–86). Hepatic mTORC1 controls the daily levels of locomotor activity, body temperature, and lipid metabolism (84) and also show circadian activity (85–87). Furthermore, mTORC1 rhythmicity is controlled by the circadian molecular clock (85, 86). *Bmal1* negatively regulates mTORC1 signaling over a 24 h cycle by affecting the expression of *mtor* and *deptor* in the liver (86). An in-depth analysis of the temporal expression of these genes in the epileptic hippocampus and their potential time-dependent functional roles in the generation/maintenance of SRS in mTLE will be needed to comprehend better the function of these genes.

Regarding the pathogenesis of mTLE, SE-induced epileptogenesis cause alterations in several biological processes, such as gene expression, cell proliferation, dendritic plasticity, which are physiologically modulated by an endogenous circadian system (76, 77, 88). The current opinion is that these changes are related to compensatory mechanisms against the insult and/or to a series of epileptogenic processes that establish an epileptic state. In this study, we did not identify diurnal variation of *Cry1, Cry*2, *Per1,* and *Per2* mRNA expression during the early post-SE, whereas *Bmal1* presented an advanced acrophase. A phase advance was also demonstrated for *Cry1*, during the epileptic condition, while *Cry2* presented a phase delay, suggesting a dysregulation in the rhythm outputs of the biological processes occurring in this period. The confirmation and the consequences of this dysregulation on the epileptogenesis remain to be investigated. On the other hand, it is plausible that these oscillatory genes play functional roles in epileptogenic processes that are independent of circadian function. Indeed, CRY1 and CRY2 interact with nuclear receptors and modulate transcriptional activity (89). From this perspective, it is possible that diminished expression of *Cry2* and elevated expression of *Cry1* in the early post-SE phase may be involved in epileptogenicity, possibly due to its role in gene expression regulation. It is known that the epilepsy induced by pilocarpine reduces RORα mRNA and protein expression in the hippocampus of rats during the early post-SE phase (90). This variation can be the responsible for the *Cry*s rhythm expression's change during the early post-SE phase. Regarding *Cry1*, studies have shown that its functional role as a negative regulator of inflammatory processes (91). The reduced expression of *Cry1* key transcriptional targets lengthens the period of circadian molecular rhythms (92). In fact, the deletion of *Cry1* increases various proinflammatory cytokines, including IL-1β and TNF-α, through the NF-kB pathway (93). Furthermore, the overexpression of *Cry1* decreased the activation of TNF-α gene expression (94). Considering these, and the fact that TNF-α and other cytokines are elevated after SE, it is possible that the *Cry1* over-expression in the early post-SE condition is a compensatory anti-inflammatory activity. *Per1* up-regulation has also been seen upon depolarization *in vitro* or in epilepsy animal models, but its functional significance on epileptogenic process remains unclear (95).Thus, the exact role of the circadian oscillatory genes in the hippocampus remains unknown and functional assays will be important to disentangle the involvement of these clock genes on generation or maintenance of seizures.

In summary, the current study provides a systematic characterization of the temporal expression of *Bmal1*, *Clock*, *Cry1, Cry2, Per1, Per2, and Per3* transcripts and the SLA during SE-induced epileptogenesis. Our findings showed that although SLA circadian cycle is preserved in early post-SE and epileptic conditions, its circadian phase is changed and the rhythms were more fragmented in epileptic rats, suggesting that the phase coupling between the central and peripheral oscillators gets impaired by SRS. Additionally, we observed that *Bmal1* oscillation is intact in the early post-SE and epileptic phases, although with a phase advanced acrophase in the epileptic condition. *Cry1* and *Cry2* circadian oscillations were not detected in the early post-SE condition, which might be due to hippocampal reorganization. Nonetheless, the rhythmicity returns in the epileptic condition, also with phase shifts. These changes support the oscillation pattern of biological outputs emerged from the hippocampus after SE, including the 24 h periodicity in seizures. *Per1*, *Per2,* and *Per3,* however, lose the circadian rhythmicity in epileptic animals, aggravating the uncoupling between the oscillator and may contribute to epileptogenic processes independent of their circadian function. In general, the expressions of clock genes were significantly dysregulated during SE-induced epileptogenesis. There are some controversies regarding the relevance of the PILO-induced SE to human TLE (96, 97). Nonetheless, this animal prototype is widely used as it replicates the progression of multiple events observed in TLE. Hence, the findings of this animal model study are relevant for understanding the role of clock genes in epileptogenic processes and the development of chronic epilepsy after SE. Therefore, performing functional assays either by modulating the expression of the core clock genes in different stages of epileptogenesis or by inducing epilepsy in animals with a knockout of specific clock genes will be of great interest in future studies for addressing the specific role of individual clock genes epileptogenic processes.

AUTHOR CONTRIBUTIONS

HM, BK, WP, and DG performed the experiments and the analysis. DG, OC, and MD designed the experiments. DG, AS, BK, TdA, JL, and MK wrote the article.

FUNDING

Fundação de Amparo à Pesquisa do Estado de São Paulo (FAPESP); Conselho Nacional de Desenvolvimento Científico e Tecnológico (CNPq); Fundação de Amparo à Pesquisa do Estado de Alagoas (FAPEAL); Coordenação de Aperfeiçoamento de Pessoal de Nível Superior (CAPES). The funders had no role in study design, data collection and analysis, decision to publish, or preparation of the manuscript.

REFERENCES

1. Marques N, Menna-Barreto L (eds.). *Cronobiologia: Princípios e Aplicações*. São Paulo: Coleção Acadêmica (2005).
2. Refinetti R. *Circadian Physiology, 3rd Edn.* CRC Press; Boise State; University Idaho (2006).
3. Li J-D, Hu W-P, Zhou Q-Y. The circadian output signals from the suprachiasmatic nuclei. *Prog Brain Res.* (2012) 199:119–27. doi: 10.1016/B978-0-444-59427-3.00028-9
4. Coomans CP, Ramkisoensing A, Meijer JH. The suprachiasmatic nuclei as a seasonal clock. *Front Neuroendocrinol.* (2015) 37:29–42. doi: 10.1016/j.yfrne.2014.11.002
5. Lee C, Etchegaray JP, Cagampang FRA, Loudon ASI, Reppert SM. Posttranslational mechanisms regulate the mammalian circadian clock. *Cell* (2001) 107:855–67. doi: 10.1016/S0092-8674(01)00610-9
6. Lowrey PL, Takahashi JS. Genetics of circadian rhythms in mammalian model organisms. *Adv Genet.* (2011) 74:175–230. doi: 10.1016/B978-0-12-387690-4.00006-4
7. Shearman LP, Sriram S, Weaver DR, Maywood ES, Chaves I, Zheng B, et al. Interacting molecular loops in the mammalian circadian clock. *Science* (2000) 288:1013–9. doi: 10.1126/science.288.5468.1013
8. Reppert SM, Weaver DR. Coordination of circadian timing in mammals. *Nature* (2002) 418:935–41. doi: 10.1038/nature00965
9. Li S, Zhang L. Circadian control of global transcription. *Biomed Res Int.* (2015) 2015:1–8. doi: 10.1155/2015/187809
10. Mazzoccoli G, Pazienza V, Vinciguerra M. Clock genes and clock-controlled genes in the regulation of metabolic rhythms. *Chronobiol Int.* (2012) 29:227–51. doi: 10.3109/07420528.2012.658127
11. Focan C. Circadian rhythms and cancer chemotherapy. *Pharmacol Ther.* (1995) 67:1–52. doi: 10.1016/0163-7258(95)00009-6
12. Gupta MA, Simpson FC, Gupta AK. Psoriasis and sleep disorders: a systematic review. *Sleep Med Rev.* (2016) 29:63–75. doi: 10.1016/j.smrv.2015.09.003
13. Hofstra-Van Oostveen WA, De Weerd AW. Seizures, epilepsy, and circadian rhythms. *Sleep Med Clin.* (2012) 7:99–104. doi: 10.1016/j.jsmc.2011.12.005
14. Knutson KL, Van Cauter E. Associations between sleep loss and increased risk of obesity and diabetes. *Ann N Y Acad Sci.* (2008) 1129:287–304. doi: 10.1196/annals.1417.033
15. Li S, Wang Y, Wang F, Hu LF, Liu CF. A new perspective for Parkinson's disease: circadian rhythm. *Neurosci Bull.* (2017) 33:62–72. doi: 10.1007/s12264-016-0089-7
16. Monteleone P, Maj M. The circadian basis of mood disorders: recent developments and treatment implications. *Eur Neuropsychopharmacol.* (2008) 18:701–11. doi: 10.1016/j.euroneuro.2008.06.007
17. Mormont MC, Waterhouse J. Contribution of the rest–activity circadian rhythm to quality of life in cancer patients. *Chronobiol Int.* (2002) 19:313–23. doi: 10.1081/CBI-120002606
18. Roenneberg T, Merrow M. The circadian clock and human health. *Curr Biol.* (2016) 26:R432–R443. doi: 10.1016/j.cub.2016.04.011
19. Smolensky MH, Hermida RC, Reinberg A, Sackett-Lundeen L, Portaluppi F. Circadian disruption: New clinical perspective of disease pathology and basis for chronotherapeutic intervention. *Chronobiol Int.* (2016) 33:1101–19. doi: 10.1080/07420528.2016.1184678
20. Mirzoev A, Bercovici E, Stewart LS, Cortez MA, Snead OC, Desrocher M. Circadian profiles of focal epileptic seizures: a need for reappraisal. *Seizure* (2012) 21:412–6. doi: 10.1016/j.seizure.2012.03.014
21. Kaleyias J, Loddenkemper T, Vendrame M, Das R, Syed TU, Alexopoulos AV, et al. Sleep-wake patterns of seizures in children with lesional epilepsy. *Pediatr Neurol.* (2011) 45:109–13. doi: 10.1016/j.pediatrneurol.2011.03.006
22. Nzwalo H, Menezes Cordeiro I, Santos AC, Peralta R, Paiva T, Bentes C. 24-hour rhythmicity of seizures in refractory focal epilepsy. *Epilepsy Behav.* (2016) 55:75–8. doi: 10.1016/j.yebeh.2015.12.005
23. Matzen J, Buchheim K, Holtkamp M. Circadian dentate gyrus excitability in a rat model of temporal lobe epilepsy. *Exp Neurol.* (2012) 234:105–11. doi: 10.1016/j.expneurol.2011.12.029
24. Tchekalarova J, Pechlivanova D, Itzev D, Lazarov N, Markova P, Stoynev A. Diurnal rhythms of spontaneous recurrent seizures and behavioral alterations of Wistar and spontaneously hypertensive rats in the kainate model of epilepsy. *Epilepsy Behav.* (2010) 17:23–32. doi: 10.1016/j.yebeh.2009.11.001
25. Tchekalarova J, Pechlivanova D, Atanasova T, Markova P, Lozanov V, Stoynev A. Diurnal variations in depression-like behavior of Wistar and spontaneously hypertensive rats in the kainate model of temporal lobe epilepsy. *Epilepsy Behav.* (2011) 20:277–85. doi: 10.1016/j.yebeh.2010.12.021
26. Van Nieuwenhuyse B, Raedt R, Sprengers M, Dauwe I, Gadeyne S, Carrette E, et al. The systemic kainic acid rat model of temporal lobe epilepsy: Long-term EEG monitoring. *Brain Res.* (2015) 1627:1–11. doi: 10.1016/j.brainres.2015.08.016
27. Quigg M, Clayburn H, Straume M, Menaker M, Bertram EH. Effects of circadian regulation and rest-activity state on spontaneous seizures in a rat model of limbic epilepsy. *Epilepsia* (2000) 41:502–9. doi: 10.1016/j.biotechadv.2011.08.021.Secreted
28. Cavalheiro EA, Leite JP, Bortolotto ZA, Turski WA, Ikonomidou C, Turski L. Long-term effects of pilocarpine in rats: structural damage of the brain triggers kindling and spontaneous i recurrent seizures. *Epilepsia* (1991) 32:778–82. doi: 10.1111/j.1528-1157.1991.tb05533.x
29. Bertram EH, Cornett JF. The evolution of a rat model of chronic spontaneous limbic seizures. *Brain Res.* (1994) 661:157–62. doi: 10.1016/0006-8993(94)91192-4
30. Arida RM, Scorza FA, De Araujo Peres C, Cavalheiro EA. The course of untreated seizures in the pilocarpine model of epilepsy. *Epilepsy Res.* (1999) 34:99–107. doi: 10.1016/S0920-1211(98)00092-8
31. Bajorat R, Wilde M, Sellmann T, Kirschstein T, Köhling R. Seizure frequency in pilocarpine-treated rats is independent of circadian rhythm. *Epilepsia* (2011) 52:e118–22. doi: 10.1111/j.1528-1167.2011.03200.x
32. Coulter DA. Chronic epileptogenic cellular alterations in the limbic system after status epilepticus. *Epilepsia* (1999) 40(Suppl. 1):S23–41. doi: 10.1111/j.1528-1157.1999.tb00875.x
33. Curia G, Lucchi C, Vinet J, Gualtieri F, Marinelli C, Torsello A, et al. Pathophysiogenesis of mesial temporal lobe epilepsy: is prevention of damage antiepileptogenic? *Curr Med Chem.* (2014) 21:663–88. doi: 10.2174/09298673206613119152201
34. Engel T, Henshall DC. Apoptosis, Bcl-2 family proteins and caspases: The ABCs of seizure-damage and epileptogenesis? *Int J Physiol Pathophysiol Pharmacol.* (2009) 1:97–115
35. Gitaí DLG, Fachin AL, Mello SS, Elias CF, Bittencourt JC, Leite JP, et al. The non-coding RNA BC1 is down-regulated in the hippocampus of Wistar Audiogenic Rat (WAR) strain after audiogenic kindling. *Brain Res.* (2011) 1367:114–21. doi: 10.1016/j.brainres.2010.10.069
36. Meldrum B. Excitotoxicity and epileptic brain damage. *Epilepsy Res.* (1991) 10:55–61.
37. Pitkänen A, Lukasiuk K. Molecular and cellular basis of epileptogenesis in symptomatic epilepsy. *Epilepsy Behav.* (2009) 14:16–25. doi: 10.1016/j.yebeh.2008.09.023
38. Vezzani A, French J, Bartfai T, Baram TZ. The role of inflammation in epilepsy. *Nat Rev Neurol.* (2011) 7:31–40. doi: 10.1038/nrneurol.2010.178
39. Amir S, Harbour VL, Robinson B. Pinealectomy does not affect diurnal PER2 expression in the rat limbic forebrain. *Neurosci Lett.* (2006) 399:147–50. doi: 10.1016/j.neulet.2006.01.041
40. Lipton JO, Boyle LM, Yuan ED, Hochstrasser KJ, Chifamba FF, Nathan A, et al. Aberrant proteostasis of BMAL1 underlies circadian abnormalities in a paradigmatic mTOR-opathy. Cell Rep. (2017) 20:868–80. doi: 10.1016/j.celrep.2017.07.008
41. Shieh KR. Distribution of the rhythm-related genes rPERIOD1, rPERIOD2, and rCLOCK, in the rat brain. *Neuroscience* (2003) 118:831–43. doi: 10.1016/S0306-4522(03)00004-6
42. Smarr BL, Jennings KJ, Driscoll JR, Kriegsfeld LJ. A time to remember: The role of circadian clocks in learning and memory. *Behav Neurosci.* (2014) 128:283–303. doi: 10.1037/a0035963
43. Uz T, Ahmed R, Akhisaroglu M, Kurtuncu M, Imbesi M, Dirim Arslan A, et al. Effect of fluoxetine and cocaine on the expression of clock genes in the mouse hippocampus and striatum. *Neuroscience* (2005) 134:1309–16. doi: 10.1016/j.neuroscience.2005.05.003
44. Wakamatsu H, Yoshinobu Y, Aida R, Moriya T, Akiyama M, Shibata S. Restricted-feeding-induced anticipatory activity rhythm is associated with a phase-shift of the expression of mPer1 and mPer2 mRNA in the cerebral cortex and hippocampus but not in the suprachiasmatic nucleus of mice. *Eur J Neurosci.* (2001) 13:1190–6. doi: 10.1046/j.0953-816x.2001.01483.x

45. Pavlova MK, Shea SA, Bromfield EB. Day/night patterns of focal seizures. *Epilepsy Behav.* (2004) 5:44–9. doi: 10.1016/j.yebeh.2003.10.013
46. Pavlova MK, Shea SA, Scheer FAJL, Bromfield EB. Is there a circadian variation of epileptiform abnormalities in idiopathic generalized epilepsy? *Epilepsy Behav.* (2009) 16:461–7. doi: 10.1016/j.yebeh.2009.08.022
47. Quigg M, Straume M, Menaker M, Bertram IIIEH. Temporal distribution of partial seizures: comparison of an animal model with human partial epilepsy. *Ann Neurol.* (1998) 43:748–55. doi: 10.1002/ana.410430609
48. Xiang Y, Li ZX, Zhang DY, He ZG, Hu J, Xiang HB. Alteration of circadian rhythm during epileptogenesis: Implications for the suprachiasmatic nucleus circuits. *Int J Physiol Pathophysiol Pharmacol.* (2017) 9:64–8
49. Stewart LS, Leung LS. Hippocampal melatonin receptors modulate seizure threshold. *Epilepsia* (2005) 46:473–80. doi: 10.1111/j.0013-9580.2005.30204.x
50. Yehuda S, Mostofsky DI. Circadian effects of β-endorphin, melatonin, DSIP, and amphetamine on pentylenetetrazol-induced seizures. *Peptides* (1993) 14:203–5. doi: 10.1016/0196-9781(93)90030-K
51. Roberts AJ, Keith LD. Sensitivity of the circadian rhythm of kainic acid-induced convulsion susceptibility to manipulations of corticosterone levels and mineralocorticoid receptor binding. *Neuropharmacology* (1994) 33:1087–93. doi: 10.1016/0028-3908(94)90147-3
52. Weiss G, Lucero K, Fernandez M, Karnaze D, Castillo N. The effect of adrenalectomy on the circadian variation in the rate of kindled seizure development. *Brain Res.* (1993) 612:354–6. doi: 10.1016/0006-8993(93)91686-M
53. Stewart LS, Leung LS, Persinger MA. Diurnal variation in pilocarpine-induced generalized tonic-clonic seizure activity. *Epilepsy Res.* (2001) 44:207–12. doi: 10.1016/S0920-1211(01)00192-9
54. Gachon F, Fonjallaz P, Damiola F, Gos P, Kodama T, Zakany J, et al. The loss of circadian PAR bZip transcription factors results in epilepsy. *Genes Dev.* (2004) 18:1397–412. doi: 10.1101/gad.301404
55. Gerstner JR, Smith GG, Lenz O, Perron IJ, Buono RJ, Ferraro TN. BMAL1 controls the diurnal rhythm and set point for electrical seizure threshold in mice. *Front Syst Neurosci.* (2014) 8:121. doi: 10.3389/fnsys.2014.00121
56. Stewart LS, Leung LS. Temporal lobe seizures alter the amplitude and timing of rat behavioral rhythms. *Epilepsy Behav.* (2003) 4:153–60. doi: 10.1016/S1525-5050(03)00006-4
57. Quigg M, Clayburn H, Straume M, Menaker M, Bertram EH. Hypothalamic neuronal loss and altered circadian rhythm of temperature in a rat model of mesial temporal lobe epilepsy. *Epilepsia* (1999) 40:1688–96. doi: 10.1111/j.1528-1157.1999.tb01585.x
58. Quigg M, Straume M, Smith T, Menaker M, Bertram EH. Seizures induce phase shifts of rat circadian rhythms. *Brain Res.* (2001) 913:165–9. doi: 10.1016/S0006-8993(01)02780-9
59. Pitsch J, Becker AJ, Schoch S, Müller JA, de Curtis M, Gnatkovsky V. Circadian clustering of spontaneous epileptic seizures emerges after pilocarpine-induced status epilepticus. *Epilepsia* (2017) 58:1159–71. doi: 10.1111/epi.13795
60. Debski K, Ceglia N, Ghestem A, Ivanov A, Brancati GE, Broer S, et al. The circadian hippocampus and its reprogramming in epilepsy: impact for chronotherapeutics. *BioRxiv* [Preprint] (2017). doi: 10.1101/199372
61. Santos EAS, MarquesTEBS, De Carvalho Matos H, Leite JP, Garcia-Cairasco N, Pa-Larson ML, et al. Diurnal variation has effect on differential gene expression analysis in the hippocampus of the pilocarpine-induced model of mesial temporal lobe epilepsy. *PLoS ONE* (2015) 10:e141121. doi: 10.1371/journal.pone.0141121
62. Turski WA, Cavalheiro EA, Schwarz M, Czuczwar SJ, Kleinrok Z, Turski L. Limbic seizures produced by pilocarpine in rats: Behavioural, electroencephalographic and neuropathological study. *Behav Brain Res.* (1983) 9:315–35. doi: 10.1016/0166-4328(83)90136-5
63. Born JPL, Matos H, de C, De Araujo MA, Castro OW, Duzzioni M, Peixoto-Santos JE, et al. Using Postmortem hippocampi tissue can interfere with differential gene expression analysis of the epileptogenic process. *PLoS ONE* (2017) 12:e182765. doi: 10.1371/journal.pone.0182765
64. Racine RJ. Modification of seizure activity by electrical stimulation: II. *Motor Seizure Electroencephalogr Clin Neurophysiol.* (1972) 32:281–94. doi: 10.1016/0013-4694(72)90177-0
65. Marques TEBS, de Mendonça LR, Pereira MG, de Andrade TG, Garcia-Cairasco N, Paçó-Larson ML, et al. Validation of suitable reference genes for expression studies in different pilocarpine-induced models of mesial temporal lobe Epilepsy. *PLoS ONE* (2013) 8:e0071892. doi: 10.1371/journal.pone.0071892
66. Livak KJ, Schmittgen TD. Analysis of relative gene expression data using realtime quantitative PCR and the 2Δ ΔC T Method. *Methods* (2001) 25:402–8. doi: 10.1006/meth.2001.1262
67. Boone DR, Sell SL, Micci M-A, Crookshanks JM, Parsley M, Uchida T, et al. Traumatic brain injury-induced dysregulation of the circadian clock. *PLoS ONE* (2012) 7:e46204. doi: 10.1371/journal.pone.0046204
68. Kondratova AA, Dubrovsky YV, Antoch MP, Kondratov RV Circadian clock proteins control adaptation to novel environment and memory formation. *Aging* (2010) 2:285–97. doi: 10.18632/aging.100142
69. Vosko AM, Hagenauer MH, Hummer DL, Lee TM. Period gene expression in the diurnal degu (Octodon degus) differs from the nocturnal laboratory rat (Rattus norvegicus). *Am J Physiol Regul Integr Comp Physiol.* (2009) 296:R353–61. doi: 10.1152/ajpregu.90392.2008
70. Stanley DA, Talathi SS, Parekh MB, Cordiner DJ, Zhou J, Mareci TH, et al. Phase shift in the 24-hour rhythm of hippocampal EEG spiking activity in a rat model of temporal lobe epilepsy. *J Neurophysiol* (2013) 110:1070–86. doi: 10.1152/jn.00911.2012
71. Bunger MK, Wilsbacher LD, Moran SM, Clendenin C, Radcliffe LA, Hogenesch JB, et al. Mop3 is an essential component of the master circadian pacemaker in mammals. *Cell* (2000) 103:1009–17. doi: 10.1016/S0092-8674(00)00205-1
72. Barca-Mayo O, Pons-Espinal M, Follert P, Armirotti A, Berdondini L, De Pietri Tonelli D. Astrocyte deletion of Bmal1 alters daily locomotor activity and cognitive functions via GABA signalling. *Nat Commun.* (2017) 8:14336. doi: 10.1038/ncomms14336
73. Quigg M. Circadian rhythms: interactions with seizures and epilepsy. *Epilepsy Res.* (2000) 42:43–55. doi: 10.1016/S0920-1211(00)00157-1
74. Cho CH. Molecular mechanism of circadian rhythmicity of seizures in temporal lobe epilepsy. *Front Cell Neurosci.* (2012) 6:55. doi: 10.3389/fncel.2012.00055
75. O'Callaghan EK, Anderson ST, Moynagh PN, Coogan AN. Long-Lasting Effects of Sepsis on Circadian Rhythms in the Mouse. *PLoS ONE* (2012) 7:e47087. doi: 10.1371/journal.pone.0047087
76. Ikeno T, Weil ZM, Nelson RJ. Photoperiod affects the diurnal rhythm of hippocampal neuronal morphology of siberian hamsters. *Chronobiol Int.* (2013) 30:1089–100. doi: 10.3109/07420528.2013.800090
77. Ikeno T, Weil ZM, Nelson RJ. Timing of light pulses and photoperiod on the diurnal rhythm of hippocampal neuronal morphology of Siberian hamsters. *Neuroscience* (2014) 270:69–75. doi: 10.1016/j.neuroscience.2014.04.002
78. Tamai SI, Sanada K, Fukada Y. Time-of-day-dependent enhancement of adult neurogenesis in the hippocampus. *PLoS ONE* (2008) 3:e3835. doi: 10.1371/journal.pone.0003835
79. Chaudhury D, Wang LM, Colwell CS. Circadian regulation of hippocampal long-term potentiation. *J Biol Rhythms* (2005) 20:225–36. doi: 10.1177/0748730405276352
80. Golombek DA, Duque DF, De Brito Sánchez MG, Burin L, Cardinali DP. Time-dependent anticonvulsant activity of melatonin in hamsters. *Eur J Pharmacol.* (1992) 210:253–8. doi: 10.1016/0014-2999(92)90412-W
81. Khedhaie W, Dridi I, Aouam K, Ben-Attia M, Reinberg A, Boughattas NA. Circadian variation in anticonvulsant activity of valproic acid in mice. *Biomed Pharmacother.* (2017) 95:25–30. doi: 10.1016/J.BIOPHA.2017.08.047
82. Talathi SS, Hwang DU, Ditto WL, Mareci T, Sepulveda H, Spano M, et al. Circadian control of neural excitability in an animal model of temporal lobe epilepsy. *Neurosci Lett.* (2009) 455:145–9. doi: 10.1016/j.neulet.2009.03.057
83. Cao R, Robinson B, Xu H, Gkogkas C, Khoutorsky A, Alain T, et al. Translational control of entrainment and synchrony of the suprachiasmatic circadian Clock by mTOR/4E-BP1 signaling. *Neuron* (2013) 79:712–24. doi: 10.1016/j.neuron.2013.06.026
84. Cornu M, Oppliger W, Albert V, Robitaille AM, Trapani F, Quagliata L, et al. Hepatic mTORC1 controls locomotor activity, body temperature, and lipid metabolism through FGF21. *PNAS* (2014) 111:11592–9. doi: 10.1073/pnas.1412047111
85. Jouffe C, Cretenet G, Symul L, Martin E, Atger F, Naef F, et al. The circadian clock coordinates ribosome biogenesis. *PLoS Biol.* (2013) 11:e1001455. doi: 10.1371/journal.pbio.1001455

86. Khapre RV, Kondratova AA, Patel S, Dubrovsky Y, Wrobel M, Antoch MP, et al. BMAL1-dependent regulation of the mTOR signaling pathway delays aging. *Aging* (2014) 6:48–57. doi: 10.18632/aging.100633
87. Hatori M, Vollmers C, Zarrinpar A, DiTacchio L, Bushong EA, Gill S, et al. Time-restricted feeding without reducing caloric intake prevents metabolic diseases in mice fed a high-fat diet. *Cell Metab.* (2012) 15:848–60. doi: 10.1016/j.cmet.2012.04.019
88. Hood S, Amir S. Neurodegeneration and the circadian clock. *Front Aging Neurosci.* (2017) 9:e00170. doi: 10.3389/fnagi.2017.00170
89. Kriebs A, Jordan SD, Soto E, Henriksson E, Sandate CR, Vaughan ME, et al. Circadian repressors CRY1 and CRY2 broadly interact with nuclear receptors and modulate transcriptional activity. *Proc Natl Acad Sci USA.* (2017) 114:8776–81. doi: 10.1073/pnas.1704955114
90. Rocha AKA, de Lima E, Amaral FG, Peres R, Cipolla-Neto J, Amado, D. Pilocarpine-induced epilepsy alters the expression and daily variation of the nuclear receptor RORα in the hippocampus of rats. *Epilepsy Behav.* (2016) 55, 38–46. doi: 10.1016/j.yebeh.2015.11.026
91. Qin B, Deng Y. Overexpression of circadian clock protein cryptochrome (CRY) 1 alleviates sleep deprivation-induced vascular inflammation in a mouse model. *Immunol Lett.* (2015) 163:76–83. doi: 10.1016/j.imlet.2014.11.014
92. Patke A, Murphy PJ, Onat OE, Krieger AC, Özçelik T, Campbell SS, et al. Mutation of the human circadian clock gene CRY1 in familial delayed sleep phase disorder. *Cell* (2017) 169:203–15.e13. doi: 10.1016/j.cell.2017.03.027
93. Hashiramoto A, Yamane T, Tsumiyama K, Yoshida K, Komai K, Yamada H, et al. Mammalian clock gene Cryptochrome regulates arthritis via proinflammatory cytokine TNF-alpha. *J Immunol.* (2010) 184:1560–5. doi: 10.4049/jimmunol.0903284
94. Yang L, Chu Y, Wang L, Wang Y, Zhao X, He W, et al. Overexpression of CRY1 protects against the development of atherosclerosis via the TLR/NF-kB pathway. *Int Immunopharmacol.* (2015) 28:525–30. doi: 10.1016/j.intimp.2015.07.001
95. Eun B, Kim HJ, Kim SY, Kim TW, Hong ST, Choi KM, et al. Induction of Per1 expression following an experimentally induced epilepsy in the mouse hippocampus. *Neurosci Lett.* (2011) 498:110–3. doi: 10.1016/J.NEULET.2011.03.039
96. Furman M. seizure initiation and propagation in the pilocarpine rat model of temporal lobe epilepsy. *J Neurosci.* (2013) 33:16409–11. doi: 10.1523/JNEUROSCI.3687-13.2013
97. Gorter JA, van Vliet EA, Lopes da Silva FH. Which insights have we gained from the kindling and post-status epilepticus models? *J Neurosci Methods* (2016) 260:96–108. doi: 10.1016/j.jneumeth.2015.03.025

Conflict of Interest Statement: The authors declare that the research was conducted in the absence of any commercial or financial relationships that could be construed as a potential conflict of interest.

frontiers in Neurology

ORIGINAL RESEARCH
published: 22 March 2018
doi: 10.3389/fneur.2018.00172

Predictability and Resetting in a Case of Convulsive Status Epilepticus

*Timothy Hutson[1], Diana Pizarro[2], Sandipan Pati[2] and Leon D. Iasemidis[1]**

[1] Department of Biomedical Engineering, Louisiana Tech University, Ruston, LA, United States, [2] Department of Neurology, University of Alabama at Birmingham, Birmingham, AL, United States

In this case study, we present evidence of resetting of brain dynamics following convulsive status epilepticus (SE) that was treated successfully with antiepileptic medications (AEDs). The measure of effective inflow (EI), a novel measure of network connectivity, was applied to the continuously recorded multichannel intracranial stereoelectroencephalographic (SEEG) signals before, during and after SE. Results from this analysis indicate trends of progressive reduction of EI over hours up to the onset of SE, mainly at sites of the epileptogenic focus with reversal of those trends upon successful treatment of SE by AEDs. The proposed analytical framework is promising for elucidation of the pathology of neuronal network dynamics that could lead to SE, evaluation of the efficacy of SE treatment strategies, as well as the development of biomarkers for susceptibility to SE.

OPEN ACCESS

Edited by:
Batool F. Kirmani, Texas A&M University College Station, United States

Reviewed by:
Satish Agadi, National Neurological Institute, United States
Olagide Wagner Castro, Federal University of Alagoas, Brazil

***Correspondence:**
Leon D. Iasemidis
leonidas@latech.edu

Specialty section:
This article was submitted to Epilepsy, a section of the journal Frontiers in Neurology

Received: *11 October 2017*
Accepted: *06 March 2018*
Published: *22 March 2018*

Citation:
Hutson T, Pizarro D, Pati S and Iasemidis LD (2018) Predictability and Resetting in a Case of Convulsive Status Epilepticus. Front. Neurol. 9:172. doi: 10.3389/fneur.2018.00172

Keywords: status epilepticus, pathological dynamics, predictability, resetting, network connectivity

INTRODUCTION

Status epilepticus (SE) is a life-threatening neurological and medical emergency seen commonly at tertiary care epilepsy centers (1, 2). SE is characterized by recurrent epileptic seizures without recovery of normal brain function between seizures or continuous seizure activity lasting long enough to produce a fixed and enduring condition (3, 4). Out of the 200,000 cases of SE diagnosed each year in the USA, the short-term (30 days) mortality rate reported in the adults ranges between 15 and 30% (2, 5). Although the disease has been reported as early as 718 BC (6), progress in developing new therapy has been slow as the underlying pathophysiological mechanism is poorly understood. Unlike seizures that can self-terminate within minutes, the neural condition of SE can self-perpetuate and self-sustain over hours to days. Both preclinical and clinical studies have demonstrated that seizures that are provoked by infection or induced by stimulants can transition to SE if the initial insult is removed, even in subjects without a known history of epilepsy (7–11). In convulsive SE, the recorded electroencephalographic (EEG) activity of the brain progresses through five visually distinguishable sequential stages that are characterized well in preclinical studies and have also been reported in patients (12, 13). All these studies suggest that SE may not be a continuum of multiple seizures but rather a distinct entity with its own underlying mechanisms.

Over the past two decades, our group as well as other researchers have demonstrated that quantitative analysis of EEG helps characterize parts of the transition of the epileptic brain into SE, namely the interictal (away from seizures), preictal (before seizures), ictal (during seizures), and postictal (after seizures) states (14–17). This analysis not only provides insight into the spatiotemporal dynamics of the epileptic brain but can impact clinical care by allowing long-term prediction of seizures and SE (18–22), as well as interictal localization of the epileptogenic focus (23, 24). By advanced analysis of scalp and intracranial EEG within the framework of nonlinear dynamics, our group first discovered that the epileptogenic focus (zone) progressively, over minutes to hours, entrains normal brain sites into a pathological state of reduced rate of information processing that could mathematically, and thus objectively, help determine preictal periods [see (20) and references therein]. Following

self-termination of seizure, there is a postictal disentrainment of the brain sites that were entrained preictally with the epileptogenic focus. We have called this phenomenon of progressive preictal entrainment and postictal disentrainment resetting of the pathology of brain dynamics (25–27). Such a functional role of seizures constitutes a new way of looking into epilepsy as a dynamical disorder and could lead to the development of innovative treatments for epilepsy. Based on these findings, we postulated that (a) subjects can transition to SE if seizures fail to reset the pathology of preictal brain dynamics and (b) successful treatment of SE may help reset this developed pathology of brain dynamics.

In the SE case we herein study, the above postulates seem to be supported. We analyzed for the first time a unique record of SE: a 24-h intracranial, high-density (94 channels) and high sampling frequency (1 kHz), stereoelectroencephalographic (SEEG) recording from a patient long before, during, and long after a 3-h SE episode that he survived. We provide evidence that this patient transitioned to SE after seizures failed to reset the preceding abnormal spatiotemporal dynamics of the focus with the rest of the brain, and that successful treatment of SE reset this pathology. Novel measures of brain dynamics were employed to quantify the route into and out of SE in this patient. The proposed analytical framework and the developed measures shed light on the physiological mechanisms of SE, are promising for evaluation of susceptibility to SE, as well as the evaluation of efficacy of SE treatments and the development of future treatment strategies for SE.

MATERIALS AND METHODS

SEEG Data

A 27-year-old, right-handed male with known medically refractory focal epilepsy that started when he was 14 years old. His epilepsy risk factor included febrile seizures with spinal meningitis during childhood (6 months old) that resolved when he was 1 year old. He was experiencing three seizure subtypes: (1) focal onset seizures without loss of awareness (previously called simple partial) (28) where he reported déjà vu, increased anxiety lasting 10–30 s with frequency 20 per day; (2) focal onset seizures with impaired awareness (previously called complex partial), lip and manual automatism lasting 2–3 min at a frequency of 1–2 times every week; and (3) focal to bilateral tonic–clonic seizures 1–2 times per year. His MRI brain was non-lesional, but 18-fluoro-2-deoxyglucose (18F-FDG) PET-imaged showed right temporal (mesial and lateral) hypometabolism. After scalp EEG monitoring, he underwent right anterior temporal lobectomy at an outside hospital when he was 21 years old. He was seizure free for first 6 months, but all his seizure subtypes gradually returned and progressively increased in frequency. He was then reevaluated for possible second epilepsy surgery at our level-IV epilepsy center (University of Alabama at Birmingham).

The patient underwent SEEG monitoring with depth electrodes implanted in the right anterior and posterior insula, right basal temporal, right anterior and posterior orbitofrontal, a remnant of right mesial temporal structures, posterior and superior temporal gyrus. The superior temporal depth electrode was extended medially to include ventrolateral thalamus. Overall, eight depth electrodes with a total of 96 contacts (i.e., 96 channels) were sampled at 1 kHz with a Natus Xltek EEG machine (see the electrode montage in **Figure 1**).

During his stay in the epilepsy monitoring unit (EMU), his home antiepileptic (AED) medications (clonazepam, calproic acid, oxcarbazepine) were gradually weaned off. Within days after weaning off medications, electroclinical seizures, and subsequently a prolonged (lasting over 3 h) SE was recorded. The SE was of focal onset around the remnant of previously resected mesial temporal structure, progressed gradually to involve insula,

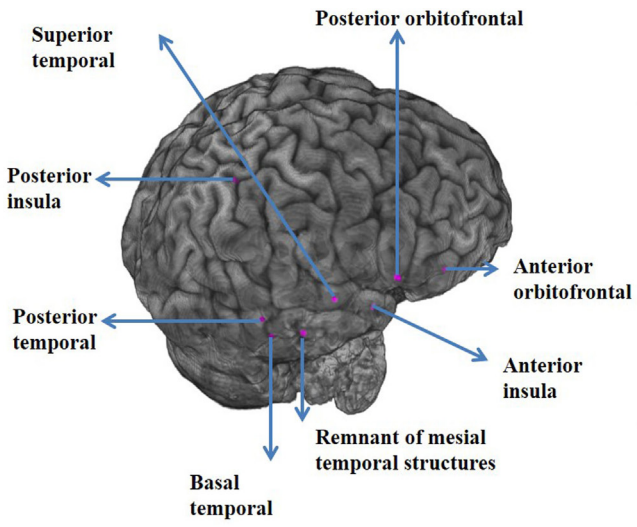

Electrode Montage	
El No.	**Brain Region**
1-8	Remnant of Mesial Temporal Structures
9-20	Posterior Temporal
21-32	Anterior OrbitoFrontal
33-46	Posterior OrbitoFrontal
46-62	Posterior Insula
63-70	Anterior Insula
71-82	Basal Temporal
83-96	Superior Temporal

FIGURE 1 | Left panel: Postoperative CT scan merged with preoperative MRI shows the location of the stereoelectroencephalographic electrodes in the right temporal and orbitofrontal structures for patient PT1. Right panel: Table with the electrode contact numbers and the corresponding eight brain regions the electrodes were implanted in.

lateral temporal structures, and orbitofrontal. The SE spread to the thalamus in the second half of the SE.

Before the onset of SE, patient was awake and alert. The patient initially had no definite clinical correlates which subsequently progressed to bilateral tonic–clonic activities. Throughout the SE, patient was examined periodically by the nurse and EEG technician in the EMU. Examination included assessment of speech (by asking to read a sign board), awareness (by asking about time, place), motor response (by asking to grab a pen), and asking the patient to self-report his feelings during the event. Patient had fluctuating consciousness in the first half of the SE but was lethargic, confused, and had minimal motor response toward the end. Immediately after SE, patient was not oriented to time or place but had appropriate motor response and had no aphasia.

The SE was successfully managed by parenteral valproic acid and two doses of lorazepam. The patient eventually underwent a large resection of temporal lobe structures that included the remnant hippocampus, superior temporal gyrus, and anterior insula [these structures were clinically identified as the seizure onset zone (SOZ)]. Eighteen months postresection the patient is seizure free (Engel's class I) and remains on AED medication.

Histopathology confirmed chronic neuronal loss, the presence of dysmorphic neurons and extensive gliosis. In particular, immunohistochemical stains for GFAP, neurofilament protein (NFP), and Neu-N neuronal marker were performed on all the tissue blocks. GFAP staining showed mild gliosis in middle temporal gyrus, moderate gliosis in superior temporal gyrus, and marked gliosis in residual hippocampus. Neu-N staining showed mild neuronal losses in hippocampus, middle and superior temporal gyrus. Staining for hyperphosphorylated NFP showed no neuronal somatic staining in middle temporal gyrus, occasional positive cortical cells in superior temporal gyrus, and also a few scattered positive neuronal cells in hippocampus. Appropriate staining was seen in the positive and negative controls. The margin of superior temporal gyrus and the remnant of right hippocampus showed dysmorphic neurons. Anterior insula and margin of middle temporal gyrus showed chronic neuronal loss and astrogliosis.

A 24-h portion of the SEEG (starting 12 h before the onset of SE) was stored and made available for retrospective mathematical analysis. This retrospective case study had institutional IRB approval from the University of Alabama at Birmingham.

Energy Measure

We employed the Teager Energy (TE) operator (29, 30) to estimate the energy of the SEEG and detect occurring seizures. TE has been used widely for seizure detection, solely or in combination with other measures of EEG characteristics (31–33). TE was applied to band-pass (5–15 Hz) filtered 60 s, non-overlapping consecutive SEEG segments over the duration of the available recording per channel. TE was estimated by:

$$\mathrm{TE}(i) = x^2(i) - x(i-1)\cdot x(i+1), \tag{1}$$

where $x(i)$ is the amplitude of the SEEG signal at time point i. With a sampling frequency of 1 kHz, 60,000 TE(i) values were produced for every 60 s SEEG segment. Then, the median ($\mathrm{TE}_{\mathrm{med}}$) of those TE values was estimated per 60 s segment generating a $\mathrm{TE}_{\mathrm{med}}$ temporal profile per electrode site every 60 s. Finally, averaging the $\mathrm{TE}_{\mathrm{med}}$ profiles across electrodes (spatial averaging) generated the $\mathrm{TE}_{\mathrm{global}}$ energy profile. We herein employed the $\mathrm{TE}_{\mathrm{global}}$ measure as a tool for detection of seizures and SE from the SEEG.

Local Effective Information Inflow Measure

We employed a recently proposed measure of the directional inflow of information a node is experiencing from its communication with the rest of the nodes in the network, the measure of the total effective inflow (TEI) of information. The TEI is estimated from the generalized partial direct coherence (GPDC) that measures the directed (causal) interactions between nodes in a network based on the principle of Granger's causality (23, 24). We have shown that GPDC outperforms many traditional measures of directed interactions in the frequency domain [e.g., partial coherence, directed coherence, partial directed coherence (PDC), normalized PDC, directed transfer function (DTF), normalized DTF] when the question of localization of the epileptogenic focus is addressed (see (23) and references therein). In particular, from such an analysis of interictal intracranial EEG recordings (23) and interictal magnetoencephalographic (MEG) recordings in respective groups of patients with focal epilepsy (24), we have found that the epileptogenic focus can be accurately localized as the region that most frequently receives the maximum effective inflow (TEI) from other brain regions in the interictal period. We briefly describe our methodology below.

A multivariate autoregressive model $\boldsymbol{X}(t) = \sum_{\tau=1}^{p} \boldsymbol{A}(\tau)\boldsymbol{X}(t-\tau) + \boldsymbol{\epsilon}(t)$, of order $\boldsymbol{p} = 7$ and dimension of vector $\boldsymbol{X}$ equal to 96, was fit to each of 60 s successive, non-overlapping SEEG segments over the available 24-h SEEG recording from our patient. Components of the vectors $\boldsymbol{X}$ were the values of SEEG from each of the 96 electrodes at every time point t. The coefficients $\boldsymbol{A}$ (7, 96) of the model were estimated *via* the Vieira-Morf partial correlation method. The GPDC value from site j to site i was estimated by:

$$\mathrm{GPDC}_{j\to i}(f) = \frac{\left|\boldsymbol{B}_{ij}(f)\right| / \sigma_{ii}}{\sqrt{\sum_{k=1}^{n}\left|\boldsymbol{B}_{kj}(f)\right|^2 / \sigma_{kk}^2}}, \tag{2}$$

where $\boldsymbol{B}(f) = \boldsymbol{I} - \sum_{k=1}^{p}\boldsymbol{A}(\tau)e^{-i2\pi f\tau}$, and σ_{ii} is the standard deviation of the generated fitting error from the model at each site i. Then, $\sum_{j=1, j\neq i}^{n} GPDC_{j\to i}(f)$ measures the effective information inflow ($\mathrm{EI}_i(f)$) to each site i from the rest $(n-1)$ of the recording sites at each frequency f with resolution of 1 Hz. The $\mathrm{EI}_i(f)$ values were then averaged over all frequencies in each of three spectral bands: 0.1–50 Hz [low frequency band (LFB)], 70–110 Hz [high frequency band (HFB)], and 130–170 Hz [ultrahigh frequency band (UFB)] producing the TEI_i values per electrode site i within specific spectral bands. TEI_i has been proven extremely valuable in localization of the epileptogenic focus from interictal periods (23).

Global EI and Local EIs

To characterize the brain's global dynamics through SE, the TEI_i measures of connectivity were averaged across all 96 electrode sites for each 60 s SEEG segment, and the TEI_{mean} (mean) and TEIσ temporal profiles were then calculated every 60 s.

To illustrate the relation over time of the effective local inflow per site versus the effective global inflow, we divided the values of each site's TEI_i by the values of TEI_{mean} within each 60 s SEEG segment, thus creating a normalized $TEI_{i,norm}$ profile over time per site *i*. In order to also gain a better insight into the relative position of each site's TEI_i values compared to the ones at other sites, we ranked the TEI_i values of the $n = 96$ individual sites within each 60 s SEEG segment and plotted the rank of each site *i* over time ($TEI_{i,rank}$ profiles).

RESULTS

We analyzed a 24-h 96 channel SEEG recording from a patient who had SE while at the EMU and survived following successful treatment with antiepileptic medications. The recording included 8-h pre-SE, 3-h SE, and 13-h post-SE SEEG. Portions of the electroencephalographic manifestation of SE in this patient are shown in **Figure 2**.

Detection of SE by Energy measure

The TE values per electrode were averaged across all electrode sites over time and the global Teager energy (TE_{global}) profile was estimated from the available 24 h SEEG record and is depicted in **Figure 3**. About 1 h before the development of SE, the patient had one clinical seizure that was well captured by the occurrence of a prominent (well above the background) peak in the global TE (black arrow in **Figure 3**). At the onset of SE, and during its 3 h duration, TE_{global} values became prominent again and stayed elevated until the end of the medical interventions (magenta arrows in the figure), after which TE_{global} abruptly assumed low, but still a bit greater than its pre-SE, values over hours (recovery period). Two points are worth noting here: (a) the resetting of TE_{global} values occurred at the end of the medical interventions, that is, about 1 h prior to the clinically assessed end of SE (green arrow). This raises the possibility for use of TE_{global} as an early biomarker of the effectiveness of the administered treatment of SE; (b) the post-SE values of TE_{global} remained elevated compared to its pre-SE values over hours, at least till the end of this recording. This raises the possibility of using the difference between pre and post-SE values of TE_{global} to objectively measure the duration of the recovery period for patients with SE. Finally, it is noteworthy that no pre-SE trends were captured by the TE profiles, that is, issue of warnings for an upcoming SE based on TE_{global} would not have been possible.

Dynamics of the SE Transition by Information Flow Profiles

The TEI profiles and their spatial average (TEI_{mean}) and standard deviation (TEIσ) were also estimated over the available 24 h SEEG record and over three different frequency bands: LFB = 0.1–50 Hz, HFB = 70–110 Hz, and UFB = 130–170 Hz. The TEI_{mean} profiles are shown in the left and the TEIσ profiles in the right panels of **Figure 4**. The TEI_{mean} profiles from LFB and UFB showed a progressively decreasing trend in values up to the onset of SE (red vertical line) with a reverse (increasing) trend thereafter and a further abrupt increase to a higher and steady level post-SE about 1 h after the onset of clinically assessed patient's recovery (green vertical line). The TEI_{mean} profile from the HFB showed a similarly progressive decrease in values pre-SE almost up to the onset of the pre-SE clinical seizure, with resetting of this trend thereafter to high values during SE and an abrupt further increase in values to

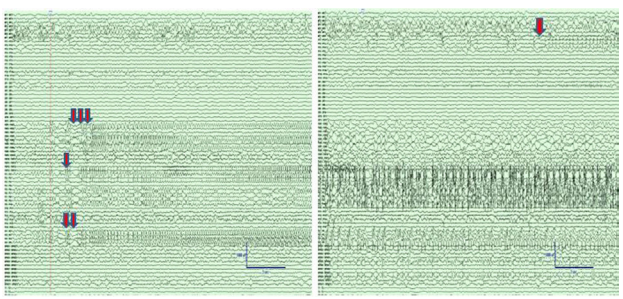

FIGURE 2 | Left panel: Intracranial electroencephalographic (EEG) recording from patient PT1 at the onset of status epilepticus (SE) in the mid insular electrodes (one red arrow) and anterior insular electrodes (two red arrows) followed by propagation to superior temporal gyrus (STG) and orbitofrontal regions (three red arrows). Right panel: Intracranial EEG recording 5 min after the onset of SE with continuous seizure activity in insula and STG, and the onset of spread to the middle temporal gyrus (orange arrow). The EEG records are illustrated with a 10 mm/s time base, sensitivity 50 μV/mm, and filtered between 1 and 100 Hz.

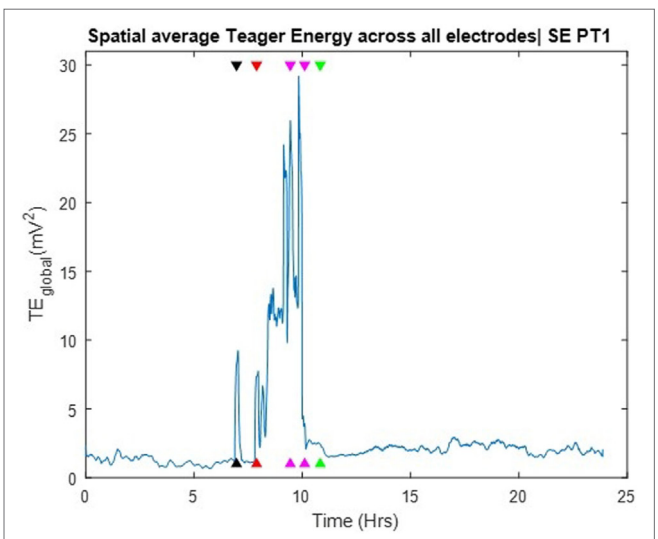

FIGURE 3 | Spatial average of Teager energy across brain sites (TE_{global}) over the entire 24 h iEEG recording from PT1. The black arrow, about 7 h into the recording, indicate the timing of a pre-status epilepticus (pre-SE) clinical seizure; the red arrow indicate the onset of SE; the magenda arrows indicate the times of the administered anti-SE medical intervention; the green arrow indicate the clinically assessed onset of recovery from SE. TE_{global} attains high values at the occurrence of the pre-SE clinical seizure as well as at the onset and during most of SE.

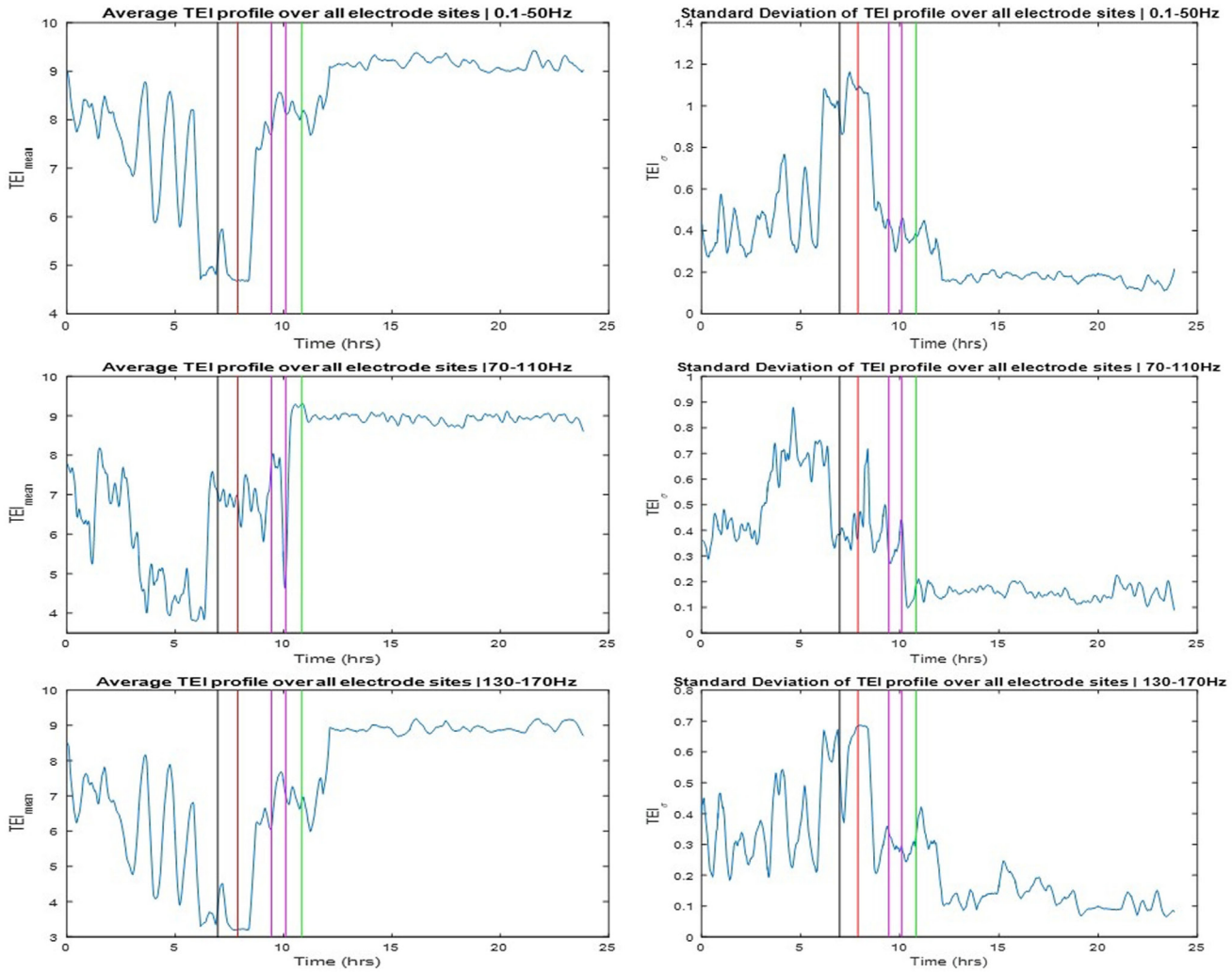

FIGURE 4 | Left panels: Averaged total effective inflow (TEI) values across brain sites over time (TEI_{mean} profiles) for three frequency bands (low frequency band top, high frequency band middle, and ultrahigh frequency band bottom panels—see text for more details). Right panels: Standard deviation of TEI values across brain sites over time (TEIσ profiles) for the same frequency bands. Color coding of the vertical lines same as the one for the arrows in **Figure 3**.

a steady higher level right after the administration of the anti-SE AED regiment (magenda lines). It is noteworthy that it was not until approximately 1 h after SE's end that TEI_{mean} values attained their maximum value in all frequency bands. It is also noteworthy that the variance in TEI values (TEIσ) in all frequency bands (illustrated in the right panels of **Figure 4**) is higher pre-SE than post-SE, implying the existence of a much more unstable pre-SE state compared to the post-SE state. Finally, it is also noteworthy, from all frequency bands, that a couple of hours after onset of patient's recovery and assuming resetting of the pathology of dynamics: (a) the TEI_{mean} obtains its highest values, that is, even higher values than the ones 8 h before the onset of SE, implying that the observed downward trend of TEI_{mean} values and the route to SE may have started even earlier than the beginning of the recording and (b) the TEIσ obtains its lowest values, that is, even lower values than the ones 8 h before the onset of SE, again implying that instabilities and the route to SE may have started even earlier than the beginning of this recording.

The SOZ of this patient was determined in a multidisciplinary patient management conference taking in consideration input from several recording modalities including EEG. We labeled electrodes within the SOZ as focal while all the rest as non-focal and examined the relation of the TEI over time between focal and non-focal sites as well as between each individual site and the spatial average (global) flow. Toward this goal, we estimated the ranking of TE values over time ($TEI_{i,rank}$) at one site i versus the rest of the sites, and the normalized TE values over time at one site i with respect to the global TE value ($TEI_{i,norm}$). In **Figure 5**, we show the $TEI_{i,norm}$ profiles (left panels) and the $TEI_{i,rank}$ (right panels) at one focal and one non-focal site. The focal site was within the mesial temporal region, the non-focal site in the posterior orbital frontal and the TE values were estimated in the three frequency bands (LFB, HFB, and UFB). From the left panels of **Figure 5**, and concentrating on the trends over time of TEI at the focal site with respect to the global EI (focal TEI_{norm} profile), we see that the focal TEI_{norm} values were less than 1 (and hence

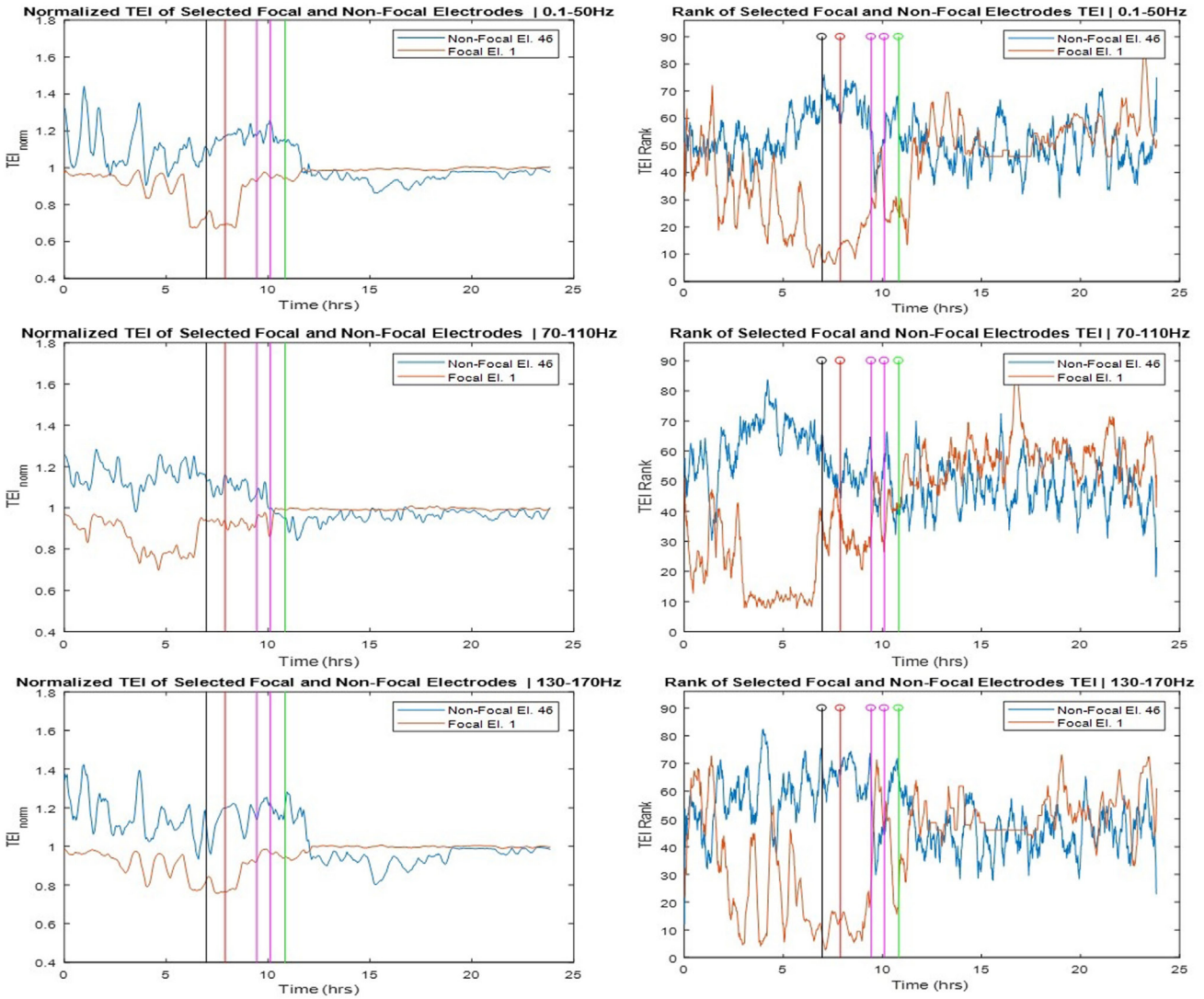

FIGURE 5 | Left panels: Normalized total effective inflow (TEI_{norm}) profiles over time at one focal (Elec. 1) and one non-focal (Elec. 46) brain site for three frequency bands (low frequency band top, high frequency band middle, and ultrahigh frequency band bottom panels—see text for more details). Right panels: Rank of the focal and non-focal electrode in terms of their TEI_{norm} values over time for the same three frequency bands.

less than the global TEI values) over the whole pre-SE period (7 h) with this difference increasing dramatically as the onset of SE approaches. After onset of SE, this difference starts to decrease and attains values close to 1 (i.e., focal site inflow approximating the global inflow values) in the post-SE period. The administration of AEDs may have assisted with this increase of the focal inflow. Also from **Figure 5**, we observe that the trend over time of TEI at the non-focal site with respect to the effective global inflow is opposite from the one at the focal site. If we compare the TEI profiles of the focal and non-focal sites, it is evident that: (a) the EI at the focal site is increasingly becoming smaller than the one at the non-focal site as SE approaches (more evident in LFB) and (b) this difference is reversed post-SE.

The corresponding rank (TEI_{rank}) profiles of TEI at the focal and non-focal sites are illustrated in the right panels of **Figure 5** and reinforce our observations from the left panels. The rank of the TEI at the focal site drops from about 50 (out of a total of 96) 7 h pre-SE to 10 at the onset of SE and back to 50 post-SE. The rank of the TEI at the non-focal site shows the opposite behavior over time especially in HFB. It is noteworthy that the pre-SE difference between the ranks of TEI at the focal and non-focal sites is reversed post-SE. This resetting is most prominent in the UFB, in which TEI at the focal site is larger than the TEI at the non-focal site (rank of 60 versus 50, respectively) at the beginning of the recording, this trend is reversed within 1.5 h into the recording en route to SE, and reversed again post-SE.

DISCUSSION

In this case study, we applied novel measures of information flow from analysis of multivariate complex networks in the frequency domain for the study of the transition of the epileptic brain to and

out of SE. We employed these measures to analyze the recorded intracranial electrical activity (SEEG) over a 24-h period from a patient who experienced SE and recovered. Using this analytical framework, we provided evidence that the route to SE involved the change of the spatial distribution of the EI of information globally, as well as locally between focal and non-focal sites. In particular, the global TEI measure showed a progressive reduction in its average and increase of its variance across brain sites over hours before the onset of SE, and resetting to its interictal high average and low variance values after the end of SE following the successful anti-SE treatment (**Figure 4**). Our subsequent analysis at the local level, in terms of TEI profiles at focal and non-focal sites, showed a progressive pre-SE reduction and post-SE resetting mainly at the focal sites, with a pre-SE gap in TEI values between focal and non-focal sites being more evident in the 70–110 Hz frequency band.

The above results, taken cumulatively, suggest that it may be possible to develop TEI-based biomarkers of an impending SE episode, as well as provide feedback on the progress of recovery of a patient in SE. Optimization of the employed frequency band toward this goal would then be necessary, as well as optimization of which and how many focal and non-focal sites to be followed over time. Also, due to the evidence we herein provided that the route to SE may start hours before its clinical onset, longer SEEG recordings before the SE onset may provide additional insight in the physiological mechanisms that lead to SE.

Epilepsy is a chronic neurological disorder believed to be due to existing imbalance between excitation and inhibition in brain's neural circuit (34, 35). However, static changes within the neural circuit fail to explain the intermittency of seizures as well as the *de novo* SE (i.e., SE occurrence in patients without prior known epilepsy). We have conceptualized in the past that effective feedback to seizure focus from other brain sites may keep the focus under control and allow the epileptic brain to operate more normally interictally (36). Failure of this control mechanism preictally can be detected as a progressive decrease of inflow of information to epileptogenic focal sites allowing them to export their destabilizing signals to the rest of the brain, eventually leading to seizures. The seizures reset this pathology of dynamics by reestablishing the internal feedback control, possibly by ictal release of suitable neurochemical agents. In this study, using GPDC, a measure of directed information flow in coupled networks (23), we showed for the first time that this hypothesis might be true in SE too. In particular, we provided evidence that progressive decrease in EI to the focus characterizes the transition from interictal period to SE and that successful administration of anti-SE AEDs reestablishes the EI to the focus.

Finally, this study was performed on rarely available SEEG data from a patient who underwent SE while at the EMU with implanted EEG electrodes (phase II recording) and needs to be replicated in a larger cohort of patients for further validation. Interinstitutional collaboration to this end would help.

CONCLUSION

We provided evidence that transition to SE could be preceded by a gradual, over hours, development of pathology in spatiotemporal dynamics of brain's electrical activity underlined by the interplay of the epileptogenic focus and controlling normal brain sites, and that successful treatment of SE resets this pathology of brain dynamics. Novel measures of brain dynamics from network analysis in the frequency domain can shed light on this transition and are thus also promising in the evaluation of susceptibility to SE, efficacy of current treatment of SE, and development of future treatment strategies for SE.

ETHICS STATEMENT

Data analysis was performed retrospectively using the EEG that was obtained for clinical reason. The study has approval from the institutional review board (UAB) to perform analysis and publish de-identified data. The patient informed consent is waived in these cases by UAB IRB. There is a collaboration agreement between the two institutes (UAB Epilepsy and Louisiana Tech) for sharing of de-identified patient data and publishing.

AUTHOR CONTRIBUTIONS

DP acquired the SEEG data for this study under the supervision of SP. TH performed the analysis of the data under the supervision of LI. All authors contributed equally to the writing of this article.

ACKNOWLEDGMENTS

We would like to acknowledge Dr. Bharat Karumuri and Mr. Omar Alamoudi in Dr. Iasemidis' Brain Dynamics Laboratory at Louisiana Tech University for assisting with modifications of the in-house developed GPDC code and its use in the conduct of this study.

FUNDING

We would like to gratefully acknowledge the support of this study by an EPSCoR grant, entitled "Probing and Understanding the Brain: Micro and Macro Dynamics of Seizure and Memory Networks" from the National Science Foundation, USA (NSF RII-2 FEC OIA1632891).

REFERENCES

1. Betjemann JP, Lowenstein DH. Status epilepticus in adults. *Lancet Neurol* (2015) 14:615–24. doi:10.1016/S1474-4422(15)00042-3
2. DeLorenzo RJ, Hauser WA, Towne AR, Boggs JG, Pellock JM, Penberthy L, et al. A prospective, population-based epidemiologic study of status epilepticus in Richmond, Virginia. *Neurology* (1996) 46:1029–35. doi:10.1212/WNL.46.4.1029
3. Brophy GM, Bell R, Claassen J, Alldredge B, Bleck TP, Glauser T, et al. Guidelines for the evaluation and management of status epilepticus. *Neurocrit Care* (2012) 17:3–23. doi:10.1007/s12028-012-9695-z
4. Trinka E, Cock H, Hesdorffer D, Rossetti AO, Scheffer IE, Shinnar S, et al. A definition and classification of status epilepticus – report of the ILAE task force on classification of status epilepticus. *Epilepsia* (2015) 56:1515–23. doi:10.1111/epi.13121

5. Betjemann JP, Josephson SA, Lowenstein DH, Burke JF. Trends in status epilepticus-related hospitalizations and mortality: redefined in US practice over time. *JAMA Neurol* (2015) 72:650–5. doi:10.1001/jamaneurol.2015.0188
6. Wilson JV, Reynolds EH. Texts and documents. Translation and analysis of a cuneiform text forming part of a Babylonian treatise on epilepsy. *Med History* (1990) 34:185–98. doi:10.1017/S0025727300050651
7. Alldredge BK, Lowenstein DH. Status epilepticus: new concepts. *Curr Opin Neurol* (1999) 12:183–90. doi:10.1097/00019052-199904000-00009
8. Seif-Eddeine H, Treiman DM. Problems and controversies in status epilepticus: a review and recommendations. *Expert Rev Neurother* (2011) 11:1747–58. doi:10.1586/ern.11.160
9. Walton NY, Treiman DM. Motor and electroencephalographic response of refractory experimental status epilepticus in rats to treatment with MK-801, diazepam, or MK-801 plus diazepam. *Brain Res* (1991) 553:97–104. doi:10.1016/0006-8993(91)90235-N
10. Wasterlain CG, Liu H, Mazarati AM, Baldwin RA, Shirasaka Y, Katsumori H, et al. Self-sustaining status epilepticus: a condition maintained by potentiation of glutamate receptors and by plastic changes in substance P and other peptide neuromodulators. *Epilepsia* (2000) 41(Suppl 6):S134–43. doi:10.1111/j.1528-1157.2000.tb01572.x
11. Mazarati AM, Wasterlain CG, Sankar R, Shin D. Self-sustaining status epilepticus after brief electrical stimulation of the perforant path. *Brain Res* (1998) 801:251–3. doi:10.1016/S0006-8993(98)00606-4
12. Treiman DM. Electroclinical features of status epilepticus. *J Clin Neurophysiol* (1995) 12:343–62. doi:10.1097/00004691-199512040-00005
13. Pender RA, Losey TE. A rapid course through the five electrographic stages of status epilepticus. *Epilepsia* (2012) 53:e193–5. doi:10.1111/j.1528-1167.2012.03655.x
14. Good LB, Sabesan S, Iasemidis LD, Tsakalis K, Treiman DM. Brain dynamical disentrainment by anti-epileptic drugs in rat and human status epilepticus. *Conference Proceedings. Annual International Conference of the IEEE Engineering in Medicine and Biology Society* (Vol. 1), San Francisco, CA: IEEE Engineering in Medicine and Biology Society (2004). p. 176–9.
15. Karunakaran S, Grasse DW, Moxon KA. Changes in network dynamics during status epilepticus. *Exp Neurol* (2012) 234:454–65. doi:10.1016/j.expneurol.2012.01.020
16. Schindler K, Elger CE, Lehnertz K. Increasing synchronization may promote seizure termination: evidence from status epilepticus. *Neurophysiol Clin* (2007) 118:1955–68. doi:10.1016/j.clinph.2007.06.006
17. Vlachos I, Faith A, Marsh S, White-James J, Tsakalis K, Treiman DM, et al. Brain network characteristics in status epilepticus. In: Rassias TM, Floudas CA, Butenko S, editors. *Optimization in Science and Engineering, Springer Series in Computational Intelligence*. New York, NY: Springer (2014). p. 543–52.
18. Iasemidis LD. Seizure prediction and its applications. *Neurosurg Clin N Am* (2011) 22:489–506. doi:10.1016/j.nec.2011.07.004
19. Good LB, Sabesan S, Marsh ST, Tsakalis K, Treiman DM, Iasemidis LD. Nonlinear dynamics of seizure prediction in a rodent model of epilepsy. *Nonlinear Dynamics Psychol Life Sci* (2010) 14:411–34.
20. Iasemidis LD. Epileptic seizure prediction and control. *IEEE Trans Biomed Eng* (2003) 50:549–58. doi:10.1109/TBME.2003.810689
21. Iasemidis LD, Shiau DS, Pardalos PM, Chaovalitwongse W, Narayanan K, Prasad A, et al. Long-term prospective on-line real-time seizure prediction. *Neurophysiol Clin* (2005) 116:532–44. doi:10.1016/j.clinph.2004.10.013
22. Sackellares JC, Shiau DS, Principe JC, Yang MC, Dance LK, Suharitdamrong W, et al. Predictability analysis for an automated seizure prediction algorithm. *J Clin Neurophysiol* (2006) 23:509–20. doi:10.1097/00004691-200612000-00003
23. Vlachos I, Krishnan B, Treiman DM, Tsakalis K, Kugiumtzis D, Iasemidis LD. The concept of effective inflow: application to interictal localization of the epileptogenic focus from iEEG. *IEEE Trans Biomed Eng* (2017) 64:2241–52. doi:10.1109/TBME.2016.2633200
24. Krishnan B, Vlachos I, Wang Z, Mosher J, Najm I, Burgess R, et al. Epileptic focus localization based on resting state interictal MEG recordings is feasible irrespective of the presence or absence of spikes. *Clin Neurophysiol* (2015) 126:667–74. doi:10.1016/j.clinph.2014.07.014
25. Iasemidis LD, Shiau DS, Sackellares JC, Pardalos PM, Prasad A. Dynamical resetting of the human brain at epileptic seizures: application of nonlinear dynamics and global optimization techniques. *IEEE Trans Biomed Eng* (2004) 51:493–506. doi:10.1109/TBME.2003.821013
26. Sabesan S, Chakravarthy N, Tsakalis K, Pardalos P, Iasemidis L. Measuring resetting of brain dynamics at epileptic seizures: application of global optimization and spatial synchronization techniques. *J Comb Optim* (2009) 17:74–97. doi:10.1007/s10878-008-9181-x
27. Krishnan B, Faith A, Vlachos I, Roth A, Williams K, Noe K, et al. Resetting of brain dynamics: epileptic versus psychogenic nonepileptic seizures. *Epilepsy Behav* (2011) 22(Suppl 1):S74–81. doi:10.1016/j.yebeh.2011.08.036
28. Fisher RS, Cross JH, French JA, Higurashi N, Hirsch E, Jansen FE, et al. Operational classification of seizure types by the international league against epilepsy: position paper of the ILAE commission for classification and terminology. *Epilepsia* (2017) 58:522–30. doi:10.1111/epi.13670
29. Maragos P, Kaiser JF, Quatieri TF. On separating amplitude from frequency modulations using energy operators. *Acoustics, Speech, and Signal Processing, IEEE International Conference*. San Francisco, CA (1992).
30. Hamila R, Astola J, Alaya Cheikh F, Gabbouj M, Renfors M. Teager energy and the ambiguity function. *IEEE Trans Sig Process* (1999) 47:260–2. doi:10.1109/78.738267
31. Solnik S, Rider P, Steinweg K, DeVita P, Hortobágyi T. Teager–Kaiser energy operator signal conditioning improves EMG onset detection. *Eur J Appl Physiol* (2010) 110(3):489–98. doi:10.1007/s00421-010-1521-8
32. Venkataraman V, Vlachos I, Faith A, Krishnan B, Tsakalis K, Treiman D, et al. Brain dynamics based automated epileptic seizure detection. Conference proceedings. *Annual International Conference of the IEEE Engineering in Medicine and Biology Society*. Chicago, IL: IEEE Engineering in Medicine and Biology Society (2014). p. 946–9.
33. Zaveri HP, Pincus SM, Goncharova EJ II, Novotny RB, Duckrow DD. Spencer, and S.S. Spencer, A decrease in EEG energy accompanies anti-epileptic drug taper during intracranial monitoring. *Epilepsy Res* (2009) 86:153–62. doi:10.1016/j.eplepsyres.2009.06.002
34. Avoli M, de Curtis M, Gnatkovsky V, Gotman J, Kohling R, Levesque M, et al. Specific imbalance of excitatory/inhibitory signaling establishes seizure onset pattern in temporal lobe epilepsy. *J Neurophysiol* (2016) 115:3229–37. doi:10.1152/jn.01128.2015
35. de Curtis M, Avoli M. Initiation, propagation, and termination of partial (focal) seizures. *Cold Spring Harb Perspect Med* (2015) 5:a022368. doi:10.1101/cshperspect.a022368
36. Chakravarthy N, Tsakalis K, Sabesan S, Iasemidis L. Homeostasis of brain dynamics in epilepsy: a feedback control systems perspective of seizures. *Ann Biomed Eng* (2009) 37:565–85. doi:10.1007/s10439-008-9625-6

Conflict of Interest Statement: The authors declare that the research was conducted in the absence of any commercial or financial relationships that could be construed as a potential conflict of interest.

frontiers in Neurology

MINI REVIEW
published: 09 May 2018
doi: 10.3389/fneur.2018.00259

Management of Autoimmune Status Epilepticus

Batool F. Kirmani[1,2†], Donald Barr[1], Diana Mungall Robinson[3], Zachary Pranske[4], Ekokobe Fonkem[2,5], Jared Benge[6], Jason H. Huang[2,5] and Geoffrey Ling[7]*

[1] Epilepsy Center, Baylor Scott and White Health Neuroscience Institute, Temple, TX, United States, [2] Texas A&M Health Science Center, College of Medicine, Temple, TX, United States, [3] Department of Psychiatry, University of Virginia, Charlottesville, VA, United States, [4] Baylor University, Waco, TX, United States, [5] Department of Neurosurgery, Baylor Scott and White Health Neuroscience Institute, Temple, TX, United States, [6] Division of Neuropsychology, Baylor Scott and White Health Neuroscience Institute, Temple, TX, United States, [7] Uniformed Services University of the Health Sciences, Bethesda, MD, United States

OPEN ACCESS

Edited by:
Fernando Cendes, Universidade Estadual de Campinas, Brazil

Reviewed by:
Luca Bartolini, National Institute of Neurological Disorders and Stroke – NINDS (NIH), United States
D. Mishra, Maulana Azad Medical College, India

***Correspondence:**
Batool F. Kirmani
fkirmani@msn.com

†Present address:
Batool F. Kirmani, Epilepsy Center, Centra Neurosciences, CentraHealth, Lynchburg, VA, United States

Specialty section:
This article was submitted to Epilepsy, a section of the journal Frontiers in Neurology

Received: *07 September 2017*
Accepted: *03 April 2018*
Published: *09 May 2018*

Citation:
Kirmani BF, Barr D, Robinson DM, Pranske Z, Fonkem E, Benge J, Huang JH and Ling G (2018) Management of Autoimmune Status Epilepticus. Front. Neurol. 9:259. doi: 10.3389/fneur.2018.00259

Status epilepticus is a neurological emergency with increased morbidity and mortality. Urgent diagnosis and treatment are crucial to prevent irreversible brain damage. In this mini review, we will discuss the recent advances in the diagnosis and treatment of autoimmune status epilepticus (ASE), a rare form of the disorder encountered in the intensive care unit. ASE can be refractory to anticonvulsant therapy and the symptoms include subacute onset of short-term memory loss with rapidly progressive encephalopathy, psychiatric symptoms with unexplained new-onset seizures, imaging findings, CSF pleocytosis, and availability of antibody testing makes an earlier diagnosis of ASE possible. Neuroimmunomodulatory therapies are the mainstay in the treatment of ASE. The goal is to maximize the effectiveness of anticonvulsant agents and find an optimal combination of therapies while undergoing immunomodulatory therapy to reduce morbidity and mortality.

Keywords: autoimmune encephalitis, status epilepticus, autoimmune antibodies, neuroimmunomodulatory therapies, autoimmune epilepsy

INTRODUCTION

Status epilepticus (SE) is defined as a condition resulting either from the failure of the mechanisms responsible for seizure termination or from the initiation of seizure inducing mechanisms, which can lead to abnormally prolonged seizures (5 min in the case of convulsive SE) (1). In more prolonged cases (greater than 30 min) (2, 3), long-term neurological injury such as neuronal death, injury, and alteration of cerebral networks can occur. The annual incidence rate of SE is 12.6 per 100,000 worldwide and 11.7 per 100,000 in developed countries (4).

While common causes of SE seen in the ICU (including stroke, infection, and subtherapeutic antiepileptic drug levels in patients with epilepsy) are often readily identified (5), a less common cause of SE is autoimmune status epilepticus (ASE). In these patients, autoantibodies against cell surface or synaptic proteins disrupt receptors or voltage-gated ion channels, resulting in rapidly progressive encephalopathy, abnormal movements, psychiatric symptoms, and often recurrent seizures. Some of these patients with autoantibodies and new-onset seizures—*autoimmune epilepsies*—will develop convulsive or non-convulsive ASE (6). There is a broad range of auto antigens in autoimmune encephalopathies with seizures both among those with intracellular antigens (GAD, Hu, DNER, Sox1 Ampiphysin, Ma, and CV2) and surface antigens (LG1, CASPR2, NMDAR, GlyR, AMPAR, $GABA_BR$, mGluR5, DPPX, $GABA_AR$, and Neurexin-3a). These patients can present with

antiepileptic drug resistant epilepsy; however, potential for reversal with immunotherapy and early treatment has shown improved survival and cognition (7).

Autoimmune status epilepticus is a rare condition, although its outcomes can be profound. In their review of 1,111 cases of autoimmune SE, Holzer et al. found the prognosis was bleak for those with ASE. 50% of cases demonstrated major morbidity or mortality, with 16% of patients dying and 35% of patients surviving with significant deficits. Age seemed to be an important factor related to likelihood of fatal outcome in the context of ASE, with those with higher age of onset being associated with greater mortality while those of younger age of onset are generally more likely to recover with major behavioral, psychiatric, or epileptogenic deficits (8). Spatola et al. reported a retrospective study of 570 episodes of SE and found that ASE accounted for just 2.4% of SE episodes. ASE was more common in younger patients (mean age: 44 vs 60 years), was more likely to be refractory to antiepileptic drug treatment, and was associated with lower morbidity (return to baseline conditions in 71%) without any difference in mortality (9). Harutyunyan et al. conducted a retrospective cohort study to characterize the underlying etiologies, clinical symptoms, reasons for ICU admission, and mortality of critically ill patients with autoimmune encephalitis and found that SE was the most common reason for admission. In this study, the median age of patients with autoimmune encephalitis was 55 years (25–87 years, $n = 16$) (10).

ESTABLISHING ETIOLOGY AND THERAPEUTIC OPTIONS IN ASE

The presence of antineuronal antibodies against central nervous system proteins is associated with a group of encephalopathies termed autoimmune encephalopathies. They may be categorized based on their antigen target (intraneuronal, surface receptor, or synaptic). Antibodies to cell surface antigens are the most common, considered idiopathic in nature, while the intraneuronal antibodies are more often associated with a neoplasm (11, 12). There are some autoimmune encephalopathies more frequently associated with seizures termed autoimmune epilepsies. These autoimmune epilepsies are seen in patients with antibodies to intracellular antigens (GAD, Hu, DNER, Sox1 Ampiphysin, Ma, and CV2) and surface antigens (LG1, CASPR2, NMDAR, GlyR, AMPAR, $GABA_BR$, mGluR5, DPPX, $GABA_AR$, and Neurexin-3a); however, there is potential for reversal with immunotherapy, and early treatment has shown a general rate of improved survival and cognition (7).

At disease onset, there is little to distinguish the different types of autoimmune encephalopathies from one another. Subacute development of short-term memory loss is among the key clinical features of autoimmune encephalopathies, along with rapid development of cognitive and working memory impairment, mood changes, and seizures (13). In their proposed diagnostic criteria for possible autoimmune encephalitis, Graus et al. included new focal CNS findings, CSF pleocytosis, MRI features suggestive of encephalitis, and seizures not explained by a previous known seizure disorder (14). Note that their criteria does not rely on antibody testing and response to immunotherapy but rather levels of evidence for autoimmune encephalitis (possible, probable, or definite) leading to earlier treatment with immunotherapy, which can lead to improved survival and cognitive outcomes (14, 15).

Sakusic and Rabinstein found that early manifestations of autoimmune encephalitis are agitation or new behavioral changes mimicking psychosis. They also note that even when CSF and MRI brain are normal, autoimmune encephalitis is still possible. In fact, the clinical presentations can vary with the same antibodies (16).

Bien and Holtkamp found that traits associated with an increased likelihood of autoimmune epilepsy included young women (15–45 years old), history of autoimmune conditions, epilepsy onset together with prominent psychiatric or cognitive impairment, and unexplained new-onset epilepsy in adults with SE or high seizure frequency (7). Electroencephalogram findings are generally non-specific in distinguishing between autoimmune epilepsies, with the exception of extreme delta brush which is seen in anti-NMDAR encephalitis (17). CSF pleocytosis is seen in majority of autoimmune epilepsies except LG1. Some seizure types can support specific autoimmune epilepsies such as faciobrachial dystonic seizures (seen in patients with LGI1 antibodies) and pilomotor seizures (seen with LGI1, Hu, and Ma antibodies).

In general, a broad spectrum of antibody testing is recommended to avoid delays that may be caused by isolated single antibody testing. Encephalopathy with seizures manifesting as rapidly evolving cognitive impairment with neuropsychiatric features or focal neurological deficits may be related to several antibodies, with NMDAR and LGI1 among the most likely. Furthermore, it is noted that the patients with voltage-gated potassium channel complex antibodies respond well and can even become seizure free with immunotherapy. Patients with faciobrachial dystonic seizures and LI1 antibodies respond well to steroids but had little response to AEDs (18). This is particularly challenging with new-onset temporal lobe seizures which are frequently accompanied by various degrees of psychiatric associations (such as depressed mood or memory deficits, for example) but may well be the onset of anti-NMDAr encephalitis (19).

There have been relatively few studies of the exact pathophysiology of ASE and even sparser characterization of outcomes related to particular pathologies. Bien found that patients with autoimmune epilepsy who presented with SE or very high seizure frequency, most cases were associated with NMDAR, LGI1, GABABR, GABAAR, and GAD antibodies (18).

In terms of treatment, corticosteroids, immunosuppressive treatments, intravenous immunoglobulin (IVIG), etc., assume that inflammation is the underlying cause of SE in patients. However, there is only limited evidence to support these treatment options. Some clinical studies have linked systemic inflammation to epilepsy; however, it is not clear from these trials alone whether inflammation directly causes SE. Children with febrile seizures have elevated levels of IL-1B, IL-6, and HMGB1, which are all inflammatory markers (18). Furthermore, histopathological findings from temporal cortex from patients with new-onset focal seizures that progressed to SE show gliosis of both astrocytes and microglia, strong IL-1B expression, and sparse lymphocytic infiltration, again suggestive of an inflammatory

pathology. In bench studies, induced SE is linked to a multitude of inflammatory cascades in animal models. Within 30–60 min of SE onset, IL-1B, TNF-a, and IL-6 transcript levels are increased for 24–72 h In compromised brains, these changes are associated with a more severe acute course and worse long-lasting neuropathological symptoms. It appears that inefficient endogenous anti-inflammatory control in the brain may be characteristic of chronic recurrent seizures and SE (18).

Despite controversy as to the exact mechanisms, limited clinical data suggest patients with known or suspected autoimmune encephalitis may still benefit from immunotherapy (18). Response to immunotherapy is commonly delayed, so caution to avoid overtreatment is advised. As with Holzer et al., first line treatments with corticosteroids, IVIG or plasma exchange may be effective, but refractory cases may require aggressive treatment regimens that may have significant side effects (8). Rituximab, cyclophosphamide, mycophenolate mofetil, tacrolimus, as well as VNS have been used in refractory cases (19–23). In their comprehensive review, Bien and Holtkamp provided an immunotherapy algorithm for conditions associated with antibodies against cell surface receptors, largely derived from reported experience with anti-NMDAR encephalitis. These include corticosteroids, IVIG, independent plasma exchange, or a combination of these symptoms (7).

Early implementation of immunomodulatory treatment may play a role for survival and better cognitive functions. In their retrospective review of 27 patients with suspected autoimmune epilepsy who underwent a 6- to 12-week trial of IV methylprednisolone, IV immune globulin, or both, Toledano et al. found that 18 patients responded with at least a 50% seizure reduction frequency, including 10 who became seizure free. 52% improved with the first agent, and of those who required a second agent, 43% responded. In addition, they found favorable response correlated with shorter interval between symptom onset and treatment initiation, and response was sustained in 11 of 13 responders followed for more than 6 months after initiating long-term oral immunosuppression with either mycophenolate mofetil or azathioprine. The authors conclude that these findings justify consideration of a trial of immunotherapy in patients with suspected autoimmune epilepsy (15).

Zeiler et al. conducted a literature review of 22 articles encompassing 27 adult patients to determine the effectiveness of plasmapheresis for refractory SE in adults. Inclusion criteria were all prospective and retrospective studies of any size, adult human subjects (≥18 years old), and use of plasmapheresis for the purpose of seizure control in the setting of refractory SE. There was a wide variety of etiologies of SE/RSE, including: unknown suspected autoimmune ($N = 8$ pts), NMDA receptor encephalitis ($N = 6$ pts), anti-GAD ($N = 3$ pts), Hashimoto's encephalitis ($N = 2$ pts), and one patient each with anti-VGCC encephalitis, anti-VGKC encephalitis, anti-SSA encephalitis, anti-GABA encephalitis, herpes simplex virus encephalitis, Creutzfeldt–Jakob disease, Rasmussen's encephalitis, and new-onset refractory SE. The most common types of seizures were generalized refractory SE ($N = 15$ pts), followed by focal refractory SE and non-convulsive SE ($N = 6$ pts each). The mean duration of treatment before starting plasmapheresis therapy was 16.2 days. The mean number of AEDs before plasmapheresis was 6.5 (18 studies; range 2–11). Other immunotherapies including corticosteroids, IVIG, and rituximab were used in most studies (21 of 22 studies). 13 patients (48%) had complete resolution of seizures, 13 patients (48%) had no response, and 1 patient (4%) had partial temporary electroencephalogram-based response. Patients with generalized refractory SE were the most likely to respond (67%, 10 of 15 patients) followed by refractory SE and non-convulsive SE (both = 33%, 2 of 6 patients). After plasmapheresis, 29% of patients who initially responded (4 of 14 patients) had seizure recurrence. Given these findings, the authors concluded that plasmapheresis as a treatment for RSE could not be recommended at this time due to patients having an uncertain response (24).

Febrile infection-related epilepsy syndrome (FIRES) is the also most catastrophic immune mediated epileptic encephalopathy which affects healthy children. The spectrum of this rare clinical illness is unknown but preceding febrile infection points toward immune etiology which is triggered by infection (25). Neuroinflammation has been shown to play a role in experimental animal models (26). The diagnosis is clinical and ranges from seizure clusters to refractory SE preceding febrile illness (25).

Conventional therapies with antiepileptic medications often fail, and early treatment with ketogenic diet, immune-modulators, and cannabidiol may help reduce seizure burden, but evidence remains anecdotal (27–29). Ketogenic diet is also utilized in other forms of super-refractory SE, both in adults and children, particularly in suspected immune related cases. Ketogenic diet can be administered parenterally and has antiepileptic effect through direct inhibition of the postsynaptic excitatory AMPA receptor by decanoic acid (30). There is also evidence that it has anti-inflammatory role which can be hypothesized as being useful in the treatment of FIRES and other related disorders (31).

FUTURE DIRECTIONS

Autoimmune status epilepticus is an infrequently observed but potentially devastating disorder with a multitude of clinical presentations depending upon the type of antibodies. During the recent years, a link has been established between various antibodies and their specific presentation Researchers continue to find new antibodies but as the available testing for antibody-mediated encephalitis expands, but physicians have limited data regarding optimal treatment regimens as it pertains to acute intervention in patients. IV immunoglobulin and plasmapheresis are also commonly included as first line therapies. Corticosteroids are also used in treatment; however, dosing, duration and threshold for response time before changing to alternative therapy remains unclear. Physicians must continue to work toward early recognition and effective interventions in patients presenting with ASE as well as understanding the underlying pathophysiology to better tailor intervention and more basic research is needed to recognize biomarkers to develop novel therapeutic agents for this life threatening condition.

AUTHOR CONTRIBUTIONS

All the authors have contributed equally to this work.

REFERENCES

1. Trinka E, Cock H, Hesdorffer D, Rossetti AO, Scheffer IE, Shinnar S, et al. A definition and classification of status epilepticus – report of the ILAE Task Force on Classification of Status Epilepticus. *Epilepsia* (2015) 56:1515–23. doi:10.3410/f.725768340.793515044
2. Treatment of convulsive status epilepticus. Recommendations of the Epilepsy Foundation of America's Working Group on Status Epilepticus. *JAMA* (1993) 270:854–9. doi:10.1001/jama.270.7.854
3. Guidelines for epidemiologic studies on epilepsy. Commission on Epidemiology and Prognosis, International League Against Epilepsy. *Epilepsia* (1993) 34:592–6. doi:10.1111/j.1528-1157.1993.tb00433.x
4. Lv RJ, Wang Q, Cui T, Zhu F, Shao XQ. Status epilepticus-related etiology, incidence and mortality: a meta-analysis. *Epilepsy Res* (2017) 136:12–7. doi:10.1016/j.eplepsyres.2017.07.006
5. Trinka E, Höfler J, Zerbs A. Causes of status epilepticus. *Epilepsia* (2012) 53:127–38. doi:10.1111/j.1528-1167.2012.03622.x
6. Holzer FJ, Rossetti AO, Heritier-Barras AC, Zumsteg D, Roebling R, Huber R, et al. Antibody-mediated status epilepticus: a retrospective multicenter survey. *Eur Neurol* (2012) 68:310–7. doi:10.1159/000341143
7. Bien CG, Holtkamp M. "Autoimmune epilepsy": encephalitis with autoantibodies for epileptologists. *Epilepsy Curr* (2017) 17:134–41. doi:10.5698/1535-7511.17.3.134
8. Holzer FJ, Seeck M, Korff CM. Autoimmunity and inflammation in status epilepticus: from concepts to therapies. *Expert Rev Neurother* (2014) 14(10): 1181–202. doi:10.1586/14737175.2014.956457
9. Spatola M, Novy J, Pasquier RD, Dalmau J, Rossetti AO. Status epilepticus of inflammatory etiology. *Neurology* (2015) 85:464–70. doi:10.1212/wnl.0000000000001717
10. Harutyunyan G, Hauer L, Dünser MW, Karamyan A, Moser T, Pikija S, et al. Autoimmune encephalitis at the neurological intensive care unit: etiologies, reasons for admission and survival. *Neurocrit Care* (2016) 27:82–9. doi:10.1007/s12028-016-0370-7
11. Louis E, Mayer S, Rowland L. *Merritt's Neurology*. Philadelphia: Wolters Kluwer (2016).
12. Tobin W, Pittock S. Autoimmune neurology of the central nervous system. *Continuum (Minneap Minn)* (2017) 23:627–53. doi:10.1212/CON.0000000000000487
13. Gultekin SH, Rosenfeld MR, Voltz R, Eichen J, Posner JB, Dalmau J. Paraneoplastic limbic encephalitis: neurological symptoms, immunological findings and tumour association in 50 patients. *Brain* (2000) 123:1481–94. doi:10.1093/brain/123.7.1481
14. Graus F, Titulaer M, Balu R, Benseler S, Bien CG, Cellucci T, et al. A clinical approach to diagnosis of autoimmune encephalitis. *Lancet Neurol* (2016) 15:391–404. doi:10.1016/S1474-4422(15)00401-9
15. Toledano M, Britton JW, McKeon A, Shin C, Lennon VA, Quek AM, et al. Utility of an immunotherapy trial in evaluating patients with presumed autoimmune epilepsy. *Neurology* (2014) 82:1578–86. doi:10.1212/wnl.0000000000000383
16. Sakusic A, Rabinstein AA. Case studies in neurocritical care. *Neurol Clin* (2016) 34(3):683–97. doi:10.1016/j.ncl.2016.04.007
17. Chanson E, Bicilli É, Lauxerois M, Kauffmann S, Chabanne R, Ducray F, et al. Anti-NMDA-R encephalitis: should we consider extreme delta brush as electrical status epilepticus? *Neurophysiol Clin* (2016) 46:17–25. doi:10.1016/j.neucli.2015.12.009
18. Bien CG. Value of autoantibodies for prediction of treatment response in patients with autoimmune epilepsy: review of the literature and suggestions for clinical management. *Epilepsia* (2013) 54:48–55. doi:10.1111/epi.12184
19. van Vliet EA, da Costa Araújo S, Redeker S, van Schaik R, Aronica E, Gorter JA. Blood-brain barrier leakage may lead to progression of temporal lobe epilepsy. *Brain* (2007) 130:521–34. doi:10.1093/brain/awl318
20. Alsaadi T, Shakra M, Turkawi L, Hamid J. VNS terminating refractory non-convulsive SE secondary to anti-NMDA encephalitis: a case report. *Epilepsy Behav Case Rep* (2015) 3:39–42. doi:10.1016/j.ebcr.2015.02.003
21. Gagnon M-M, Savard M, Amari KM. Refractory status epilepticus and autoimmune encephalitis with GABA A R and GAD65 antibodies: a case report. *Seizure* (2016) 37:25–7. doi:10.1016/j.seizure.2016.02.006
22. Dillien P, Ferrao Santos S, Van Pesch V, Suin V, Lamoral S, Hantson P. New-onset refractory status epilepticus: more investigations, more questions. *Case Rep Neurol* (2016) 8:127–33. doi:10.1159/000447295
23. Ramanathan S, Wong CH, Rahman Z, Dale RC, Fulcher D, Bleasel AF. Myoclonic status epilepticus as a presentation of caspr2 antibody-associated autoimmune encephalitis. *Epileptic Disord* (2014) 16:477–81. doi:10.1684/epd.2014.0707
24. Zeiler F, Matuszczak M, Teitelbaum J, Kazina C, Gillman L. Plasmapheresis for refractory status epilepticus, part I: a scoping systematic review of the adult literature. *Seizure* (2016) 43:14–22. doi:10.1016/j.seizure.2016.10.012
25. van Baalen A, Vezzani A, Häusler M, Kluger G. Febrile infection-related epilepsy syndrome: clinical review and hypotheses of epileptogenesis. *Neuropediatrics* (2017) 48(01):005–018. doi:10.1055/s-0036-1597271
26. Riazi K, Galic MA, Pittman QJ. Contributions of peripheral inflammation to seizure susceptibility: cytokines and brain excitability. *Epilepsy Res* (2010) 89(1):34–42. doi:10.1016/j.eplepsyres.2009.09.004
27. Kossoff EH, Hartman AL. Ketogenic diets: new advances for metabolism-based therapies. *Curr Opin Neurol* (2012) 25(2):173–8. doi:10.1097/WCO.0b013e3283515e4a
28. Gofshteyn JS, Wilfong A, Devinsky O, Bluvstein J, Charuta J, et al. Cannabidiol as a potential treatment for febrile infection-related epilepsy syndrome (FIRES) in the acute and chronic phases. *J Child Neurol* (2016) 32(1):35–40. doi:10.1177/0883073816669450
29. Sivakumar S, Ibrahim M, Parker D Jr, Norris G, Shah A, Mohamed W. Clobazam: an effective add-on therapy in refractory status epilepticus. *Epilepsia* (2015) 56(6):e83–9. doi:10.1111/epi.13013
30. Chang P, Augustin K, Boddum K, Williams S, Sun M, Terschak JA, et al. Seizure control by decanoic acid through direct AMPA receptor inhibition. *Brain* (2016) 139(Pt 2):431–43. doi:10.1093/brain/awv325
31. Dupuis N, Curatolo N, Benoist JF, Auvin S. Ketogenic diet exhibits anti-inflammatory properties. *Epilepsia* (2015) 56(7):e95–8. doi:10.1111/epi.13038

Conflict of Interest Statement: The authors declare that the research was conducted in the absence of any commercial or financial relationships that could be construed as a potential conflict of interest.

frontiers in Neurology

ORIGINAL RESEARCH
published: 18 December 2017
doi: 10.3389/fneur.2017.00700

Status Epilepticus Triggers Time-Dependent Alterations in Microglia Abundance and Morphological Phenotypes in the Hippocampus

Season K. Wyatt-Johnson[1†], Seth A. Herr[1†] and Amy L. Brewster[1,2]*

[1] Department of Psychological Sciences, College of Health and Human Sciences, Purdue University, West Lafayette, IN, United States, [2] Weldon School of Biomedical Engineering, West Lafayette, IN, United States

Status epilepticus (SE) is defined by the occurrence of prolonged "non-stop" seizures that last for at least 5 min. SE provokes inflammatory responses including the activation of microglial cells, the brain's resident immune cells, which are thought to contribute to the neuropathology and pathophysiology of epilepsy. Microglia are professional phagocytes that resemble peripheral macrophages. Upon sensing immune disturbances, including SE, microglia become reactive, produce inflammatory cytokines, and alter their actin cytoskeleton to transform from ramified to amoeboid shapes. It is widely known that SE triggers time-dependent microglial expression of pro-inflammatory cytokines that include TNFα and IL-1β. However, less is known in regards to the spatiotemporal progression of the morphological changes, which may help define the extent of microglia reactivity after SE and potential function (surveillance, inflammatory, phagocytic). Therefore, in this study, we used the microglia/macrophage IBA1 marker to identify and count these cells in hippocampi from control rats and at 4 h, 3 days, and 2 weeks after a single episode of pilocarpine-induced SE. We identified, categorized, and counted the IBA1-positive cells with the different morphologies observed after SE in the hippocampal areas CA1, CA3, and dentate gyrus. These included ramified, hypertrophic, bushy, amoeboid, and rod. We found that the ramified phenotype was the most abundant in control hippocampi. In contrast, SE provoked time-dependent changes in the microglial morphology that was characterized by significant increases in the abundance of bushy-shaped cells at 4 h and amoeboid-shaped cells at 3 days and 2 weeks. Interestingly, a significant increase in the number of rod-shaped cells was only evident in the CA1 region at 2 weeks after SE. Taken together, these data suggest that SE triggers time-dependent alterations in the morphology of microglial cells. This detailed description of the spatiotemporal profile of SE-induced microglial morphological changes may help provide insight into their contribution to epileptogenesis.

Keywords: status epilepticus, epilepsy, hippocampus, microglia morphology, microglia

OPEN ACCESS

Edited by:
Lee A. Shapiro, Texas A&M University System Health Science Center College of Medicine, United States

Reviewed by:
Thimmasettappa Thippeswamy, Iowa State University, United States
João P. Leite, University of São Paulo, Brazil

***Correspondence:**
Amy L. Brewster
abrewst@purdue.edu

†These authors have contributed equally to this work.

Specialty section:
This article was submitted to Epilepsy, a section of the journal Frontiers in Neurology

Received: *21 August 2017*
Accepted: *06 December 2017*
Published: *18 December 2017*

Citation:
Wyatt-Johnson SK, Herr SA and Brewster AL (2017) Status Epilepticus Triggers Time-Dependent Alterations in Microglia Abundance and Morphological Phenotypes in the Hippocampus. Front. Neurol. 8:700. doi: 10.3389/fneur.2017.00700

INTRODUCTION

Status epilepticus (SE) is defined by the occurrence of prolonged "non-stop" seizures that last for at least 5 min (1). In the United States, it is estimated that up to 41 out of 100K individuals are affected by SE, and that one or two SE events can increase the risk of future unprovoked seizures by 40–52 and 73%, respectively (1). SE is a clinical emergency for which rapid intervention can

help to prevent or reduce the risk for subsequent neuronal injury and neurological sequelae that includes epilepsy and cognitive disturbances (1, 2). Extensive evidence supports that SE provokes an array of inflammatory responses including activation of microglial cells, the resident immune cells of the CNS, which are thought to contribute to the neuropathology and pathophysiology of epilepsy (3, 4).

Microglial cells are highly dynamic professional phagocytes that resemble peripheral macrophages. Under physiological conditions, these cells occupy non-overlapping territories where they constantly survey their surrounding environment for signals that indicate injury and immune disturbances, as well as altered neuronal activity (5–10). Upon sensing pathological signals, including seizures and SE, microglia become reactive and promptly undergo biochemical changes, producing pro-inflammatory cytokines, such as tumor necrosis factor-alpha (TNFα) and interleukin 1- beta (IL-1β) (4). In parallel, reactive microglia go through morphological changes that range from a phenotype of small cell bodies with vastly ramified processes (surveilling microglia) to small amoeboid shapes with little to no processes (activated/phagocytic) that can alternate between transitional states/phenotypes that include slightly enlarged cell bodies with thickened processes that may be long or short (10–16). Both inflammatory and morphological microglial alterations have been widely described in human epileptic brain tissues (4, 17–21) as well as in animal models of SE and experimental epilepsy (4, 22–28). While these and numerous additional studies support that areas such as the hippocampus are particularly vulnerable to SE-induced injury and show highly activated inflammatory responses, less is known in regards to the spatiotemporal progression of microglial morphological changes. Understanding these phenotypes may help define the extent of microglia reactivity and potential function after SE.

Previously, we reported that SE promoted an increase in the microglial levels in the CA1 hippocampal area that peaked at 2 weeks following the prolonged seizures (22). However, this finding was based on densitometry analysis from the immunoreactivity of the ionized calcium-binding adaptor molecule 1 (IBA1), a protein found specifically in microglia and macrophages (29). Thus, in order to determine the extent to which SE modulates the hippocampal microglial population and morphological phenotypes in the current study, we determined (i) the abundance of microglia by immunohistochemistry (IHC) and flow cytometry and (ii) the percentage of microglial morphological phenotypes (ramified, hypertrophied, bushy, amoeboid, and rod) present in different hippocampal areas at 4 h, 3 days, and 2 weeks following a single episode of SE using the pilocarpine rat model of SE and acquired temporal lobe epilepsy.

MATERIALS AND METHODS

Animals

Male Sprague Dawley rats (150–175 g) (Envigo Laboratories) were housed at the Psychological Sciences Building at an ambient temperature of 22°C, with 12-h light and 12-h dark (0800 to 2000 hours) cycles, and unlimited access to food and water. All animal procedures were approved by the Purdue Animal Care and Use Committee and followed the approved Institutional and NIH guidelines.

Pilocarpine-Induced SE

Status epilepticus inductions were done following previously described protocols (22, 23). Scopolamine methylbromide (1 mg/kg) was given 30 min (min) prior to injections (i.p.) of saline (Sham-Control) or pilocarpine (280–300 mg/kg; Sigma Chemical Co., St. Louis, MO, USA) (SE group). SE was stopped after 1 h with diazepam (10 mg/kg; i.p.; Sigma Chemical Co.). When rats reached class 5 limbic motor seizures (rearing and falling) (30), they were considered to be in SE. Two hours after SE, all rats were given injections (i.p.) of sterile 0.9% saline (AddiPak) for hydration and as needed thereafter. Rat chow was supplemented with sliced peeled apples and Kellogg's Fruit Loop cereal for up to 1 week after SE inductions. From our studies in the pilocarpine model of SE and acquired TLE, we calculated that pilocarpine promotes SE at 4.5–6 seizure stages according to the Racine scale (30) in approximately 67.1% of the rats. Rats that did not reach a seizure score of 4.5–6 were not used in this study. Animals for histology were sacrificed at 4 h ($N = 4$), 3 days ($N = 8$), or 2 weeks following SE ($N = 5$); controls ($N = 5$). Animals for flow cytometry were sacrificed at 2 weeks following SE ($N = 5$); Controls ($N = 5$). The sample size per group was determined using a power level of 0.80 and $\alpha = 0.05$ (*post hoc* power analysis, GPower).

Flow Cytometry

Animals were anesthetized with beuthanasia (200 mg/kg) and perfused with ice cold 1× phosphate buffered saline (PBS). Hippocampi were rapidly dissected on ice and processed using the NeuroCult™ Enzymatic Dissociation Kit for Adult CNS Tissue (Mouse and Rat) according to manufacturer's instructions (Stemcell Technologies) with minor modifications. At this point, all samples were coded for experimenter to be blinded of treatment groups for the rest of the tissue processing and flowcytometric analysis. Hippocampal tissue samples were then placed into a 70-μm nylon cell strainer rinsed with 100 μL of cold NeuroCult Tissue Collection Solution and gently pressed, using fingertips, through the filter into the 15-mL tube on ice. The collected tissue homogenate was then similarly gently pressed through a 40-μm nylon cell strainer, collected, and transferred into a 1.5–2 mL tube using a glass Pasteur Pipette. The samples were centrifuged at 100 *g* for 7 min at 4°C. Pellets were suspended with 500 μL NeuroCult Enzymatic Dissociation Solution and incubated for 14 min at 37°C. Then, 500 μL of NeuroCult Inhibition Solution was gently mixed and samples were centrifuged at 100 *g* for 7 min at 4°C. The following steps were done using previously described protocols with minor modifications (31–34). Pellets were suspended with 3.5 mL of resuspension solution and 1.5 mL of Percoll gel for a 30% total Percoll (v/v) and centrifuged at 700 *g* for 11 min at RT. The resulting pellets were suspended in eBioscience Flow Cytometry Staining Buffer according to manufacturer's instructions. Cells in staining buffer were divided equally into

four, 1 mL volumes and the number of viable cells per milliliter was estimated with a hemocytometer and Trypan Blue dye (~1 × 10^6 cells/mL). Immunophenotyping categories identified microglia/macrophages expressing high or low levels of cluster of differentiation molecule 11b (CD11b), cluster of differentiation 45 (CD45), and major histocompatibility complex class II (MHCII) (10) using the following antibodies: APC/Cy7 anti-rat CD45 (BioLegend Cat# 202216 RRID:AB_1236411), APC anti-rat CD11b/c Antibody (BioLegend Cat# 201809 RRID:AB_313995), and PE anti-rat RT1B Antibody (BioLegend Cat# 205308 RRID:AB_1595483). Antibodies were incubated for 30 min at 2–8°C in the dark followed by centrifugation at 400 *g* for 5 min at RT. Cells were washed and centrifuged at 100 *g* for 7 min, following pellet suspension with the Viability Dye (eBioscience, Grand Island, NY, USA, cat. 65-0863). The dye was titrated and added, immediately mixed, and incubated in the dark at 2–8°C for 30 min. Cells were washed and centrifuged at 400 *g* (2×), and pellets were suspended 1:1 of flow cytometry staining buffer and IC Fixation Buffer (eBioscience, Grand Island, NY, USA, cat. 00-8222). Samples were stored at 2–8°C in the dark and analyzed within 3 days. Stained samples were acquired on a BD Facs Aria flow cytometer (BD Biosciences) fitted with a 355 nm-UV laser, 405-nm violet laser, 488 nm-blue laser, a 561-yellow-green laser, and a 627-nm red laser. Data were acquired using DIVA v. 7 (BD Biosciences, San Jose, CA, USA) software. Analysis of the populations was performed in Flowjo v.8.7.3 (Treestar) using bi-exponential display and was based on "fluorescent minus one" gating controls to ensure the proper identification of true positive and negative events. Live cells were gated for CD45/CD11b positive cells and from these the percent of the population of MHCII-positive cells was determined.

Immunohistochemistry

Animals and tissues were processed for IHC as described in our previous study (22). The tissues used for IHC and densitometry analysis in Schartz et al. (22) were further analyzed for microglia/macrophage cell and morphology counts in the current study. Briefly, animals were anesthetized with beuthanasia (200 mg/kg) and perfused with ice cold 1× PBS followed by 4% paraformaldehyde (PFA). After overnight post-fixation (4%-PFA) and cryoprotection (30% sucrose), brains were frozen in pre-chilled isopentane and stored at −80°C until used. Coronal brain sections (50 µm) were stored in 1×PBS + 0.1% sodium azide at 4°C. Serial sections from rostral to caudal (4–6 sections per brain) were collected at approximately every 500 µm along the dorsoventral axis between the Bregma coordinates −3.00 mm and −5.28 mm. These sections were immunostained with anti-rabbit IBA1 (1:500; Wako Chemicals Cat# 019-19741, RRID: AB_839504) followed by biotinylated goat anti-rabbit secondary antibodies (1:2,000; Vector Laboratories Cat# BA-1000 RRID:AB_2313606), incubated in ABC avidin/biotin complex solution and developed using the DAB Peroxidase (HRP) Substrate Kit, 3,3′-diaminobenzidine (Vector Laboratories). Brain sections were mounted on gelatin-coated slides, Nissl stained, dehydrated in alcohol, de-fatted in Xylene, and coverslipped using Permount mounting media. All chemicals were obtained from Fisher Scientific unless otherwise indicated.

Morphological Assessment and Cell Counts

The ionized calcium-binding adapter molecule 1 (IBA1) was used to identify microglia. Note that in addition to its specificity for microglial cells, IBA1 also stains infiltrated macrophages and/or monocytes (29). Therefore, to include the possibility of non-microglia cells stained with IBA1, we refer to the IBA1-positive cells as microglia/macrophages. The morphologies of IBA1-positive microglia/macrophages were sorted into categories from 1 to 5: 1—ramified; 2—hypertrophic; 3—bushy; 4—amoeboid; and 5—rod. Cells were categorized based on overall diameter including processes and evident changes in process thickness. These classification guidelines and categories were adopted based on published literature with detailed descriptions of microglia morphology (10–14, 35–37). The descriptions and cellular diameters for each category are as follows: (1) ramified cells had a diameter of 50+ µm with fine and highly branched processes; (2) hypertrophic cells had a diameter of 40–50 µm with thick and highly branched processes; (3) bushy cells had a diameter of 20–25 µm with thick, dense, and shorter processes; (4) amoeboid cells had a diameter smaller than 10–15 µm with retracted processes and irregular shapes; (5) rod cells did not display circular diameters but had long, slender cell bodies and short fine processes. Although not described in this study, we also observed rod microglia/macrophages on train formation, which included two or more connecting rod-shaped cells (13, 14). Cells were categorized in the hippocampal CA1, CA3, and dentate gyrus (DG). IBA1-positive cells were only counted if more than 75% of their staining was inside the boundaries of the counting frame and met the criteria of one of the different diameters (35). Cell overlapping, broken tissue areas, or cells with very light staining were not counted. Cellular nuclei were identified through Nissl staining. To remain unbiased, often multiple cells were counted as one: (1) if microglia appeared to be in cell division or (2) if clumps of amoeboid-shaped microglia were observed, in this case the distinct cells at the edge of the clump were counted but the center of the mass was counted as one cell. A Leica DM500 microscope with high resolution digital camera (Leica MC120 HD) and LAS4.4 software was used for image acquisition using a 40× objective. All image groups were blinded to the researcher for cell counts and morphological quantification and IBA1-positive cells within the entire 40× image frame were counted. We analyzed 4–6 sections per brain bilaterally distributed from rostral to caudal. Four pictures were taken in non-overlapping locations in each of the different hippocampal areas and the average of cell counts was calculated for section area and then for each brain. Cells were counted using ImageJ with scaled circle frames for diameter reference. Total number of cells per frame was counted first, followed by the count of the different morphologies. The percentage of each morphological phenotype was calculated based on the total number of IBA1-positive cells per hippocampal area.

Statistical Analyses

Graphpad Prism was used for data analysis. *T*-test or analysis of variance were used to determine statistical associations between the experimental groups from flow cytometry and histological data. Statistical significance was set at $\alpha < 0.05$. Data values are reported as means (M) ± SEM. Figures were generated using Adobe Photoshop (CS6).

RESULTS

We previously reported that a single episode of SE provoked an increase in the immunoreactivity for the microglial/macrophage marker IBA1 in the hippocampus that peaked at 2 weeks after the induction of SE (22). To further determine potential alterations in the population of IBA1-positive microglia/macrophages in the hippocampus, we counted the number of these cells in control samples as well as at 4 h, 3 days, and 2 weeks after SE (**Figures 1A–G**). Statistical analyses showed that the number of IBA1-positive cells in the hippocampal areas CA1, CA3, and DG was not different between the control group and the 4 h- or 3 day-SE groups ($p > 0.05$). Statistically significant differences were found between the control and 2-week-SE group. The highest SE-induced increases in the number of IBA1-positive cells at this time point occurred in the CA1 region (~1.9-fold, $p = 0.0036$) followed by DG (~1.3-fold, $p = 0.0010$) and CA3 (~1.2-fold, $p = 0.0056$) relative to control hippocampi. The increase in the abundance of microglia/macrophages at 2 weeks after SE was also evident through flow cytometry analyses (**Figures 1H–K**). Microglia/macrophages were identified with antibodies against CD45 and CD11b, and surface expression of the MHCII that was used to also label reactive/inflammatory cells (10). **Figure 1H** shows that whole hippocampal live-cell suspensions gated for CD45 and CD11b displayed significantly more labeled cells in the 2-week-SE samples than the controls ($p = 0.0423$) (**Figures 1H,J**). Similarly, a significant increase in the number of CD45/CD11b positive expressing MHCII was evident at the 2-week time point relative to controls ($p = 0.0070$) (**Figures 1I,K**). Together these data suggest that SE triggers an increase in the population of activated microglia/macrophages in the hippocampus.

During the cell quantification analyses, we observed that IBA1-positive cells displayed a variety of heterogeneous morphologies, suggesting different activation and/or transitional states. We identified at least five different types of morphologies in the control and experimental SE tissues, and categorized them as follows: 1—ramified; 2—hypertrophic; 3—bushy; 4—amoeboid; and 5—rod (**Figure 2**). Some of these phenotypes such as 2- and 3- have been referred to as primed and reactive/activated, respectively (12). However, given that the function of these morphological phenotypes is not definitively known we based the nomenclature strictly on the physical appearance of the IBA1-positive cells.

We calculated the percentage of IBA1-positive cells that displayed each of these morphologies from the total cell numbers in the different hippocampal regions CA1, CA3, and DG in control brains, as well as at 4 h, 3 days, and 2 weeks (**Figure 3**; Figure S1 in Supplementary Material) after SE. **Figure 3A** shows that in the CA1 area of control hippocampi 74% of microglia were ramified with highly branched, thin, and elongated processes with an overall diameter of 40–50 μm, while 19% were hypertrophied and the remaining (~8%) were bushy. In CA3 area, 64% of the microglia displayed the ramified phenotype while 30% were hypertrophic, and in DG a mixed population of microglial/macrophage morphologies ranging from 1 to 4 was observed with 50% ramified, 24% hypertrophic, 19% bushy, and 6% amoeboid (**Figure 3A**).

Although the total microglia/macrophage numbers were similar in CA1 ($p = 0.2777$), CA3 ($p = 0.2830$), and DG ($p = 0.8612$) between the control and 4-h-SE groups (**Figure 1**), we found drastic changes in the microglia/macrophage morphology at this time point (**Figure 3B**). In the 4-h-SE group, the population of microglia/macrophage cells displayed mainly the bushy phenotype and represented 54% in CA1, 57% in CA3, and 36% in DG. Similarly, at 3 days after SE, the total number of IBA1-positive cells in the hippocampus was not significantly different to that of the control group (CA1, $p = 0.0845$; CA3, $p = 0.0629$; DG, $p = 0.0654$). However, the morphology of these cells was altered in all hippocampal regions of the 3-day-SE group (**Figure 3C**). In CA1, the bushy, amoeboid, and rod phenotypes contributed to 33, 40, and 12% of the population of IBA1-positive cells, respectively, in the 3-day-SE group. The bushy and amoeboid phenotypes also were the most abundant morphologies in the CA3 (27 and 50%, respectively) and DG areas (31 and 64%, respectively).

At 2 weeks after SE, the increase in the numbers of microglia in the hippocampus was significantly different when compared to control (**Figure 1**), and was coupled with a change in the morphology from 1—ramified to 2- through 5- phenotypes (**Figure 3D**). The distribution of the microglia/macrophage population in the 2-week-SE CA1 hippocampi was 6% ramified, 8% hypertrophic, 19% bushy, 42% amoeboid, and 25% rod. In the CA3 area of the 2-week-SE group, only 10% of the IBA1-positive cells were ramified while the larger population consisted of hypertrophic (17%), bushy (34%), and amoeboid (38%) with few rods (1%). In the DG, we observed a population that consisted of 2% ramified, 9% hypertrophic, 40% bushy, and 48% amoeboid cells.

Overall, we found that the SE-induced changes in the microglia/macrophage morphological phenotype occurred as early as 4 hrs and persisted for at least 2 weeks after the prolonged seizures in all hippocampal areas (**Figure 4**). Statistical analyses between the control group and the 4-h-, 3-day-, and 2-week-SE groups showed a significant decrease in the population of ramified cells in CA1 (4 h/3 day: $p = 0.0001$; 2 week, $p < 0.0001$) (**Figure 4A**), CA3 (4 h, $p = 0.0029$; 3 day, $p = 0.0001$; 2 week: $p = 0.0008$) (**Figure 4B**), and DG (4 h, $p = 0.0332$; 3 day, $p = 0.0028$; 2 week: $p = 0.0067$) (**Figure 4C**). Across this time line, the bushy phenotype peaked at 4 h (Ctl vs. 4-h-SE, bushy: CA1, $p = 0.0171$; CA3, $p = 0.0084$; DG, $p = 0.2202$) and slightly decreased thereafter. The amoeboid phenotype was significantly more abundant in the 3day-SE (Ctl vs. 3-day-SE, amoeboid: CA1, $p = 0.0185$; CA3, $p = 0.0268$; DG, $p = 0.0054$) and 2-week-SE groups compared to controls (Ctl vs. 2-week-SE, amoeboid: CA1, $p = 0.0043$; CA3, $p = 0.0047$; DG, $p = 0.0013$), where few cells

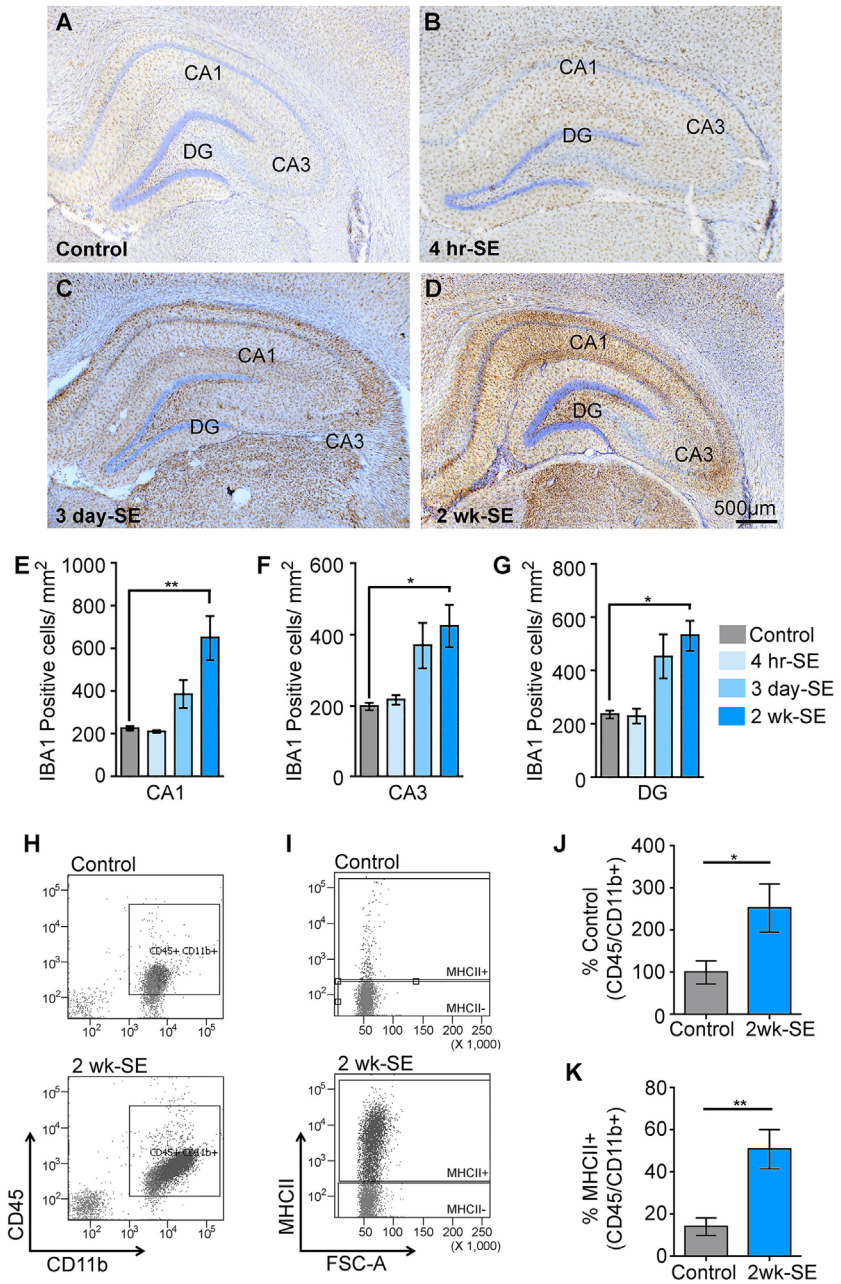

FIGURE 1 | Status epilepticus (SE) provokes an increase in the number of microglia/macrophages in the hippocampus. **(A–D)** Representative images showing IBA1-postivibe immunoreactive cells in hippocampi from control **(A)** and SE groups at 4 h **(B)**, 3 days **(C)**, and 2 weeks **(D)** after the prolonged seizures. Nissl-stained nuclei are shown in blue. **(E–G)** Quantitative analysis of IBA1-positive cells in the hippocampal regions CA1 **(E)**, CA3 **(F)**, and dentate gyrus (DG) **(G)** from controls and SE groups. **(H–K)** Flow cytometry gating analysis of cluster of differentiation 45 (CD45) and cluster of differentiation molecule 11b (CD11b) **(H,J)**, and major histocompatibility complex class II (MHCII) **(I,K)** positive microglia/macrophages in hippocampal cell suspensions from control and 2-week-SE groups are shown **(J–K)**, show the analysis of the percentage of CD45/Cd11b+ positive cells **(J)** and from those the number of MHC11+ cell **(K)**. Data are shown as M ± SEM. $^{*}p < 0.05$, $^{**}p < 0.002$ by analysis of variance with Dunnett's multiple comparison test.

displayed that morphology. Interestingly, a significant increase in the percentage of rod microglia was only found in the CA1 area of the 2-week-SE group (Ctl vs. 2-week-SE, rod: CA1, $p = 0.0063$; CA3, $p = 0.1436$; DG, $p = 0.3653$). Taken together, these data support that SE induces time-dependent changes in microglia/macrophage morphology throughout the hippocampus.

DISCUSSION

The main findings of this study are that a single episode of SE triggers: (1) an increase in the number of microglia/macrophages in the hippocampus that is significantly different from controls at 2 weeks after SE (**Figure 1**); (2) time-dependent changes that

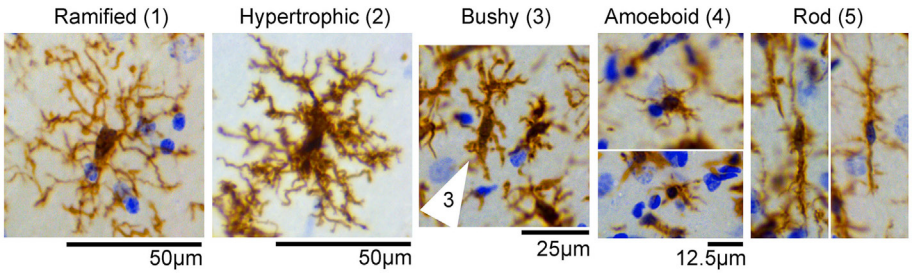

FIGURE 2 | IBA1-positive cells display different morphologies in the hippocampus. Representative images of microglia/macrophage cells (brown) with different morphological phenotypes observed in control and status epilepticus (SE) groups included (1) ramified, (2) hypertrophic, (3) bushy (cell indicated by arrow), (4) amoeboid, and (5) rod. Images were taken from hippocampi of control or SE animals. Nissl-stained nuclei are shown in blue.

are characterized by an increase in the population of microglia/macrophage with bushy shapes which peak at 4 h and are followed by an increase in the abundance of amoeboid cells at 3 days and 2 weeks after the prolonged seizures (**Figures 3** and **4**); and (3) a significant increase in the number of rod-shaped cells was only evident in the CA1 region at 2 weeks post-SE (**Figures 3** and **4**). Substantial evidence supports activation of microglial cells in humans and experimental epilepsy (4, 5). However, to our knowledge, this is the first study to perform a spatiotemporal analysis of the *population* of hippocampal IBA1-positive cells with different morphologies in the adult rat pilocarpine model of SE and acquired temporal lobe epilepsy.

Altered morphologies from the typical ramified phenotype, as well as expression and levels of cytokines and chemokines, have been widely used to identify microglial activation in human and experimental epilepsy, including in response to SE (17, 22, 24, 25, 27, 38, 39). For instance, using 3D reconstructions and morphometric analysis, Shapiro et al. (25) reported that following pilocarpine-induced SE, the IBA1-positive microglial cells in the adult hilus displayed different morphologies that included cells with larger and elongated cell bodies with thick and dense processes (hypertrophic), cells with thickened but complexed processes (bushy), and cells with rod cell body morphology at 1-, 3-, and 5-days, respectively, after the prolonged seizures (25). Consistent with their findings, we identified multiple microglia/macrophages with these morphologies in the DG area at all time points. We also found an increase in the amount of MHCII-positive cells at 2 weeks after SE suggesting a heterologous population of microglia with different M1/M2 polarization phenotypes at this time point (40). Furthermore, a comparable spatial and temporal profile of microglial morphological changes along with an increased population of microglia in the CA1 area were reported in the adult hippocampus following kainic acid and ischemic insults (41, 42) as well as microgliosis after corneal kindling and Theiler murine encephalomyelitis virus (26). Together, these studies, in different models that promote SE and epilepsy, suggest the possibility that neuronal hyperexcitability and injury may contribute to the microglial changes.

Similar to the adult brain, microglia/macrophages in the developing hippocampus also respond with evident morphological changes when exposed to SE (27, 43–45). For example, Patterson et al. (27) demonstrated that early-life SE induced by fever is associated with an acute increase in the abundance of amoeboid IBA1-positive cells, but not total microglia/macrophages, throughout the hippocampus. This was coupled to increased levels of TNFα (27). In the adult hippocampus, it is noticeable that the appearance of hypertrophic/bushy phenotypes parallels the time points when the cytokines TNFα and IL-1β were highest in the hippocampus after pilocarpine-induced SE (22, 24). Although the specific functional role of each of the morphologies is not definitively known, this observation suggests the possibility that hypertrophic/bushy microglia/macrophages may be associated with the production and release of inflammatory molecules.

One of the most interesting observations was the accumulation of rod-shaped microglial cells in the CA1 area of the 2-week-SE group (**Figure 3**). This type of microglia is also found in human brain samples associated with drug-resistant epilepsy (39). Interestingly, rod microglia have been found wrapped along apical dendrites of cortical neurons that were also surrounded by activated microglia in the human epileptic tissue samples (39). This type of interaction has also been reported in other human neurological and psychiatric disorders that include viral infections and dementia (11, 46). Evidence suggests that the interactions between rod microglia and dendrites also occur following brain injury (14, 47). While the physiological significance of rod-shaped microglia and their tight interactions with dendritic processes remains to be defined, it has been argued that rod microglia may be required to prevent further damage to injured areas (47). In addition, it is also possible that the microglia–dendritic contacts, independent of microglial morphology, may result in synaptic stripping (48–50). Recent studies support that microglia–dendritic interactions increase after SE (5–7, 23, 51). Interestingly, we reported a spatiotemporal correlation between increased IBA1 immunoreactivity, loss of Map2 immunostaining, and a reduction in dendritic spines in the CA1 hippocampus (22). These paralleled colocalization of multiple IBA1-labeled microglial processes with Map2-labeled CA1 apical dendrites 2 weeks following SE (23), when the population of microglia is mostly amoeboid and rod. Thus, we speculate that these microglia morphologies may contribute to the dendritic structural plasticity in CA1. However, whether these neuro–immune interactions are beneficial or detrimental for synaptodendritic stability after SE requires investigation.

Overall, the time course of the SE-induced microglia/macrophage morphological alterations and activation follows the

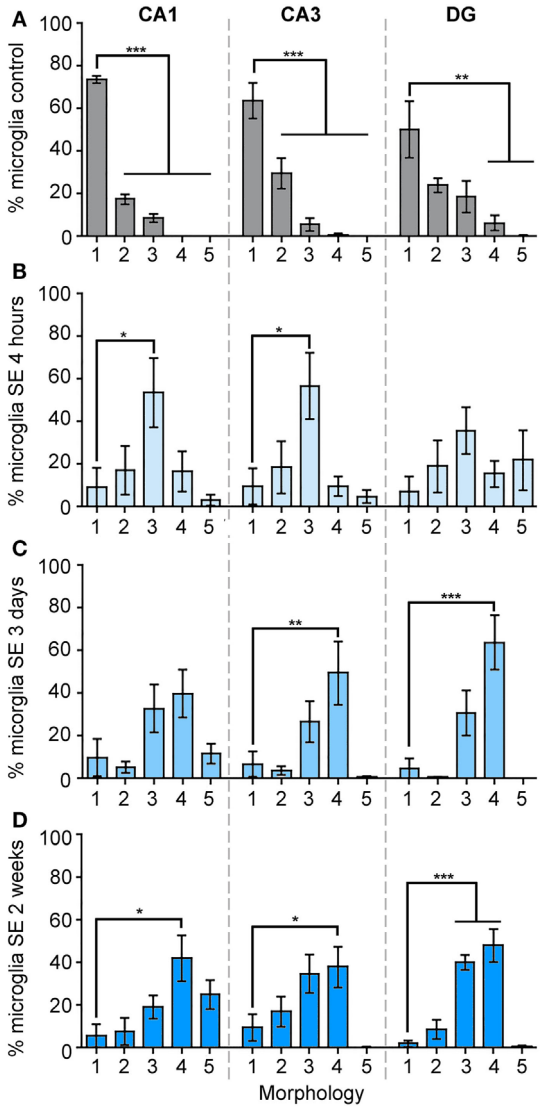

FIGURE 3 | The morphology of IBA1-positive cells is mainly ramified in control hippocampi, and mainly bushy at 4 h, amoeboid at 3 days, and bushy/amoeboid at 2 weeks following status epilepticus (SE). Panels **(A–D)** show the analysis of the percentage of IBA1-positive cells of different morphologies: (1) ramified, (2) hypertrophic, (3) bushy, (4) amoeboid, and (5) rod, in the hippocampal CA1, CA3, and dentate gyrus areas in the control samples **(A)**, and in 4 h **(B)**, 3 days **(C)**, and 2 weeks **(D)** following SE samples. Data are shown as M ± SEM. *$p < 0.05$, **$p < 0.001$, ***$p < 0.0001$ by analysis of variance with Dunnett's multiple comparison test.

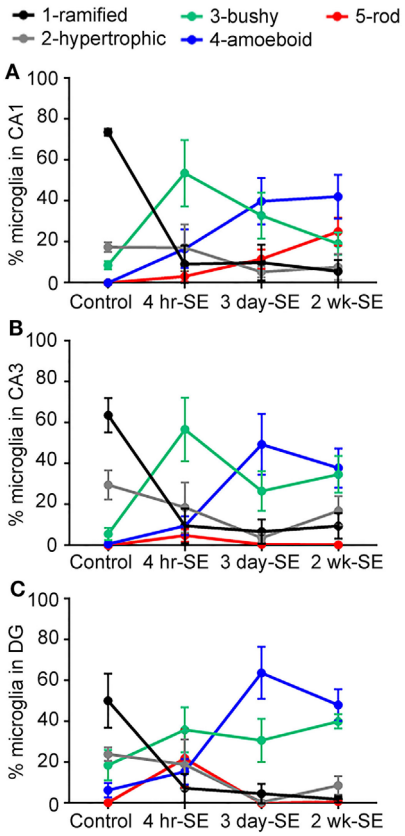

FIGURE 4 | Status epilepticus (SE) triggers time-dependent changes in the morphology of IBA1-positive cells in the hippocampus. Panels **(A–C)** show the percentage of total hippocampal microglia/macrophage population of the different morphologies (1) ramified (black), (2) hypertrophic (gray), (3) bushy (green), (4) amoeboid (blue), and (5) rod (red) in the CA1 **(A)**, CA3 **(B)**, and dentate gyrus **(C)** hippocampal areas of control, 4-hr-SE, 3-day-SE, and 2-wk-SE groups. Note that the exact *p* values calculated from the statistical analyses of all data shown in this figure are described in the Section "Results."

classical descriptions of microglial plasticity from the ramified to the amoeboid morphology which may be associated with different functional roles (10, 15, 52). Ramified microglia are very dynamic and contribute to the physiology of developing and adult brains (8, 15, 52, 53). For instance, *in vivo* imaging studies demonstrated that ramified microglial cells are highly active, regularly survey their microenvironment, and make direct contacts with synaptodendritic structures in an activity-dependent manner (7, 8, 54, 55). Ramified microglia help maintain homeostasis in neuronal circuities by promoting, for example, dendritic spine growth (56), elimination of extranumerary synapses in developing networks (49, 50) as well as phagocytosis of the excessive apoptotic newborn cells in the hippocampal sub-ventricular zone (9, 28). Moreover, in response to immune disturbances, these cells alter their actin cytoskeleton to the different morphological phenotypes that include but are not limited to hypertrophic, bushy, and amoeboid. Based on our observations, the increased microgliosis seen at 3 days after SE (**Figure 1**) with bushy and amoeboid morphologies (**Figure 3**) paralleled an increase in the number of cleaved caspase 3-positive cells in CA1 hippocampus (22). This suggests the possibility that the microgliosis seen at 3 days after SE may be linked to the need for clearing the apoptotic cells. Although the amoeboid and bushy morphologies are often associated with inflammatory responses, as well as a high phagocytic capacity, the extent to which each of the morphologies relates to specific functions in the brain is still unclear. This is because most available evidence for morphology–function associations comes from *in vitro* cell culture studies (10, 15).

CONCLUSION

This study shows that the abundance of microglia/macrophage of different morphologies (ramified, hypertrophic, bushy, amoeboid, and rod) in the hippocampus evolves between 4 h and 2 weeks following a single episode of SE. These data suggest that at different time points, distinct populations of microglia may serve specific functions, such as surveillance for ramified cells, perhaps inflammatory for hypertrophic and bushy at 4 h and 3 days after SE, and potentially highly phagocytic at the amoeboid stage (3 days and 2 weeks after SE). However, to determine these possibilities, comprehensive histological studies that directly identify their biochemical profile with specific inflammatory (M1/M2 polarization) (53) and phagocytic makers/indexes (57) are required. Substantial evidence supports that microglia activation plays a critical role in some of the neuropathology and pathophysiology associated with SE, and has been linked to the modulation of memory (58, 59), psychiatric disorders (60), and even suicide (61), all of which have been reported in epilepsy (62, 63). Studies using immunosuppressant drugs such as rapamycin, FK506, and minocycline, which modulate microglial activation (64), support that reactive microglia contribute to seizure-induced cell death and spine loss in the hippocampus as well as the development of spontaneous seizures and cognitive decline in some models of SE and epilepsy (23, 65–71). However, here, we show that there is a heterologous population of microglia of different morphologies throughout the hippocampus that can potentially promote neuroprotection and/or neurodegeneration to their surrounding neurons. Thus, understanding the morphologies of microglia, and their associated inflammatory/phagocytic phenotypes throughout the development of epilepsy after SE could allow for more targeted treatments focused on specifically altering the detrimental signals. This may provide different insights and potentially new directions in how we target and manage SE.

ETHICS STATEMENT

This study was carried out in accordance with the recommendations of Institutional and NIH guidelines and Purdue Animal Care and Use Committee.

AUTHOR CONTRIBUTIONS

SW-J conducted induction of SE, perfusions, immunohistochemistry, imaging acquisition, analysis, performed cell counts along with densitometry analyses blinded to treatment groups, flow cytometry, and wrote the manuscript. SH conducted imaging acquisition, analysis, performed cell counts along with densitometry analyses blinded to treatment groups, flow cytometry, and wrote the manuscript. AB designed and initiated the project, and wrote the manuscript. SW-J, SH, and AB participated in the discussion of the experiments, data, and manuscript.

ACKNOWLEDGMENTS

The authors thank Drs. Jeff Woodliff and Jill Hutchcroft, from the Bindley Bioscience Flow Cytometry and Cell Separation Facility, for their assistance with the flow cytometry data collection, analysis, and interpretation; Dr. Jorge Iván Alvarez for technical advice on brain tissue processing and cell labeling for flow cytometry; and gratefully acknowledge the Purdue Flow Core support from the Purdue University Center for Cancer Research, NIH grant P30 CA023168.

FUNDING

The flow cytometry experiments were supported, in part, with support from the Indiana Clinical and Translational Sciences Institute funded, in part by Award Number UL1TR001108 from the National Institutes of Health, National Center for Advancing Translational Sciences, and Clinical and Translational Sciences Award (ALB). The content is solely the responsibility of the authors and does not necessarily represent the official views of the National Institutes of Health.

SUPPLEMENTARY MATERIAL

The Supplementary Material for this article can be found online at http://www.frontiersin.org/articles/10.3389/fneur.2017.00700/full#supplementary-material.

REFERENCES

1. Lawson T, Yeager S. Status epilepticus in adults: a review of diagnosis and treatment. *Crit Care Nurse* (2016) 36:62–73. doi:10.4037/ccn2016892
2. Jensen FE. Epilepsy as a spectrum disorder: implications from novel clinical and basic neuroscience. *Epilepsia* (2011) 52(Suppl 1):1–6. doi:10.1111/j.1528-1167.2010.02904.x
3. Devinsky O, Vezzani A, Najjar S, De Lanerolle NC, Rogawski MA. Glia and epilepsy: excitability and inflammation. *Trends Neurosci* (2013) 36:174–84. doi:10.1016/j.tins.2012.11.008
4. Vezzani A, French J, Bartfai T, Baram TZ. The role of inflammation in epilepsy. *Nat Rev Neurol* (2011) 7:31–40. doi:10.1038/nrneurol.2010.178
5. Eyo UB, Murugan M, Wu LJ. Microglia-neuron communication in epilepsy. *Glia* (2016) 65:5–18. doi:10.1002/glia.23006
6. Eyo UB, Gu N, De S, Dong H, Richardson JR, Wu LJ. Modulation of microglial process convergence toward neuronal dendrites by extracellular calcium. *J Neurosci* (2015) 35:2417–22. doi:10.1523/JNEUROSCI.3279-14.2015
7. Eyo UB, Peng J, Swiatkowski P, Mukherjee A, Bispo A, Wu LJ. Neuronal hyperactivity recruits microglial processes via neuronal NMDA receptors and microglial P2Y12 receptors after status epilepticus. *J Neurosci* (2014) 34:10528–40. doi:10.1523/JNEUROSCI.0416-14.2014
8. Tremblay ME, Stevens B, Sierra A, Wake H, Bessis A, Nimmerjahn A. The role of microglia in the healthy brain. *J Neurosci* (2011) 31:16064–9. doi:10.1523/JNEUROSCI.4158-11.2011
9. Sierra A, Encinas JM, Deudero JJ, Chancey JH, Enikolopov G, Overstreet-Wadiche LS, et al. Microglia shape adult hippocampal neurogenesis through apoptosis-coupled phagocytosis. *Cell Stem Cell* (2010) 7:483–95. doi:10.1016/j.stem.2010.08.014
10. Kettenmann H, Hanisch UK, Noda M, Verkhratsky A. Physiology of microglia. *Physiol Rev* (2011) 91:461–553. doi:10.1152/physrev.00011.2010
11. Graeber MB. Changing face of microglia. *Science* (2010) 330:783–8. doi:10.1126/science.1190929
12. Torres-Platas SG, Comeau S, Rachalski A, Bo GD, Cruceanu C, Turecki G, et al. Morphometric characterization of microglial phenotypes in human cerebral cortex. *J Neuroinflammation* (2014) 11:12. doi:10.1186/1742-2094-11-12

13. Taylor SE, Morganti-Kossmann C, Lifshitz J, Ziebell JM. Rod microglia: a morphological definition. *PLoS One* (2014) 9:e97096. doi:10.1371/journal.pone.0097096
14. Ziebell JM, Taylor SE, Cao T, Harrison JL, Lifshitz J. Rod microglia: elongation, alignment, and coupling to form trains across the somatosensory cortex after experimental diffuse brain injury. *J Neuroinflammation* (2012) 9:247. doi:10.1186/1742-2094-9-247
15. Sierra A, Abiega O, Shahraz A, Neumann H. Janus-faced microglia: beneficial and detrimental consequences of microglial phagocytosis. *Front Cell Neurosci* (2013) 7:6. doi:10.3389/fncel.2013.00006
16. Morrison HW, Filosa JA. A quantitative spatiotemporal analysis of microglia morphology during ischemic stroke and reperfusion. *J Neuroinflammation* (2013) 10:4. doi:10.1186/1742-2094-10-4
17. Wyatt SK, Witt T, Barbaro NM, Cohen-Gadol AA, Brewster AL. Enhanced classical complement pathway activation and altered phagocytosis signaling molecules in human epilepsy. *Exp Neurol* (2017) 295:184–93. doi:10.1016/j.expneurol.2017.06.009
18. Schiering IA, de Haan TR, Niermeijer JM, Koelman JH, Majoie CB, Reneman L, et al. Correlation between clinical and histologic findings in the human neonatal hippocampus after perinatal asphyxia. *J Neuropathol Exp Neurol* (2014) 73:324–34. doi:10.1097/NEN.0000000000000056
19. Boer K, Jansen F, Nellist M, Redeker S, van den Ouweland AM, Spliet WG, et al. Inflammatory processes in cortical tubers and subependymal giant cell tumors of tuberous sclerosis complex. *Epilepsy Res* (2008) 78:7–21. doi:10.1016/j.eplepsyres.2007.10.002
20. Aronica E, Boer K, van Vliet EA, Redeker S, Baayen JC, Spliet WG, et al. Complement activation in experimental and human temporal lobe epilepsy. *Neurobiol Dis* (2007) 26:497–511. doi:10.1016/j.nbd.2007.01.015
21. Dachet F, Bagla S, Keren-Aviram G, Morton A, Balan K, Saadat L, et al. Predicting novel histopathological microlesions in human epileptic brain through transcriptional clustering. *Brain* (2015) 138:356–70. doi:10.1093/brain/awu350
22. Schartz ND, Herr SA, Madsen L, Butts SJ, Torres C, Mendez LB, et al. Spatiotemporal profile of Map2 and microglial changes in the hippocampal CA1 region following pilocarpine-induced status epilepticus. *Sci Rep* (2016) 6:24988. doi:10.1038/srep24988
23. Brewster AL, Lugo JN, Patil VV, Lee WL, Qian Y, Vanegas F, et al. Rapamycin reverses status epilepticus-induced memory deficits and dendritic damage. *PLoS One* (2013) 8:e57808. doi:10.1371/journal.pone.0057808
24. Arisi GM, Foresti ML, Katki K, Shapiro LA. Increased CCL2, CCL3, CCL5, and IL-1beta cytokine concentration in piriform cortex, hippocampus, and neocortex after pilocarpine-induced seizures. *J Neuroinflammation* (2015) 12:129. doi:10.1186/s12974-015-0347-z
25. Shapiro LA, Wang L, Ribak CE. Rapid astrocyte and microglial activation following pilocarpine-induced seizures in rats. *Epilepsia* (2008) 49:33–41. doi:10.1111/j.1528-1167.2008.01491.x
26. Loewen JL, Barker-Haliski ML, Dahle EJ, White HS, Wilcox KS. Neuronal injury, gliosis, and glial proliferation in two models of temporal lobe epilepsy. *J Neuropathol Exp Neurol* (2016) 75:366–78. doi:10.1093/jnen/nlw008
27. Patterson KP, Brennan GP, Curran M, Kinney-Lang E, Dube C, Rashid F, et al. Rapid, coordinate inflammatory responses after experimental febrile status epilepticus: implications for epileptogenesis. *eNeuro* (2015) 2:1–13. doi:10.1523/ENEURO.0034-15.2015
28. Abiega O, Beccari S, Diaz-Aparicio I, Nadjar A, Laye S, Leyrolle Q, et al. Neuronal hyperactivity disturbs ATP microgradients, impairs microglial motility, and reduces phagocytic receptor expression triggering apoptosis/microglial phagocytosis uncoupling. *PLoS Biol* (2016) 14:e1002466. doi:10.1371/journal.pbio.1002466
29. Konishi H, Kobayashi M, Kunisawa T, Imai K, Sayo A, Malissen B, et al. Siglec-H is a microglia-specific marker that discriminates microglia from CNS-associated macrophages and CNS-infiltrating monocytes. *Glia* (2017) 65(12):1927–43. doi:10.1002/glia.23204
30. Racine RJ. Modification of seizure activity by electrical stimulation. II. Motor seizure. *Electroencephalogr Clin Neurophysiol* (1972) 32:281–94. doi:10.1016/0013-4694(72)90177-0
31. Nikodemova M, Watters JJ. Efficient isolation of live microglia with preserved phenotypes from adult mouse brain. *J Neuroinflammation* (2012) 9:147. doi:10.1186/1742-2094-9-147
32. Guez-Barber D, Fanous S, Harvey BK, Zhang Y, Lehrmann E, Becker KG, et al. FACS purification of immunolabeled cell types from adult rat brain. *J Neurosci Methods* (2012) 203:10–8. doi:10.1016/j.jneumeth.2011.08.045
33. Alvarez JI, Saint-Laurent O, Godschalk A, Terouz S, Briels C, Larouche S, et al. Focal disturbances in the blood-brain barrier are associated with formation of neuroinflammatory lesions. *Neurobiol Dis* (2015) 74:14–24. doi:10.1016/j.nbd.2014.09.016
34. Alvarez JI, Kebir H, Cheslow L, Chabarati M, Larochelle C, Prat A. JAML mediates monocyte and CD8 T cell migration across the brain endothelium. *Ann Clin Transl Neurol* (2015) 2:1032–7. doi:10.1002/acn3.255
35. Long JM, Kalehua AN, Muth NJ, Hengemihle JM, Jucker M, Calhoun ME, et al. Stereological estimation of total microglia number in mouse hippocampus. *J Neurosci Methods* (1998) 84:101–8. doi:10.1016/S0165-0270(98)00100-9
36. Sadasivan S, Pond BB, Pani AK, Qu C, Jiao Y, Smeyne RJ. Methylphenidate exposure induces dopamine neuron loss and activation of microglia in the basal ganglia of mice. *PLoS One* (2012) 7:e33693. doi:10.1371/journal.pone.0033693
37. Kosonowska E, Janeczko K, Setkowicz Z. Inflammation induced at different developmental stages affects differently the range of microglial reactivity and the course of seizures evoked in the adult rat. *Epilepsy Behav* (2015) 49:66–70. doi:10.1016/j.yebeh.2015.04.063
38. Choi J, Koh S. Role of brain inflammation in epileptogenesis. *Yonsei Med J* (2008) 49:1–18. doi:10.3349/ymj.2008.49.1.1
39. Wirenfeldt M, Clare R, Tung S, Bottini A, Mathern GW, Vinters HV. Increased activation of Iba1+ microglia in pediatric epilepsy patients with Rasmussen's encephalitis compared with cortical dysplasia and tuberous sclerosis complex. *Neurobiol Dis* (2009) 34:432–40. doi:10.1016/j.nbd.2009.02.015
40. Ponomarev ED, Veremeyko T, Weiner HL. MicroRNAs are universal regulators of differentiation, activation, and polarization of microglia and macrophages in normal and diseased CNS. *Glia* (2013) 61:91–103. doi:10.1002/glia.22363
41. Jorgensen MB, Finsen BR, Jensen MB, Castellano B, Diemer NH, Zimmer J. Microglial and astroglial reactions to ischemic and kainic acid-induced lesions of the adult rat hippocampus. *Exp Neurol* (1993) 120:70–88. doi:10.1006/exnr.1993.1041
42. Varvel NH, Neher JJ, Bosch A, Wang W, Ransohoff RM, Miller RJ, et al. Infiltrating monocytes promote brain inflammation and exacerbate neuronal damage after status epilepticus. *Proc Natl Acad Sci U S A* (2016) 113:E5665–74. doi:10.1073/pnas.1604263113
43. Ravizza T, Rizzi M, Perego C, Richichi C, Veliskova J, Moshe SL, et al. Inflammatory response and glia activation in developing rat hippocampus after status epilepticus. *Epilepsia* (2005) 46:113–7. doi:10.1111/j.1528-1167.2005.01006.x
44. Rizzi M, Perego C, Aliprandi M, Richichi C, Ravizza T, Colella D, et al. Glia activation and cytokine increase in rat hippocampus by kainic acid-induced status epilepticus during postnatal development. *Neurobiol Dis* (2003) 14:494–503. doi:10.1016/j.nbd.2003.08.001
45. Kazl C, Foote LT, Kim MJ, Koh S. Early-life experience alters response of developing brain to seizures. *Brain Res* (2009) 1285:174–81. doi:10.1016/j.brainres.2009.05.082
46. Bachstetter AD, Van Eldik LJ, Schmitt FA, Neltner JH, Ighodaro ET, Webster SJ, et al. Disease-related microglia heterogeneity in the hippocampus of Alzheimer's disease, dementia with Lewy bodies, and hippocampal sclerosis of aging. *Acta Neuropathol Commun* (2015) 3:32. doi:10.1186/s40478-015-0209-z
47. Au NPB, Ma CHE. Recent advances in the study of bipolar/rod-shaped microglia and their roles in neurodegeneration. *Front Aging Neurosci* (2017) 9:128. doi:10.3389/fnagi.2017.00128
48. Schafer DP, Lehrman EK, Stevens B. The "quad-partite" synapse: microglia-synapse interactions in the developing and mature CNS. *Glia* (2013) 61:24–36. doi:10.1002/glia.22389
49. Schafer DP, Lehrman EK, Kautzman AG, Koyama R, Mardinly AR, Yamasaki R, et al. Microglia sculpt postnatal neural circuits in an activity and complement-dependent manner. *Neuron* (2012) 74:691–705. doi:10.1016/j.neuron.2012.03.026
50. Paolicelli RC, Bolasco G, Pagani F, Maggi L, Scianni M, Panzanelli P, et al. Synaptic pruning by microglia is necessary for normal brain development. *Science* (2011) 333:1456–8. doi:10.1126/science.1202529

51. Eyo UB, Peng J, Murugan M, Mo M, Lalani A, Xie P, et al. Regulation of physical microglia-neuron interactions by Fractalkine signaling after status epilepticus. *eNeuro* (2016) 3:1–14. doi:10.1523/ENEURO.0209-16.2016
52. Tay TL, Savage JC, Hui CW, Bisht K, Tremblay ME. Microglia across the lifespan: from origin to function in brain development, plasticity and cognition. *J Physiol* (2017) 595:1929–45. doi:10.1113/JP272134
53. Boche D, Perry VH, Nicoll JA. Review: activation patterns of microglia and their identification in the human brain. *Neuropathol Appl Neurobiol* (2013) 39:3–18. doi:10.1111/nan.12011
54. Nimmerjahn A. Two-photon imaging of microglia in the mouse cortex in vivo. *Cold Spring Harb Protoc* (2012) 2012:594–603. doi:10.1101/pdb.prot069294
55. Nimmerjahn A, Kirchhoff F, Helmchen F. Resting microglial cells are highly dynamic surveillants of brain parenchyma in vivo. *Science* (2005) 308:1314–8. doi:10.1126/science.1110647
56. Parkhurst CN, Yang G, Ninan I, Savas JN, Yates JR III, Lafaille JJ, et al. Microglia promote learning-dependent synapse formation through brain-derived neurotrophic factor. *Cell* (2013) 155:1596–609. doi:10.1016/j.cell.2013.11.030
57. Diaz-Aparicio I, Beccari S, Abiega O, Sierra A. Clearing the corpses: regulatory mechanisms, novel tools, and therapeutic potential of harnessing microglial phagocytosis in the diseased brain. *Neural Regen Res* (2016) 11:1533–9. doi:10.4103/1673-5374.193220
58. Williamson LL, Sholar PW, Mistry RS, Smith SH, Bilbo SD. Microglia and memory: modulation by early-life infection. *J Neurosci* (2011) 31:15511–21. doi:10.1523/JNEUROSCI.3688-11.2011
59. Morris GP, Clark IA, Zinn R, Vissel B. Microglia: a new frontier for synaptic plasticity, learning and memory, and neurodegenerative disease research. *Neurobiol Learn Mem* (2013) 105:40–53. doi:10.1016/j.nlm.2013.07.002
60. Kandratavicius L, Peixoto-Santos JE, Monteiro MR, Scandiuzzi RC, Carlotti CG Jr, Assirati JA Jr, et al. Mesial temporal lobe epilepsy with psychiatric comorbidities: a place for differential neuroinflammatory interplay. *J Neuroinflammation* (2015) 12:38. doi:10.1186/s12974-015-0266-z
61. Steiner J, Bielau H, Brisch R, Danos P, Ullrich O, Mawrin C, et al. Immunological aspects in the neurobiology of suicide: elevated microglial density in schizophrenia and depression is associated with suicide. *J Psychiatr Res* (2008) 42:151–7. doi:10.1016/j.jpsychires.2006.10.013
62. Tellez-Zenteno JF, Patten SB, Jette N, Williams J, Wiebe S. Psychiatric comorbidity in epilepsy: a population-based analysis. *Epilepsia* (2007) 48:2336–44. doi:10.1111/j.1528-1167.2007.01222.x
63. Rzezak P, Lima EM, Gargaro AC, Coimbra E, de Vincentiis S, Velasco TR, et al. Everyday memory impairment in patients with temporal lobe epilepsy caused by hippocampal sclerosis. *Epilepsy Behav* (2017) 69:31–6. doi:10.1016/j.yebeh.2017.01.008
64. Hailer NP. Immunosuppression after traumatic or ischemic CNS damage: it is neuroprotective and illuminates the role of microglial cells. *Prog Neurobiol* (2008) 84:211–33. doi:10.1016/j.pneurobio.2007.12.001
65. Zeng LH, Rensing NR, Wong M. The mammalian target of rapamycin signaling pathway mediates epileptogenesis in a model of temporal lobe epilepsy. *J Neurosci* (2009) 29:6964–72. doi:10.1523/JNEUROSCI.0066-09.2009
66. Moriwaki A, Lu YF, Tomizawa K, Matsui H. An immunosuppressant, FK506, protects against neuronal dysfunction and death but has no effect on electrographic and behavioral activities induced by systemic kainate. *Neuroscience* (1998) 86:855–65. doi:10.1016/S0306-4522(98)00071-2
67. Nishimura T, Imai H, Minabe Y, Sawa A, Kato N. Beneficial effects of FK506 for experimental temporal lobe epilepsy. *Neurosci Res* (2006) 56:386–90. doi:10.1016/j.neures.2006.08.006
68. Yilmaz I, Adiguzel E, Akdogan I, Kaya E, Hatip-Al-Khatib I. Effects of second generation tetracyclines on penicillin-epilepsy-induced hippocampal neuronal loss and motor incoordination in rats. *Life Sci* (2006) 79:784–90. doi:10.1016/j.lfs.2006.02.027
69. Heo K, Cho YJ, Cho KJ, Kim HW, Kim HJ, Shin HY, et al. Minocycline inhibits caspase-dependent and -independent cell death pathways and is neuroprotective against hippocampal damage after treatment with kainic acid in mice. *Neurosci Lett* (2006) 398:195–200. doi:10.1016/j.neulet.2006.01.027
70. Kwon YS, Pineda E, Auvin S, Shin D, Mazarati A, Sankar R. Neuroprotective and antiepileptogenic effects of combination of anti-inflammatory drugs in the immature brain. *J Neuroinflammation* (2013) 10:30. doi:10.1186/1742-2094-10-30
71. van Vliet EA, Otte WM, Wadman WJ, Aronica E, Kooij G, de Vries HE, et al. Blood-brain barrier leakage after status epilepticus in rapamycin-treated rats II: potential mechanisms. *Epilepsia* (2016) 57:70–8. doi:10.1111/epi.13245

Conflict of Interest Statement: The authors declare that the research was conducted in the absence of any commercial or financial relationship that could be construed as a potential conflict of interest.

frontiers in Neurology

ORIGINAL RESEARCH
published: 26 September 2017
doi: 10.3389/fneur.2017.00507

Socioeconomic Outcome and Quality of Life in Adults after Status Epilepticus: A Multicenter, Longitudinal, Matched Case–Control Analysis from Germany

*Lena-Marie Kortland[1], Susanne Knake[1], Felix von Podewils[2], Felix Rosenow[1,3] and Adam Strzelczyk[1,3]**

[1] Epilepsy Center Hessen, Philipps-University, Marburg, Germany, [2] Epilepsy Center Greifswald, Ernst-Moritz-Arndt-University, Greifswald, Germany, [3] Epilepsy Center Frankfurt Rhine-Main, Goethe-University, Frankfurt am Main, Germany

OPEN ACCESS

Edited by:
Batool F. Kirmani, Texas A&M Health Science Center College of Medicine, United States

Reviewed by:
Fengfei Wang, Texas A&M College of Medicine, United States
Dieter Schmidt, Epilepsy Research Group, Germany

***Correspondence:**
Adam Strzelczyk
strzelczyk@med.uni-frankfurt.de

Specialty section:
This article was submitted to Epilepsy, a section of the journal Frontiers in Neurology

Received: *18 August 2017*
Accepted: *08 September 2017*
Published: *26 September 2017*

Citation:
Kortland LM, Knake S, von Podewils F, Rosenow F and Strzelczyk A (2017) Socioeconomic Outcome and Quality of Life in Adults after Status Epilepticus: A Multicenter, Longitudinal, Matched Case–Control Analysis from Germany. Front. Neurol. 8:507. doi: 10.3389/fneur.2017.00507

Background: There is a lack of data concerning socioeconomic outcome and quality of life (QoL) in patients after status epilepticus (SE) in Germany.

Patients and methods: Adult patients treated between 2011 and 2015 due to SE at the university hospitals in Frankfurt, Greifswald, and Marburg were asked to fill out a questionnaire regarding long-term outcome of at least 3 months after discharge. The SE cohort consisted of 25.9% patients with an acute symptomatic, 42% with a remote symptomatic and previous epilepsy, 22.2% with a new-onset remote symptomatic, and 9.9% with other or unknown etiology. A matched case–control analysis was applied for comparison with patients with drug refractory epilepsy and seizure remission, both not previously affected by SE.

Results: A total of 81 patients (mean age: 58.7 ± 18.0 years; 58% female) participated. A non-refractory course was present in 59.3%, while 27.2% had a refractory SE (RSE) and 13.6% had a superrefractory SE (SRSE). Before admission, a favorable modified Rankin Scale (mRS) of 0–3 was found in 82.7% (67/81), deteriorating to 38.3% (31/81) ($p = 0.003$) at discharge. The majority returned home [51.9% (42/81)], 32.1% entered a rehabilitation facility, while 12.3% were transferred to a nursing home and 3.7% to another hospital. The overall mRS at follow-up did not change; 61.8% (45/74) reached an mRS of 0–3. In RSE and SRSE, the proportion with a favorable mRS increased from 45.5% at discharge to 70% at follow-up, while QoL was comparable to a non-refractory SE course. Matched epilepsy controls in seizure remission were treated with a lower mean number of anticonvulsants (1.3 ± 0.7) compared to controls with drug refractory epilepsy (1.9 ± 0.8; $p < 0.001$) or SE (1.9 ± 1.1; $p < 0.001$). A major depression was found in 32.8% of patients with SE and in 36.8% of drug refractory epilepsy, but only in 20.3% of patients in seizure remission. QoL was reduced in all categories (QOLIE-31) in SE patients in comparison with patients in seizure remission, but was comparable to patients with drug refractory epilepsy.

Discussion: Patients after SE show substantial impairments in their QoL and daily life activities. However, in the long term, patients with RSE and SRSE had a relatively

favorable outcome comparable to that of patients with a non-refractory SE course. This underlines the need for efficient therapeutic options in SE.

Keywords: epilepsy, seizure, anticonvulsants, morbidity, mortality

INTRODUCTION

Status epilepticus (SE) presents as a major neurological emergency and is associated with a substantial burden on individuals and society (1–3). Prolonged inpatient treatment and neurological sequelae due to SE lead to substantial direct and indirect costs and result in reduced quality of life (QoL). Rehabilitation and informal care are often necessary following discharge from acute treatment and might result in further costs. Studies on outcome show a substantial portion of patients who are discharged with a neurologic deficit, while overall hospital mortality is about 15–20%. Both SE related morbidity and mortality increase with a refractory course and prolonged inpatient treatment (4–6). Prehospital and in-hospital treatment strategies aim at a timely cessation of seizure activity and consist of benzodiazepines, intravenous anticonvulsants, and anesthetic drugs in selected cases (7).

Given the reduced QoL and increased rate of depression in patients with drug refractory epilepsy, as proven by several studies (8–11), patients with SE are very likely to suffer from decreased QoL and mood disorders. However, there is a paucity of data concerning socioeconomic outcome and QoL in patients after an SE, especially as there is no study on this topic from Germany.

Thus, the objective of this multicenter study is to determine the outcome, resource utilization, and QoL indicators following an episode of SE. For comparison, patients suffering from epilepsy who had never previously experienced an episode of SE were matched by age and gender: we matched two groups, one with a drug refractory epilepsy (DRE) and one with epilepsy patients in seizure remission (SRE) for more than 1 year as they show distinct outcomes regarding QoL, health resource utilization, and mood disorders.

PATIENTS AND METHODS

Study Settings and Design

This longitudinal study on outcome, QoL, and resource utilization was performed by means of a bottom-up approach from the perspective of the statutory health insurer at the university hospitals in Frankfurt am Main, Greifswald, and Marburg. The study was granted approval by the local ethics committees and registered at the German Clinical Trials Register (DRKS00008718). The Strengthening the Reporting of Observational Studies in Epidemiology (STROBE) guidelines were followed (12).

Adult patients of 18 years or older treated due to SE at the participating university hospitals during the 5-year study period of 2011–2015 were asked to fill out a questionnaire regarding long-term outcome for at least 3 months after discharge. Overall, 669 patients were treated due to SE during the study period with an average in-hospital mortality of 18.8% ($n = 126$). Therefore, responder rate was 15% regarding 81 of 543 survivors. The questionnaire was validated for use in people with epilepsy (13, 14). Patients with SE received standard care with no intervention due to the study, and a decision for rehabilitation after SE was at the discretion of the treating physician. An operational definition consistent with ILAE guidelines was adopted that defines convulsive SE as ≥5 min of continuous seizure or two or more discrete seizures, between which there is an incomplete recovery (15, 16). In case of focal SE or absence SE, the definition encompassed at least 5 min of seizure duration; however, none of the patients were identified with a focal SE or absence SE below duration of 20 min (1). Refractory SE (RSE) was defined as recurrent seizure activity despite two appropriately selected and dosed antiepileptic drugs, including benzodiazepine, and superrefractory SE (SRSE) was referred to as a SE that continues or recurs 24 h or more after the initiation of treatment with anesthetic drugs, including cases in which seizure control is attained after induction of anesthesia, but recurs on weaning the patient off the anesthetic agent (4, 17, 18). Patients were assigned to four major groups based on etiology and onset of SE with (1) acute symptomatic SE, due to an acute brain injury as defined by the ILAE (19); (2) new-onset, remote symptomatic SE, with no history of epilepsy or SE; (3) remote symptomatic SE, with history of epilepsy or SE; and (4) other etiologies, such as idiopathic generalized epilepsy or progressive symptomatic causes. The epilepsy diagnosis was based on the definitions proposed by the ILAE and the International Bureau for Epilepsy (20). Patients were excluded if the diagnosis of SE could not be unequivocally determined, or if SE was due to hypoxia after cardiopulmonary resuscitation.

We employed a matched case–control analysis to compare the SE group with two control groups of epilepsy patients, either with drug refractory epilepsy (DRE) or in seizure remission (SRE) for more than 1 year. None of the patients from the epilepsy control groups suffered from an SE during their lifetime. Patients were matched by age and gender. The distribution of age and gender did not differ significantly across the groups, except for SRE patients, who were, in mean, 2 years younger than patients in the SE group.

Instruments

To analyze the health-related QoL, we used scales, such as Quality of Life in Epilepsy Inventory (QOLIE-31) (21), Neurological Disorders Depression Inventory for Epilepsy (NDDI-E) (22), A-B neuropsychological assessment schedule (ABNAS, originally the A-B neurotoxicity scale) (23), Liverpool Adverse Events Profile (LAEP) (24), and the EuroQol questionnaire (EQ-5D) (25). Measures of severity of illness and long-term outcome included the modified Rankin Scale (mRS) (26) on admission, discharge, and follow-up. Healthcare resource utilization is reported as use of inpatient, outpatient, rehabilitation, and anticonvulsive treatment. For cost unit data and details of evaluation, please refer to previous publications (27, 28).

Data Entry and Statistical Analysis

Statistical analyses were performed using IBM SPSS Statistics, version 22.0 (IBM Corp., Armonk, NY, USA). Most data are

presented as percentage or mean ± SD and as minimum and maximum. Comparisons between groups were accomplished using adequate parametric and non-parametric tests. Since the study was planned to have an explorative nature, no further adjustment for multiple testing was performed.

RESULTS

Characteristics of Patients with SE

During the 5-year study period, a total of 81 patients (mean age: 58.7 ± 18.0 years, range: 21–97 years; 58.0% female) participated in the study. An acute symptomatic etiology was present in 25.9% ($n = 21$), a remote symptomatic SE was attributed in 22.2% ($n = 18$) with new-onset SE, and in 42.0% ($n = 34$) of patients with history of epilepsy, other or unknown etiologies were seen in 9.9% (n = 8). Of these cases, 59.3% ($n = 48$) had a non-RSE, 27.2% ($n = 22$) an RSE, and 13.6% ($n = 11$) had an SRSE. Details of clinical or socioeconomic characteristics and QoL at least 3 months after SE are provided in **Table 1**.

Before admission, a favorable mRS of 0–3 was present in 82.7% ($n = 67$), while an unfavorable mRS of 4–5 was seen in 17.3% ($n = 14$) of the SE population. On discharge, mRS decreased significantly with 31 patients (38.3%, $p = 0.003$) rated at an unfavorable mRS of 4–5. The mRS at follow-up did not differ from the one at discharge; 60.8% (45/74) presented an mRS of 0–3 and 39.2% (29/74) an mRS of 4–5 (**Figure 1**); seven patients did not report their mRS on follow-up. Regarding RSE and SRSE, a favorable mRS of 0–3 was present in 45.5% at discharge and increased to 70% at follow-up.

At discharge, the majority returned home (51.9%, $n = 42$), 32.1% ($n = 26$) entered a rehabilitation facility, 12.3% ($n = 10$) were transferred into a nursing home, and 3.7% ($n = 3$) to another hospital. At the time of follow-up, 21 patients (25.9%) lived at home without any help, 43 (54%) depended on aid of their families, and partners or of ambulatory nursing care, while 16 patients (19.8%) lived in a nursing home. A care level (Pflegestufe) was attributed to 56.8% and a grade of disability to 79% of the SE patients. Only 9 of 49 patients of working age (18.4%) had been employed at follow-up.

Regarding healthcare resource utilization within the last 3 months, an ambulance transport to hospital was necessary in 13.2%. The mean number of outpatient consultations due to epilepsy amounted to 3.1 ± 3.3 (range 1–17). Overall, 22.5% ($n = 18/81$) of the SE patients were hospitalized due to epilepsy for a mean of 6.8 days within the last 3 months. Patients were in need of ancillary therapies, such as physiotherapy, occupational therapy, or speech therapy, with a mean number of 22.1 ± 18.3 (range 1–80) sessions within the previous 3 months. The number of AEDs did not differ at follow-up compared to discharge (see **Figure 2**).

The evaluation of QoL using the EQ-5D-Index showed 0.57 ± 0.36 on average (0 = death to 1 = full health). Most of the patients showed impairments due to side effects of anticonvulsants; the mean ABNAS score amounted to 34.9 ± 20.8 and 73.6% of the patients reported a high score (ABNAS 0–99, 99 = the worst score, >15=high score, and ≤15=low score) (23).

TABLE 1 | Socioeconomic and clinical characteristics in patients with SE provided for all patients ($n = 81$) and according to a non-RSE ($n = 48$) and RSE or SRSE course ($n = 33$).

	All patients with SE ($n = 81$)	Non-RSE ($n = 48$)	RSE/SRSE ($n = 33$)	p Value[a]
Age (years) at admission				
Mean ± SD	58.7 ± 18.0	61.8 ± 16.8	54.2 ± 18.9	0.063
Range	21–97	23–97	21–80	
Sex	% (*n*)	% (*n*)	% (*n*)	
Male	42.0 (34)	35.4 (17)	51.5 (17)	0.225
Female	58.0 (47)	64.6 (31)	48.5 (16)	
Etiology	% (*n*)	% (*n*)	% (*n*)	
Acute symptomatic	25.9 (21)	16.7 (8)	39.4 (13)	0.021 (Acute vs non-acute)
Remote symptomatic	42.0 (34)	43.8 (21)	39.4 (13)	
New onset SE	22.2 (18)	27.1 (13)	15.2 (5)	
Other or unknown	9.9 (8)	12.5 (6)	6.1 (2)	
mRS at admission	% (*n*)	% (*n*)	% (*n*)	
mRS 0–3	82.7 (67)	81.3 (39)	84.8 (28)	0.673
mRS 4–5	17.3 (14)	18.8 (9)	15.2 (5)	
mRS at discharge	% (*n*)	% (*n*)	% (*n*)	
mRS 0–3	61.7 (50)	72.9 (35)	45.5 (15)	0.012
mRS 4–5	38.3 (31)	27.1 (13)	54.5 (18)	
mRS at follow-up	% (*n*)	% (*n*)	% (*n*)	
mRS 0–3	60.8 (45)	54.5 (24)	70.0 (21)	0.180
mRS 4–5	39.2 (29)	45.5 (20)	30.0 (9)	
Discharge destination	% (*n*)	% (*n*)	% (*n*)	
Home	51.9 (42)	64.6 (31)	33.3 (11)	0.013 (home vs other)
Rehabilitation	32.1 (26)	16.7 (8)	54.5 (18)	
Other hospital	3.7 (3)	2.1 (1)	6.1 (2)	
Nursing home	12.3 (10)	16.7 (8)	6.1 (2)	
Living situation	% (*n*)	% (*n*)	% (*n*)	
At home without help	25.9 (21)	27.1 (13)	24.2 (8)	0.732
At home with help (family, nursing, etc.)	54.0 (43)	47.9 (23)	60.6 (20)	
Nursing home	19.8 (16)	22.9 (11)	15.2 (5)	
n.a.	(1)	(1)		
Care level	% (*n*)	% (*n*)	% (*n*)	
None	33.3 (27)	33.3 (16)	33.3 (11)	0.947
None, but in need of care	8.6 (7)	10.4 (5)	6.1 (2)	
Care level existing	56.8 (46)	54.2 (26)	60.6 (20)	
n.a.	(1)	(1)		
Grade of disability	% (*n*)	% (*n*)	% (*n*)	
Yes	79.0 (64)	79.2 (38)	78.8 (26)	0.820
None	19.8 (16)	18.8 (9)	21.2 (7)	
n.a.	(1)	(1)		
Number of AEDs at discharge	% (*n*)	% (*n*)	% (*n*)	
0	1.2 (1)	-	3.0 (1)	
1	33.3 (27)	43.8 (21)	18.2 (6)	
2	32.1 (26)	35.4 (17)	27.3 (9)	
≥3	33.3 (27)	20.8 (10)	51.5 (17)	
Total (mean ± SD)	2.1 ± 1.0	1.8 ± 0.9	2.5 ± 1.1	0.007
Number of AEDs at follow-up	% (*n*)	% (*n*)	% (*n*)	
0	4.2 (3)	2.4 (1)	6.7 (2)	
1	40.3 (29)	50.0 (21)	26.7 (8)	
2	19.4 (14)	23.8 (10)	13.3 (4)	
≥3	36.1 (26)	23.8 (10)	53.3 (16)	
Total (mean ± SD)	1.9 ± 1.1	1.8 ± 1.0	2.2 ± 1.1	0.113

(*Continued*)

TABLE 1 | Continued

	All patients with SE (n = 81)	Non-RSE (n = 48)	RSE/SRSE (n = 33)	p Value[a]
Healthcare resource utilization within the last 3 months				
Inpatient treatment due to epilepsy	% (n)	% (n)	% (n)	
Yes	22.2 (18)	17.0 (8)	30.3 (10)	0.146
None	77.7 (63)	83.0 (40)	69.7 (23)	
Outpatient hospital treatment due to epilepsy	% (n)	% (n)	% (n)	
Yes	14.3 (11)	11.1 (5)	18.8 (6)	0.316
None	85.7 (70)	88.9 (43)	81.3 (27)	
NDDI-E	% (n)	% (n)	% (n)	
Major depression (Score >15)	32.8 (19)	30.3 (10)	36.0 (9)	0.647
No major depression (Score ≤15)	67.2 (39)	69.7 (23)	64.0 (16)	
ABNAS				
Total (mean ± SD)	34.9 ± 20.8	34.6 ± 20.1	35.2 ± 22.0	0.351
Range	0–72	3–71	0–72	
LAEP				
Total (mean ± SD)	41.9 ± 10.4	41.5 ± 10.3	42.3 ± 10.8	0.997
Range	14–63	20–62	14–63	
QOLIE-31				
Overall T (mean ± SD)	43.5 ± 13.7	44.2 ± 13.9	42.5 ± 13.6	0.870
Range	11–73	11–73	16–66	
VAS (mean ± SD)	48.3 ± 24.5	49.2 ± 22.7	47.2 ± 27.0	0.618

[a]*Comparison between non-RSE and RSE/SRSE.*

SE, status epilepticus; RSE, refractory SE; SRSE, superrefractory SE; mRS, modified Rankin Scale; AEDs, antiepileptic drugs; NIDDI-E, Neurological Disorders Depression inventory for Epilepsy; LAEP, Liverpool Adverse Events Profile; QOLIE, Quality of Life in Epilepsy Inventory; VAS, visual analog scale; ABNAS, A-B neuropsychological assessment schedule.

Table 1 presents the socioeconomic characteristics and QoL in relation to the severity of SE. Admissions were more likely due to an acute symptomatic etiology in patients with RSE or SRSE (39.4%) than with a non-refractory course (16.7%, $p = 0.021$). Furthermore, the course of SE had a significant impact on the degree of disability, as measured by mRS at discharge [mRS 0–3 in 72.9% (35/48) vs 45.5% (15/33); $p = 0.012$]. Patients with RSE and SRSE were discharged with more AEDs [2.5 ± 1.1 (mean ± SD) vs 1.8 ± 0.9; $p = 0.007$], while this difference was not detectable at follow-up ($p = 0.113$). Patients with non-RSE were more frequently discharged home (64.6 vs 33.3%; $p = 0.013$), while more patients with RSE or SRSE were transferred into a rehabilitation center (54.5 vs 16.7%; $p < 0.001$). Concerning the QoL, patients after an RSE or SRSE achieved the same outcome as patients with a non-refractory course, as measured by NDDI-E, ABNAS, LAEP, QOLIE-31, or VAS.

Comparison of QoL between Patients after SE and Patients with Drug Refractory Epilepsy and in Seizure Remission

For each patient after SE, one patient with DRE and one with SRE were matched by age and gender. The mean length of epilepsy amounted to 19.9 ± 17.6 years in DRE and to 17.0 ± 16.0 years in SRE. SE patients had a significantly shorter length of epilepsy (9.3 ± 14.2 years, $p < 0.001$ DRE and $p = 0.001$ SRE) at follow-up.

Table 2 shows the socioeconomic and clinical characteristics and QoL of SE patients at follow-up compared to patients with DRE and SRE. In the two control groups, significantly more patients lived at home independently than in the SE group

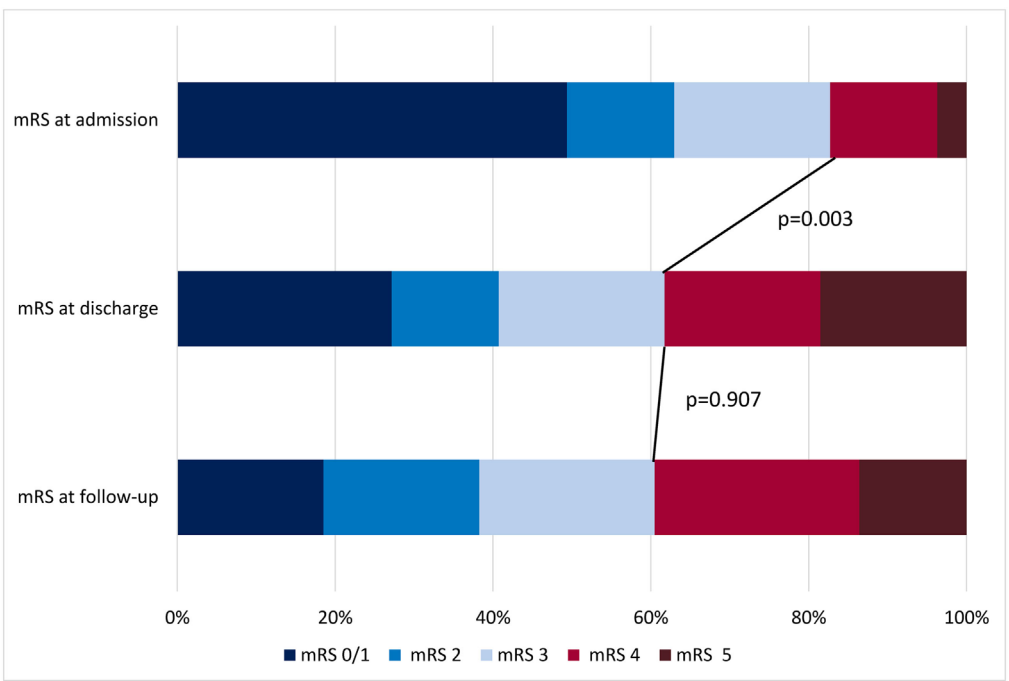

FIGURE 1 | Modified Rankin Scale (mRS) at admission, discharge, and follow-up in patients with status epilepticus.

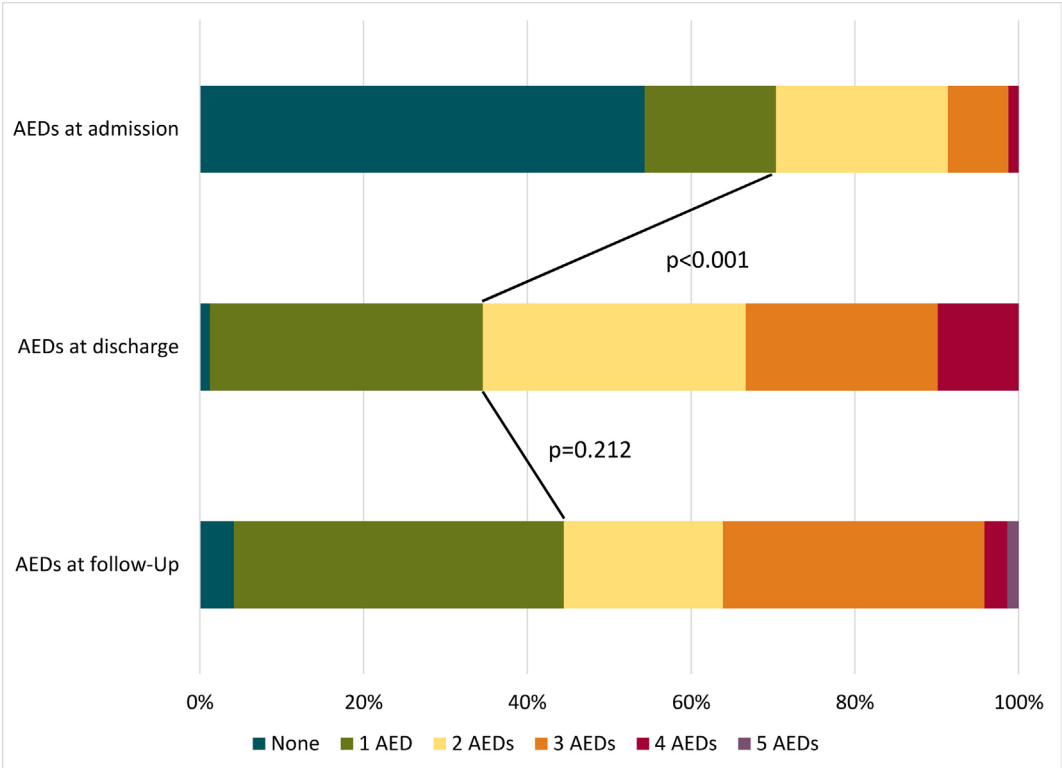

FIGURE 2 | Number of used anticonvulsants at admission, discharge, and follow-up in patients with status epilepticus. AEDs, antiepileptic drugs.

(SE: 25.9%; DRE: 46.3%; $p = 0.008$, SRE: 64.6%; $p < 0.001$), in particular, in the cohort with SRE, no patient lived in a nursing home. Concerning marital status, 70.3% of patients with SRE were married in comparison to 55.6% ($p = 0.048$) of patients in the SE cohort. The mRS at follow-up documented a better state of health for both control groups (mRS 0–3: DRE 98.8%, SRE 97.5%) in comparison to the SE group (mRS 0–3 in 60.8%; $p < 0.001$ each). Regarding epilepsy-related healthcare resource utilization, about 22.2% ($n = 18$) of the SE patients were treated in a hospital, whereas fewer patients with drug refractory epilepsy (11.1%; $n = 9$, $p = 0.057$) and with SRE (1.2%; $n = 1$, $p < 0.001$) were hospitalized due to epilepsy within the last 3 months. Mean length of stay amounted to 6.8 ± 5.9 days (range 1–20) for SE, 7.0 ± 5.2 days (range 1–18) for DRE, and 7.0 days for SRE. An outpatient hospital treatment due to epilepsy was necessary for 14.3% patients with SE, 23.8% of patients with DRE, and 7.9% of patients in SRE. Patients in SRE were treated with a mean number of 1.3 ± 0.7 anticonvulsants (AEDs) and with significantly fewer AEDs than those with drug refractory epilepsy (1.9 ± 0.8; $p < 0.001$) or SE (1.9 ± 1.1; $p < 0.001$).

A major depression, as indicated by NDDI-E, was found in nearly one-third of patients with SE (32.8%) and DRE (36.8%), but only in 20.3% of patients with SRE. Side effects intensity evaluated by the LAEP score was 41.9 ± 10.4 in SE patients, 40.5 ± 11.8 in DRE patients, and lower in SRE patients (37.0 ± 11.8; $p = 0.011$). A better QoL, measured by QOLIE-31 and VAS, was seen for patients in SRE in all categories compared to patients after SE. Regarding the subcategory QoL, both patients with DRE ($p = 0.013$) and SRE ($p < 0.001$) scored better than patients after SE; for details, please refer to **Table 2**.

DISCUSSION

This study on QoL and socioeconomic outcome after an episode of SE is the first comprehensive evaluation to address sequelae and outcome of adult patients with SE and compare them with matched epilepsy controls with a drug refractory course or in SRE. We can show that patients with RSE and SRSE had a deterioration in neurological functions at discharge, which can be set off at follow-up. Furthermore, patients after RSE and SRSE may achieve an equivalent QoL compared to patients after a non-RSE. Despite persistent and increased neurological deficits in patients after SE, these patients may achieve similar QoL values to patients with DRE who have no neurological deficits. However, QoL was reduced in all subcategories of QOLIE-31 when compared to patients in SRE.

Our findings underline the need for an efficient therapy of RSE and SRSE, as these patients will, on average, achieve outcomes comparable to patients with a non-RSE and patients with DRE. That is remarkable as these patients are suffering from persisting neurological deficits, as measured by mRS, and show

TABLE 2 | Socioeconomic and clinical characteristics of patients with SE in comparison to matched epilepsy patients with drug refractory course and in seizure remission (n = 81 in each group).

	SE (n = 81)	Drug-resistant epilepsy (n = 81)	Epilepsy in SRE >1 year (n = 81)	p Value
Age (years) at survey				
Mean ± SD	58.7 ± 18.0	57.3 ± 15.6	56.2 ± 14.0	0.082 (SE vs DRE)
Range	21–97	21–94	20–87	0.001 (SE vs SRE)
Sex	% (n)	% (n)	% (n)	
Male	42.0 (34)	42.0 (34)	42.0 (34)	1.0
Female	58.0 (47)	58.0 (47)	58.0 (47)	
Marital status	% (n)	% (n)	% (n)	
Married or with partner	55.6 (45)	64.2 (52)	70.4 (57)	0.302 (SE vs DRE)
Divorced or in separation	6.2 (5)	7.4 (6)	9.9 (8)	0.048 (SE vs SRE)
Living with family/relatives	7.4 (6)	11.1 (9)	12.3 (10)	
Widowed	29.6 (24)	17.3 (14)	6.2 (5)	
n.a.	(1)		(1)	
Living situation	% (n)	% (n)	% (n)	
At home without help	25.9 (21)	45.7 (37)	62.9 (51)	0.008 (SE vs DRE)
At home with help (family, nursing service)	54.0 (43)	50.6 (41)	34.6 (28)	<0.001 (SE vs SRE)
Nursing home	19.8 (16)	2.5 (2)	–	
n.a.	(1)	(1)	2.5 (2)	
mRS at follow-up	% (n)	% (n)	% (n)	
mRS 0–3	60.8 (45)	98.8 (80)	97.5 (79)	<0.001 each
mRS 4–5	39.2 (29)	1.2 (1)	2.5 (2)	
Number of AEDs at follow-up	% (n)	% (n)	% (n)	
0	4.2 (3)	–	4.9 (4)	
1	40.3 (29)	40.7 (33)	65.4 (53)	
2	19.4 (14)	35.8 (29)	25.9 (21)	
≥3	36.1 (26)	23.5 (19)	3.7 (3)	
Number of AEDs (mean ± SD)	1.9 ± 1.1	1.9 ± 0.8	1.3 ± 0.7	0.632 (SE vs DRE); <0.001 (SE vs SRE)
Healthcare resource utilization within the last 3 months				
Inpatient treatment due to epilepsy	% (n)	% (n)	% (n)	
Yes	22.2 (18)	11.1 (9)	1.2 (1)	0.057 (SE vs DRE)
None	77.7 (63)	88.9 (72)	98.8 (80)	<0.001 (SE vs SRE)
Length of stay (mean ± SD)	6.8 ± 5.9	7.0 ± 5.2	7.0	
Outpatient hospital treatment due to epilepsy	% (n)	% (n)	% (n)	
Yes	14.3 (11)	23.8 (19)	7.9 (6)	0.105 (SE vs DRE)
None	85.7 (70)	76.3 (62)	92.1 (75)	0.2 (SE vs SRE)
NDDI-E	% (n)	% (n)	% (n)	
Major depression (>15 points)	32.8 (19)	36.8 (21)	20.3 (12)	0.79 (SE vs DRE)
No major depression (≤15 points)	67.2 (39)	63.2 (36)	79.7 (47)	0.128 (SE vs SRE)
LAEP	% (n)	% (n)	% (n)	
Total score (mean ± SD)	41.9 ± 10.4	40.5 ± 11.8	37.0 ± 11.8	0.375 (SE vs DRE)
Range	14–63	19–69	19–45	0.011 (SE vs SRE)
QOLIE-31 (1–100, 100 best QoL)	% (n)	% (n)	% (n)	
Overall T	43.5 ± 13.7	44.8 ± 12.8	51.8 ± 12.5	0.698 (SE vs DRE); <0.001 (SE vs SRE)
Quality of Life T	41.7 ± 11.5	46.6 ± 9.7	50.2 ± 11.2	0.013 (SE vs DRE); <0.001 (SE vs SRE)
Seizure Worry T	51.3 ± 12.3	48.9 ± 10.5	56.0 ± 9.7	0.084 (SE vs DRE); 0.042 (SE vs SRE)
Emotional Well-Being T	43.8 ± 11.2	46.3 ± 10.7	49.4 ± 10.8	0.296 (SE vs DRE); 0.009 (SE vs SRE)
Energy-Fatigue T	43.6 ± 9.2	46.3 ± 9.8	49.6 ± 10.1	0.114 (SE vs DRE); 0.002 (SE vs SRE)
Cognitive Functioning T	45.8 ± 12.6	46.8 ± 12.0	50.6 ± 11.9	0.832 (SE vs DRE); 0.011 (SE vs SRE)
Medication Effects T	49.0 ± 10.7	50.8 ± 9.6	53.8 ± 9.3	0.328 (SE vs DRE); 0.011 (SE vs SRE)
Social Functioning T	44.3 ± 11.8	45.2 ± 10.5	52.0 ± 10.4	0.909 (SE vs DRE); <0.001 (SE vs SRE)
VAS (mean ± SD)	48.3 ± 24.5	55.3 ± 22.9	65.3 ± 22.1	0.269 (SE vs DRE) <0.001 (SE vs SRE)

AEDs, antiepileptic drugs; SE, status epilepticus; DRE, drug refractory epilepsy; mRS, modified Rankin Scale; NIDDI-E, Neurological Disorders Depression Inventory for Epilepsy; LAEP, Liverpool Adverse Events Profile; QOLIE, Quality of Life in Epilepsy Inventory; VAS, visual analog scale; SRE, seizure remission.

an increased need for assistance in daily activities. Furthermore, patients with RSE and SRSE improve in neurological outcome over time. This is in line with previous findings, as reported by Lai et al. (29). They reported functional outcome using the mRS in patients with prolonged RSE on admission, discharge, and 1 year after discharge. In their cohort, a favorable outcome of mRS 0–3 increased from 11.5% of patients at discharge to 17.1% of patients at follow-up (29). Ferlisi and Shorvon reported on long-term outcomes of RSE and SRSE, providing mortality rates and data on neurologic defects in 596 cases (4). Overall, 35% of the patients were able to return to baseline, while 13% suffered a severe neurologic deficit, a further 13% had a mild

neurologic deficit and 4% had an undefined neurologic deficit. Mortality accumulated to 35% (4). The preliminary report of the global audit from 44 countries on treatment of RSE and SRSE (30) showed a favorable outcome with an mRS of 0–3 in 36% of the patients at discharge (26.6% = mRS 0–2; 9.4% = mRS 3), which improved to 63.8% at follow-up (42.6% = mRS 0–2; 21.3% = mRS 3). The follow-up was available for 108 patients with an obvious selection bias, as noted by the authors.

A retrospective study from India used the Glasgow Outcome Scale (GOS) to describe outcome. They reported that SRSE had a worse outcome after 6 months in comparison with RSE (33.3 vs 57.1%; $p = 0.055$) and non-RSE (33.3 vs 79.1%; $p < 0.0001$) (31). These findings are well explained by encephalitis as the main underlying etiology in SRSE cases reported from India, an etiology that is independently associated with a poor outcome.

Sutter et al. reported on identification of predictors for outcome involving clinical features such as age, history of prior seizures or epilepsy, SE etiology, level of consciousness, and seizure type at SE onset (6). Determination of predictors from our study is hindered by the limited sample size. However, overall mortality rates of the overall SE group and outcome measures (mRS or GOS) are in line with previous publications (4, 5, 29, 31).

Patients after SE achieved QoL scores comparable to patients with DRE who had never suffered from SE. Given the neurological deficits in the SE group, these seem rather surprising. Strong determinants of reduced QoL in DRE are depression and anxiety, as shown by multiple studies (9, 32, 33). Furthermore, tolerability and efficacy of AEDs, employment, seizure frequency and semiology, and comorbidities will influence some aspects of QoL in DRE (9, 32–35). These factors are also present in patients after SE, e.g., depression in one-third of our SE cohort, and should be kept in mind during rehabilitation and further outpatient treatment. Use of inpatient and outpatient services after SE remains high, showing the ongoing need for neurological care to this potentially vulnerable patient group. Most of the studies on outcome of SE focused on the first months to a year after discharge, which might influence the QoL outcome. DRE patients in our study suffered for two decades from epilepsy, which likely explains some of the deterioration in QoL.

Limitations of the Study

Despite a careful design and strong efforts to gather follow-up data, this study has certain limitations. Direct comparison to other studies is difficult because of different healthcare settings, differences in etiology between different regions, age considerations (children are not included in our study), and varying treatment approaches. Definition of RSE might differ among studies with varying amount of drugs or time passed to define an SE as being refractory.

Due to the study design, which implies a questionnaire that was filled out by patients or their families, we cannot exclude a misunderstanding sometimes leading to incorrect answers. Furthermore, results of this survey are probably biased by selection due to the SE-associated mortality (overall 18.8%) and morbidity that were also described in other studies (30). Morbidity and mortality after discharge might explain the low responder rate of 15%, and mortality at discharge and during follow-up might be the main confounder in our study. The average in-hospital mortality in our SE cohort is 5.8% for non-RSE and 20.1% for RSE and SRSE (1) and matches nationwide evaluations of mortality in SE (3). We have to assume that participating patients were able to write or communicate with their relatives to complete the questionnaire. Adults who depend on help of their family members, who live in a nursing home, or who suffer a severe disability might be underrepresented in this evaluation. As we used patient questionnaires to collect data regarding resource utilization, the possibility of incomplete patient recall in some of the categories cannot be excluded and could have resulted in an underestimation of resource use. Another limitation of the study is the relatively short evaluation period of 3 months, which could have led to large variability in estimates.

CONCLUSION

Patients after SE show substantial impairments in their QoL and daily life activities. However, QoL is comparable to patients with DRE, despite more SE patients being affected by neurological deficits. Further studies and treatment evaluations are warranted to answer questions on the outcome of SE patients in the future, especially if new treatment strategies might improve initial outcome and reduce in-hospital mortality. In the long term, patients with RSE and SRSE might have a favorable outcome regarding QoL and neurological functions compared to patients with a non-refractory course. This underlines the need for efficient therapeutic options in these challenging situations.

ETHICS STATEMENT

We confirm that we have read the Frontiers in Neurology position on ethics and procedures and confirm that this report is consistent with these guidelines.

AUTHOR CONTRIBUTIONS

LMK and AS generated the research idea, study design, and concept. LMK, FP, and AS acquired the data. LMK and AS analyzed the data and drafted the work. LMK, SK, FP, FR, and AS made critical revisions for important intellectual content and interpreted the data. LMK and AS wrote the manuscript. LMK, SK, FP, FR, and AS approved the final manuscript.

ACKNOWLEDGMENTS

We are grateful to all of our colleagues and the staff at the study centers in Frankfurt, Greifswald, and Marburg for their assistance in conducting this study. This study was conceptually supported by "Epilepsie-Förderverein Hessen e.V." and by an unrestricted grant from UCB Pharma, Monheim. The funding sources had no role in the study design, data collection, data analysis, data interpretation, or writing of the manuscript.

REFERENCES

1. Kortland LM, Alfter A, Bahr O, Carl B, Dodel R, Freiman TM, et al. Costs and cost-driving factors for acute treatment of adults with status epilepticus: a multicenter cohort study from Germany. *Epilepsia* (2016) 57:2056–66. doi:10.1111/epi.13584
2. Kortland LM, Knake S, Rosenow F, Strzelczyk A. Cost of status epilepticus: a systematic review. *Seizure* (2015) 24:17–20. doi:10.1016/j.seizure.2014.11.003
3. Strzelczyk A, Ansorge S, Hapfelmeier J, Bonthapally V, Erder MH, Rosenow F. Costs, length of stay, and mortality of super-refractory status epilepticus: a population-based study from Germany. *Epilepsia* (2017) 58:1533–41. doi:10.1111/epi.13837
4. Ferlisi M, Shorvon S. The outcome of therapies in refractory and super-refractory convulsive status epilepticus and recommendations for therapy. *Brain* (2012) 135:2314–28. doi:10.1093/brain/aws091
5. Hocker SE, Britton JW, Mandrekar JN, Wijdicks EF, Rabinstein AA. Predictors of outcome in refractory status epilepticus. *JAMA Neurol* (2013) 70:72–7. doi:10.1001/jamaneurol.2013.578
6. Sutter R, Kaplan PW, Ruegg S. Outcome predictors for status epilepticus – what really counts. *Nat Rev Neurol* (2013) 9:525–34. doi:10.1038/nrneurol.2013.154
7. Sutter R, Marsch S, Fuhr P, Kaplan PW, Ruegg S. Anesthetic drugs in status epilepticus: risk or rescue? A 6-year cohort study. *Neurology* (2014) 82:656–64. doi:10.1212/WNL.0000000000000009
8. Kerr C, Nixon A, Angalakuditi M. The impact of epilepsy on children and adult patients' lives: development of a conceptual model from qualitative literature. *Seizure* (2011) 20:764–74. doi:10.1016/j.seizure.2011.07.007
9. Taylor RS, Sander JW, Taylor RJ, Baker GA. Predictors of health-related quality of life and costs in adults with epilepsy: a systematic review. *Epilepsia* (2011) 52:2168–80. doi:10.1111/j.1528-1167.2011.03213.x
10. Mula M, Cock HR. More than seizures: improving the lives of people with refractory epilepsy. *Eur J Neurol* (2015) 22:24–30. doi:10.1111/ene.12603
11. Kwon OY, Park SP. Depression and anxiety in people with epilepsy. *J Clin Neurol* (2014) 10:175–88. doi:10.3988/jcn.2014.10.3.175
12. von Elm E, Altman DG, Egger M, Pocock SJ, Gotzsche PC, Vandenbroucke JP, et al. Strengthening the Reporting of Observational Studies in Epidemiology (STROBE) statement: guidelines for reporting observational studies. *BMJ* (2007) 335:806–8. doi:10.1136/bmj.39335.541782.AD
13. Hamer HM, Spottke A, Aletsee C, Knake S, Reis J, Strzelczyk A, et al. Direct and indirect costs of refractory epilepsy in a tertiary epilepsy center in Germany. *Epilepsia* (2006) 47:2165–72. doi:10.1111/j.1528-1167.2006.00889.x
14. Strzelczyk A, Nickolay T, Bauer S, Haag A, Knake S, Oertel WH, et al. Evaluation of health-care utilization among adult patients with epilepsy in Germany. *Epilepsy Behav* (2012) 23:451–7. doi:10.1016/j.yebeh.2012.01.021
15. Trinka E, Cock H, Hesdorffer D, Rossetti AO, Scheffer IE, Shinnar S, et al. A definition and classification of status epilepticus – report of the ILAE task force on classification of status epilepticus. *Epilepsia* (2015) 56:1515–23. doi:10.1111/epi.13121
16. Fisher RS, Cross JH, French JA, Higurashi N, Hirsch E, Jansen FE, et al. Operational classification of seizure types by the International League Against Epilepsy: position paper of the ILAE commission for classification and terminology. *Epilepsia* (2017) 58:522–30. doi:10.1111/epi.13670
17. Shorvon S, Ferlisi M. The treatment of super-refractory status epilepticus: a critical review of available therapies and a clinical treatment protocol. *Brain* (2011) 134:2802–18. doi:10.1093/brain/awr215
18. Betjemann JP, Lowenstein DH. Status epilepticus in adults. *Lancet Neurol* (2015) 14:615–24. doi:10.1016/S1474-4422(15)00042-3
19. Beghi E, Carpio A, Forsgren L, Hesdorffer DC, Malmgren K, Sander JW, et al. Recommendation for a definition of acute symptomatic seizure. *Epilepsia* (2010) 51:671–5. doi:10.1111/j.1528-1167.2009.02285.x
20. Fisher RS, Acevedo C, Arzimanoglou A, Bogacz A, Cross JH, Elger CE, et al. ILAE official report: a practical clinical definition of epilepsy. *Epilepsia* (2014) 55:475–82. doi:10.1111/epi.12550
21. May TW, Pfafflin M, Cramer JA. Psychometric properties of the German translation of the QOLIE-31. *Epilepsy Behav* (2001) 2:106–14. doi:10.1006/ebeh.2001.0170
22. Metternich B, Wagner K, Buschmann F, Anger R, Schulze-Bonhage A. Validation of a German version of the neurological disorders depression inventory for epilepsy (NDDI-E). *Epilepsy Behav* (2012) 25:485–8. doi:10.1016/j.yebeh.2012.10.004
23. Aldenkamp AP, van Meel HF, Baker GA, Brooks J, Hendriks MP. The A-B neuropsychological assessment schedule (ABNAS): the relationship between patient-perceived drug related cognitive impairment and results of neuropsychological tests. *Seizure* (2002) 11:231–7. doi:10.1053/seiz.2002.0672
24. Panelli RJ, Kilpatrick C, Moore SM, Matkovic Z, D'Souza WJ, O'Brien TJ. The Liverpool adverse events profile: relation to AED use and mood. *Epilepsia* (2007) 48:456–63. doi:10.1111/j.1528-1167.2006.00956.x
25. EuroQol Group. EuroQol – a new facility for the measurement of health-related quality of life. *Health Policy* (1990) 16:199–208. doi:10.1016/0168-8510(90)90421-9
26. Banks JL, Marotta CA. Outcomes validity and reliability of the modified Rankin scale: implications for stroke clinical trials: a literature review and synthesis. *Stroke* (2007) 38:1091–6. doi:10.1161/01.STR.0000258355.23810.c6
27. Noda AH, Hermsen A, Berkenfeld R, Dennig D, Endrass G, Kaltofen J, et al. Evaluation of costs of epilepsy using an electronic practice management software in Germany. *Seizure* (2015) 26:49–55. doi:10.1016/j.seizure.2015.01.010
28. Strzelczyk A, Bergmann A, Biermann V, Braune S, Dieterle L, Forth B, et al. Neurologist adherence to clinical practice guidelines and costs in patients with newly diagnosed and chronic epilepsy in Germany. *Epilepsy Behav* (2016) 64:75–82. doi:10.1016/j.yebeh.2016.07.037
29. Lai A, Outin HD, Jabot J, Megarbane B, Gaudry S, Coudroy R, et al. Functional outcome of prolonged refractory status epilepticus. *Crit Care* (2015) 19:199. doi:10.1186/s13054-015-0914-9
30. Ferlisi M, Hocker S, Grade M, Trinka E, Shorvon S; International Steering Committee of the StEp A. Preliminary results of the global audit of treatment of refractory status epilepticus. *Epilepsy Behav* (2015) 49:318–24. doi:10.1016/j.yebeh.2015.04.010
31. Jayalakshmi S, Ruikar D, Vooturi S, Alladi S, Sahu S, Kaul S, et al. Determinants and predictors of outcome in super refractory status epilepticus – a developing country perspective. *Epilepsy Res* (2014) 108:1609–17. doi:10.1016/j.eplepsyres.2014.08.010
32. Elsharkawy AE, Thorbecke R, Ebner A, May TW. Determinants of quality of life in patients with refractory focal epilepsy who were not eligible for surgery or who rejected surgery. *Epilepsy Behav* (2012) 24:249–55. doi:10.1016/j.yebeh.2012.03.012
33. Gilliam F. Optimizing health outcomes in active epilepsy. *Neurology* (2002) 58:S9–20. doi:10.1212/WNL.58.8_suppl_5.S9
34. Zhao Y, Wu H, Li J, Dong Y, Liang J, Zhu J, et al. Quality of life and related factors in adult patients with epilepsy in China. *Epilepsy Behav* (2011) 22:376–9. doi:10.1016/j.yebeh.2011.07.025
35. Ferro MA, Camfield CS, Levin SD, Smith ML, Wiebe S, Zou G, et al. Trajectories of health-related quality of life in children with epilepsy: a cohort study. *Epilepsia* (2013) 54:1889–97. doi:10.1111/epi.12388

Conflict of Interest Statement: LMK reports personal fees from Desitin Arzneimittel. SK reports personal fees from Desitin Arzneimittel and UCB Pharma. FP reports industry-funded travel with support of Desitin Arzneimittel, Eisai, and UCB Pharma obtained honoraria for speaking engagements from Desitin Arzneimittel, Eisai, and UCB Pharma, was part of a speaker's bureau of Desitin Arzneimittel, Eisai, and UCB Pharma. FR reports grants and personal fees from Eisai, UCB Pharma, Desitin Arzneimittel, Novartis, Medtronic, Cerbomed, Sandoz, Shire, and the VfA (Verband der Forschenden Arzneimittelhersteller) and grants from European Union and Deutsche Forschungsgemeinschaft. AS reports grants and personal fees from Bayer HealthCare, Boehringer Ingelheim, Desitin Arzneimittel, Eisai, LivaNova, Pfizer, Sage Therapeutics, UCB Pharma, and Zogenix.

The reviewer FW and handling editor declared their shared affiliation.

frontiers in Neurology

ORIGINAL RESEARCH
published: 06 November 2017
doi: 10.3389/fneur.2017.00588

Kainic Acid-Induced Post-Status Epilepticus Models of Temporal Lobe Epilepsy with Diverging Seizure Phenotype and Neuropathology

Daniele Bertoglio†, Halima Amhaoul†, Annemie Van Eetveldt, Ruben Houbrechts, Sebastiaan Van De Vijver, Idrish Ali and Stefanie Dedeurwaerdere‡*

Department of Translational Neurosciences, University of Antwerp, Antwerp, Belgium

OPEN ACCESS

Edited by:
Lee A. Shapiro, Texas A&M University System Health Science Center College of Medicine, United States

Reviewed by:
Luiz E. Mello, Federal University of São Paulo, Brazil
Qianfa Long, Xi'an Central Hospital, China

***Correspondence:**
Stefanie Dedeurwaerdere
stefanie.dedeurwaerdere@hotmail.com

†These authors have contributed equally to this work.

‡Present address:
Stefanie Dedeurwaerdere, UCB Pharma, Braine l-Alleud, Belgium

Specialty section:
This article was submitted to Epilepsy, a section of the journal Frontiers in Neurology

Received: *04 August 2017*
Accepted: *20 October 2017*
Published: *06 November 2017*

Citation:
Bertoglio D, Amhaoul H, Van Eetveldt A, Houbrechts R, Van De Vijver S, Ali I and Dedeurwaerdere S (2017) Kainic Acid-Induced Post-Status Epilepticus Models of Temporal Lobe Epilepsy with Diverging Seizure Phenotype and Neuropathology. Front. Neurol. 8:588. doi: 10.3389/fneur.2017.00588

The aim of epilepsy models is to investigate disease ontogenesis and therapeutic interventions in a consistent and prospective manner. The kainic acid-induced *status epilepticus* (KASE) rat model is a widely used, well-validated model for temporal lobe epilepsy (TLE). As we noted significant variability within the model between labs potentially related to the rat strain used, we aimed to describe two variants of this model with diverging seizure phenotype and neuropathology. In addition, we evaluated two different protocols to induce status epilepticus (SE). Wistar Han (Charles River, France) and Sprague-Dawley (Harlan, The Netherlands) rats were subjected to KASE using the Hellier kainic acid (KA) and a modified injection scheme. Duration of SE and latent phase were characterized by video-electroencephalography (vEEG) in a subgroup of animals, while animals were sacrificed 1 week (subacute phase) and 12 weeks (chronic phase) post-SE. In the 12 weeks post-SE groups, seizures were monitored with vEEG. Neuronal loss (neuronal nuclei), microglial activation (OX-42 and translocator protein), and neurodegeneration (Fluorojade C) were assessed. First, the Hellier protocol caused very high mortality in WH/CR rats compared to SD/H animals. The modified protocol resulted in a similar SE severity for WH/CR and SD/H rats, but effectively improved survival rates. The latent phase was significantly shorter ($p < 0.0001$) in SD/H (median 8.3 days) animals compared to WH/CR (median 15.4 days). During the chronic phase, SD/H rats had more seizures/day compared to WH/CR animals ($p < 0.01$). However, neuronal degeneration and cell loss were overall more extensive in WH/CR than in SD/H rats; microglia activation was similar between the two strains 1 week post-SE, but higher in WH/CR rats 12 weeks post-SE. These neuropathological differences may be more related to the distinct neurotoxic effects of KA in the two rat strains than being the outcome of seizure burden itself. The divergences in disease progression and seizure outcome, in addition to the histopathological dissimilarities, further substantiate the existence of strain differences for the KASE rat model of TLE.

Keywords: epilepsy model, status epilepticus, spontaneous recurrent seizures, translocator protein, epileptogenesis, strain

INTRODUCTION

Animal models are very important for biomedical researchers to investigate disease ontogenesis or to evaluate pharmacological interventions. They have been essential tools in the discovery of antiepileptic drugs (AEDs) (1, 2). Moreover, chronic epilepsy models with high etiological relevance, such as the *status epilepticus* (SE), febrile seizure, and traumatic brain injury models, have played an important role in disentangling the pathophysiological processes involved in human epilepsy (1, 3–5). The advantage of these chronic models is that they enable to study epileptogenesis in a consistent and prospective manner, which is almost impossible to accomplish in patients due to heterogeneity of disease ontogenesis and interfering factors, such as antiepileptic medication, during clinical studies. In addition, models provide the possibility to test new drug targets for disease-modifying potential, a needed paradigm shift in respect to the current availability of symptomatic AEDs only.

Careful consideration in the selection of one or the other animal model is required. This choice depends on several factors, including the epilepsy subtype to be modeled as well as the research aims. The kainic acid-induced *status epilepticus* (KASE) model is a well-validated model of temporal lobe epilepsy (TLE) (6). TLE is the most common form of focal epilepsy in adults and often refractory epilepsy to medication (7). The KASE model involves induction of SE, which is characterized by a continuous seizure activity or as a series of seizures without retaining full consciousness in between (8). In the majority of animals, this subsequently initiates a process of epileptogenesis, which later leads to the development of spontaneous epileptic seizures. The model allows studying the different stages between SE and the development of TLE including SE, the acute and latent stages of epileptogenesis and chronic epilepsy. TLE models reflect similar neuropathological characteristics as seen in patients with TLE including mild (MRI negative) to severe structural changes such as hippocampal sclerosis (HS) (MRI positive) (9–11), accompanied by several processes such as cell loss and inflammation. HS is a common pathology in patients with mesial TLE (approximately 65% of patients) and can be classified into typical (type 1) and atypical (type 2 and 3), based on the histological patterns of neuronal loss and gliosis (12). Nearly 60–80% of patients with mesial TLE are affected by type 1 HS, which is characterized by neuronal loss predominantly in CA1 but also CA4 and CA3. Accordingly, in the KASE rat model of TLE, a high proportion of animals is characterized by a histological pattern similar to type 1 HS in patients (13).

At our laboratory, the KASE model is used to study the role of brain inflammation as well as its association with chronic seizure burden in epileptic rats (14). Earlier experiments in our group utilized Wistar Han rats from Charles River (WH/CR; France) (14, 15). We noticed that across different laboratories, Wistar Han rats have a relatively low number (on average <1/day) of spontaneous recurrent seizures (SRS) during the chronic period (11, 13–16), and extensive microgliosis and neurodegeneration (13, 15, 17, 18). Nevertheless, studies in models with low seizure frequency or an overall lower susceptibility to develop seizures after an epileptogenic insult are very useful in investigating molecular, epigenetic, and neurobiological alterations associated with epileptogenesis and seizure susceptibility. Such models could provide important insights in the identification and evaluation of risk and precipitating factors, which could otherwise be less evident. Besides, these models could be useful in the evaluation of anti-epileptogenic treatments interfering with epileptogenic mechanisms to delay or prevent development of epilepsy.

In addition to striving for a better understanding of epileptogenesis, an important part of epilepsy research is to find new treatments. For evaluating novel antiepileptic treatments, a model with higher seizure burden could be attractive. This would allow detecting more subtle effects of the treatment on the number and severity of SRS (instead of an all-or-none effect). An extensive literature search indicated that Sprague-Dawley rats from the Harlan Laboratories (SD/H; The Netherlands) have frequent SRS during the chronic period when subjected to KASE (17, 19–22).

With this study, we aimed to describe two rat strains subjected to KASE that express either a low or a high prevalence of SRS during the chronic period using the same initial trigger, i.e., KASE. A second aim was to investigate neuropathological differences (neurodegeneration and cell loss, and microgliosis) during both subacute and chronic stages of KASE-induced TLE. To fulfill these goals, we first compared two protocols for the induction of SE as described by and modified from Hellier (8) [5 mg/kg every hour and 2.5 mg/kg every 30 min kainic acid (KA), respectively] to assess the vulnerability of the two strains to KA. Second, seizure phenotype was determined by means of continuous (24 h/day) video-electroencephalography (vEEG) and neuropathological changes with *postmortem* analysis, respectively.

MATERIALS AND METHODS

Animal Ethics and Care

Male WH and SD rats were bought from Charles River (France) and Harlan Laboratories (The Netherlands), respectively. WH/CR were the standardly used animals at the laboratory, while SD/H were chosen due to their high chronic seizure frequency reported in the literature. All rats were single housed under a 12 h light/dark cycle, in a temperature (22 ± 2°C) and humidity (55 ± 10%) controlled environment. Food and water were available *ad libitum*. Animals were allowed 6 days of acclimatization to the animal facilities before the start of the experiments and were treated in accordance with the guidelines approved by the European Directive (2010/63/EU) on the protection of animals used for experimental and other scientific purposes. All animal experiments were approved (ECD 2014-39) by the ethical committee of the University of Antwerp (Belgium).

Study Design

A total of 121 animals were included in the study from which 97 rats (WH/CR, $n = 57$; SD/H, $n = 40$) were subjected to the multiple, low-dose injection KASE model. The other 24 animals represented the control group. In a first step, the severity and mortality of SE were compared between the Hellier protocol (8) and a modified protocol as we noticed that the WH/CR were strikingly sensitive to the standard Hellier protocol. As there was a high mortality in the WH/CR strain after SE induced by the

Hellier protocol, vEEG and histopathological evaluations were limited to animals subjected to the modified protocol. In addition, a control group ($n = 5$–7) for each strain and each time point was also included. The study design is summarized in **Figure 1**: a group of animals was used to evaluate SE duration and the latency to the first SRS by means of vEEG recording, a second group was sacrificed 1 week post-SE (subacute phase), while a third group of animals was followed up longitudinally until the chronic period (12 weeks post-SE) to determine SRS outcome by means of vEEG recording. Differences in the two strains were evaluated at each of the time points investigated.

Induction of SE

At SE induction, the rats were 7.5 weeks old with an average weight of 231.3 ± 1.8 g for WH/CR and 238.4 ± 2.3 g for SD/H rats. In a first group of animals (WH/CR $n = 6$; SD/H $n = 15$), the Hellier protocol was used to induce SE (8). Briefly, they received an initial dose of 5 mg/kg KA [subcutaneously (s.c.); sourced from A.G. Scientific, USA for all experiments], repeated every hour until the animals displayed four convulsive seizures (type S4–S5) (Table S1 in Supplementary Material). To assure SE was induced, the animal had to experience four convulsive seizures within 1 h. This protocol is referred to as the Hellier protocol (8). The modified protocol was based on previous studies in which repeated doses of KA have been tapered down to 2.5 mg/kg in Wistar Han rats to improve survival and welfare requirements from local ethical committees (11, 23, 24). The protocol presented here results from optimizing its efficiency regarding epilepsy outcomes and to provide excellent survival rate at the same time. The modified protocol (WH/CR $n = 51$; SD/H $n = 25$) involved an initial dose of 7.5 mg/kg. After 45 min, repetitive injections of 2.5 mg/kg were given every 30 min (14). Injections were repeated until convulsive seizures were induced and then stopped to avoid overdose. According to the protocol, if an animal did not present four convulsive seizures within 1 h, injections would be continued. However, it was never required since all animals reached the criterion. After 4 h of SE (induction score ≥3), diazepam (4 mg/kg, i.p.; NV Roche SA, Belgium) was given to reduce the mortality, although this dose

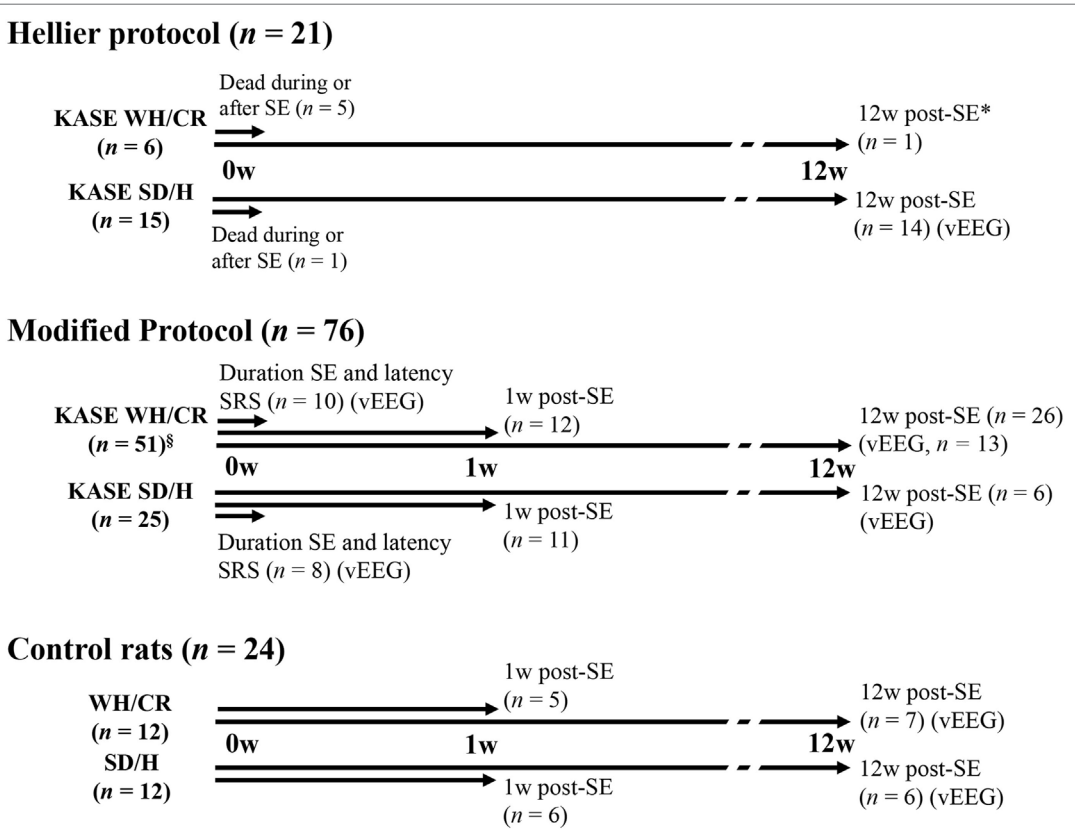

FIGURE 1 | Schematic diagram illustrating the experimental design, the number of animals used for each SE induction protocol, and strain. Three animal groups were included in the study: a group of animals (duration SE and latency SRS) was vEEG monitored to determine the duration of SE and the latency to the first SRS (modified protocol: KASE WH/CR, $n = 10$; KASE SD/H, $n = 8$). A second group of animals (1 w post-SE) was sacrificed at subacute phase for *postmortem* analysis (modified protocol: KASE WH/CR, $n = 12$; KASE SD/H, $n = 11$; control rats: WH/CR, $n = 5$; SD/H, $n = 6$). Finally, a third group of animals (12 w post-SE) was vEEG monitored during chronic epilepsy and sacrificed for *postmortem* analysis (Hellier protocol: KASE SD/H, $n = 14$, only vEEG; modified protocol: KASE WH/CR, $n = 26$; SD/H, $n = 6$; control rats: WH/CR, $n = 7$; SD/H, $n = 6$). vEEG indicates animal that underwent vEEG monitoring. * was not included for further vEEG analysis or *postmortem* evaluation. §Three WH/CR died during SE. vEEG indicates animals underwent electrode implantation and were vEEG monitored. SE, *status epilepticus*; w, weeks; KASE, kainic acid-induced *status epilepticus*; WH/CR, Wistar Han/Charles River; SD/H, Sprague-Dawley/Harlan; *n*, number; vEEG, video-electroencephalography; SRS, spontaneous recurrent seizures.

did not terminate SE (24). For both protocols, the first convulsive seizure was considered as the start of SE. The number of injections was limited to a maximum of 10, although rarely more than 8 injections were needed, and all animals entered SE. Hartmann's solution (10 ml/kg, s.c.) was administered to prevent dehydration (15). All control animals ($n = 24$) received saline injections only (range of 3–6 injections, s.c.). Additional care was taken the days following SE by providing the animals with enriched soft food pellets, manual feeding, and Hartmann's solution (10 ml/kg, s.c.) if required (15).

Several induction variables were determined for statistical analysis including the induction score, which represented the severity of the SE (score ranging from 0 to 7, with 0 indicating no SE and 7 a very severe SE) (Table S2 in Supplementary Material), sickness behavior, and body weight change (%). Sickness behavior was determined as composite score of different criteria, where for each criterion (namely feeding and drinking, mobility, visible stress or discomfort, signs of pain, respiration, fur, and body weight) a score from 0 (normal) to 2 (highly abnormal) was given. Intermediate scores were included when only a mild change was visible. The sum of all criteria defined the composite score.

Evaluation of SE and SRS by Means of vEEG

To determine the duration of SE and the latency to first SRS, animals (WH/CR $n = 10$; SD/H $n = 8$) were implanted with epidural electrodes 2 weeks before the induction of SE with modified protocol as previously described (14). After 4 h of observation of SE, the animals were connected to the vEEG system (14). From the EEG, we considered the SE terminated when the last high-amplitude periodic epileptiform discharge occurred as previously described (14, 21).

To investigate SRS during chronic epilepsy, KASE animals (modified protocol: WH/CR $n = 13$; SD/H $n = 6$; Hellier protocol: SD/H $n = 14$) were followed up with vEEG for a period of 14 days. The implantation of the epidural electrodes was performed 8 weeks after SE to provide the animals with a recovery period of at least 2 weeks before the start of the recording. The first day of vEEG recording was excluded from the analysis to allow the animals to acclimatize to the vEEG setup. Analysis of vEEG recordings was performed manually using Neuroscore 3.0 (Data Sciences International, USA) by an experienced investigator. The identification of SRS was executed as previously described (25). The severity of SRS was determined according to the modified scale of Racine (26). Duration of SE, latency to the first SRS, duration of SRS, severity of SRS, circadian distribution of SRS, and number of SRS were determined for each strain following SE induction with the modified protocol.

Tissue Collection

All animals were sacrificed by rapid decapitation. Brains were immediately removed from the skull and directly fresh-frozen in 2-methylbutane at −35°C and further preserved at −80°C. Serial coronal sections (20 µm of thickness) were collected for analysis starting at −3.0 mm from bregma (dorsal hippocampus; Figure S1 in Supplementary Material) (27) until −3.6 mm from bregma, in triplicate, on positively charged glass slides (Menzel-Gläser, Thermo Fischer Scientific, USA) using a cryostat (Leica, Germany).

Histopathology

Neuronal nuclei (NeuN), OX-42, and Fluorojade C (FjC) staining were performed as previously described (15, 25, 28) to visualize neurons, microglial activation, and degenerating neurons, respectively. Staining was quantified in the hippocampal subregions cornu ammonis 1, 3, 4, and dentate hilus (DH), and in the piriform cortex (PC) (Figure S1 in Supplementary Material). These regions were chosen for histopathological analysis given their implication in TLE. They are highly interconnected with other limbic nuclei, providing the substrate for the hypersynchrony and hyperexcitability associated with seizure generation and propagation.

Neuronal nuclei and OX-42 immunostaining were performed for neuronal loss and microglia activation, respectively. Briefly, after fixating and blocking, sections were incubated overnight with the primary antibody [mouse anti-rat NeuN, 1:2.000, Merck Millipore, Germany or mouse anti-rat OX-42 (CD11b), 1:1.000, AbD Serotec, UK] in blocking solution. The next morning sections were incubated with peroxidase-conjugated secondary antibody (donkey anti-mouse IgG-HRP, 1:500, Jackson Immunoresearch, UK) in antibody diluent. Finally, to visualize the binding, sections were exposed for 10 min to the colorimetric diaminobenzidine staining.

Fluorojade C staining was performed to visualize degenerating neurons. Briefly, sections were first immersed in a solution consisting of 1% sodium hydroxide in 80% ethanol for 5 min, then rinsed for 2 min in 70% ethanol, 2 min in distilled water, and incubated in 0.06% potassium permanganate solution for 10 min. After 5 min in distilled water, sections were transferred to a 0.0005% solution of FjC (Merck Millipore, Germany) dissolved in 0.1% acetic acid vehicle. Following three 2 min rinses in distilled water, the sections were dehydrated and cleared in xylene for at least 1 min and then coverslipped.

Quantification of the number of neurons was performed using ImageJ software (National Institute of Health, USA) as previous described (29) in CA1, CA3, CA4, DH, and PC (Figure S1 in Supplementary Material). The intensity threshold and the minimum and maximum cell size parameter values were initially determined in an empirical manner under blind conditions. Automatic quantification was done blinded for treatment on triplicate sections of which the mean score was used for statistical analysis.

Area of increased OX-42 staining was quantitatively evaluated in the same regions as for NeuN staining using ImageJ software as previously described (13). FjC-positive cells were manually counted by two investigators blinded to treatment in the same regions used for the other variables (Figure S1 in Supplementary Material). Quantification was performed on triplicate sections of which the mean score was used for statistical analysis.

Autoradiography

Translocator protein (TSPO) expression was determined by *in vitro* autoradiography with ^{3}H-PK11195 (PerkinElmer, USA)

as previously described (15). This is a valuable tool as it has potential translational clinical use due to the availability of TSPO PET tracers for non-invasive imaging. The TSPO focal binding (TSPO binding in the focal region; Bq/mg tissue) and the TSPO% area (area with increased TSPO) were determined as previously described (15) for the KASE animals. TSPO expression was quantitatively measured in the following ROIs: CA1, CA3, CA4, DH, and PC (Figure S1 in Supplementary Material). The specific binding of the radioligand (TSPO-specific binding; Bq/mg tissue) was determined for the control and KASE groups. In addition, the TSPO focal binding (TSPO binding in the focal region; Bq/mg tissue) and the TSPO% area (area with increased TSPO) were determined as previously described for the KASE animals (15, 25).

Statistical Analysis

The Kolmogorov–Smirnov test showed that not all data were normally distributed and, therefore, it was decided to use non-parametric tests for the analyses. A Mann–Whitney *U* test was used to compare the two KASE groups (KASE WH/CR and KASE SD/H), whereas a Kruskal–Wallis test with *post hoc* Dunn's multiple comparisons test to evaluate the four different groups at once (namely, the control WH/CR, KASE WH/CR, control SD/H, and KASE SD/H groups). The Fischer's exact test was used to compare severity of SRS and circadian distribution of SRS between KASE groups. Spearman's rank test was used to evaluate correlations. Data from the two time points were analyzed separately. Data are represented as box plot and reported as median ± interquartile ranges (IQRs), unless specified. GraphPad Prism 6 (GraphPad Software, USA) was used for all analyses. Tests were two-tailed and statistical significance was set at $p < 0.05$.

RESULTS

Mortality, Severity, and Duration of the KA-Induced SE

Two similar SE induction protocols were evaluated in both the WH/CR and SD/H strains to compare their responsiveness to each protocol. Following Hellier protocol, all SD/H rats went into SE for at least 4 h without any mortality, and only 1/15 animal did not recover from the SE and died 2 days post-SE (7% mortality) (**Figure 2A**). Instead, four WH/CR rats died within 4 h from the induction of SE and one rat died due to SE-related sickness 3 days post-SE (83% mortality). The considerable mortality associated with the Hellier protocol in the WH/CR rats underlines the need for a different SE induction protocol in this strain. While using the modified protocol, none of the SD/H rats ($n = 25$) died during the induction of SE (0% mortality) and only 3/51 WH/CR rats died during or the days following induction of SE (6% mortality) (**Figure 2A**). No significant difference was found in the induction score of the SE between WH/CR and SD/H when using the modified protocol (**Figure 2B**). The duration of SE was evaluated by means of vEEG monitoring in a subset of animals and no difference between strains could be found [WH/CR = 15.26 h (IQR = 13.72–16.19 h); SD/H = 13.87 h (IQR = 11.68–14.86 h)] (**Figure 2C**). During post-SE follow-up, strains did not display any significant difference in sickness behavior [sickness score: WH/CR = 4 (IQR = 3–6.5), while SD/H = 4.5 (IQR = 3–7.5)] or body weight change 1 day post-SE (WH/CR = −14.9 ± 3.2%, while SD/H = −14.3 ± 3.6%, compared to the day of induction of SE). All animals fully recovered the weight loss within 4 days' post-SE. No differences were seen in SD/H animals between the two protocols for any of the parameters evaluated.

The Two Strains Are Characterized by Different SRS Outcome

For a cohort of animals, vEEG monitoring was started at SE to determine the duration of SE and the latency to the first SRS. These animals underwent surgical implantation of the recording electrodes 2 weeks before SE. WH/CR rats experienced a significantly longer latency to the first SRS compared to SD/H animals [WH/CR = 15.4 days (IQR = 14.5–32.4), SD/H = 8.3 days (IQR = 3.7–12.6); $p < 0.0001$] (**Figure 3A**). In the cohort of animals allocated for the vEEG monitoring during chronic epilepsy, the surgical implantation of the recording electrodes occurred 6 weeks post-SE. This was followed by a 2 weeks recovery before the start of the recording. During vEEG monitoring in the chronic phase, 10 out of 13 KASE WH/CR rats experienced SRS, while all KASE SD/H rats did

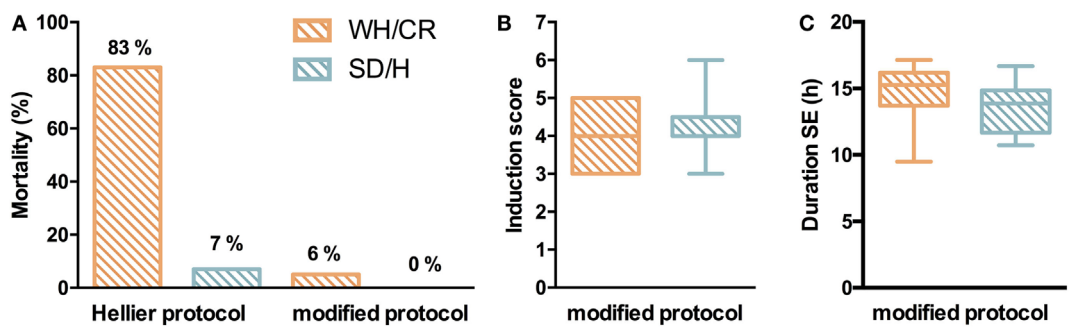

FIGURE 2 | Status epilepticus (SE) in KASE WH/CR and KASE SD/H rats. **(A)** Mortality rates for both rat strains during SE induction. **(B)** Severity of the SE between the two strains during the modified protocol. Hellier protocol: WH/CR $n = 6$ and SD/H $n = 15$; modified protocol: WH/CR $n = 51$ and SD/H $n = 25$ **(A,B)**. **(C)** Duration of SE in WH/CR ($n = 10$) and SD/H ($n = 8$) during the modified protocol. WH/CR, Wistar Han/Charles River; SD/H, Sprague-Dawley/Harlan; KASE, kainic acid-induced *status epilepticus*.

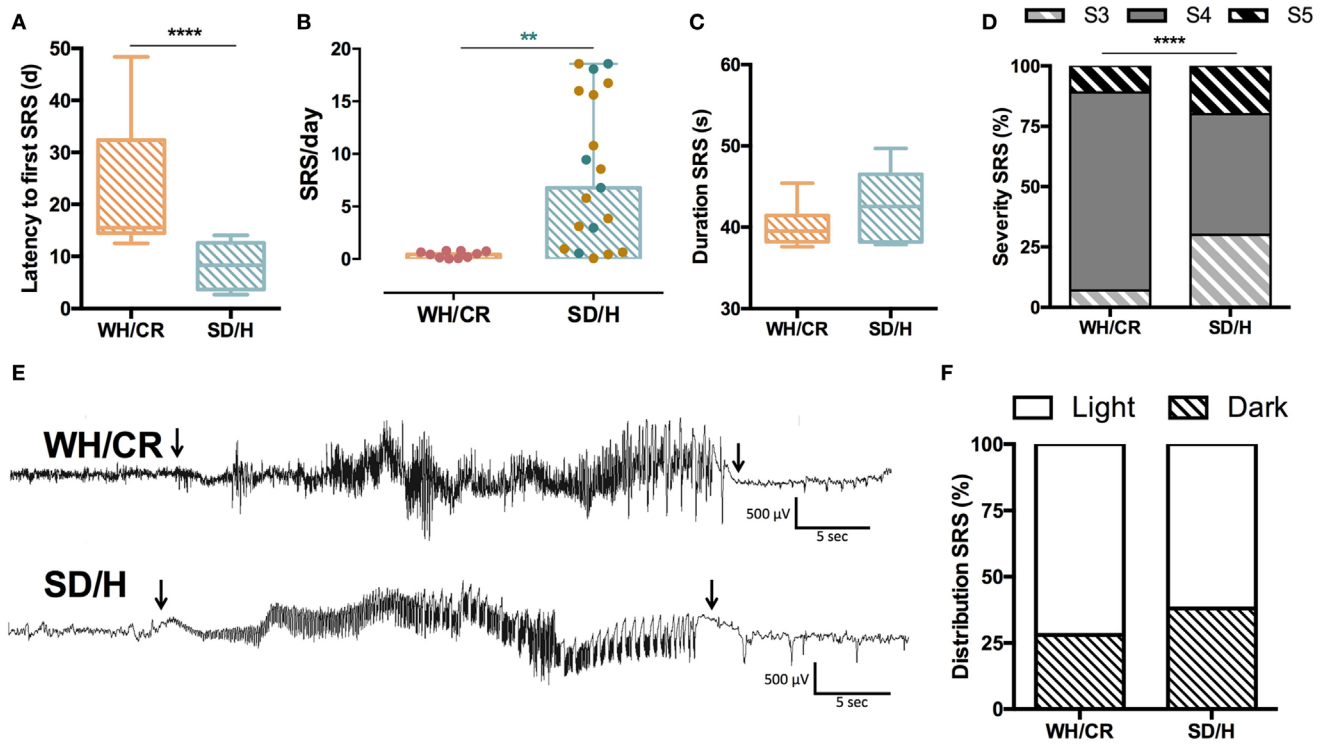

FIGURE 3 | SRS characterization in kainic acid-induced SE (KASE) WH/CR and KASE SD/H rats. **(A)** WH/CR rats ($n = 10$) showed a significant longer latency to the first SRS when compared to SD/H ($n = 8$). Mann–Whitney U test. ****$p < 0.0001$. **(B)** SRS frequency during the chronic period. A significant higher number of SRS per day was demonstrated for the SD/H rats compared to the WH/CR rats 12 weeks post-status epilepticus (SE). Red and blue dots represent WH/CR and SD/H, respectively, following modified protocol; brown dots represent SD/H following Hellier protocol. Mann–Whitney U test. **$p < 0.01$ after considering only animals that underwent modified SE protocol. **(C)** The duration of SRS was similar in both strains. **(D)** WH/CR and SD/H were characterized by different distribution of SRS. ****$p < 0.0001$. Fischer's exact test. **(E)** Representative spontaneous electrographic seizure (S4) during chronic period (12 weeks post-SE) of a WH/CR and SD/H rat. Arrows indicate the onset and the end of the seizure. **(F)** The circadian distribution of SRS was similar in both strains with a higher frequency of SRS during the light phase. WH/CR $n = 10$ and SD/H $n = 6$ **(C,D,F)**. WH/CR, Wistar Han/Charles River; SD/H, Sprague-Dawley/Harlan; SRS, spontaneous recurrent seizures; d, days. Graph B is reported as mean ± SD.

following both protocols (Hellier protocol = 14/14, modified protocol = 6/6). To compare SRS outcome parameters side-by-side between the two strains, only data following the modified protocol were included. After excluding the non-seizing KASE WH/CR rats, the number of SRS per day was still significantly lower compared to KASE SD/H rats [WH/CR = 0.46 SRS/day (IQR = 0.12–0.75), SD/H = 6.78 SRS/day (IQR = 0.96–17.98); $p < 0.01$] (**Figures 3B,E**). The average duration of SRS was similar in the two strains [WH/CR = 39.5 s (IQR = 38.2–41.4 s), SD/H = 42.5 s (IQR = 38.2–46.5 s)] (**Figure 3C**), whereas the SRS severity was significantly different between the two strains ($p < 0.0001$) (**Figure 3D**). Finally, both strains displayed a similar SRS distribution between light phase (WH/CR = 72%; SD/H = 62%) and dark phase (WH/CR = 28%; SD/H = 38%) of the day (**Figure 3F**).

Neuronal Loss Is More Extensive in KASE WH/CR Rats than KASE SD/H Rats

One week post-SE significant neuronal loss was present in all hippocampal sub-regions and PC in KASE WH/CR rats in comparison to control rats ($p < 0.05$) (**Figure 4**). On the contrary, in the SD/H rats, significant neuronal loss was found only in CA3 and DH. In addition, KASE WH/CR rats showed significant neuronal loss in CA1 and CA4 compared to KASE SD/H animals ($p < 0.05$).

Twelve weeks post-SE, significant neuronal loss was observed for all investigated regions in KASE WH/CR compared to the control rats ($p < 0.05$) (**Figure 4**), while significant neuronal loss was limited to CA3, DH, and PC in KASE SD/H rats compared to the controls ($p < 0.05$).

KASE WH/CR and SD/H Rats Show Similar OX-42 Immunoreactivity Only at Subacute Phase

Kainic acid-induced *status epilepticus* WH/CR rats displayed increased OX-42 immunoreactivity compared to controls in hippocampal sub-regions and PC 1 week post-SE ($p < 0.01$) (**Figure 5**). In KASE SD/H rats, only CA3 and PC were significantly increased compared to control SD/H rats ($p < 0.05$) (**Figure 5**).

Twelve weeks post-SE microglial activation was relatively less evident, however, it was still significantly increased in KASE

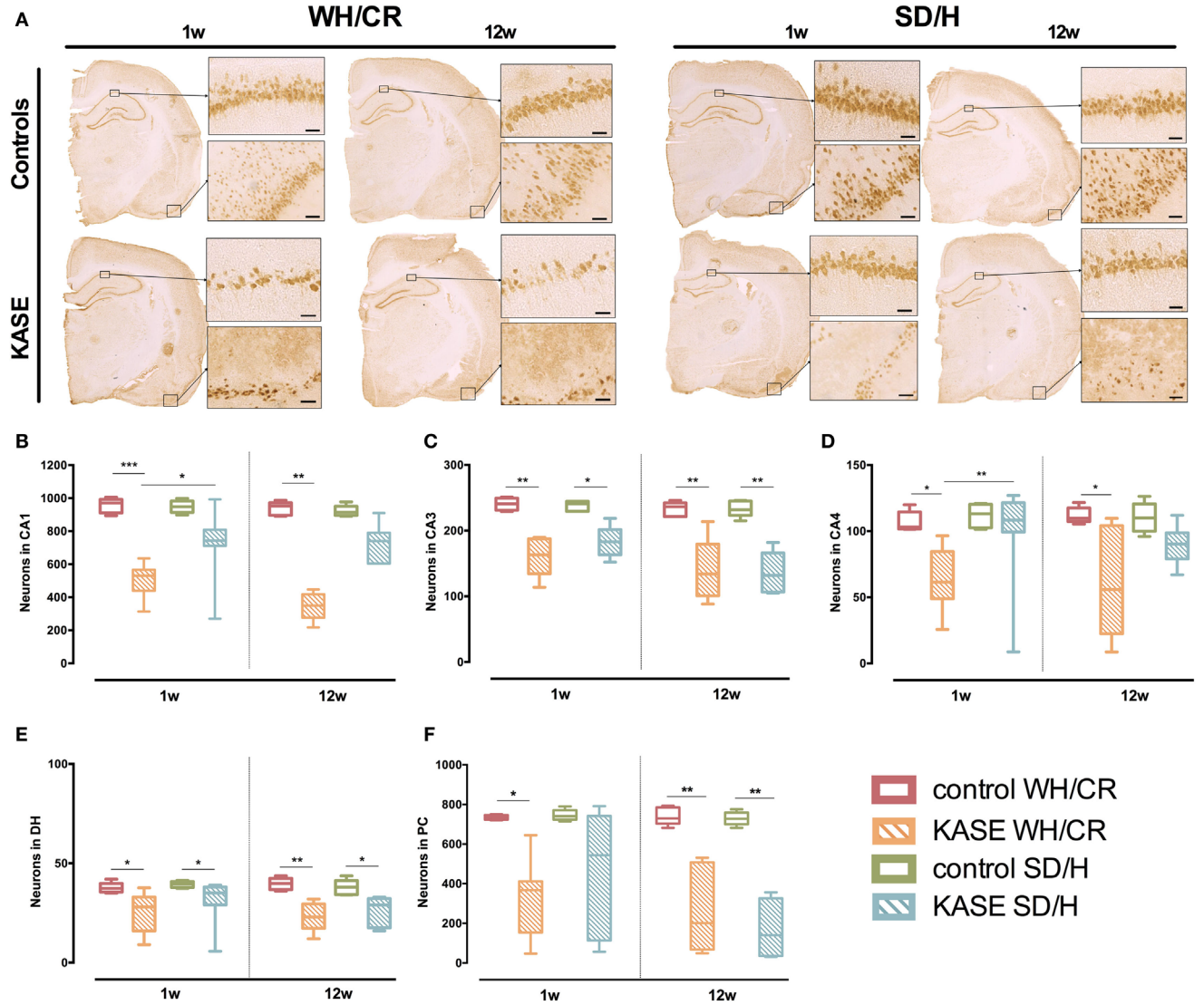

FIGURE 4 | Neuronal loss in KASE WH/CR and KASE SD/H rats. **(A)** Representative KASE and control rats 1 and 12 weeks post-status epilepticus (SE). At both time points, a significant difference could be demonstrated for the investigated regions **(B–F)** between the respective control and KASE WH/CR animals, while for the SD/H animals only in CA3 and DH 1 week post-SE, and CA3, DH, and PC 12 weeks post-SE **(C,E,F)**. In addition, for the CA1 and CA4 sub-regions, significant higher neuronal loss could be demonstrated for the KASE WH/CR animals compared to KASE SD/H rats 1 week post-SE. Kruskal–Wallis test with *post hoc* Dunn's test **(B–F)**. 1 week post-SE: control WH/CR $n = 5$, KASE WH/CR $n = 10$, control SD/H $n = 5$ and KASE SD/H $n = 9$; 12 weeks post-SE: control WH/CR $n = 7$, KASE WH/CR $n = 6$, control SD/H $n = 6$ and KASE SD/H $n = 6$. Insets were taken at 10× magnification. Scale bar = 50 µm. $^{*}p < 0.05$, $^{**}p < 0.01$. WH/CR, Wistar Han/Charles River; SD/H, Sprague-Dawley/Harlan; w, week; CA, cornu ammonis; DH, dentate hilus; PC, piriform cortex; KASE, kainic acid-induced *status epilepticus*.

WH/CR animals compared to controls in all the investigated regions ($p < 0.01$) (**Figure 5**). On the other hand, in KASE SD/H animals, increased OX-42 immunoreactivity was confined to PC ($p < 0.05$) (**Figure 5F**).

TSPO Displays Different Upregulation Patterns in KASE WH/CR and SD/H Rats

During subacute phase, KASE animals of both strains had significantly increased TSPO-specific binding in all evaluated regions compared to controls ($p < 0.05$) (Figure S2 in Supplementary Material). Accordingly, the TSPO focal binding was similar between the two KASE groups (**Figures 6A,B**), whereas TSPO% area was significantly increased in KASE SD/H rats compared to KASE WH/CR in CA1 and DH ($p < 0.05$) (**Figure 6C**).

Translocator protein upregulation was less evident 12 weeks post-SE, nevertheless all evaluated brain regions were increased in KASE SD/H compared to control SD/H rats ($p < 0.01$) and a significant increase in TSPO-specific binding was also demonstrated in the CA1 of KASE WH/CR rats compared to controls

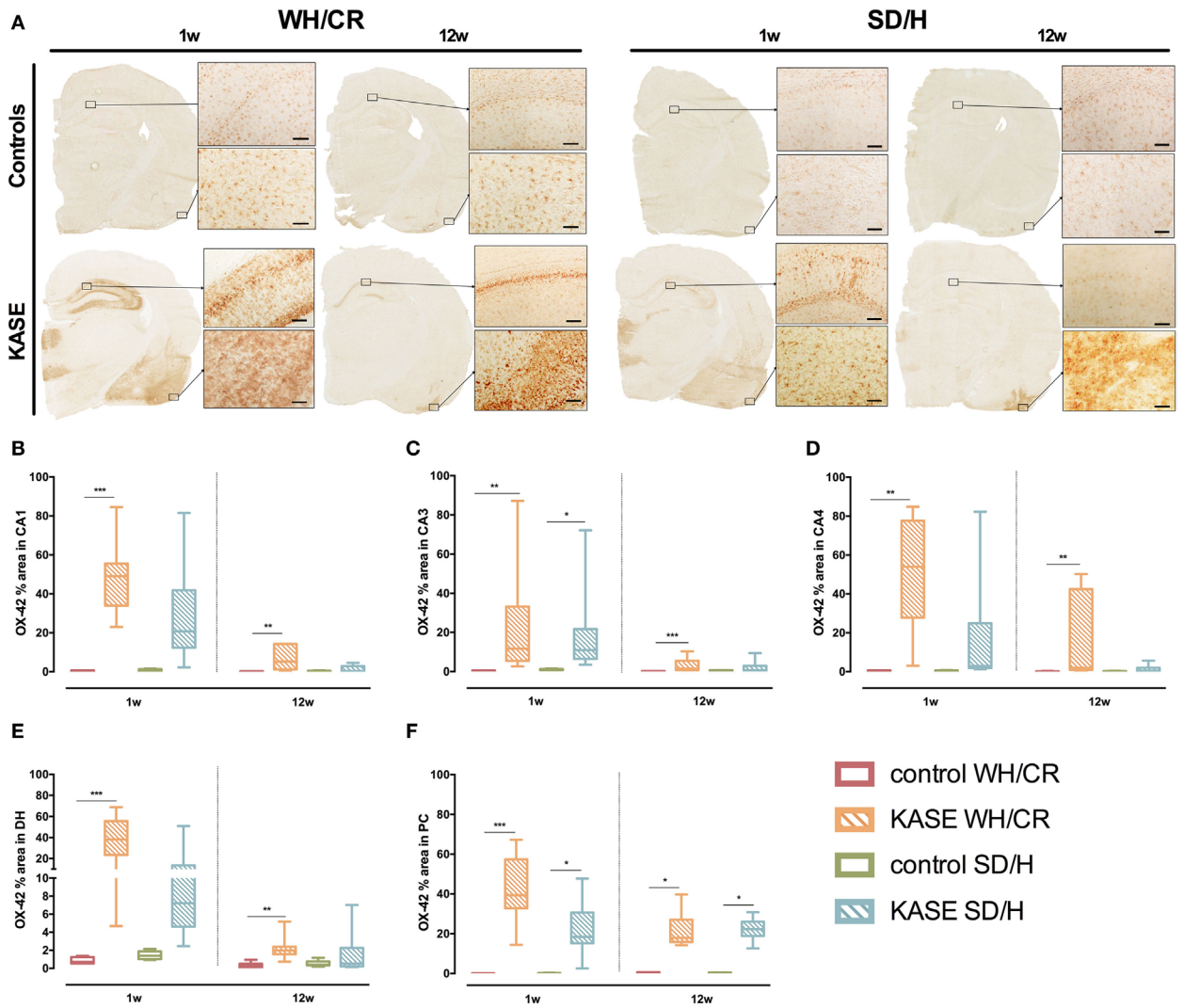

FIGURE 5 | Microglial activation in KASE WH/CR and KASE SD/H rats. **(A)** Representative KASE and control rats 1 and 12 weeks post-status epilepticus (SE). For all investigated regions, a significant difference could be demonstrated between WH/CR controls and KASE rats 1 week post-SE as well as 12 weeks post-SE **(B–F)**. For the SD/H rats, this was only observed for the CA3 sub-region of the hippocampus and PC 1 week post-SE, while only in PC during the chronic period. Kruskal–Wallis test with *post hoc* Dunn's test **(B–F)**. *$p < 0.05$, **$p < 0.01$, ***$p < 0.001$. 1 week post-SE: control WH/CR $n = 4$–5, KASE WH/CR $n = 8$–10, control SD/H $n = 5$ and KASE SD/H $n = 6$; 12 weeks post-SE: control WH/CR $n = 5$–6, KASE WH/CR $n = 7$, control SD/H $n = 4$–6 and KASE SD/H $n = 6$–8. Insets were taken at 10× magnification. Scale bar = 100 µm. WH/CR, Wistar Han/Charles River; SD/H, Sprague-Dawley/Harlan; w, week; CA, cornu ammonis; DH, dentate hilus; PC, piriform cortex; KASE, kainic acid-induced *status epilepticus*.

($p < 0.05$) (Figure S3 in Supplementary Material). Interestingly, TSPO focal binding was significantly higher in KASE WH/CR rats compared to KASE SD/H animals in CA1, CA3, and DH ($p < 0.05$) (**Figure 6B**), whereas TSPO% area between the two KASE groups did not differ in any investigated region (**Figure 6C**).

Neurodegeneration Is More Extensive in KASE WH/CR than KASE SD/H Rats and Continues in the Chronic Phase Reflecting Neuronal Loss and Microglial Activation

During the subacute phase, KASE WH/CR rats displayed significant neurodegeneration in CA1, CA3, DH, and PC compared to controls ($p < 0.01$), while for the KASE SD/H animals, this was observed only in PC ($p < 0.05$) (**Figure 7**). In addition, KASE WH/CR displayed a significantly higher number of FjC positive neurons in DH compared to KASE SD/H ($p < 0.05$). The number of FjC-positive cells during the subacute phase inversely correlated with the number of neurons in all investigated regions ($R = -0.46$ to -0.77; $p < 0.05$) (Figure S4 in Supplementary Material). In addition, the number of FjC-positive cells during the subacute phase correlated with the % area of OX-42 immunoreactivity in all investigated regions ($R = 0.55$ to 0.94; $p < 0.01$) (Figure S5 in Supplementary Material).

Kainic acid-induced *status epilepticus* WH/CR animals displayed ongoing neurodegeneration even during the chronic

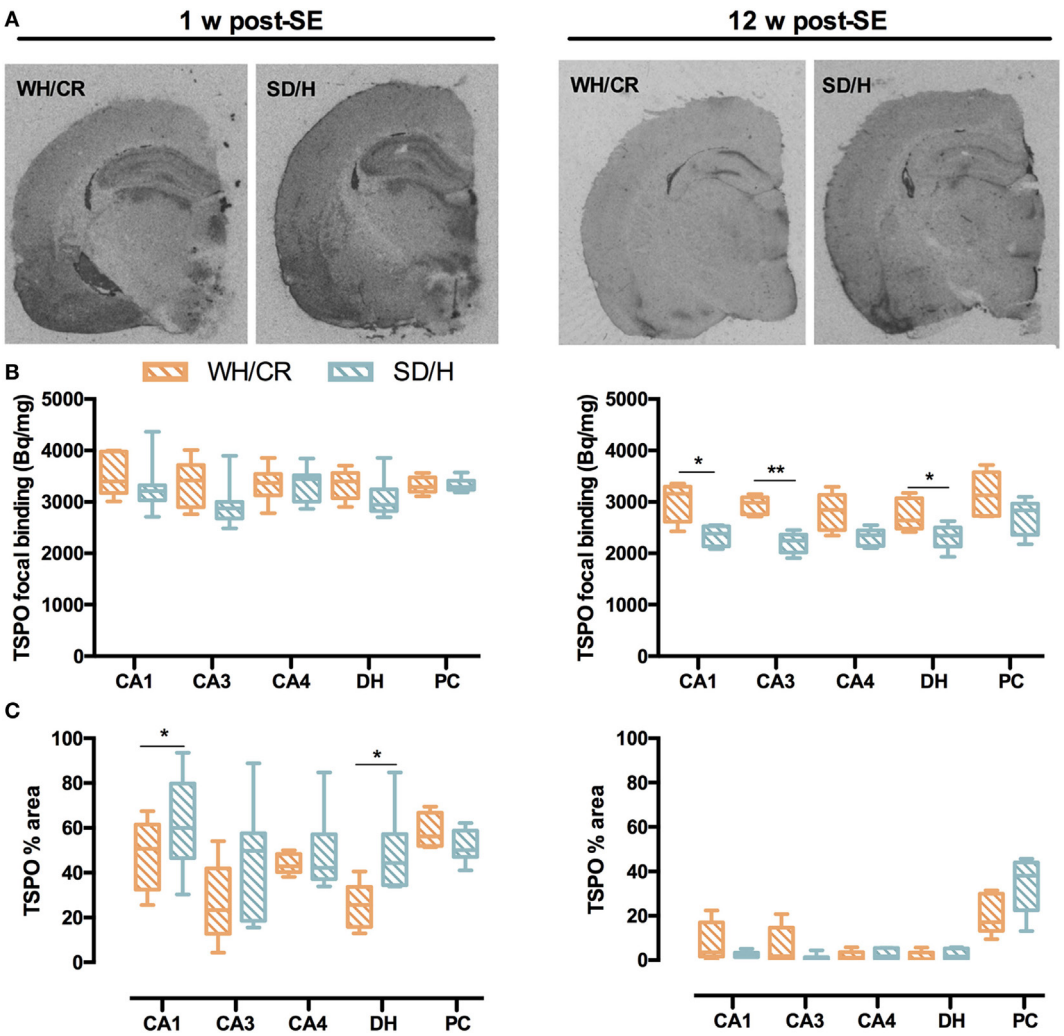

FIGURE 6 | TSPO focal binding and % area in WH/CR and SD/H rats. **(A)** Representative autoradiograms showing TSPO expression 1 and 12 weeks post-status epilepticus (SE). **(B)** TSPO focal binding in the subacute phase was similar for the two strains, while in the chronic phase, it was higher for the KASE WH/CR rats for all the brain regions except for the CA4 and PC when compared to KASE SD/H animals. **(C)** The TSPO% area was significantly increased in the KASE SD/H animals in the CA1 and DH when compared to the KASE WH/CR rats 1 week post-SE. Twelve weeks post-SE no differences could be determined. Mann–Whitney *U* test **(B,C)**. $^{*}p < 0.05$, $^{**}p < 0.01$. KASE WH/CR $n = 5$–7 and KASE SD/H $n = 6$. TSPO, translocator protein; WH/CR, Wistar Han/Charles River; SD/H, Sprague-Dawley/Harlan; w, week; CA, cornu ammonis; DH, dentate hilus; PC, piriform cortex; KASE, kainic acid-induced *status epilepticus*.

epilepsy period in the CA1, CA4, and PC when compared to the controls ($p < 0.05$). Whereas for the SD/H animals, neurodegeneration was limited to the PC at the chronic phase ($p < 0.05$) (**Figure 7**). Accordingly, in CA1 and CA4 sub-regions, a significant higher number of degenerative neurons was observed for the KASE WH/CR animals compared to KASE SD/H rats ($p < 0.05$).

DISCUSSION

In this study, we describe two rat strains subjected to the KASE model and their differences in seizure phenotype and neuropathology. We also compared the Hellier protocol and a modified milder protocol for SE induction to determine the most suitable protocol in terms of mortality.

Using the Hellier protocol to induce SE led to high mortality in the WH/CR rats, which underlined the impossibility to use such protocol in this rat strain. When continuing with the modified protocol (2.5 mg/kg for repeated injections), this was well tolerated by both WH/CR and SD/H rats and resulted in a SE with similar severity and duration. This modified protocol allowed to substantially increase the survival of WH/CR rats without affecting the SE, thus reducing the overall number of animals needed in agreement with the refinement and reduction principles of the *in vivo* research.

Although only timing and dose of the repeated KA injections differed between the Hellier and our modified protocol, these results seem to suggest that the WH/CR rats handle KA differently than SD/H rats, which showed no/minimal mortality with

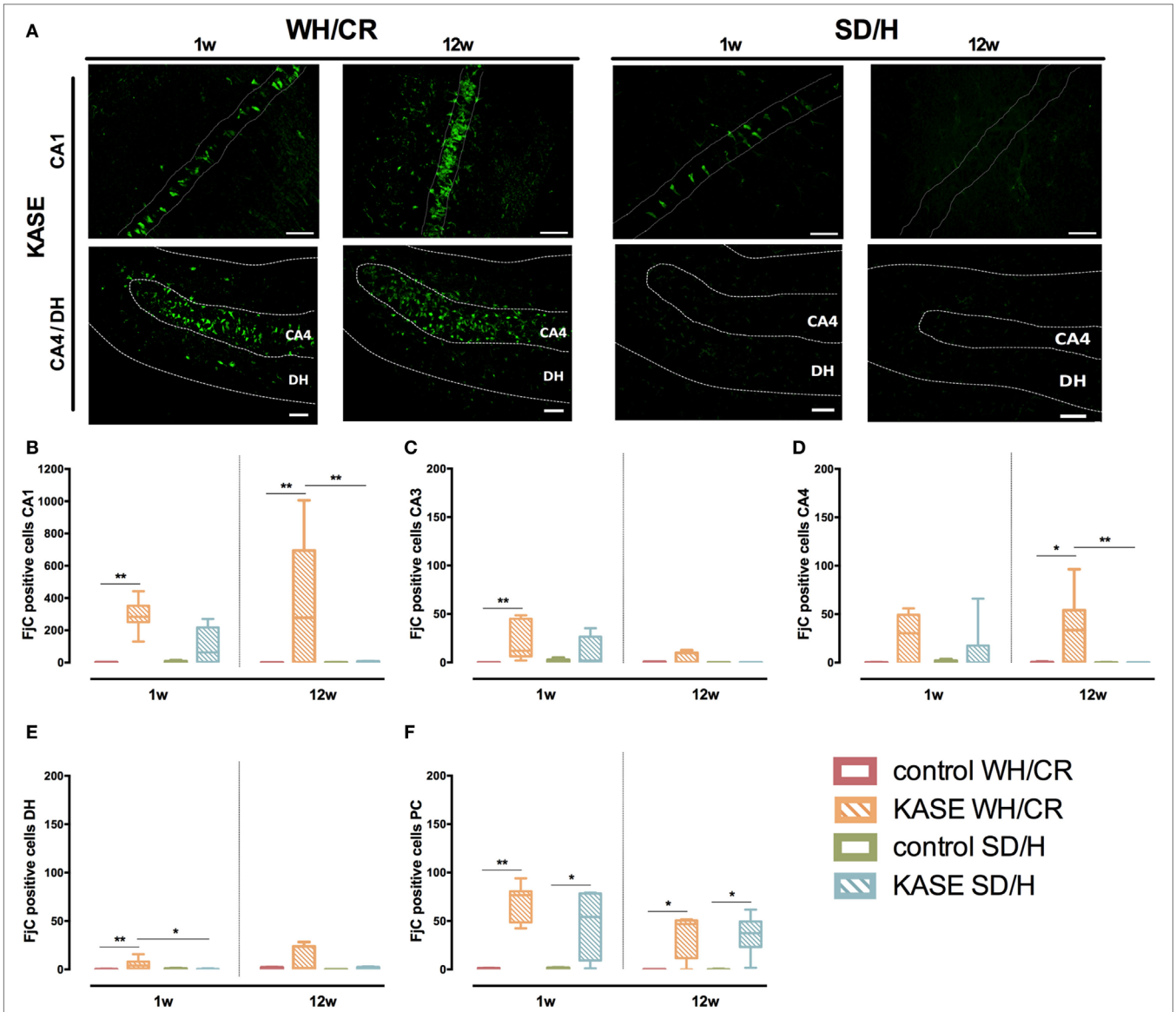

FIGURE 7 | Neurodegeneration in KASE WH/CR and KASE SD/H rats. **(A)** Representative CA1 and CA4/DH images for KASE rats 1 and 12 weeks post-status epilepticus (SE). During both subacute and chronic phases, KASE WH/CR displayed an overall more extensive neurodegeneration than KASE SD/H in the investigated regions **(B–F)**. Kruskal–Wallis test with *post hoc* Dunn's test **(B–F)**. $^{*}p < 0.05$, $^{**}p < 0.01$. One week post-SE: control WH/CR $n = 4–5$, KASE WH/CR $n = 8–10$, control SD/H $n = 5$ and KASE SD/H $n = 6$; 12 weeks post-SE: control WH/CR $n = 5–6$, KASE WH/CR $n = 7$, control SD/H $n = 4–6$ and KASE SD/H $n = 6$. Representative images: CA1 = 40× magnification, CA4/DH = 20× magnification. Scale bar = 50 μm. WH/CR, Wistar Han/Charles River; SD/H, Sprague-Dawley/Harlan; w, week; CA, cornu ammonis; DH, dentate hilus; PC, piriform cortex; KASE, kainic acid-induced *status epilepticus*.

both protocols. The large difference in mortality rate between the WH/CR and SD/H rats may be due to dissimilarities in pharmacokinetics and pharmacodynamics of KA in the WH/CR and SD/H rats. Indeed, WH rats are reported to be more sensitive to the excitotoxic agents including KA when compared to the SD rats (30, 31), and this major sensitivity of WH might result in the higher mortality observed in this strain.

The latent phase to disease onset represents a crucial period of time to investigate mechanisms involved in epileptogenesis. Here, we have shown how this time window is significantly shorter in SD/H rats. During chronic epilepsy, SD/H rats displayed on average 15 times higher SRS frequency than WH/CR animals. These remarkable findings might suggest that the KASE WH/CR rats are more resistant to epilepsy or they are characterized by a slower disease progression.

The high divergence in SRS frequency of the two strains offers the possibility to choose the most appropriate strain to answer specific research questions. The WH/CR strain following modified protocol is characterized by a longer latent phase and low prevalence of SRS, meaning that it is useful to evaluate changes during epileptogenesis. For instance, such strain can be relevant in the identification and evaluation of risk (e.g., prenatal

or early life stress) (32, 33) and precipitating factors (e.g., sleep deprivation) (34), which could aggravate epileptogenesis and seizure susceptibility. This model could be of great relevance in the evaluation of anti-epileptogenic treatments to halt or prevent epileptogenesis, especially to investigate the effect of anti-inflammatory treatments on the development of epilepsy. Given the strong microgliosis occurring in this model, it could be preferred in the evaluation of anti-inflammatory treatments. In addition, it is relevant to underline how WH/CR rats display HS similar to the majority of patient with TLE (type 1 HS). However, it is important to note that animal models with a more equal proportion of epileptic and non-epileptic animals would be needed to determine the specificity and sensitivity of biomarkers to predict acquired epilepsy (35, 36).

On the other hand, the SD/H strain is characterized by a short latent phase and high prevalence of SRS, which makes this strain appropriate for the evaluation of novel antiepileptic treatments or disease modification of existing epilepsy. The high SRS frequency would allow detecting more subtle effects of the treatment on the number and severity of SRS. Another feature of this strain is that all the animals subjected to KASE develop SRS as also confirmed by several independent *in-house* and previously published studies (22, 25). An important downside when performing intervention studies is the high variability in SRS frequency in this model. We observed that a proportion of animals was having very few seizures. This can be circumvented by pre-selection of a homogenous group of animals before entering the treatment study.

It is relevant to underline that several studies have demonstrated intra- and inter-strain variations in both focal and systemically induced TLE models regarding the SE and development of SRS (37–43). WH as well as SD rats are outbred strains with a high genetic heterogeneity and high intra-strain variation (37, 44). Moreover, epigenetic and environmental factors, including vendor-related effects, can also be important contributors in the intra-strain differences seen (37, 45).

The two rat strains present different pattern of neuronal loss. Although it may be expected that the rat strain with higher seizure burden would be characterized by more severe neuronal loss, it is important to underline that neuronal loss and seizure frequency are not univocally linked to each other as supported by previous studies (17, 46–49). Indeed, we observed that the KASE WH/CR rats had neuronal loss across all the investigated regions, while the KASE SD/H rats showed focal neuronal loss mainly in the PC. The two different patterns suggest neuronal loss could be the result of different processes. In particular, possible mechanisms involved in the extensive neuronal loss in CA1 of WH/CR animals could be a consequence of hypoxia and ischemia, which are known to occur during SE (50), and their effects could be more pronounced in this strain. Another possible explanation could be that WH/CR rats are more susceptible to the neurotoxic effect of KA and/or seizure-induced excitotoxicity, leading to increased cell loss as well as higher mortality.

The strong inflammatory response seen with both OX-42 and TSPO 1 week post-SE might be mainly driven by response to the primary injury, which was similar for both strains when using the modified induction protocol. This is supported by studies showing that high microglial activation is typically seen during the early phases of disease ontogenesis in different models of CNS injury (51–53). During the chronic period, the % area of microglial activation was overall reduced, however, still strongly increased in PC of both strains, and hippocampal sub-regions of WH/CR. In addition, chronic neurodegeneration was strikingly different between the two rat strains. The extensive neurodegeneration in WH/CR animals suggests the presence of abundant cell death, which might be the result or cause of the chronic microglial response seen in KASE WH/CR, explaining the higher TSPO focal binding seen in WH/CR compared to SD/H. Indeed, the high levels of cellular debris derived from the neuronal loss may trigger chronic microglial activation promoting neurodegeneration and establishing a vicious cycle that persists during chronic epilepsy. In accordance, a previous study (54) reported concurrent neurodegeneration and microgliosis in WH rats during chronic epilepsy in the KASE model of TLE. On the contrary, for SD/H rats, neuronal loss may be only related to SE insult, as previously shown (17), and the occurrence of SRS may result in a limited involvement of microglial activation and neurodegeneration in hippocampus as previously reported (48, 55). Furthermore, in agreement with our finding, neurodegeneration in the parahippocampal regions has been reported until 3 months' post-SE in the KASE model of TLE in SD rats (56).

In conclusion, we described two rat strains subjected to KASE, one with a low (WH/CR) and one with a high (SD/H) prevalence of SRS during the chronic period. The differences in disease progression and seizure outcome between strains may help to select the appropriate strain to study different research questions, including mechanisms of epileptogenesis, the search for prognostic factors, and the effect of treatments. In particular, these strain-related seizure phenotype and neuropathology indicate WH/CR as a more appropriate strain to investigate epileptogenesis, while SD/H to develop antiepileptic treatments. This work also confirms that in the same epilepsy model, the disease outcome can develop with different timing, features, and severity in different strains. This provides valuable information to reduce time, variables, and number of animals needed to achieve the specific research question in future studies. In addition, studying these diverging strains may lead to new insights regarding mechanisms underlying epilepsy.

ETHICS STATEMENT

This study was carried out in accordance with the recommendations of the European Directive (2010/63/EU) on the protection of animals used for experimental and other scientific purposes. The protocol was approved (ECD 2014-39) by the ethical committee of the University of Antwerp (Belgium).

AUTHOR CONTRIBUTIONS

HA and SD conceived and designed the study. DB, HA, AE, RH, SV, and IA were involved in execution of the experimental design, data acquisition, and data interpretation for the study. DB, HA, IA, and SD were involved in drafting and editing the manuscript and figures. All authors approved the final manuscript and they are accountable for the content of the work.

ACKNOWLEDGMENTS

The authors are thankful to P. Ponsaerts for his help regarding the NeuN immunohistochemistry and providing the fluorescent microscope for FjC analysis. We are grateful to UCB Biopharma and to Georges Mairet-Coello, Mathieu Schmitt, and Tania Deprez for the use of the slide scanner. Our gratitude also goes to K. Szewczyk for her support in the performance of the experimental procedures.

FUNDING

This work was supported by the Research Foundation Flanders (FWO, grant numbers 1.5.110.14N, 1.5.144.12N, G.A009.13N); and the Queen Elisabeth Medical Foundation for Neurosciences (SD). Support was also granted from the Bijzonder Onderzoeks Fonds of the University of Antwerp (HA and SD) and the FWO (11W2516N) (DB).

SUPPLEMENTARY MATERIAL

The Supplementary Material for this article can be found online at http://www.frontiersin.org/article/10.3389/fneur.2017.00588/full#supplementary-material.

FIGURE S1 | Representative delineation of the investigated regions.

FIGURE S2 | TSPO-specific binding 1 week post-SE in WH/CR and SD/H rats. For all brain regions and for both strains studied, a significant difference could be demonstrated between control and KASE animals 1 week post-SE. Kruskal–Wallis test with *post hoc* Dunn's test. $*p < 0.05$, $**p < 0.01$, $***p < 0.001$. KASE, kainic acid-induced *status epilepticus*; TSPO, translocator protein; status epilepticus, SE.

FIGURE S3 | TSPO-specific binding 12 weeks post-SE in WH/CR and SD/H rats. In the KASE WH/CR animals, increased TSPO-specific binding 12 weeks post-SE could only be demonstrated in the CA1 when compared to control WH/CR rats. On the contrary, KASE SD/H rats showed a significant increase in all regions investigated compared to control SD/H animals. Kruskal–Wallis test with *post hoc* Dunn's test. $*p < 0.05$, $**p < 0.01$, $***p < 0.001$. KASE, kainic acid-induced *status epilepticus*; TSPO, translocator protein; status epilepticus, SE.

FIGURE S4 | The number of fluorojade C (FjC)-positive cells inversely correlated with the number of neurons 1 week post-status epilepticus in WH/CR and SD/H rats. A statistically significant correlation between the number of FjC-positive cells and neurons was determined in all investigated regions. Spearman's rank test.

FIGURE S5 | The number of fluorojade C (FjC)-positive cells correlated with the % area of OX-42 1 week post-status epilepticus in WH/CR and SD/H rats. A statistically significant correlation between the % area of OX-42 and the number of FjC-positive cells was determined in all investigated regions. Spearman's rank test.

REFERENCES

1. Loscher W. Critical review of current animal models of seizures and epilepsy used in the discovery and development of new antiepileptic drugs. *Seizure* (2011) 20(5):359–68. doi:10.1016/j.seizure.2011.01.003
2. Loscher W, Klitgaard H, Twyman RE, Schmidt D. New avenues for anti-epileptic drug discovery and development. *Nat Rev Drug Discov* (2013) 12(10):757–76. doi:10.1038/nrd4126
3. Levesque M, Avoli M, Bernard C. Animal models of temporal lobe epilepsy following systemic chemoconvulsant administration. *J Neurosci Methods* (2016) 260:45–52. doi:10.1016/j.jneumeth.2015.03.009
4. Morimoto K, Fahnestock M, Racine RJ. Kindling and status epilepticus models of epilepsy: rewiring the brain. *Prog Neurobiol* (2004) 73(1):1–60. doi:10.1016/j.pneurobio.2004.03.009
5. Grone BP, Baraban SC. Animal models in epilepsy research: legacies and new directions. *Nat Neurosci* (2015) 18(3):339–43. doi:10.1038/nn.3934
6. Loscher W, Brandt C. High seizure frequency prior to antiepileptic treatment is a predictor of pharmacoresistant epilepsy in a rat model of temporal lobe epilepsy. *Epilepsia* (2010) 51(1):89–97. doi:10.1111/j.1528-1167.2009.02183.x
7. Tellez-Zenteno JF, Hernandez-Ronquillo L. A review of the epidemiology of temporal lobe epilepsy. *Epilepsy Res Treat* (2012) 2012:630853. doi:10.1155/2012/630853
8. Hellier JL, Patrylo PR, Buckmaster PS, Dudek FE. Recurrent spontaneous motor seizures after repeated low-dose systemic treatment with kainate: assessment of a rat model of temporal lobe epilepsy. *Epilepsy Res* (1998) 31(1):73–84. doi:10.1016/S0920-1211(98)00017-5
9. Doelken MT, Stefan H, Pauli E, Stadlbauer A, Struffert T, Engelhorn T, et al. (1)H-MRS profile in MRI positive- versus MRI negative patients with temporal lobe epilepsy. *Seizure* (2008) 17(6):490–7. doi:10.1016/j.seizure.2008.01.008
10. Nairismagi J, Pitkanen A, Kettunen MI, Kauppinen RA, Kubova H. Status epilepticus in 12-day-old rats leads to temporal lobe neurodegeneration and volume reduction: a histologic and MRI study. *Epilepsia* (2006) 47(3):479–88. doi:10.1111/j.1528-1167.2006.00455.x
11. Vivash L, Gregoire MC, Bouilleret V, Berard A, Wimberley C, Binns D, et al. In vivo measurement of hippocampal GABAA/cBZR density with [18F]-flumazenil PET for the study of disease progression in an animal model of temporal lobe epilepsy. *PLoS One* (2014) 9(1):e86722. doi:10.1371/journal.pone.0086722
12. Thom M. Review: hippocampal sclerosis in epilepsy: a neuropathology review. *Neuropathol Appl Neurobiol* (2014) 40(5):520–43. doi:10.1111/nan.12150
13. Dedeurwaerdere S, Fang K, Chow M, Shen YT, Noordman I, van Raay L, et al. Manganese-enhanced MRI reflects seizure outcome in a model for mesial temporal lobe epilepsy. *Neuroimage* (2013) 68:30–8. doi:10.1016/j.neuroimage.2012.11.054
14. Bertoglio D, Verhaeghe J, Santermans E, Amhaoul H, Jonckers E, Wyffels L, et al. Non-invasive PET imaging of brain inflammation at disease onset predicts spontaneous recurrent seizures and reflects comorbidities. *Brain Behav Immun* (2017) 61:69–79. doi:10.1016/j.bbi.2016.12.015
15. Amhaoul H, Hamaide J, Bertoglio D, Reichel SN, Verhaeghe J, Geerts E, et al. Brain inflammation in a chronic epilepsy model: evolving pattern of the translocator protein during epileptogenesis. *Neurobiol Dis* (2015) 82:526–39. doi:10.1016/j.nbd.2015.09.004
16. Vivash L, Tostevin A, Liu DS, Dalic L, Dedeurwaerdere S, Hicks RJ, et al. Changes in hippocampal GABAA/cBZR density during limbic epileptogenesis: relationship to cell loss and mossy fibre sprouting. *Neurobiol Dis* (2011) 41(2):227–36. doi:10.1016/j.nbd.2010.08.021
17. Gorter JA, Goncalves Pereira PM, van Vliet EA, Aronica E, Lopes da Silva FH, Lucassen PJ. Neuronal cell death in a rat model for mesial temporal lobe epilepsy is induced by the initial status epilepticus and not by later repeated spontaneous seizures. *Epilepsia* (2003) 44(5):647–58. doi:10.1046/j.1528-1157.2003.53902.x
18. Akiyama H, Tooyama I, Kondo H, Ikeda K, Kimura H, McGeer EG, et al. Early response of brain resident microglia to kainic acid-induced hippocampal lesions. *Brain Res* (1994) 635(1–2):257–68. doi:10.1016/0006-8993(94)91447-8
19. van Vliet EA, da Costa Araujo S, Redeker S, van Schaik R, Aronica E, Gorter JA. Blood-brain barrier leakage may lead to progression of temporal lobe epilepsy. *Brain* (2007) 130(Pt 2):521–34. doi:10.1093/brain/awl318
20. van Vliet EA, Holtman L, Aronica E, Schmitz LJ, Wadman WJ, Gorter JA. Atorvastatin treatment during epileptogenesis in a rat model for temporal lobe epilepsy. *Epilepsia* (2011) 52(7):1319–30. doi:10.1111/j.1528-1167.2011.03073.x
21. Van Nieuwenhuyse B, Raedt R, Sprengers M, Dauwe I, Gadeyne S, Carrette E, et al. The systemic kainic acid rat model of temporal lobe epilepsy:

long-term EEG monitoring. *Brain Res* (2015) 1627:1–11. doi:10.1016/j.brainres.2015.08.016
22. Van Nieuwenhuyse B, Raedt R, Delbeke J, Wadman WJ, Boon P, Vonck K. In search of optimal DBS paradigms to treat epilepsy: bilateral versus unilateral hippocampal stimulation in a rat model for temporal lobe epilepsy. *Brain Stimul* (2015) 8(2):192–9. doi:10.1016/j.brs.2014.11.016
23. Powell KL, Ng C, O'Brien TJ, Xu SH, Williams DA, Foote SJ, et al. Decreases in HCN mRNA expression in the hippocampus after kindling and status epilepticus in adult rats. *Epilepsia* (2008) 49(10):1686–95. doi:10.1111/j.1528-1167.2008.01593.x
24. Dedeurwaerdere S, Callaghan PD, Pham T, Rahardjo GL, Amhaoul H, Berghofer P, et al. PET imaging of brain inflammation during early epileptogenesis in a rat model of temporal lobe epilepsy. *EJNMMI Res* (2012) 2(1):60. doi:10.1186/2191-219X-2-60
25. Amhaoul H, Ali I, Mola M, Van Eetveldt A, Szewczyk K, Missault S, et al. P2X7 receptor antagonism reduces the severity of spontaneous seizures in a chronic model of temporal lobe epilepsy. *Neuropharmacology* (2016) 105:175–85. doi:10.1016/j.neuropharm.2016.01.018
26. Racine RJ. Modification of seizure activity by electrical stimulation. II. Motor seizure. *Electroencephalogr Clin Neurophysiol* (1972) 32(3):281–94. doi:10.1016/0013-4694(72)90176-9
27. Paxinos C, Watson C. *The Rat Brain in Stereotaxic Coordinates*. Elsevier Inc. (2007).
28. Schmued LC, Stowers CC, Scallet AC, Xu L. Fluoro-Jade C results in ultra high resolution and contrast labeling of degenerating neurons. *Brain Res* (2005) 1035(1):24–31. doi:10.1016/j.brainres.2004.11.054
29. Tedesco V, Ravagnani C, Bertoglio D, Chiamulera C. Acute ketamine-induced neuroplasticity: ribosomal protein S6 phosphorylation expression in drug addiction-related rat brain areas. *Neuroreport* (2013) 24(7):388–93. doi:10.1097/WNR.0b013e32836131ad
30. Golden GT, Smith GG, Ferraro TN, Reyes PF, Kulp JK, Fariello RG. Strain differences in convulsive response to the excitotoxin kainic acid. *Neuroreport* (1991) 2(3):141–4. doi:10.1097/00001756-199103000-00008
31. Golden GT, Smith GG, Ferraro TN, Reyes PF. Rat strain and age differences in kainic acid induced seizures. *Epilepsy Res* (1995) 20(2):151–9. doi:10.1016/0920-1211(94)00079-C
32. Ali I, O'Brien P, Kumar G, Zheng T, Jones NC, Pinault D, et al. Enduring effects of early life stress on firing patterns of hippocampal and thalamocortical neurons in rats: implications for limbic epilepsy. *PLoS One* (2013) 8(6):e66962. doi:10.1371/journal.pone.0066962
33. Yin P, Liu J, Li Z, Wang YY, Qiao NN, Huang SY, et al. Prenatal immune challenge in rats increases susceptibility to seizure-induced brain injury in adulthood. *Brain Res* (2013) 1519:78–86. doi:10.1016/j.brainres.2013.04.047
34. Matos G, Scorza FA, Mazzotti DR, Guindalini C, Cavalheiro EA, Tufik S, et al. The effects of sleep deprivation on microRNA expression in rats submitted to pilocarpine-induced status epilepticus. *Prog Neuropsychopharmacol Biol Psychiatry* (2014) 51:159–65. doi:10.1016/j.pnpbp.2014.02.001
35. Choy M, Dube CM, Patterson K, Barnes SR, Maras P, Blood AB, et al. A novel, noninvasive, predictive epilepsy biomarker with clinical potential. *J Neurosci* (2014) 34(26):8672–84. doi:10.1523/JNEUROSCI.4806-13.2014
36. Pascente R, Frigerio F, Rizzi M, Porcu L, Boido M, Davids J, et al. Cognitive deficits and brain myo-Inositol are early biomarkers of epileptogenesis in a rat model of epilepsy. *Neurobiol Dis* (2016) 93:146–55. doi:10.1016/j.nbd.2016.05.001
37. Portelli J, Aourz N, De Bundel D, Meurs A, Smolders I, Michotte Y, et al. Intrastrain differences in seizure susceptibility, pharmacological response and basal neurochemistry of Wistar rats. *Epilepsy Res* (2009) 87(2–3):234–46. doi:10.1016/j.eplepsyres.2009.09.009
38. Langer M, Brandt C, Loscher W. Marked strain and substrain differences in induction of status epilepticus and subsequent development of neurodegeneration, epilepsy, and behavioral alterations in rats. [corrected]. *Epilepsy Res* (2011) 96(3):207–24. doi:10.1016/j.eplepsyres.2011.06.005
39. Brandt C, Bankstahl M, Tollner K, Klee R, Loscher W. The pilocarpine model of temporal lobe epilepsy: marked intrastrain differences in female Sprague-Dawley rats and the effect of estrous cycle. *Epilepsy Behav* (2016) 61:141–52. doi:10.1016/j.yebeh.2016.05.020
40. Loscher W, Ferland RJ, Ferraro TN. The relevance of inter- and intrastrain differences in mice and rats and their implications for models of seizures and epilepsy. *Epilepsy Behav* (2017) 73:214–35. doi:10.1016/j.yebeh.2017.05.040
41. Hort J, Brozek G, Komarek V, Langmeier M, Mares P. Interstrain differences in cognitive functions in rats in relation to status epilepticus. *Behav Brain Res* (2000) 112(1–2):77–83. doi:10.1016/S0166-4328(00)00163-7
42. Becker A, Krug M, Schroder H. Strain differences in pentylenetetrazol-kindling development and subsequent potentiation effects. *Brain Res* (1997) 763(1):87–92. doi:10.1016/S0006-8993(97)00409-5
43. Schauwecker PE. Strain differences in seizure-induced cell death following pilocarpine-induced status epilepticus. *Neurobiol Dis* (2012) 45(1):297–304. doi:10.1016/j.nbd.2011.08.013
44. Yilmazer-Hanke DM. Morphological correlates of emotional and cognitive behaviour: insights from studies on inbred and outbred rodent strains and their crosses. *Behav Pharmacol* (2008) 19(5–6):403–34. doi:10.1097/FBP.0b013e32830dc0de
45. Schridde U, Strauss U, Brauer AU, van Luijtelaar G. Environmental manipulations early in development alter seizure activity, Ih and HCN1 protein expression later in life. *Eur J Neurosci* (2006) 23(12):3346–58. doi:10.1111/j.1460-9568.2006.04865.x
46. Dingledine R, Varvel NH, Dudek FE. When and how do seizures kill neurons, and is cell death relevant to epileptogenesis? *Adv Exp Med Biol* (2014) 813:109–22. doi:10.1007/978-94-017-8914-1_9
47. Mathern GW, Adelson PD, Cahan LD, Leite JP. Hippocampal neuron damage in human epilepsy: Meyer's hypothesis revisited. *Prog Brain Res* (2002) 135:237–51. doi:10.1016/S0079-6123(02)35023-4
48. Pitkanen A, Nissinen J, Nairismagi J, Lukasiuk K, Grohn OH, Miettinen R, et al. Progression of neuronal damage after status epilepticus and during spontaneous seizures in a rat model of temporal lobe epilepsy. *Prog Brain Res* (2002) 135:67–83. doi:10.1016/S0079-6123(02)35008-8
49. Arida RM, Scorza FA, de Amorim Carvalho R, Cavalheiro EA. *Proechimys guyannensis*: an animal model of resistance to epilepsy. *Epilepsia* (2005) 46(Suppl 5):189–97. doi:10.1111/j.1528-1167.2005.01065.x
50. Lucchi C, Vinet J, Meletti S, Biagini G. Ischemic-hypoxic mechanisms leading to hippocampal dysfunction as a consequence of status epilepticus. *Epilepsy Behav* (2015) 49:47–54. doi:10.1016/j.yebeh.2015.04.003
51. Jack C, Ruffini F, Bar-Or A, Antel JP. Microglia and multiple sclerosis. *J Neurosci Res* (2005) 81(3):363–73. doi:10.1002/jnr.20482
52. Loane DJ, Byrnes KR. Role of microglia in neurotrauma. *Neurotherapeutics* (2010) 7(4):366–77. doi:10.1016/j.nurt.2010.07.002
53. Weinstein JR, Koerner IP, Moller T. Microglia in ischemic brain injury. *Future Neurol* (2010) 5(2):227–46. doi:10.2217/fnl.10.1
54. Immonen RJ, Kharatishvili I, Sierra A, Einula C, Pitkanen A, Grohn OH. Manganese enhanced MRI detects mossy fiber sprouting rather than neurodegeneration, gliosis or seizure-activity in the epileptic rat hippocampus. *Neuroimage* (2008) 40(4):1718–30. doi:10.1016/j.neuroimage.2008.01.042
55. Hopkins KJ, Wang G, Schmued LC. Temporal progression of kainic acid induced neuronal and myelin degeneration in the rat forebrain. *Brain Res* (2000) 864(1):69–80. doi:10.1016/S0006-8993(00)02137-5
56. Drexel M, Preidt AP, Sperk G. Sequel of spontaneous seizures after kainic acid-induced status epilepticus and associated neuropathological changes in the subiculum and entorhinal cortex. *Neuropharmacology* (2012) 63(5):806–17. doi:10.1016/j.neuropharm.2012.06.009

Conflict of Interest Statement: None of the authors has any conflict of interest to disclose. The authors declare that the research was conducted in the absence of any commercial or financial relationships that could be construed as a potential conflict of interest.

frontiers in Neurology

REVIEW
published: 13 November 2017
doi: 10.3389/fneur.2017.00603

Resveratrol for Easing Status Epilepticus Induced Brain Injury, Inflammation, Epileptogenesis, and Cognitive and Memory Dysfunction—Are We There Yet?

Olagide W. Castro[1,2,3†], Dinesh Upadhya[1,2,4†], Maheedhar Kodali[1,2] and Ashok K. Shetty[1,2]*

[1] Olin E. Teague Veterans' Medical Center, Central Texas Veterans Health Care System, Temple, Texas, United States, [2] Institute for Regenerative Medicine, Department of Molecular and Cellular Medicine, Texas A&M Health Science Center College of Medicine, College Station, Texas, United States, [3] Institute of Biological Sciences and Health, Federal University of Alagoas (UFAL), Maceio, Brazil, [4] Department of Anatomy, Kasturba Medical College, Manipal University, Manipal, India

OPEN ACCESS

Edited by:
Patrick A. Forcelli, Georgetown University, United States

Reviewed by:
Luiz E. Mello, Federal University of São Paulo, Brazil
Thimmasettappa Thippeswamy, Iowa State University, United States

***Correspondence:**
Ashok K. Shetty
shetty@medicine.tamhsc.edu

[†]These authors have contributed equally to this work.

Specialty section:
This article was submitted to Epilepsy, a section of the journal Frontiers in Neurology

Received: 22 July 2017
Accepted: 30 October 2017
Published: 13 November 2017

Citation:
Castro OW, Upadhya D, Kodali M and Shetty AK (2017) Resveratrol for Easing Status Epilepticus Induced Brain Injury, Inflammation, Epileptogenesis, and Cognitive and Memory Dysfunction—Are We There Yet? Front. Neurol. 8:603. doi: 10.3389/fneur.2017.00603

Status epilepticus (SE) is a medical emergency exemplified by self-sustaining, unceasing seizures or swiftly recurring seizure events with no recovery between seizures. The early phase after SE event is associated with neurodegeneration, neuroinflammation, and abnormal neurogenesis in the hippocampus though the extent of these changes depends on the severity and duration of seizures. In many instances, over a period, the initial precipitating injury caused by SE leads to temporal lobe epilepsy (TLE), typified by spontaneous recurrent seizures, cognitive, memory and mood impairments associated with chronic inflammation, reduced neurogenesis, abnormal synaptic reorganization, and multiple molecular changes in the hippocampus. While antiepileptic drugs are efficacious for terminating or greatly reducing seizures in most cases of SE, they have proved ineffective for easing SE-induced epileptogenesis and TLE. Despite considerable advances in elucidating SE-induced multiple cellular, electrophysiological, and molecular changes in the brain, efficient strategies that prevent SE-induced TLE development are yet to be discovered. This review critically confers the efficacy and promise of resveratrol, a phytoalexin found in the skin of red grapes, for easing SE-induced neurodegeneration, neuroinflammation, aberrant neurogenesis, and for restraining the evolution of SE-induced brain injury into a chronic epileptic state typified by spontaneous recurrent seizures, and learning, memory, and mood impairments.

Keywords: epilepsy, seizures, memory impairment, neuroprotection, GABA-ergic interneurons, hippocampal neurogenesis, neuroinflammation, oxidative stress

INTRODUCTION

Status epilepticus (SE) is a medical emergency exemplified by continuous tonic-clonic seizure activity lasting five or more minutes or a series of seizures with no recovery between them (1). The incidence of SE varies from 10 to 61 per 100,000 population each year. The frequency of SE is higher in children and the aged population, and the overall SE-related mortality is ~20% (2–4). SE

can occur from multiple causes, including head injury, febrile seizures, stroke, brain infections, sleep deprivation, withdrawal from alcohol and drugs of abuse, or pre-existing conditions, such as brain tumor, congenital malformations, and Alzheimer's disease. Although a combination of antiepileptic drugs (AEDs) terminate seizures in most cases of SE, the first line of AEDs, such as benzodiazepines and phenytoin are ineffective for ceasing seizures in 30–40% of SE cases (2, 5, 6). Moreover, AEDs have undesirable side effects and do not positively modulate the pathological sequelae of SE. Indeed, significant numbers of SE-survivors display morbidity characterized by cognitive, memory, and mood dysfunction with an enhanced risk for developing chronic temporal lobe epilepsy (TLE). Hence, alternative therapies, alone or in combination with AEDs, are necessary for reducing SE-induced mortality, as well as easing SE-induced pathological ramifications, such as neurodegeneration; neuroinflammation; abnormal hippocampal neurogenesis; epileptogenesis; cognitive, memory, and mood dysfunction; and chronic TLE.

The hippocampus is one of the highly susceptible regions of the brain to be inflicted with SE-induced injury and for developing enduring pathological alterations in structure and function (7, 8). For example, in the early phase after SE elicited by chemo-convulsants, such as the kainic acid (KA) or pilocarpine, degeneration of some dentate hilar neurons and CA1 and CA3 pyramidal neurons is consistently seen in the hippocampus (9–13). Moreover, such neurodegeneration is associated with increased as well as aberrant neurogenesis (14–19). SE enhances neural stem cell (NSC) proliferation in the hippocampus, which is likely triggered by the release of NSC mitogenic factors from dying neurons, deafferented granule cells, and reactive glia (20–22) and elevated gamma-amino butyric acid (GABA) levels (23). These alterations cause increased neurogenesis as well as an abnormal migration of newly born neurons to the dentate hilus (DH) and the dentate molecular layer (ML). The addition of greater numbers of new neurons to the granule cell layer (GCL) after SE has been recognized to be beneficial due to their reduced excitability feature (24). However, abnormal migration of a substantial number of newly born neurons has been suggested to be detrimental due to their propensity for forming epileptogenic circuitry (17, 25–28).

The hippocampal neurodegeneration resulting from SE typically ensues with persistently increased oxidative stress and inflammation (29–32), declined neurogenesis (16, 33, 34), and aberrant sprouting of dentate granule cell axons (mossy fibers) into the inner ML of the dentate gyrus (DG) (35–39). Furthermore, learning and memory impairments (40–44), loss of calbindin expression in dentate granule cells and CA1 pyramidal neurons (45, 46), alterations in neurotransmitter and other receptors (47–49), and functional modifications in astrocytes (50) also occur. Considerably waned neurogenesis in the chronic phase after SE appears to be due to an altered fate-choice decision of newly born cells with a preference to differentiate into glia rather than neurons, likely due to changes in the neurotrophic milieu of neurogenic niches (16, 22, 51) and continued inflammation (30, 31, 44). Importantly, a greater portion of residual neurogenesis in the chronic phase remains aberrant with much of newly born neurons migrating into the DH or giving rise to basal dendrites (34). Both decreased and abnormal neurogenesis in the chronic phase likely contribute to learning, memory, and mood impairments, in addition to enhancing epileptogenic circuitry. Aberrant mossy fiber sprouting is another prominent structural change in the hippocampus after SE. Many studies have suggested that aberrant mossy fiber sprouting is one of the major causes of TLE (52–54). Although there is no consensus on this issue, there is enough evidence to believe that aberrant mossy fiber sprouting contributes at least some extent to the frequency and/or intensity of spontaneous recurrent seizures (SRS) in TLE (55–58).

Thus, multiple epileptogenic and neurogenic changes contribute to the progression of SE-induced injury into chronic epilepsy, typified by SRS, and learning, memory, and mood impairments (59–62). However, the manifestation of TLE in humans following SE may take months, years, or even decades, depending on the degree and the swiftness by which the various epileptogenic changes achieve required ceilings to produce hippocampal hyperexcitability. The delay provides a large window to intervene with promising alternative drugs or natural compounds that are efficacious for alleviating oxidative stress, inflammation, and abnormal neurogenesis. While intervention in the early phase after SE may considerably reduce neurodegeneration, intervention in both early and latent phases or in the latent phase alone may block or slow-down the subsequent epileptogenic changes, thwart or delay the development of SRS and/or prevent cognitive, memory, and mood impairments. However, it is important to note that partial neuroprotection or limited suppression of ensuing inflammation provided by drugs does not necessarily prevent epileptogenesis and/or the related comorbidities. For example, anticonvulsant drugs, such as dizocilpine and retigabine, interleukin-1 receptor antagonist anakinra, interleukin-1β inhibitor VX765, or a melatonin receptor agonist agomelatine, can provide partial protection against SE-induced neuron loss and inflammation but cannot prevent epileptogenesis (63–65). This discrepancy reflects the fact that neurodegeneration and neuroinflammation are not the exclusive reasons driving epileptogenesis and the occurrence of SRS after SE or brain injury (66). Therefore, it is imperative to identify drugs that not only provide neuroprotection and suppress inflammation but also reduce multiple other epileptogenic changes after SE. In addition, it will be essential to determine for every candidate drug, whether short-term treatment in the immediate post-SE period or prolonged treatment for several weeks after SE is needed. In this review, we focus on discussing the promise of resveratrol (RESV), a phytoalexin found in the skin of red grapes, certain berries, and peanuts, for easing SE-induced neurodegeneration, neuroinflammation, epileptogenesis, chronic seizures and the associated comorbidities.

SOURCE OF RESV AND ITS KNOWN BIOLOGICAL ACTIVITIES

Resveratrol (3,5,4′-trihydroxystilbene) is a natural phytoalexin, produced by grapevines, pines, and legumes in response to bacterial or fungal infections, injury, or stress (67, 68). RESV is

also found in raspberries, mulberries, plums, peanuts, bilberries, blueberries, cranberries, Scots pine, and Japanese knotweed. A vast majority of these sources contain both cis- and trans-isomeric forms of RESV. However, the trans-isomer has received the utmost attention because of its role in beneficial effects of RESV (69).

Numerous studies have shown that RESV facilitates a range of biological activities, including longevity and prevention of cancer (70–72). Studies in animal models of human diseases have pointed out that RESV has anti-ischemic, antiviral, antioxidant, and antiinflammatory properties (73–76). Besides, RESV has been shown to delay several age-related diseases (70, 77, 78). Its neuroprotective property has been seen in several cell culture models (79, 80) as well as *in vivo* models of neuroinflammation (81), stroke (82), spinal cord injury (83), multiple sclerosis (84), Huntington's disease (85), and traumatic brain injury (86). The other features of RESV that are attractive for therapeutic use include its ability to cross the blood–brain barrier after peripheral administration, its minimal side effects and its prolonged activity in the brain (~4 h) after peripheral administration (87–89).

RESULTS FROM CLINICAL TRIALS REGARDING THE BENEFICIAL EFFECTS OF RESV ON HUMAN HEALTH

The effects of RESV on insulin sensitivity has been somewhat controversial. Two clinical trials in obese humans and type 2 diabetes patients demonstrated that 4-weeks of RESV treatment improved insulin sensitivity associated with reductions in low-level inflammation, blood pressure, and liver fat accumulation (80–91). However, other clinical trials showed no such improvement in non-obese women with normal glucose tolerance (92) and obese healthy men (93). Discrepancies in results between these studies have been attributed to differences in study designs, populations, and resveratrol formulations (94). It is also likely that RESV is not efficacious for enhancing glucose handling in subjects where normal glucose homeostasis is already maintained but effective in subjects suffering from insulin resistance. In line with this notion, a recent clinical trial showed that 4 months of RESV treatment in middle-aged men with metabolic syndrome could induce increased muscle turnover, lipid metabolism, and accumulation of long-chain saturated, monounsaturated, and polyunsaturated free fatty acids, and beneficial alterations in gut microbiota (94). Another recent clinical trial showed that incorporation of RESV to standard antihypertensive treatment is adequate for reducing blood pressure to normal levels, without the need for additional antihypertensive drugs (95). This study also implied prevention of liver damage with RESV intake, based on lower levels of hepatic enzyme glutamate-pyruvate transaminase in the serum.

Several clinical trials have also suggested that RESV treatment is beneficial for improving human brain function. For instance, improved memory performance allied with enhanced hippocampal functional connectivity between the hippocampus and the medial prefrontal cortex has been observed with RESV treatment in healthy overweight elderly individuals (96). RESV has also been shown to enhance neurovascular coupling and cognitive performance in type 2 diabetes patients (97). Furthermore, in individuals with mild to moderate Alzheimer disease, RESV treatment modulated amyloid β-40 levels in both plasma and cerebrospinal fluid, in comparison to the placebo-treated group (98). Overall, clinical studies conducted so far imply that RESV is safe, well-tolerated and beneficial with minimal side effects. Nonetheless, detailed, long-term follow-up studies are needed to fully understand the efficacy of RESV for improving the health in people with brain diseases.

POTENTIAL MECHANISMS UNDERLYING THE NEUROPROTECTIVE PROPERTIES OF RESV

Many studies have suggested that RESV mediates protective effects through its robust antioxidant and antiinflammatory activities, more so in aging or disease conditions (32, 99–101). First, RESV can reduce reactive oxygen species (ROS) generation through several mechanisms. It can suppress mitochondrial complex III activity, and the release of cytochrome *C* (102, 103) as well as modulate *N*-methyl-D-aspartate, α-amino-3-hydroxy-5-methyl-4-isoxazolepropionic acid or KA receptor, and intracellular Ca^{2+} pathway. RESV can also prevent mitochondrial dysfunction and impairments in $Na^{+}K^{+}$-ATPase activity after glutamate activation (104). Second, RESV can inhibit lipid peroxidation and enhance antioxidant and heme oxygenase 1 activity (89, 105). Third, RESV can restrain the loss of proteins that are implicated in cognitive disorders (106), stimulate AMP kinase activity and mitochondrial biogenesis (107), and dampen the increased electrical activity of neurons (108). Fourth, RESV can indirectly mediate beneficial effects through activation of sirtuin 1 (SIRT1). SIRT1, a class III histone deacetylase, can regulate multiple biological activities, including oxidative stress, inflammation, cellular senescence, autophagy, apoptosis, differentiation, stem cell pluripotency, metabolism, and mitochondrial biogenesis (109). In the brain, SIRT1 can influence chromatin remodeling, DNA repair, cell survival, neurogenesis, synaptic plasticity, and memory (110, 111). Finally, RESV can mediate antiinflammatory actions through activation of AMP kinase and subsequent inhibition of mammalian target of rapamycin pathway. These, in turn, inhibit the activation of nuclear factor-kappa B and the production of proinflammatory molecules induced by SE (112).

EFFECTS OF RESV PRE-TREATMENT ON EXCITOTOXIC BRAIN INJURY OR ACUTE SEIZURES

Neuroprotective effects of RESV has been seen in several animal models of excitotoxic brain injury. Most of the earlier studies have, however, examined the effects of pre-treating animals with RESV on subsequent neurodegeneration mediated by excitotoxic agents. Numerous beneficial effects were observed with a variety of pre-treatment approaches. While one study showed reduced brain damage with KA administration after chronic

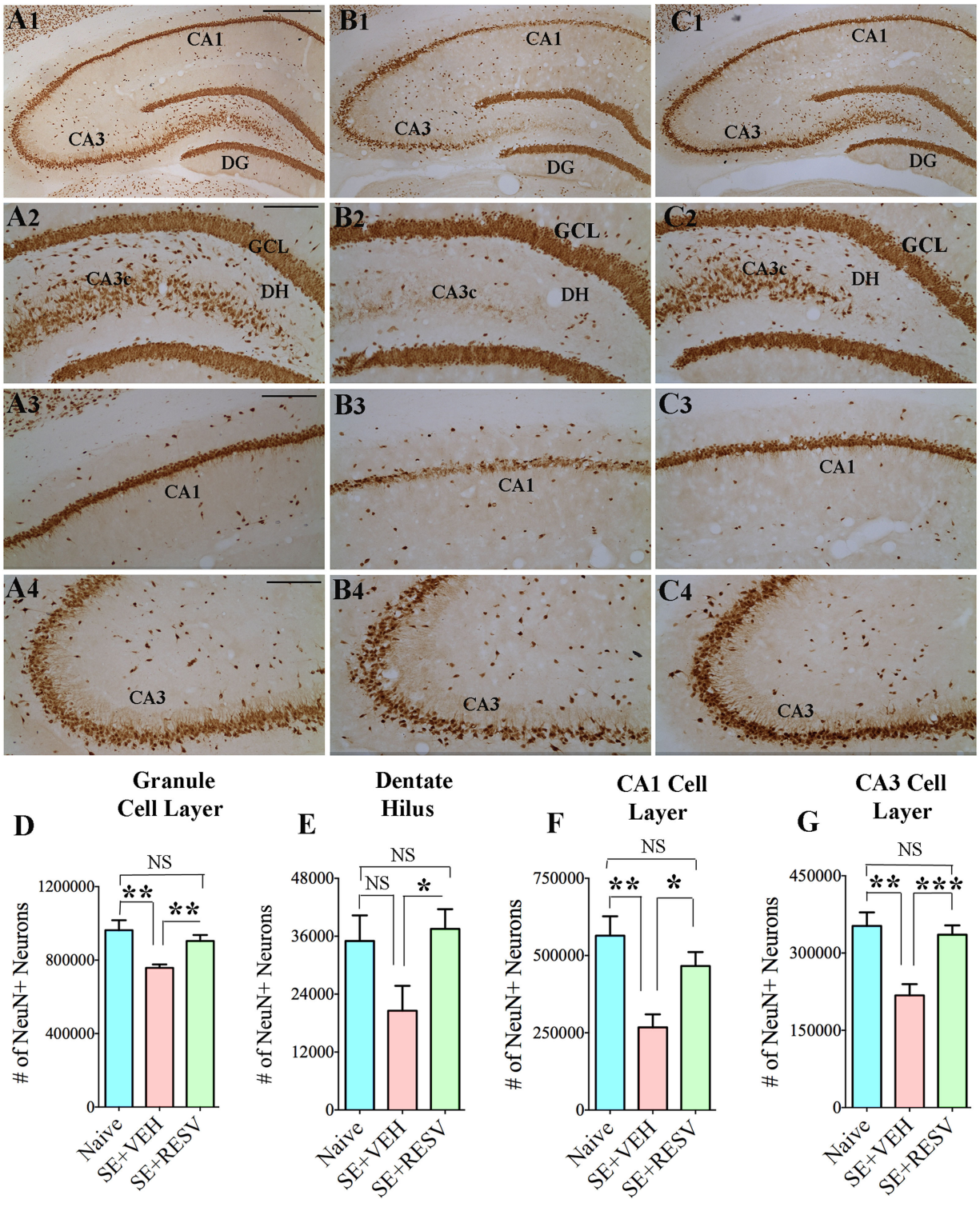

FIGURE 1 | Four days of resveratrol (RESV) treatment after status epilepticus (SE) considerably curtailed neuron loss in the dentate hilus (DH), granule cell layer (GCL), and hippocampal CA1 and CA3 pyramidal cell layers. Panels **(A1–C4)** illustrate neuron-specific nuclear antigen (NeuN) positive neurons in different subfields of the hippocampus from a naïve control animal **(A1–A4)**, an animal receiving vehicle (VEH) after SE **(B1–B4)**, and an animal receiving RESV after SE **(C1–C4)**. Scale bar, **(A1,B1,C1)**, 500 µm; **(A2–A4,B2–B4,C2–C4)**, 200 µm. Bar charts display numbers of NeuN + neurons in distinct hippocampal cell layers. Animals receiving VEH after SE displayed considerably diminished numbers of neurons in the DH **(D)**, GCL **(E)**, and the CA1 and CA3 pyramidal cell layers **(F,G)**. However, neuron numbers were comparable between animals receiving RESV after SE and naïve control animals **(D–G)**, implying robust neuroprotection by RESV. $^{*}p < 0.05$; $^{**}p < 0.01$; $^{***}p < 0.001$; NS, not significant. Figure reproduced from Mishra et al. (32).

RESV pre-treatment (113), another study demonstrated significant protection against KA-induced seizures and increased oxidative stress with the administration of RESV performed 5 min before KA treatment (114). Moreover, delayed onset of the epileptiform electroencephalographic (EEG) discharges, and reduced malondialdehyde (MDA, a byproduct of lipid peroxidation) levels were observed with RESV treatment occurring 30 min before intracortical placement of ferric chloride (115).

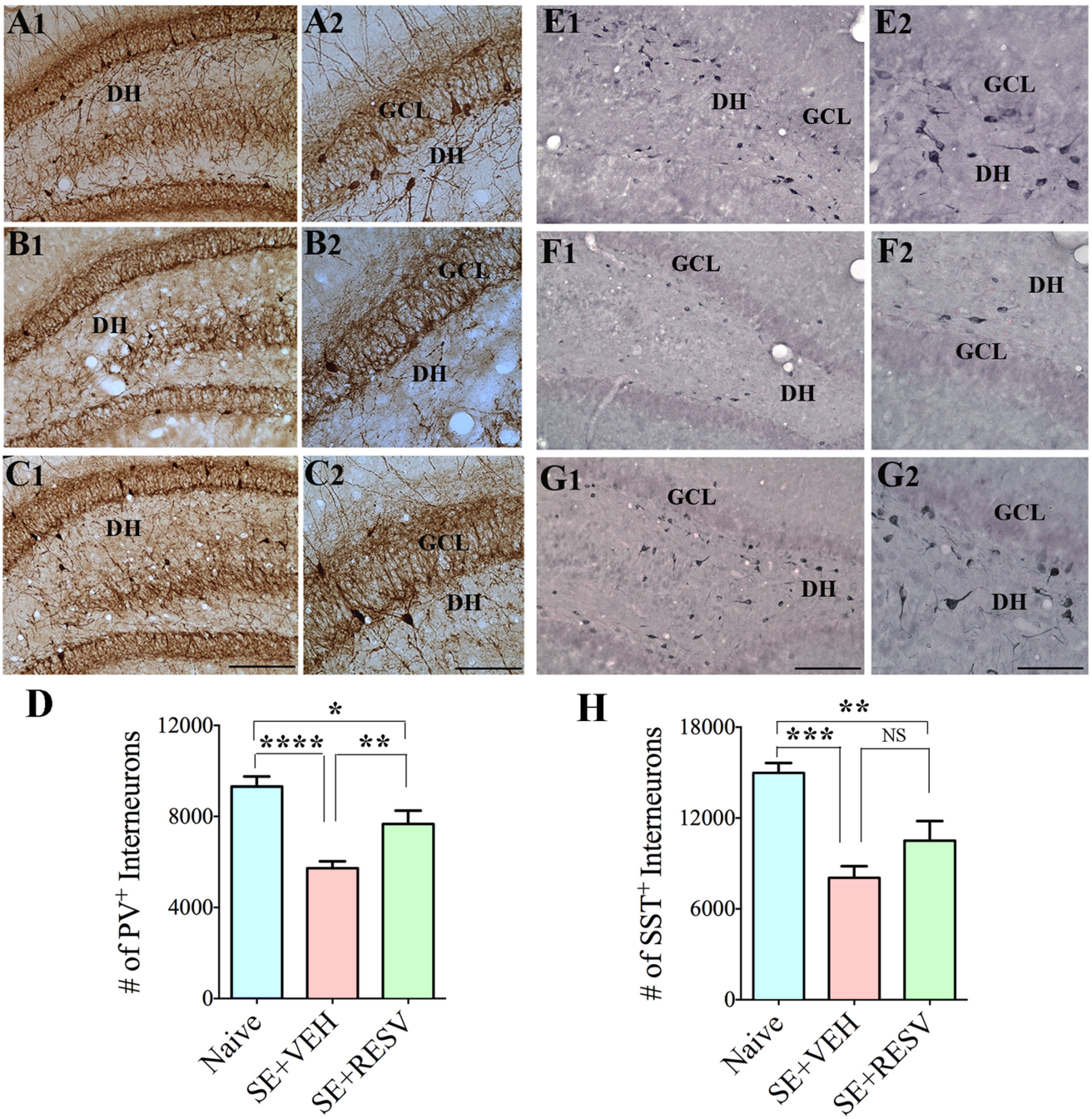

FIGURE 2 | Four days of resveratrol (RESV) treatment after status epilepticus (SE) restrained the loss of inhibitory interneurons expressing the calcium-binding protein parvalbumin (PV) and the neuropeptide somatostatin (SST) in the dentate gyrus (DG). **(A1–C2)** and **(E1–G2)**, respectively, illustrate PV+ interneurons and SST+ interneurons in the DG from a naïve control animal **(A1–A2**, **E1–E2)**, an animal receiving vehicle (VEH) after SE **(B1–B2,F1–F2)**, and an animal receiving RESV after SE **(C1–C2,G1–G2)**. DH, Dentate hilus; GCL, granule cell layer. Scale bar: **(A1,B1,C1,E1,F1,G1)**, 200 μm; **(A2,B2,C2,E2,F2,G2)**, 100 μm. Bar charts display numbers of PV+ **(D)** and SST+ **(H)** interneurons in the DG. Animals receiving VEH after SE displayed considerable loss of PV+ and SST+ interneurons. However, animals receiving RESV showed only modest loss of PV+ and SST+ interneuron numbers. *$p < 0.05$; **$p < 0.01$; ***$p < 0.001$; ****$p < 0.0001$. Figure reproduced from Mishra et al. (32).

Additional studies demonstrated neuroprotection against pilocarpine-induced SE with RESV administration occurring 30 min before pilocarpine treatment (112) and reduced seizure activity and mortality with 6 weeks of RESV treatment prior to KA administration (116). Furthermore, increased latency to myoclonic jerks and seizures, decreased number of myoclonic jerks, reduced neuronal injury, oxidative stress, and apoptosis were observed in Wistar rats receiving RESV 30 min prior to pentylenetetrazole (PTZ)-induced kindling (135). A subsequent study also showed that concurrently treating animals with KA and RESV (daily for 5 days) results in significant neuroprotection (117).

Multiple mechanisms have been suggested for the neuroprotective effects of RESV pre-treatment against seizures. A few studies showed that RESV moderates excitatory synaptic neurotransmission *via* inhibition of the voltage-gated potassium currents, and post-synaptic glutamate receptors (108, 118). The other studies showed the ability of RESV for suppressing reactive astrocytes and activated microglia (117), scavenging and opposing the production of ROS, antioxidant, antiapoptotic, and antiinflammatory activity (102, 112, 116, 119). Considering the effects of RESV on excitatory synaptic neurotransmission and post-synaptic glutamate receptors, it is plausible that RESV pre-treatment impacts the overall SE activity, which likely influences pathogenesis that follows SE. However, detailed EEG studies on the intensity of SE in RESV pre-treated animals vis-à-vis untreated animals are lacking. Although the beneficial effects of RESV pre-treatment or concurrent treatment of excitotoxins and RESV

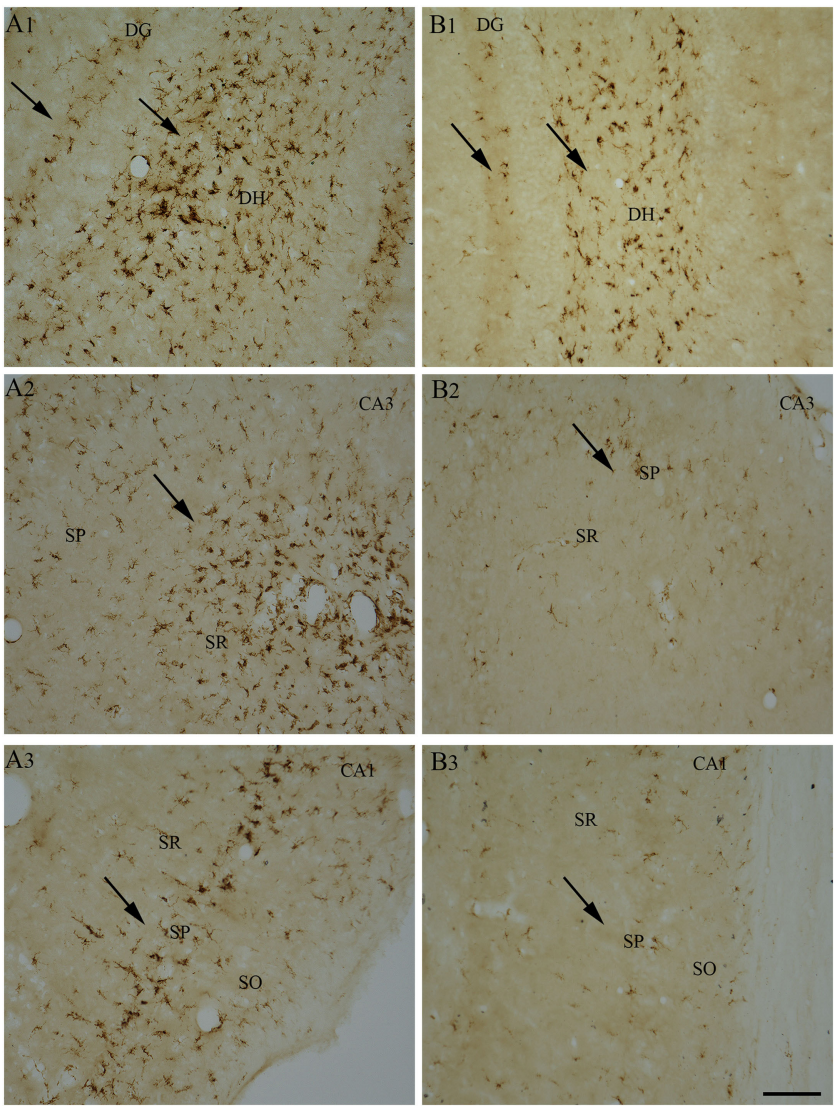

FIGURE 3 | Four days of resveratrol (RESV) treatment after status epilepticus (SE) reduced the signs of inflammatory processes in the dentate gyrus (DG) and CA1 and CA3 subfields. A robust inflammation, indicated by large numbers of ED-1+activated microglia, is obvious in the DG, CA1, and CA3 hippocampal subfields of the animal receiving vehicle after SE **(A1–A3)**, in comparison to a reduced inflammation in the animal receiving RESV after SE **(B1–B3)**. SO, Stratum oriens. SP, Stratus pyramidale, SR, Stratus radiatum. Scale bar: **(A1–B3)**, 100 μm.

in different animal models are useful for understanding mechanisms by which RESV mediates neuroprotection, there is little translational value with this approach. Pre-treatment approach may, however, be relevant to a smaller percentage of people who take RESV daily as an antioxidant or antiinflammatory dietary supplement. However, it remains to be determined whether such small daily doses would be adequate to have protective effects against brain insults.

EFFICACY OF RESV TREATMENT COMMENCING AFTER THE ONSET OF SE ON SEIZURE-INDUCED NEURODEGENERATION, NEUROINFLAMMATION, AND ABNORMAL NEUROGENESIS

So far, only a few studies have analyzed the effects of RESV treatment starting hours after the onset of SE on SE-induced detrimental effects. A recent study, using a graded intraperitoneal KA administration model of SE provided the first proof that RESV treatment starting 1 h after SE onset was effective for considerably restraining SE-induced hippocampal damage (32). In this study, 4 days of RESV treatment (3 hourly doses on SE day commencing 1 h after SE, twice daily doses on SE days 2–4) was found efficacious for providing robust neuroprotection against SE. In comparison to animals receiving vehicle after SE, animals receiving RESV after SE demonstrated robust preservation of glutamatergic neurons in the GCL, DH, and CA1 and CA3 subfields of the hippocampus (**Figure 1**), and greater levels of maintenance of subclasses of GABA-ergic interneurons expressing parvalbumin, somatostatin (**Figure 2**), and neuropeptide Y. Moreover, RESV treatment after SE resulted in normalization of seizure-induced increased oxidative stress. This was evidenced in RESV treated rats by the maintenance of hippocampal MDA and the expression of multiple genes related to oxidative stress response to levels seen in naïve control animals. Controlling oxidative stress after SE has great significance as greatly elevated oxidative stress can facilitate progressive neuron loss and impair the function of remaining neurons. Indeed, increased levels of MDA has been seen in epileptic patients (120, 121). However,

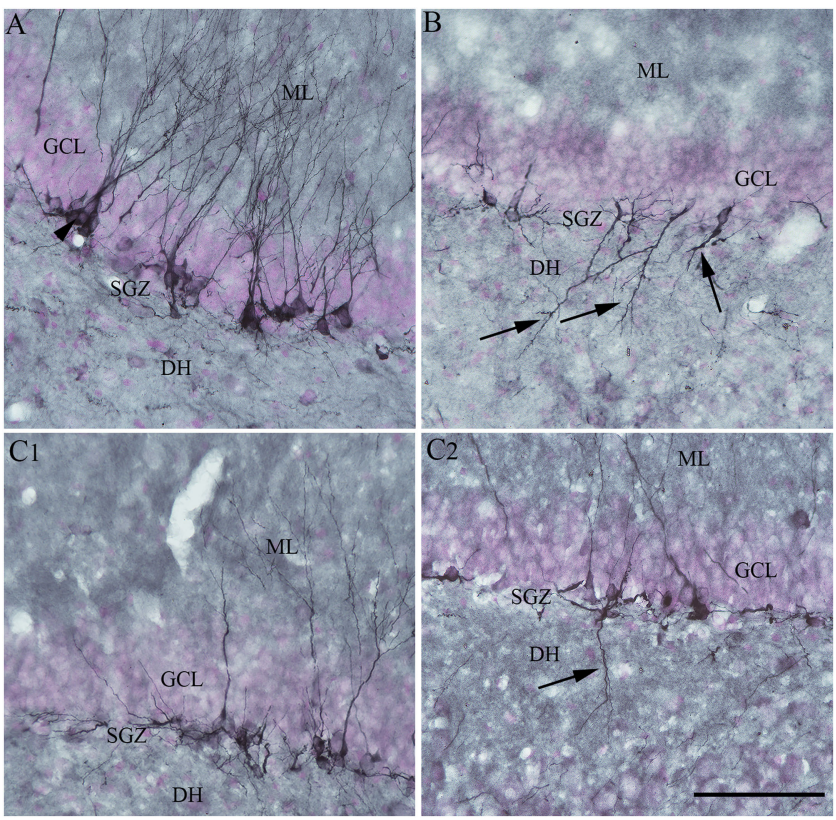

FIGURE 4 | Four days of resveratrol (RESV) treatment after status epilepticus (SE) restrained the dendrites of newly born neurons projecting into the dentate hilus (DH). In the naïve control animal **(A)**, the normal polarity of newly born neurons is apparent from virtually all dendrites projecting into the molecular layer (ML) of the dentate gyrus. Contrastingly, in the animal receiving vehicle after SE **(B)**, a significant number of newly born neurons showed either abnormal polarity with apical dendrites projecting into the dentate hilus (DH; arrows) or basal dendrites projecting into the hilus. Interestingly, in animals receiving RESV after SE **(C1,C2)**, there were no newly born neurons with apical dendrites projecting into the dentate hilus **(C1)**. In addition, the occurrence of newly born neurons with basal dendrites projecting into the hilus was reduced [arrow in **(C2)**]. Scale bar = 100 μm.

in a seizure study using neonatal animals, RESV therapy did not restrain SE-induced brain damage because SE in neonatal animals does not elevate oxidative stress (122). From this perspective, it is noteworthy that RESV therapy for SE is effective only in conditions where elevated oxidative stress is one of the major initial sequels of SE. Thus, RESV therapy for SE is likely more suitable for the adult and aged populations where oxidative stress is among the prominent initial pathological changes. Furthermore, 4 days of RESV therapy was effective for suppressing SE-induced inflammation in the hippocampus. This was evinced mainly through reduced concentration of tumor necrosis factor-alpha protein and diminished numbers of activated microglia in the hippocampus (**Figure 3**) but did not involve modulation of nuclear factor-kappa B or SIRT1 activity (32).

Moreover, RESV treatment after SE in the above study reduced aberrant neurogenesis (**Figure 4**). Both numbers of newly born neurons that migrated abnormally into the DH and occurrences of basal dendrites from newly born neurons were diminished. Reduced aberrant neurogenesis mediated by RESV has functional implications because such neurogenesis promotes epileptogenic circuitry between ectopically placed granule cells

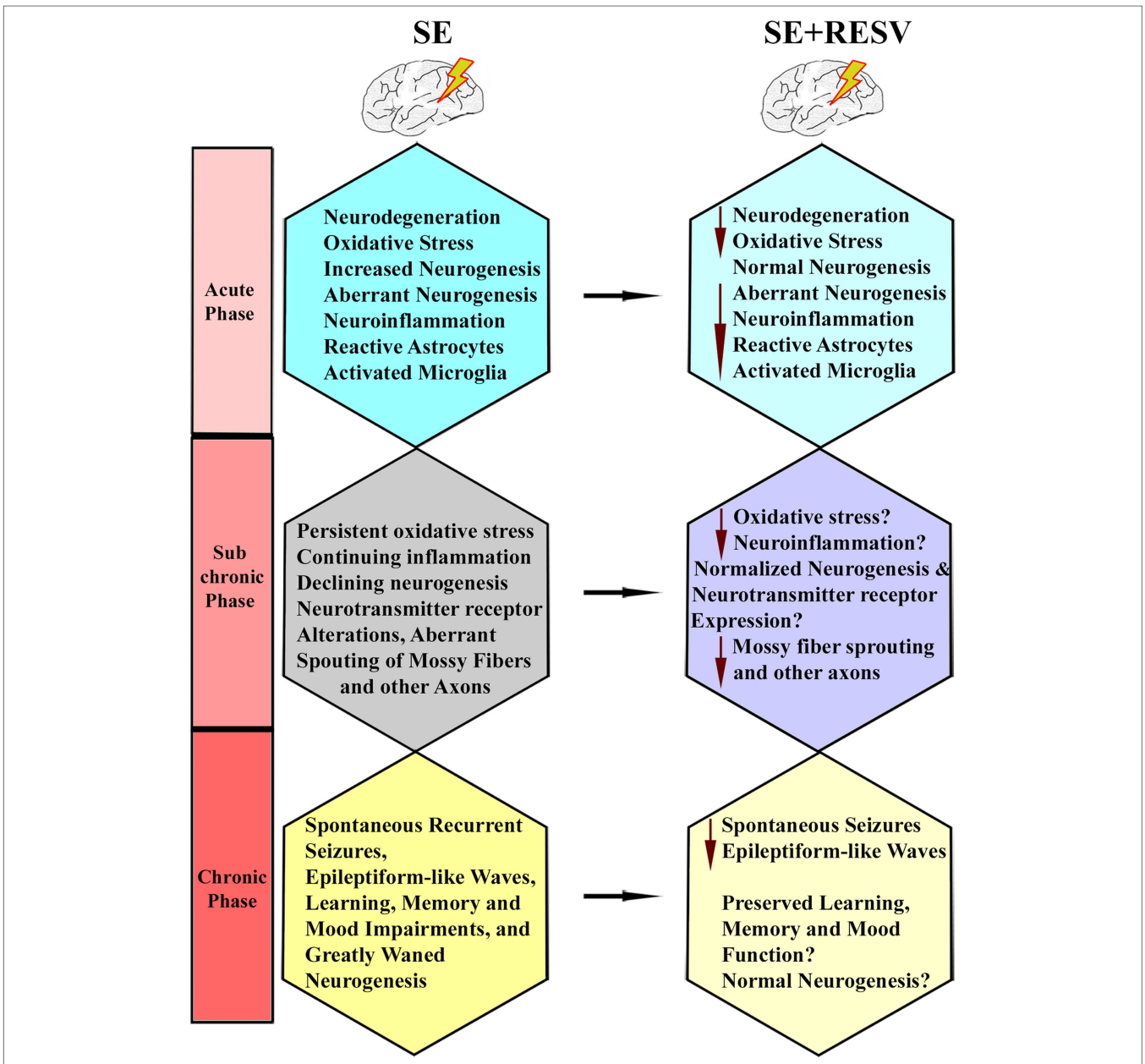

FIGURE 5 | Illustration of how resveratrol (RESV) treatment after status epilepticus likely restrains or modifies the various detrimental effects of SE in the acute, subchronic, and chronic phases.

and the CA3 pyramidal neurons, and between basal dendrites of granule cells projecting into the DH and granule cell axons (mossy fibers). These abnormal synaptic connectivities may contribute to occurrences of SRS in the chronic phase after SE (25–28, 123–126). In summary, the above study provided novel proof that RESV treatment starting 1 h after SE is also favorable for curtailing SE-caused elevated oxidative stress, neuron loss, inflammatory cascade, and anomalous neurogenesis, all of which can contribute to the development of a chronic epileptic state after SE.

EFFICACY OF RESV TREATMENT FOR EASING EPILEPTOGENESIS AND CHRONIC EPILEPSY

A study by Wu and colleagues examined the effects of oral administration of RESV for 10 days after an intrahippocampal injection of KA into anesthetized rats (127). They found that a reduced percentage of animals receiving RESV after KA displayed behavioral SRS at 9-weeks post-KA, in comparison to rats receiving KA alone. Besides, 2 h of EEG recordings showed diminished epileptiform-like waves in rats receiving RESV after KA, associated with some neuroprotection in the CA1 and CA3a cell layer and reduced aberrant mossy fiber sprouting into the dentate supragranular layer. These results suggest that RESV treatment starting after the induction of hippocampal injury has the potential for reducing the incidence and intensity of injury-induced chronic epilepsy. However, there are several caveats in this study. Since KA was administered directly into the hippocampus under chloral hydrate anesthesia, the influence of anesthesia on the intensity of SE is an issue. Furthermore, direct application of KA caused considerable neurodegeneration in the DH and CA3b and CA3c subregions, likely due to localized excitotoxicity. Hence, the neuroprotective effect of RESV that commenced after KA injection could not be ascertained on dentate hilar and CA3b and CA3c pyramidal neurons. Also, SRS and epileptogenic changes were measured only in the early phase after KA administration during which minimal SRS are seen. Another study evaluated the effects of RESV on a few behavioral and pathological changes in a rat model of epilepsy induced *via* PTZ kindling (128). The results suggested improved cognitive function, diminished neuronal loss in CA1 and CA3 hippocampal subfields, and reduced S100-beta protein levels in the cerebrospinal fluid and serum, in animals receiving RESV after PTZ. Furthermore, a recent study showed that acute RESV treatment after an intrahippocampal injection of KA partially inhibits evoked epileptiform discharges in the hippocampal CA1 region (129). Additional analyses demonstrated that long-term RESV treatment in this model could normalize the expression of hippocampal kainate glutamate receptors and the $GABA_A$ receptor alpha1 subunit, and inhibit the KA-induced increased glutamate/GABA ratio in the hippocampus (129). Overall, the results of a few studies on anti-epileptogenic effects of RESV are promising but not conclusive. Additional rigorous longitudinal studies in animal models of epilepsy on specific epileptogenic changes are required to understand the extent to which RESV treatment can curtail epileptogenic changes that ensue after SE. **Figure 5** illustrates the known and likely beneficial effects of early RESV treatment after SE on the various detrimental sequelae in the acute, subchronic, and chronic phases.

CONCLUSION AND FUTURE DIRECTIONS

From the results of pre-clinical studies performed so far, RESV appears to be a promising compound to employ as an adjunct to AED therapy for SE. The idea is to use AEDs for terminating SE and then employ RESV for prolonged periods to block or lessen SE-induced maladaptive structural changes as well as the development of epileptogenic circuitry. Nonetheless, additional studies are critically required prior to clinical application to ascertain whether the amount of neuroprotective, antioxidant, antiinflammatory, and normal-neurogenesis promoting effects offered by RESV therapy after SE is adequate for thwarting or at least greatly restraining the progression of SE-induced hippocampal injury into a chronic epileptic state exemplified by SRS and cognitive, memory, and mood impairments. Particularly, the following issues need to be addressed. First, SRS develop progressively after an incidence of SE and typically require 3–5 months of time to exhibit a consistent frequency and intensity of SRS over weeks (12, 13, 130, 131). Therefore, to determine the benefits of RESV administration after SE, detailed analyses of SRS through chronic EEG recordings are required at 3–5 months post-SE. Second, validation of the efficacy of RESV for preventing or greatly restraining SE-induced epileptogenic changes and the associated comorbidities will be required at different time-points after SE. These should comprise quantification of the (i) progressive loss of both glutamatergic neurons and GABA-ergic interneurons in the hippocampus and the various extrahippocampal regions; (ii) continued abnormal migration of newly generated neurons into the hilus and the ML of the DG, in relation to the survival of reelin-positive interneurons that aid the migration of newly born neurons (32, 44); (iii) extent of abnormal synaptic reorganization of dentate mossy fibers and entorhinal axons (37, 132); (iv) alterations in astrocyte function (133, 134); (v) progression of neuroinflammation (30, 31); (vi) attainment of chronic epileptic state typified by SRS; (vii) cognitive and memory impairments; and (viii) extent of depression. Third, it will be important to identify the time-point after SE at which commencement of RESV treatment provides maximal neuroprotection and prevents the progression of SE-induced brain damage into a state typified by SRS and cognitive, memory, and mood impairments. Fourth, it will be necessary to know the effects of different doses of RESV treatment occurring for shorter periods after SE (e.g., 4–14 days of treatment) and continuing for longer durations after SE (e.g., 3–12 weeks) on outcomes such as SRS frequency and intensity, and cognitive, memory and mood function. Furthermore, determining the best route of RESV administration after SE for achieving maximal efficacy with minimal side effects will be important. Routes of administration that are clinically practical for repeated administration may be examined, which may include oral and intranasal routes. Finally, any potential

adverse effects of long-term administration of higher doses of RESV after SE need to be examined.

AUTHOR CONTRIBUTIONS

OC and DU wrote the first draft of the manuscript text and prepared figures. MK provided input to the first draft and prepared the reference list. AS edited and prepared the final version of the manuscript text and figures.

ACKNOWLEDGMENTS

This work was supported by grants from the Department of Veterans Affairs Merit Award I01BX000883 (AS), Department of Veterans Affairs BLR&D Research Career Scientist award 1IK6BX003612 (AS), Department of Defense (GWIRP grant, W81XWH-14-1-0572 to AKS), and a Visiting Scientist Award from CAPES Foundation, Ministry of Education, Government of Brazil (OC).

REFERENCES

1. Trinka E, Kalviainen R. 25 years of advances in the definition, classification and treatment of status epilepticus. *Seizure* (2017) 44:65–73. doi:10.1016/j.seizure.2016.11.001
2. Sirven JI, Waterhouse E. Management of status epilepticus. *Am Fam Physician* (2003) 68(3):469–76.
3. Betjemann JP, Lowenstein DH. Status epilepticus in adults. *Lancet Neurol* (2015) 14(6):615–24. doi:10.1016/S1474-4422(15)00042-3
4. Sanchez S, Rincon F. Status epilepticus: epidemiology and public health needs. *J Clin Med* (2016) 5:E71. doi:10.3390/jcm5080071
5. Shaner DM, McCurdy SA, Herring MO, Gabor AJ. Treatment of status epilepticus: a prospective comparison of diazepam and phenytoin versus phenobarbital and optional phenytoin. *Neurology* (1988) 38:202–7. doi:10.1212/WNL.38.2.202
6. Knake S, Hamer HM, Rosenow F. Status epilepticus: a critical review. *Epilepsy Behav* (2009) 15:10–4. doi:10.1016/j.yebeh.2009.02.027
7. Sankar R, Shin DH, Liu H, Mazarati A, Pereira de Vasconcelos A, Wasterlain CG. Patterns of status epilepticus-induced neuronal injury during development and long-term consequences. *J Neurosci* (1998) 18:8382–93.
8. Sloviter RS. Excitatory dentate granule cells normally contain GAD and GABA, but does that make them GABAergic, and do seizures shift granule cell function in the inhibitory direction? *Epilepsy Curr* (2003) 3:3–5. doi:10.1046/j.1535-7597.2003.03101.x
9. Hellier JL, Patrylo PR, Buckmaster PS, Dudek FE. Recurrent spontaneous motor seizures after repeated low-dose systemic treatment with kainate: assessment of a rat model of temporal lobe epilepsy. *Epilepsy Res* (1998) 31:73–84. doi:10.1016/S0920-1211(98)00017-5
10. Castro OW, Furtado MA, Tilelli CQ, Fernandes A, Pajolla GP, Garcia-Cairasco N. Comparative neuroanatomical and temporal characterization of FluoroJade-positive neurodegeneration after status epilepticus induced by systemic and intrahippocampal pilocarpine in Wistar rats. *Brain Res* (2011) 1374:43–55. doi:10.1016/j.brainres.2010.12.012
11. Bengzon J, Mohapel P, Ekdahl CT, Lindvall O. Neuronal apoptosis after brief and prolonged seizures. *Prog Brain Res* (2002) 135:111–9. doi:10.1016/S0079-6123(02)35011-8
12. Rao MS, Hattiangady B, Reddy DS, Shetty AK. Hippocampal neurodegeneration, spontaneous seizures, and mossy fiber sprouting in the F344 rat model of temporal lobe epilepsy. *J Neurosci Res* (2006) 83:1088–105. doi:10.1002/jnr.20802
13. Rao MS, Hattiangady B, Rai KS, Shetty AK. Strategies for promoting anti-seizure effects of hippocampal fetal cells grafted into the hippocampus of rats exhibiting chronic temporal lobe epilepsy. *Neurobiol Dis* (2007) 27:117–32. doi:10.1016/j.nbd.2007.03.016
14. Parent JM, Yu TW, Leibowitz RT, Geschwind DH, Sloviter RS, Lowenstein DH. Dentate granule cell neurogenesis is increased by seizures and contributes to aberrant network reorganization in the adult rat hippocampus. *J Neurosci* (1997) 17:3727–38.
15. Gray WP, Sundstrom LE. Kainic acid increases the proliferation of granule cell progenitors in the dentate gyrus of the adult rat. *Brain Res* (1998) 790:52–9. doi:10.1016/S0006-8993(98)00030-4
16. Hattiangady B, Rao MS, Shetty AK. Chronic temporal lobe epilepsy is associated with severely declined dentate neurogenesis in the adult hippocampus. *Neurobiol Dis* (2004) 17:473–90. doi:10.1016/j.nbd.2004.08.008
17. Shetty AK, Hattiangady B. Concise review: prospects of stem cell therapy for temporal lobe epilepsy. *Stem Cells* (2007) 25:2396–407. doi:10.1634/stemcells.2007-0313
18. Rao MS, Hattiangady B, Shetty AK. Status epilepticus during old age is not associated with enhanced hippocampal neurogenesis. *Hippocampus* (2008) 18:931–44. doi:10.1002/hipo.20449
19. Shetty AK, Hattiangady B, Rao MS, Shuai B. Neurogenesis response of middle-aged hippocampus to acute seizure activity. *PLoS One* (2012) 7:e43286. doi:10.1371/journal.pone.0043286
20. Lowenstein DH, Seren MS, Longo FM. Prolonged increases in neurotrophic activity associated with kainate-induced hippocampal synaptic reorganization. *Neuroscience* (1993) 56:597–604. doi:10.1016/0306-4522(93)90359-N
21. Shetty AK, Zaman V, Shetty GA. Hippocampal neurotrophin levels in a kainate model of temporal lobe epilepsy: a lack of correlation between brain-derived neurotrophic factor content and progression of aberrant dentate mossy fiber sprouting. *J Neurochem* (2003) 87:147–59. doi:10.1046/j.1471-4159.2003.01979.x
22. Shetty AK, Rao MS, Hattiangady B, Zaman V, Shetty GA. Hippocampal neurotrophin levels after injury: relationship to the age of the hippocampus at the time of injury. *J Neurosci Res* (2004) 78:520–32. doi:10.1002/jnr.20302
23. Ge S, Pradhan DA, Ming GL, Song H. GABA sets the tempo for activity-dependent adult neurogenesis. *Trends Neurosci* (2007) 30:1–8. doi:10.1016/j.tins.2006.11.001
24. Jakubs K, Nanobashvili A, Bonde S, Ekdahl CT, Kokaia Z, Kokaia M, et al. Environment matters: synaptic properties of neurons born in the epileptic adult brain develop to reduce excitability. *Neuron* (2006) 52:1047–59. doi:10.1016/j.neuron.2006.11.004
25. Scharfman HE, Goodman JH, Sollas AL. Granule-like neurons at the hilar/CA3 border after status epilepticus and their synchrony with area CA3 pyramidal cells: functional implications of seizure-induced neurogenesis. *J Neurosci* (2000) 20:6144–58.
26. Scharfman HE, Sollas AL, Goodman JH. Spontaneous recurrent seizures after pilocarpine-induced status epilepticus activate calbindin-immunoreactive hilar cells of the rat dentate gyrus. *Neuroscience* (2002) 111:71–81. doi:10.1016/S0306-4522(01)00599-1
27. Scharfman HE, Sollas AL, Smith KL, Jackson MB, Goodman JH. Structural and functional asymmetry in the normal and epileptic rat dentate gyrus. *J Comp Neurol* (2002) 454:424–39. doi:10.1002/cne.10449
28. McCloskey DP, Hintz TM, Pierce JP, Scharfman HE. Stereological methods reveal the robust size and stability of ectopic hilar granule cells after pilocarpine-induced status epilepticus in the adult rat. *Eur J Neurosci* (2006) 24:2203–10. doi:10.1111/j.1460-9568.2006.05101.x
29. Rowley S, Patel M. Mitochondrial involvement and oxidative stress in temporal lobe epilepsy. *Free Radic Biol Med* (2013) 62:121–31. doi:10.1016/j.freeradbiomed.2013.02.002
30. Vezzani A, Bartfai T, Bianchi M, Rossetti C, French J. Therapeutic potential of new antiinflammatory drugs. *Epilepsia* (2011) 52(Suppl 8):67–9. doi:10.1111/j.1528-1167.2011.03242.x
31. Vezzani A, Lang B, Aronica E. Immunity and inflammation in epilepsy. *Cold Spring Harb Perspect Med* (2015) 6:a022699. doi:10.1101/cshperspect.a022699
32. Mishra V, Shuai B, Kodali M, Shetty GA, Hattiangady B, Rao X, et al. Resveratrol treatment after status epilepticus restrains neurodegeneration and abnormal neurogenesis with suppression of oxidative stress and inflammation. *Sci Rep* (2015) 5:17807. doi:10.1038/srep17807

33. Scharfman HE, Gray WP. Relevance of seizure-induced neurogenesis in animal models of epilepsy to the etiology of temporal lobe epilepsy. *Epilepsia* (2007) 48(Suppl 2):33–41. doi:10.1111/j.1528-1167.2007.01065.x
34. Hattiangady B, Shetty AK. Implications of decreased hippocampal neurogenesis in chronic temporal lobe epilepsy. *Epilepsia* (2008) 49(Suppl 5):26–41. doi:10.1111/j.1528-1167.2008.01635.x
35. Shetty AK, Turner DA. Fetal hippocampal cells grafted to kainate-lesioned CA3 region of adult hippocampus suppress aberrant supragranular sprouting of host mossy fibers. *Exp Neurol* (1997) 143:231–45. doi:10.1006/exnr.1996.6363
36. Shetty AK, Turner DA. Aging impairs axonal sprouting response of dentate granule cells following target loss and partial deafferentation. *J Comp Neurol* (1999) 414:238–54. doi:10.1002/(SICI)1096-9861(19991115)414:2<238::AID-CNE7>3.0.CO;2-A
37. Shetty AK, Zaman V, Hattiangady B. Repair of the injured adult hippocampus through graft-mediated modulation of the plasticity of the dentate gyrus in a rat model of temporal lobe epilepsy. *J Neurosci* (2005) 25:8391–401. doi:10.1523/JNEUROSCI.1538-05.2005
38. Buckmaster PS. Does mossy fiber sprouting give rise to the epileptic state? *Adv Exp Med Biol* (2014) 813:161–8. doi:10.1007/978-94-017-8914-1_13
39. Koyama R. Dentate circuitry as a model to study epileptogenesis. *Biol Pharm Bull* (2016) 39:891–6. doi:10.1248/bpb.b16-00125
40. Groticke I, Hoffmann K, Loscher W. Behavioral alterations in the pilocarpine model of temporal lobe epilepsy in mice. *Exp Neurol* (2007) 207:329–49. doi:10.1016/j.expneurol.2007.06.021
41. Khalil A, Kovac S, Morris G, Walker MC. Carvacrol after status epilepticus (SE) prevents recurrent SE, early seizures, cell death, and cognitive decline. *Epilepsia* (2017) 58(2):263–73. doi:10.1111/epi.13645
42. Lenck-Santini PP, Holmes GL. Altered phase precession and compression of temporal sequences by place cells in epileptic rats. *J Neurosci* (2008) 28:5053–62. doi:10.1523/JNEUROSCI.5024-07.2008
43. Shetty AK. Hippocampal injury-induced cognitive and mood dysfunction, altered neurogenesis, and epilepsy: can early neural stem cell grafting intervention provide protection? *Epilepsy Behav* (2014) 38:117–24. doi:10.1016/j.yebeh.2013.12.001
44. Long Q, Upadhya D, Hattiangady B, Kim DK, An SY, Shuai B, et al. Intranasal MSC-derived A1-exosomes ease inflammation, and prevent abnormal neurogenesis and memory dysfunction after status epilepticus. *Proc Natl Acad Sci U S A* (2017) 114:E3536–45. doi:10.1073/pnas.1703920114
45. Shetty AK, Turner DA. Intracerebroventricular kainic acid administration in adult rat alters hippocampal calbindin and non-phosphorylated neurofilament expression. *J Comp Neurol* (1995) 363(4):581–99. doi:10.1002/cne.903630406
46. Shetty AK, Hattiangady B. Restoration of calbindin after fetal hippocampal CA3 cell grafting into the injured hippocampus in a rat model of temporal lobe epilepsy. *Hippocampus* (2007) 17:943–56. doi:10.1002/hipo.20311
47. Scharfman HE, Brooks-Kayal AR. Is plasticity of GABAergic mechanisms relevant to epileptogenesis? *Adv Exp Med Biol* (2014) 813:133–50. doi:10.1007/978-94-017-8914-1_11
48. Szczurowska E, Mares P. NMDA and AMPA receptors: development and status epilepticus. *Physiol Res* (2013) 62(Suppl 1):S21–38.
49. Qian F, Tang FR. Metabotropic glutamate receptors and interacting proteins in epileptogenesis. *Curr Neuropharmacol* (2016) 14:551–62. doi:10.2174/1570159X14666160331142228
50. Coulter DA, Steinhauser C. Role of astrocytes in epilepsy. *Cold Spring Harb Perspect Med* (2015) 5:a022434. doi:10.1101/cshperspect.a022434
51. Hattiangady B, Shetty AK. Decreased neuronal differentiation of newly generated cells underlies reduced hippocampal neurogenesis in chronic temporal lobe epilepsy. *Hippocampus* (2010) 20:97–112. doi:10.1002/hipo.20594
52. Bender RA, Dube C, Gonzalez-Vega R, Mina EW, Baram TZ. Mossy fiber plasticity and enhanced hippocampal excitability, without hippocampal cell loss or altered neurogenesis, in an animal model of prolonged febrile seizures. *Hippocampus* (2003) 13:399–412. doi:10.1002/hipo.10089
53. Sloviter RS. Possible functional consequences of synaptic reorganization in the dentate gyrus of kainate-treated rats. *Neurosci Lett* (1992) 137:91–6. doi:10.1016/0304-3940(92)90306-R
54. Shao LR, Dudek FE. Changes in mIPSCs and sIPSCs after kainate treatment: evidence for loss of inhibitory input to dentate granule cells and possible compensatory responses. *J Neurophysiol* (2005) 94:952–60. doi:10.1152/jn.01342.2004
55. Zhang X, Cui SS, Wallace AE, Hannesson DK, Schmued LC, Saucier DM, et al. Relations between brain pathology and temporal lobe epilepsy. *J Neurosci* (2002) 22:6052–61.
56. Nadler JV. The recurrent mossy fiber pathway of the epileptic brain. *Neurochem Res* (2003) 28:1649–58. doi:10.1023/A:1026004904199
57. Koyama R, Ikegaya Y. Mossy fiber sprouting as a potential therapeutic target for epilepsy. *Curr Neurovasc Res* (2004) 1:3–10. doi:10.2174/1567202043480242
58. Santhakumar V, Aradi I, Soltesz I. Role of mossy fiber sprouting and mossy cell loss in hyperexcitability: a network model of the dentate gyrus incorporating cell types and axonal topography. *J Neurophysiol* (2005) 93:437–53. doi:10.1152/jn.00777.2004
59. Blumcke I, Thom M, Aronica E, Armstrong DD, Bartolomei F, Bernasconi A, et al. International consensus classification of hippocampal sclerosis in temporal lobe epilepsy: a Task Force report from the ILAE Commission on Diagnostic Methods. *Epilepsia* (2013) 54:1315–29. doi:10.1111/epi.12220
60. Devinsky O, Vickrey BG, Cramer J, Perrine K, Hermann B, Meador K, et al. Development of the quality of life in epilepsy inventory. *Epilepsia* (1995) 36:1089–104. doi:10.1111/j.1528-1157.1995.tb00467.x
61. Peixoto-Santos JE, Velasco TR, Galvis-Alonso OY, Araujo D, Kandratavicius L, Assirati JA, et al. Temporal lobe epilepsy patients with severe hippocampal neuron loss but normal hippocampal volume: Extracellular matrix molecules are important for the maintenance of hippocampal volume. *Epilepsia* (2015) 56:1562–70. doi:10.1111/epi.13082
62. Shetty AK. Progress in cell grafting therapy for temporal lobe epilepsy. *Neurotherapeutics* (2011) 8(4):721–35. doi:10.1007/s13311-011-0064-y
63. Ebert U, Brandt C, Löscher W. Delayed sclerosis, neuroprotection, and limbic epileptogenesis after status epilepticus in the rat. *Epilepsia* (2002) 43(Suppl 5):86–95. doi:10.1046/j.1528-1157.43.s.5.39.x
64. Noe FM, Polascheck N, Frigerio F, Bankstahl M, Ravizza T, Marchini S, et al. Pharmacological blockade of IL-1β/IL-1 receptor type 1 axis during epileptogenesis provides neuroprotection in two rat models of temporal lobe epilepsy. *Neurobiol Dis* (2013) 59:183–93. doi:10.1016/j.nbd.2013.07.015
65. Tchekalarova J, Atanasova D, Nenchovska Z, Atanasova M, Kortenska L, Gesheva R, et al. Agomelatine protects against neuronal damage without preventing epileptogenesis in the kainate model of temporal lobe epilepsy. *Neurobiol Dis* (2017) 104:1–14. doi:10.1016/j.nbd.2017.04.017
66. Dudek FE, Williams PA. Does neuroprotection prevent epileptogenesis? *Epilepsy Curr* (2003) 3(2):68–9. doi:10.1046/j.1535-7597.2003.03213.x
67. Lancake P, Pryce RJ. A new class of phytoalexins from grapevines. *Experientia* (1977) 33:151–2. doi:10.1007/BF02124034
68. Soleas GJ, Diamandis EP, Goldberg DM. Resveratrol: a molecule whose time has come? And gone? *Clin Biochem* (1997) 30:91–113. doi:10.1016/S0009-9120(96)00155-5
69. Fremont L. Biological effects of resveratrol. *Life Sci* (2000) 66:663–73. doi:10.1016/S0024-3205(99)00410-5
70. Orallo F. Trans-resveratrol: a magical elixir of eternal youth? *Curr Med Chem* (2008) 15:1887–98. doi:10.2174/092986708785132951
71. Baur JA, Pearson KJ, Price NL, Jamieson HA, Lerin C, Kalra A, et al. Resveratrol improves health and survival of mice on a high-calorie diet. *Nature* (2006) 444:337–42. doi:10.1038/nature05354
72. Baur JA, Sinclair DA. Therapeutic potential of resveratrol: the in vivo evidence. *Nat Rev Drug Discov* (2006) 5:493–506. doi:10.1038/nrd2060
73. Campagna M, Rivas C. Antiviral activity of resveratrol. *Biochem Soc Trans* (2010) 38:50–3. doi:10.1042/BST0380050
74. Robich MP, Chu LM, Chaudray M, Nezafat R, Han Y, Clements RT, et al. Anti-angiogenic effect of high-dose resveratrol in a swine model of metabolic syndrome. *Surgery* (2010) 148:453–62. doi:10.1016/j.surg.2010.04.013
75. Robich MP, Osipov RM, Nezafat R, Feng J, Clements RT, Bianchi C, et al. Resveratrol improves myocardial perfusion in a swine model of hypercholesterolemia and chronic myocardial ischemia. *Circulation* (2010) 122:S142–9. doi:10.1161/CIRCULATIONAHA.109.920132
76. Sun YA, Wang Q, Simonyi A, Sun GY. Resveratrol as a therapeutic agent for neurodegenerative diseases. *Mol Neurobiol* (2010) 41:375–83. doi:10.1007/s12035-010-8111-y
77. Karuppagounder SS, Pinto JT, Xu H, Chen HL, Beal MF, Gibson GE. Dietary supplementation with resveratrol reduces plaque pathology in a transgenic model of Alzheimer's disease. *Neurochem Int* (2009) 54:111–8. doi:10.1016/j.neuint.2008.10.008

78. Shetty AK. Promise of resveratrol for easing status epilepticus and epilepsy. *Pharmacol Ther* (2011) 131:269–86. doi:10.1016/j.pharmthera.2011.04.008
79. Sun AY, Chen YM, James-Kracke M, Wixom P, Cheng Y. Ethanol-induced cell death by lipid peroxidation in PC12 cells. *Neurochem Res* (1997) 22:1187–92. doi:10.1023/A:1021968526696
80. Han YS, Zheng WH, Bastianetto S, Chabot JG, Quirion R. Neuroprotective effects of resveratrol against beta-amyloid-induced neurotoxicity in rat hippocampal neurons: involvement of protein kinase C. *Br J Pharmacol* (2004) 141:997–1005. doi:10.1038/sj.bjp.0705688
81. Zhang F, Liu J, Shi JS. Anti-inflammatory activities of resveratrol in the brain: role of resveratrol in microglial activation. *Eur J Pharmacol* (2010) 636:1–7. doi:10.1016/j.ejphar.2010.03.043
82. Sakata Y, Zhuang H, Kwansa H, Koehler RC, Dore S. Resveratrol protects against experimental stroke: putative neuroprotective role of heme oxygenase 1. *Exp Neurol* (2010) 224:325–9. doi:10.1016/j.expneurol.2010.03.032
83. Liu C, Shi Z, Fan L, Zhang C, Wang K, Wang B. Resveratrol improves neuron protection and functional recovery in rat model of spinal cord injury. *Brain Res* (2011) 1374:100–9. doi:10.1016/j.brainres.2010.11.061
84. Shindler KS, Ventura E, Dutt M, Elliott P, Fitzgerald DC, Rostami A. Oral resveratrol reduces neuronal damage in a model of multiple sclerosis. *J Neuroophthalmol* (2010) 30:328–39. doi:10.1097/WNO.0b013e3181f7f833
85. Maher P, Dargusch R, Bodai L, Gerard PE, Purcell JM, Marsh JL. ERK activation by the polyphenols fisetin and resveratrol provides neuroprotection in multiple models of Huntington's disease. *Hum Mol Genet* (2011) 20:261–70. doi:10.1093/hmg/ddq460
86. Singleton RH, Yan HQ, Fellows-Mayle W, Dixon CE. Resveratrol attenuates behavioral impairments and reduces cortical and hippocampal loss in a rat controlled cortical impact model of traumatic brain injury. *J Neurotrauma* (2010) 27:1091–9. doi:10.1089/neu.2010.1291
87. Wang Q, Xu J, Rottinghaus GE, Simonyi A, Lubahn D, Sun GY, et al. Resveratrol protects against global cerebral ischemic injury in gerbils. *Brain Res* (2002) 958:439–47. doi:10.1016/S0006-8993(02)03543-6
88. Abd El-Mohsen M, Bayele H, Kuhnle G, Gibson G, Debnam E, Kaila Srai S, et al. Distribution of [3H]trans-resveratrol in rat tissues following oral administration. *Br J Nutr* (2006) 96:62–70. doi:10.1079/BJN20061810
89. Mokni M, Elkahoui S, Limam F, Amri M, Aouani E. Effect of resveratrol on antioxidant enzyme activities in the brain of healthy rat. *Neurochem Res* (2007) 32:981–7. doi:10.1007/s11064-006-9255-z
90. Timmers S, Konings E, Bilet L, Houtkooper RH, van de Weijer T, Goossens GH, et al. Calorie restriction-like effects of 30 days of resveratrol supplementation on energy metabolism and metabolic profile in obese humans. *Cell Metab* (2011) 14:612–22. doi:10.1016/j.cmet.2011.10.002
91. Brasnyo P, Molnar GA, Mohas M, Marko L, Laczy B, Cseh J, et al. Resveratrol improves insulin sensitivity, reduces oxidative stress and activates the Akt pathway in type 2 diabetic patients. *Br J Nutr* (2011) 106:383–9. doi:10.1017/S0007114511000316
92. Yoshino J, Conte C, Fontana L, Mittendorfer B, Imai S, Schechtman KB, et al. Resveratrol supplementation does not improve metabolic function in nonobese women with normal glucose tolerance. *Cell Press* (2012) 16:658–64.
93. Poulsen MM, Vestergaard PF, Clasen BF, Radko Y, Christensen LP, Stodkilde-Jorgensen H, et al. High-dose resveratrol supplementation in obese men: an investigator-initiated, randomized, placebo-controlled clinical trial of substrate metabolism, insulin sensitivity, and body composition. *Diabetes* (2013) 62:1186–95. doi:10.2337/db12-0975
94. Korsholm AS, Kjaer TN, Ornstrup MJ, Pedersen SB. Comprehensive metabolomic analysis in blood, urine, fat, and muscle in men with metabolic syndrome: a randomized, placebo-controlled clinical trial on the effects of resveratrol after four months' treatment. *Int J Mol Sci* (2017) 18:E554. doi:10.3390/ijms18030554
95. Theodotou M, Fokianos K, Mouzouridou A, Konstantinou C, Aristotelous A, Prodromou D, et al. The effect of resveratrol on hypertension: a clinical trial. *Exp Ther Med* (2017) 13:295–301. doi:10.3892/etm.2016.3958
96. Witte AV, Kerti L, Margulies DS, Floel A. Effects of resveratrol on memory performance, hippocampal functional connectivity, and glucose metabolism in healthy older adults. *J Neurosci* (2014) 34:7862–70. doi:10.1523/JNEUROSCI.0385-14.2014
97. Wong RH, Raederstorff D, Howe PR. Acute resveratrol consumption improves neurovascular coupling capacity in adults with type 2 diabetes mellitus. *Nutrients* (2016) 8:E425. doi:10.3390/nu8070425
98. Turner RS, Thomas RG, Craft S, van Dyck CH, Mintzer J, Reynolds BA, et al. A randomized, double-blind, placebo-controlled trial of resveratrol for Alzheimer disease. *Neurology* (2015) 85:1383–91. doi:10.1212/WNL.0000000000002035
99. Golkar L, Ding XZ, Ujiki MB, Salabat MR, Kelly DL, Scholtens D, et al. Resveratrol inhibits pancreatic cancer cell proliferation through transcriptional induction of macrophage inhibitory cytokine-1. *J Surg Res* (2007) 138:163–9. doi:10.1016/j.jss.2006.05.037
100. Bonkowski MS, Sinclair DA. Slowing ageing by design: the rise of NAD^+ and sirtuin-activating compounds. *Nat Rev Mol Cell Biol* (2016) 17(11):679–90. doi:10.1038/nrm.2016.93
101. Kodali M, Parihar VK, Hattiangady B, Mishra V, Shuai B, Shetty AK. Resveratrol prevents age-related memory and mood dysfunction with increased hippocampal neurogenesis and microvasculature, and reduced glial activation. *Sci Rep* (2015) 5:8075. doi:10.1038/srep08075
102. Zini R, Morin C, Bertelli A, Bertelli AA, Tillement JP. Effects of resveratrol on the rat brain respiratory chain. *Drugs Exp Clin Res* (1999) 25:87–97.
103. Zini R, Morin C, Bertelli A, Bertelli AA, Tillement JP. Resveratrol-induced limitation of dysfunction of mitochondria isolated from rat brain in an anoxia-reoxygenation model. *Life Sci* (2002) 71:3091–108. doi:10.1016/S0024-3205(02)02161-6
104. Quincozes-Santos A, Bobermin LD, Tramontina AC, Wartchow KM, Tagliari B, Souza DO, et al. Oxidative stress mediated by NMDA, AMPA/KA channels in acute hippocampal slices: neuroprotective effect of resveratrol. *Toxicol In Vitro* (2014) 28:544–51. doi:10.1016/j.tiv.2013.12.021
105. Zhuang H, Kim YS, Koehler RC, Dore S. Potential mechanism by which resveratrol, a red wine constituent, protects neurons. *Ann N Y Acad Sci* (2003) 993:276,86. doi:10.1111/j.1749-6632.2003.tb07534.x
106. Kim H, Deshane J, Barnes S, Meleth S. Proteomics analysis of the actions of grape seed extract in rat brain: technological and biological implications for the study of the actions of psychoactive compounds. *Life Sci* (2006) 78(18):2060–5. doi:10.1016/j.lfs.2005.12.008
107. Dasgupta B, Milbrandt J. Resveratrol stimulates AMP kinase activity in neurons. *Proc Natl Acad Sci U S A* (2007) 104:7217–22. doi:10.1073/pnas.0610068104
108. Gao ZB, Hu GY. Trans-resveratrol, a red wine ingredient, inhibits voltage-activated potassium currents in rat hippocampal neurons. *Brain Res* (2005) 1056:68–75. doi:10.1016/j.brainres.2005.07.013
109. Chung S, Yao H, Caito S, Hwang JW, Arunachalam G, Rahman I. Regulation of SIRT1 in cellular functions: role of polyphenols. *Arch Biochem Biophys* (2010) 501:79–90. doi:10.1016/j.abb.2010.05.003
110. Michan S, Li Y, Chou MM, Parrella E, Ge H, Long JM, et al. SIRT1 is essential for normal cognitive function and synaptic plasticity. *J Neurosci* (2010) 30:9695–707. doi:10.1523/JNEUROSCI.0027-10.2010
111. Gao J, Wang WY, Mao YW, Graff J, Guan JS, Pan L, et al. A novel pathway regulates memory and plasticity via SIRT1 and miR-134. *Nature* (2010) 466:1105–9. doi:10.1038/nature09271
112. Wang SJ, Bo QY, Zhao XH, Yang X, Chi ZF, Liu XW. Resveratrol pretreatment reduces early inflammatory responses induced by status epilepticus via mTOR signaling. *Brain Res* (2013) 1492:122–9. doi:10.1016/j.brainres.2012.11.027
113. Virgili M, Contestabile A. Partial neuroprotection of in vivo excitotoxic brain damage by chronic administration of the red wine antioxidant agent, trans-resveratrol in rats. *Neurosci Lett* (2000) 281:123–6. doi:10.1016/S0304-3940(00)00820-X
114. Gupta YK, Briyal S, Chaudhary G. Protective effect of trans-resveratrol against kainic acid-induced seizures and oxidative stress in rats. *Pharmacol Biochem Behav* (2002) 71:245–9. doi:10.1016/S0091-3057(01)00663-3
115. Gupta YK, Chaudhary G, Sinha K, Srivastava AK. Protective effect of resveratrol against intracortical FeCl3-induced model of posttraumatic seizures in rats. *Methods Find Exp Clin Pharmacol* (2001) 23:241–4. doi:10.1358/mf.2001.23.5.662120
116. Kim HJ, Kim IK, Song W, Lee J, Park S. The synergic effect of regular exercise and resveratrol on kainate-induced oxidative stress and seizure activity in mice. *Neurochem Res* (2013) 38:117–22. doi:10.1007/s11064-012-0897-8
117. Wang Q, Yu S, Simonyi A, Rottinghaus G, Sun GY, Sun AY. Resveratrol protects against neurotoxicity induced by kainic acid. *Neurochem Res* (2004) 29:2105–12. doi:10.1007/s11064-004-6883-z

118. Li M, Wang QS, Chen Y, Wang ZM, Liu Z, Guo SM. Resveratrol inhibits the electrical activity of subfornical organ neurons in rat. *Sheng Li Xue Bao* (2005) 57(4):523–8.
119. Nicolini G, Rigolio R, Miloso M, Bertelli AA, Tredici G. Anti-apoptotic effect of trans-resveratrol on paclitaxel-induced apoptosis in the human neuroblastoma SH-SY5Y cell line. *Neurosci Lett* (2001) 302:41–4. doi:10.1016/S0304-3940(01)01654-8
120. Waldbaum S, Patel M. Mitochondria, oxidative stress, and temporal lobe epilepsy. *Epilepsy Res* (2010) 88:23–45. doi:10.1016/j.eplepsyres.2009.09.020
121. Menon B, Ramalingam K, Kumar RV. Oxidative stress in patients with epilepsy is independent of antiepileptic drugs. *Seizure* (2012) 21:780–4. doi:10.1016/j.seizure.2012.09.003
122. Friedman LK, Mancuso J, Patel A, Kudur V, Leheste JR, Iacobas S, et al. Transcriptome profiling of hippocampal CA1 after early-life seizure-induced preconditioning may elucidate new genetic therapies for epilepsy. *Eur J Neurosci* (2013) 38:2139–52. doi:10.1111/ejn.12168
123. Kuruba R, Hattiangady B, Shetty AK. Hippocampal neurogenesis and neural stem cells in temporal lobe epilepsy. *Epilepsy Behav* (2009) 14(Suppl 1):65–73. doi:10.1016/j.yebeh.2008.08.020
124. Cho KO, Lybrand ZR, Ito N, Brulet R, Tafacory F, Zhang L, et al. Aberrant hippocampal neurogenesis contributes to epilepsy and associated cognitive decline. *Nat Commun* (2015) 6:6606. doi:10.1038/ncomms7606
125. Scharfman HE, Sollas AL, Berger RE, Goodman JH. Electrophysiological evidence of monosynaptic excitatory transmission between granule cells after seizure-induced mossy fiber sprouting. *J Neurophysiol* (2003) 90:2536–47. doi:10.1152/jn.00251.2003
126. Hester MS, Danzer SC. Hippocampal granule cell pathology in epilepsy – a possible structural basis for comorbidities of epilepsy? *Epilepsy Behav* (2014) 38:105–16. doi:10.1016/j.yebeh.2013.12.022
127. Wu Z, Xu Q, Zhang L, Kong D, Ma R, Wang L. Protective effect of resveratrol against kainate-induced temporal lobe epilepsy in rats. *Neurochem Res* (2009) 34:1393–400. doi:10.1007/s11064-009-9920-0
128. Meng XJ, Wang F, Li CK. Resveratrol is neuroprotective and improves cognition in pentylenetetrazole-kindling model of epilepsy in rats. *Indian J Pharm Sci* (2014) 76:125–31.
129. Li Z, You Z, Li M, Pang L, Cheng J, Wang L. Protective effect of resveratrol on the brain in a rat model of epilepsy. *Neurosci Bull* (2017) 33:273–80. doi:10.1007/s12264-017-0097-2
130. Waldau B, Hattiangady B, Kuruba R, Shetty AK. Medial ganglionic eminence-derived neural stem cell grafts ease spontaneous seizures and restore GDNF expression in a rat model of chronic temporal lobe epilepsy. *Stem Cells* (2010) 28:1153–64. doi:10.1002/stem.446
131. Upadhya D, Hattiangady B, Shetty GA, Zanirati G, Kodali M, Shetty AK. Neural stem cell or human induced pluripotent stem cell-derived GABAergic progenitor cell grafting in an animal model of chronic temporal lobe epilepsy. *Curr Protoc Stem Cell Biol* (2016) 38:2D.7.1,2D.7.47. doi:10.1002/cpsc.9
132. Shetty AK. Entorhinal axons exhibit sprouting in CA1 subfield of the adult hippocampus in a rat model of temporal lobe epilepsy. *Hippocampus* (2002) 12:534–42. doi:10.1002/hipo.10031
133. Wilcox KS, Gee JM, Gibbons MB, Tvrdik P, White JA. Altered structure and function of astrocytes following status epilepticus. *Epilepsy Behav* (2015) 49:17–9. doi:10.1016/j.yebeh.2015.05.002
134. Kielbinski M, Gzielo K, Soltys Z. Review: roles for astrocytes in epilepsy: insights from malformations of cortical development. *Neuropathol Appl Neurobiol* (2016) 42:593–606. doi:10.1111/nan.12331
135. Saha L, Chakrabarti A. Understanding the anti-kindling role and its mechanism of Resveratrol in Pentylenetetrazole induced-kindling in a rat model. *Pharmacol Biochem Behav* (2014) 120:57–64. doi:10.1016/j.pbb.2014.01.010

Disclaimer: Department of Veterans Affairs, Department of Defense, United States Government Disclaimer: The contents of this article suggest the views of authors and do not represent the views of the U.S. Department of Veterans Affairs, Department of Defense or the United States Government.

Conflict of Interest Statement: The authors declare that the research was conducted in the absence of any commercial or financial relationships that could be construed as a potential conflict of interest.

frontiers in Neurology

MINI REVIEW
published: 23 January 2018
doi: 10.3389/fneur.2018.00007

Status Epilepticus: Behavioral and Electroencephalography Seizure Correlates in Kainate Experimental Models

*Shaunik Sharma[1], Sreekanth Puttachary[2], Achala Thippeswamy[1], Anumantha G. Kanthasamy[3] and Thimmasettappa Thippeswamy[1]**

[1] Epilepsy Research Laboratory, Department of Biomedical Sciences, College of Veterinary Medicine, Iowa State University, Ames, IA, United States, [2] Veterinary Biomedical Sciences, College of Veterinary Medicine, Oregon State University, Corvallis, OR, United States, [3] Parkinson's Research Laboratory, Department of Biomedical Sciences, College of Veterinary Medicine, Iowa State University, Ames, IA, United States

Various etiological factors, such as head injury, chemical intoxication, tumors, and gene mutation, can induce epileptogenesis. In animal models, *status epilepticus* (SE) triggers epileptogenesis. In humans, convulsive SE for >30 min can be a life-threatening medical emergency. The duration and severity of convulsive SE are highly variable in chemoconvulsant animal models. A continuous video-electroencephalography (EEG) recording, and/or diligent direct observation, facilitates quantification of exact duration of different stages of convulsive seizures (Racine stages 3–5) to determine the severity of SE. A continuous convulsive SE for >30 min usually causes high mortality in some rodents and results in widespread brain damage in the surviving animals, in spite of treating with antiepileptic drugs (AEDs). AEDs control behavioral seizures but not EEG seizures. The severity of initial SE impacts epileptogenesis and cognitive function; therefore, quantitative assessment of behavioral SE and EEG in animal models will help to understand the impact of SE severity on epileptogenesis. There are several excellent reviews on experimental models of seizure/SE/epilepsy. This review focusses on the comparison of induction and characterization of behavioral SE and EEG correlates in mice and rats induced by kainate. We also discuss the advantages of repeated low dose of kainate (i.p. route), which minimizes variability in the initial SE severity between animals and reduces mortality rate. A refined approach to induce SE with kainate also addresses the two of the 3Rs (i.e., refinement and reduction), the guiding principles for ethical and scientific standpoint of animal research.

Keywords: status epilepticus, kainate, repeated low dose, electroencephalography seizures, behavioral seizures

OPEN ACCESS

Edited by:
Ashok K. Shetty, Texas A&M University College of Medicine, United States

Reviewed by:
Yogendra H. Raol, University of Colorado Denver, United States
Olagide Wagner Castro, Federal University of Alagoas, Brazil

****Correspondence:***
Thimmasettappa Thippeswamy
tswamy@iastate.edu

Specialty section:
This article was submitted to Epilepsy, a section of the journal Frontiers in Neurology

Received: *20 July 2017*
Accepted: *03 January 2018*
Published: *23 January 2018*

Citation:
Sharma S, Puttachary S, Thippeswamy A, Kanthasamy AG and Thippeswamy T (2018) Status Epilepticus: Behavioral and Electroencephalography Seizure Correlates in Kainate Experimental Models. Front. Neurol. 9:7. doi: 10.3389/fneur.2018.00007

INTRODUCTION

The PubMed search, using *status epilepticus* (SE) and epilepsy as key words, yielded >1,600 articles on SE. In a recent review on bibliometric analysis of top 100 articles on both SE and epilepsy, as expected, revealed that the majority of these articles are from animal studies (1). In these literature, the duration of SE is discussed, but the information on quantification of the severity of SE is lacking (2, 3). In general, the duration of SE in experimental models is between the time of administration of chemoconvulsant (assuming the onset of convulsive SE) and the end of behavioral seizures. Traditionally, the behavioral seizures are scored based on the Racine scale (4–6). However, the

electroencephalography (EEG) quantification to determine the severity of SE in animal models is lacking in the literature. There are numerous reports on qualitative EEG that has been used as an evidence to demonstrate the occurrence of SE and to support the idea that benzodiazepines are ineffective in controlling the epileptiform spiking activity after certain time-point (7, 8). We have recently described both behavioral and EEG seizures' quantification methods from the kainate-induced SE in both mice and rat models (2, 9, 10). In this mini-review, we discuss SE in the context of its onset, duration, types of seizures during SE, quantitative measures of behavioral and electrographic seizures to determine SE severity, and the impact of SE severity on epileptogenesis in the rat and mouse kainate models of temporal lobe epilepsy (TLE).

The definition of SE has been constantly changing. It is also suggested that it depends on the context of SE, in humans or experimental models (11, 12). There has been a consensus that the duration or length of convulsive seizures (CS) during SE should be sufficient to cause long-term brain injury, enabling the brain to generate spontaneous seizures i.e., "an enduring epilepticus" (13). According to the Commission of Epidemiology Prognosis (1993) and Dodson et al. (14), initial duration of SE for humans was set at 60 min. This was later reduced to 30 min, which is now widely accepted for studies that investigate the long-term consequences of SE, i.e., epileptogenesis and epilepsy. Seizures are normally self-terminated by activating inhibitory mechanisms. Failure of these mechanisms can result in prolonged seizures (SE), which may require interventional drugs (12). However, according to the clinical trial guidelines, the treatment should be initiated only if the CS last for ~5 min (11, 14–16). According to the recommendation of the Commission on Classification and Terminology, and the Commission on Epidemiology of the International League Against Epilepsy (ILAE), the SE is defined as "*a condition resulting either from the failure of the mechanisms responsible for seizure termination or from the initiation of mechanisms, which lead to abnormally, prolonged seizures (after time point t1). It is a condition, which can have long-term consequences (after time point t2), including neuronal death, neuronal injury, and alteration of neuronal networks, depending on the type and duration of seizures*" (17). In this review, we discuss the types and duration of seizures during SE in mice and rat kainate models of TLE. We also discuss SE in these models on the background of a new definition of SE proposed by the ILAE.

SE IN ANIMAL MODELS: THE TYPES OF SEIZURES

In the literature on chemoconvulsant models of seizure/epilepsy, the types of behavioral seizures during SE are generally well defined based on the (modified) Racine scale (4–6, 18). However, the scoring pattern varies between the literature, models, stimulus, strains, and species used in the experiment. The most acceptable broad classification of behavioral seizures, for quantification purpose, are non-convulsive seizure (NCS) and CS (tonic–clonic, tonic, and clonic). For the sake of clarity, the following five stages of behavioral seizures were considered for SE quantification for mice and rat kainate models: stage 1, absence-like immobility; stage 2, hunching with facial automatism (exaggerated upper lip movement as evident from vibrissae movement with or without salivation) and/or abducted forelimb/s, wet-dog shaking (in rats); stage 3, rearing with facial automatism and forelimb clonus (excessive salivation in some animals); stage 4, repeated rearing with continuous forelimb clonus and falling (loss of righting reflex); and stage 5, generalized tonic–clonic convulsions with lateral recumbence or jumping (more common in mice) and wild running followed by generalized convulsions (**Figures 1A,B**) (2, 9).

SE ONSET AND ITS LENGTH OR DURATION IN ANIMAL MODELS

Unlike electroconvulsant models, such as the maximal electroshock seizure model (19–21), the time of onset and length of convulsive SE are highly variable in chemoconvulsant models. This depends on numerous factors, such as drug and its route of administration, species, sex, age groups, strain, and genetic background (22–25). In the kainate model, intraperitoneal administration of a single high dose (SHD) of kainate (20–30 mg/kg) induced convulsive SE between 5 and 49 min in 86% of inbred C57BL/6J mice. Out of these, 63% of mice had >30 min and 23% had <30 min of convulsive SE (**Figure 1E**). The duration of SE (stages 1–5) was usually greater than 2 h in these animals (**Figure 2A**). However, 21% of mice died due to the severity of CS, and the vast majority of deaths occurred in mice that reached stage 5 seizures in <15 min of kainate administration (data not shown). A similar pattern of quick onset of convulsive SE with kainate (i.p.), but >80% mortality was observed in mixed genetic background mice (C57 × Balb-c) (**Figures 1C–E**). In Sprague Dawley rats, the convulsive SE onset with a SHD of kainate (12.5–15.0 mg/kg, i.p.) occurred between 30 and 40 min, with 12% mortality, and the percentage of animals that achieved CS for ≥30 min was 46% (**Figures 1C–E**).

The type of seizures and their duration determine the severity of SE. It has been proposed that >10 min of convulsive SE is sufficient to cause brain damage and to induce TLE in chemoconvulsant animal models (10, 26). However, in some of the literature, there is limited information on whether the CS (stage ≥3) were continuous or intermittent in a given time (for example, during the 2–3 h of drug administration), and whether the behavioral SE was terminated with an antiepileptic drug (AED) or not. We used both behavioral methods and EEG parameters to accurately quantify the duration of convulsive SE. Interestingly, in C57BL/6J mouse kainate model, about 50% of behavioral seizures did not correspond to the epileptiform activity detected on the EEG (10). This implies that in some chemoconvulsant models, there is an exaggerated behavioral response that could be due to the peripheral effects (27).

QUANTITATIVE MEASURE OF BEHAVIORAL AND ELECTROGRAPHIC SEIZURES TO DETERMINE SE SEVERITY

In a pilocarpine mouse model (C57BL/129Sv genetic background) of acute seizures, both video and quantitative EEG

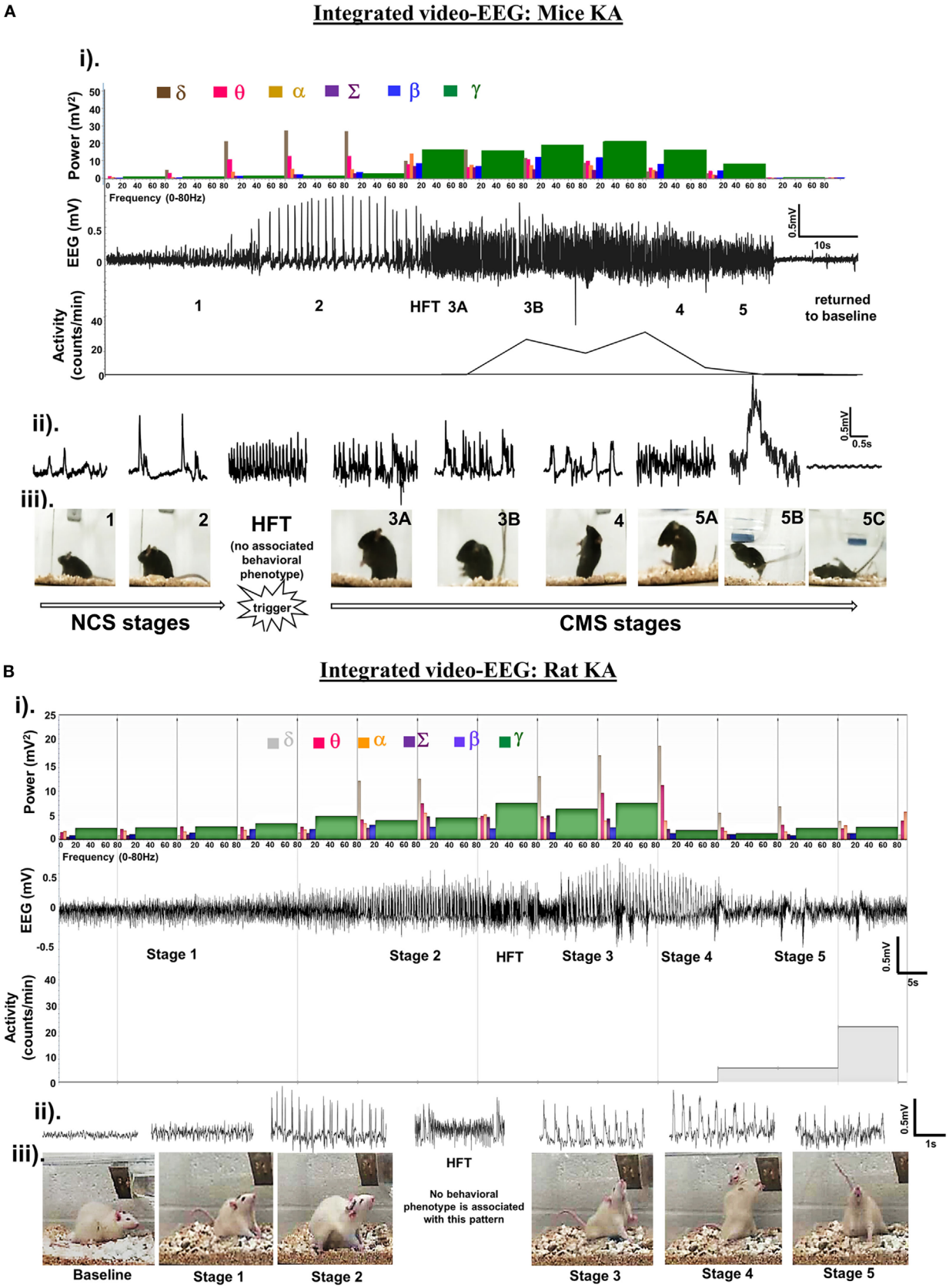

FIGURE 1 | **Continued**

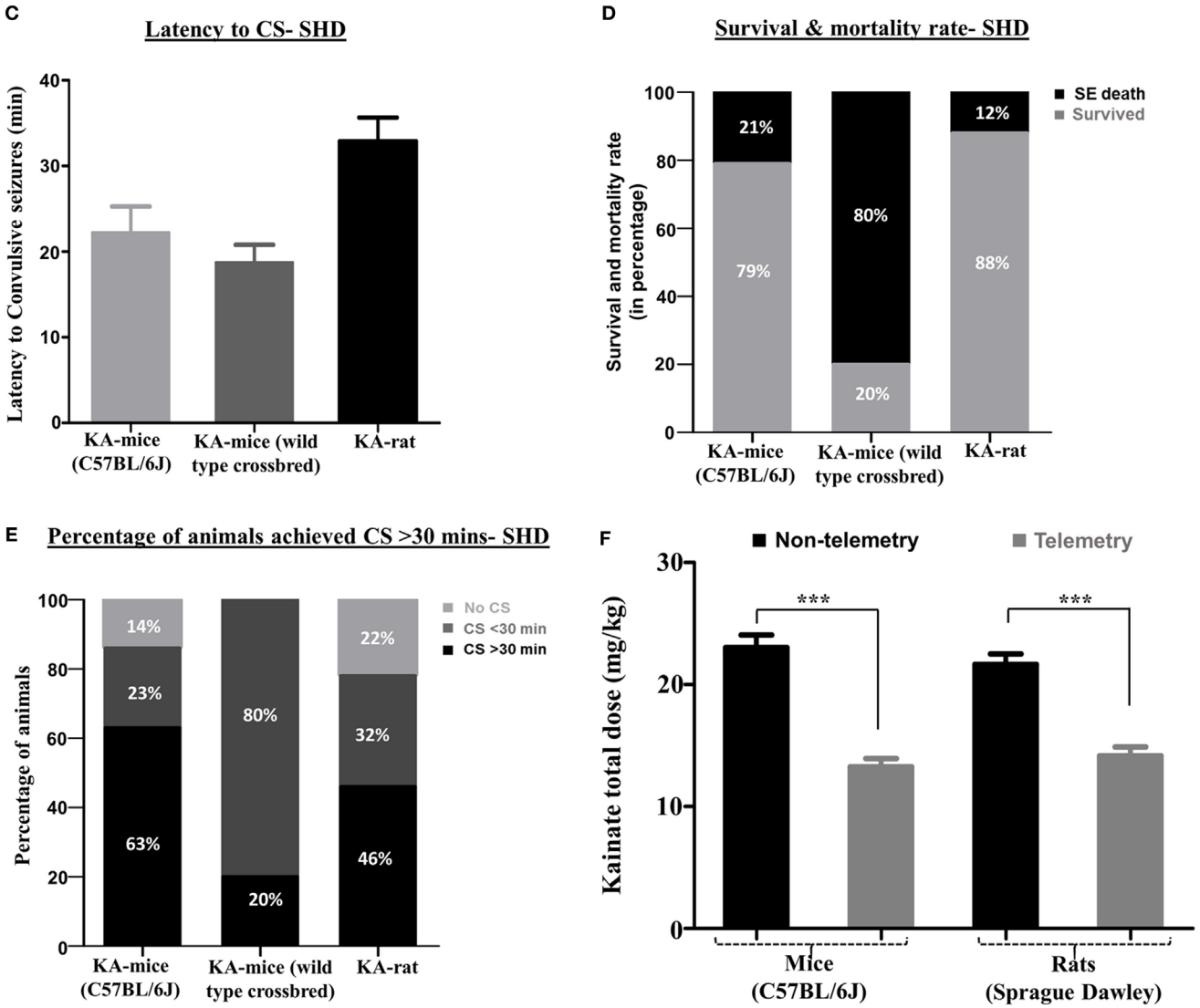

FIGURE 1 | **(A,B)** An example of an electroencephalography (EEG) trace showing different stages of seizures, induced by kainate in C57BL/6J mouse **(A)** and Sprague Dawley rat **(B)**. The corresponding power spectra, activity level, and real-time behavioral seizures captured from the video-EEG recording are illustrated. (i) EEG trace in the middle shows the changes in electrical activity as the seizure severity progressed from NCS to CS over time. A brief HFT pattern on the EEG, which had no behavioral correlate, preceded the CS. The photographs show different stages of behavioral seizures (iii). Magnified 2-s EEG traces that correspond to each stage of behavioral seizures are shown in the panel (ii). The histograms at the top panel in "i" represent power bands. As the seizure progressed from NCS to CS, the power bands, especially the gamma power increased (shown in green) at stage 3, but decreased during stages 4 and 5. The delta and theta power bands increased during the stage 2 NCS. The gamma power band increased after HFT, peaked at stage 3B, and declined in stages 4 and 5 before returning to the baseline. One interesting finding in the power spectra of the rat kainate model **(B)**, in contrast to the mouse kainate model **(A)**, was an increase in theta and delta power bands during CS. Activity counts represent brisk locomotor activity, which is shown below the EEG trace, increased from stage 3A onward and peaked in stage 3B and 4. Activity counts reduced in stage 5 when the mouse was recumbent or showed generalized rigidity but increased when the mouse displayed jumping behavior. In the rat KA model, the delta power persisted at high levels during pre- and post-CS stage, but the theta, beta, and gamma powers increased during the CS stages. **(C–E)** The comparison of latency to the onset of CS **(C)**, mortality rate **(D)**, and the time spent by the number of animals (in percentage) in CS stages **(E)** in C57BL/6J mice, the crossbred mice on C57BL/6J genetic background (C57 × Balb-c) and the Sprague Dawley rats in response to SHD of kainate. **(F)** Comparison between the total amounts of kainate, given 5 mg/kg at 30 min interval, required to induce CS in telemetry and non-telemetry groups of mice and rats. The animals with telemetry required about ~40% less kainate to reach CS when compared to the non-telemetry group in both rats and mice. Mann–Whitney test, ***$p < 0.001$, $n = 30$–40 per group. RLD, repeated low dose; SHD, single high dose; CS, convulsive seizures; NCS, non-convulsive seizures; HFT, high frequency trigger. Adopted and modified from Tse et al. (2) and Puttachary et al. (9).

analyses (fast Fourier transformation) were used to correlate the electrographic seizures with the convulsive behaviors (6). In this study, the authors graded the seizures on the Racine scale, and the root-mean-square (RMS) power analysis of EEG was performed using Sirenia Seizure Pro software. They found a weak correlation between the RMS power and convulsive behavior, induced

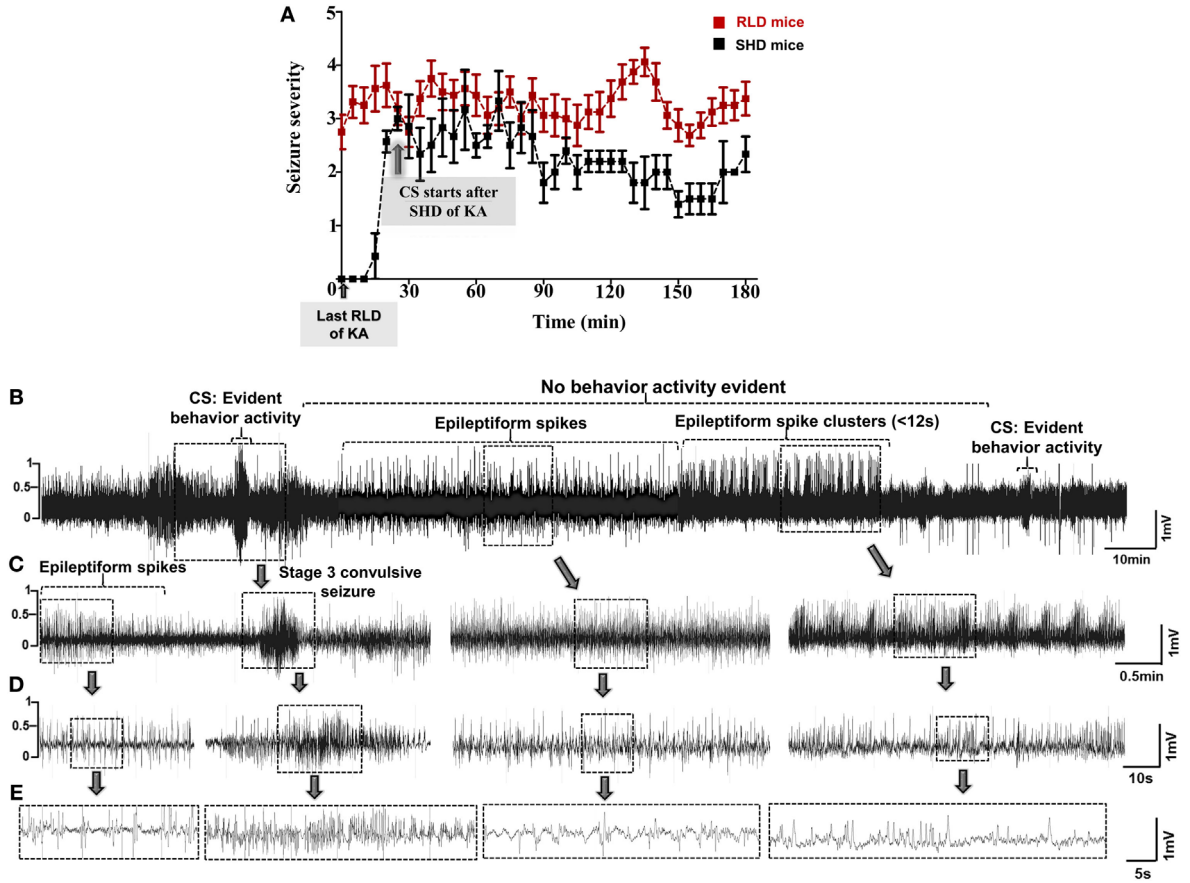

FIGURE 2 | **(A)** Seizure severity comparison between single high dose (SHD) and repeated low dose (RLD) of KA in mice during SE. Animals in RLD group showed more severe seizures and spent more time in ≥3 stage when compared to the SHD group during the 3 h of SE. Animals in both groups were given 20–30 mg/kg kainate (i.p.) (***$p < 0.0001$, two-way ANOVA between 1 and 719 degrees of freedom, $F = 148.60$, $n = 30$ for each group). Adopted and modified from Tse et al. (2). **(B–E)** An example of a 30-min EEG trace, during SE, showing inter-ictal activity that comprises of continuous epileptiform spikes and seizure cluster <12 s without any behavioral phenotype. Convulsive seizures (CS) and non-convulsive seizures (NCS) were observed throughout SE, but behavior activity was evident only during CS, i.e., stage ≥3. Expanded electroencephalography (EEG) traces of **(B)** are shown in panels **(C–E)**.

by the pilocarpine, suggesting that power spectral analysis alone is insufficient to quantitatively correlate the behavioral seizures with electrographic seizures (6). In the mouse (C57BL/6J) kainate model, we determined the power spectrum for frequencies ranging from 0.5 to 80 Hz based on stage-specific behavioral and EEG seizure correlates (2). In our studies, the power band spectrum analysis included delta (δ, 0–4 Hz), theta (θ, 4–8 Hz), alpha (α, 8–12 Hz), sigma (Σ, 12–16 Hz), beta (β, 16–24 Hz), and gamma (γ, 24–80 Hz) frequencies in 10-s epochs on a continuous EEG during SE with power ranging from 200 to 2,000 mV^2. As the seizure stages progressed from stages 1–5, the EEG patterns with increase in power bands began to emerge in real-time as measured by the Neuroscore software (**Figures 1A,B**). A magnified EEG traces shown above the behavioral stages in these figures demonstrate stage-specific spike characteristics (amplitude, duration, and inter-spike intervals). When the seizures progressed from NCS (stages 1 and 2) to CS (stages 3–5), the power in different bands also changed. The gamma power peaked during stage 3, but declined in stages 4 and 5 before reaching the baseline (**Figures 1A,B**). Higher delta and theta powers were the hallmarks of stage-2 spikes. A reduced delta power, but the increased beta and gamma powers marked the progression from NCS to CS. The high frequency trigger (HFT) pattern was frequently observed during the transition from NCS to CS, which was characterized by a brief peak in alpha and sigma powers (**Figures 1A,B**). To determine the severity of SE, in addition to the power spectral analysis, it is useful to quantify stage-specific spike frequencies during SE to correlate with the behavioral seizures as described in the mouse and rat kainate models (2, 9, 10). However, it is plausible that the type of chemoconvulsant [for example, parasympathomimetics (pilocarpine) versus glutamate agonists (kainate)] could affect the extent of correlation between the power, EEG, and behavioral seizures.

SEVERITY OF SE AND ITS IMPACT ON EPILEPTOGENESIS

Several review articles have documented the impact of the severity of initial SE on epileptogenesis and epilepsy in the long term (28–32). The majority of chemoconvulsant-induced SE in rats

and mice will develop progressive epilepsy, which is generally characterized by reactive gliosis, neurodegeneration, spontaneous recurrent seizures, and cognitive deficits (10, 31–37). A recent article by Loscher et al. (22) has highlighted the relevance of strain-specific differences in mice and rats and their implications in determining the choice of experimental models of seizure/epilepsy. The vast variation in seizure susceptibility in animal models is due to the diversity of their outbred genetic backgrounds. However, the C57BL/6J inbred mice response to chemoconvulsants such as kainate also varies between batches of mice and the source (22, 38–41). SE induction by chemoconvulsants in mice and rats revealed a huge variation in latency to convulsive SE onset, duration of CS, and mortality (**Figures 1C–E** and **2A**). A refined method of inducing SE with repeated low dose (RLD) of kainate, 5 mg/kg, administered at 30 min intervals *via* the intraperitoneal route, has shown to reduce inconsistency in SE severity across different strains (2, 42–44). Moreover, the RLD method of kainate administration revealed that the surgical procedure for intracranial electrode implantation reduces the threshold for CS onset. About 40% less kainate was required to induce convulsive SE in the telemetry animals when compared to the non-telemetry animals (**Figure 1F**) (2, 9, 10). The SE induction by either SHD or RLD of kainate (i.p.) will lead to the development of epilepsy in the majority of animals. However, the frequency of spontaneous convulsive (tonic–clonic) seizures significantly varies between models. For example, the RLD method in both rats and mice induced epilepsy and the C57BL/6J mice had almost the same numbers of spontaneous CS as the rats during the first 4 weeks, but the frequency of seizures reduced after 4–6 weeks in the mice (9, 10, 45). In both rats and mice, the electrodes were implanted epidurally on the surface of the cortices as described previously (2, 10, 46). Interestingly, in a 4-month continuous video-EEG study from the C57BL/6J mouse kainate model, irrespective of initial severity of SE (severe or mild SE), high numbers of electrographic NCS were detected on EEG, which persisted during entire length of the study (10). However, the frequency of spontaneous CS, a readout for the classification of the severity of disease, was related to the initial severity of SE in both rats and mice (9, 10, 47, 48). Therefore, it is imperative to review and refine the methods of induction and quantification of severity of SE (the type and duration of seizures) to understand its impact on the disease progression and, importantly, to determine disease-modifying effects of drugs in experimental models of TLE.

Considering one of the operational dimensions of the ILAE recommendations for SE, we further focus the review on "*the length of the seizure and the time point (t1) beyond which the seizure should be regarded as 'continuous seizure activity'*" (11, 17). Hitherto, the SE in animal models has been defined as the duration from the onset of seizures until they stop on their own or intervention by an AED, most commonly diazepam (DZP). This means the length of behavioral seizures, i.e., SE could vary between animals. This can cause problems in animals that are intended for interventional and long-term studies (for example, vehicle treated versus test drug treated group/s), and would yield confounding results. Since DZP has little or no effect on EEG seizures, it is unlikely to have an impact on brain pathology in animals that experience severe SE (49, 50). However, DZP treatment controlled behavioral seizures and suppressed epileptiform spikes or electrographic seizures in mice that had mild SE (45). According to the NIH CounterACT program, administering DZP or other AEDs to control behavioral seizures prior to testing disease-modifying agent is recommended for translational studies. The length of SE also depends on the type of chemoconvulsant and the method of administration. For example, SHD method of kainate (i.p.) produces inconsistent seizure response with high variability in SE duration, while the RLD method of administration (i.p.) produces relatively consistent SE (stage ≥3) with longer duration in both mice and rats (2, 9). Therefore, the RLD method is useful to develop animal models of varying SE severity, such as mild or severe groups, for any chosen experiment.

Several studies have shown huge variations in SE response to a SHD of kainate in various strains of mice and rats in terms of SE onset and duration (2, 23, 43, 51, 52). Unlike in humans, the convulsive SE is not always continuous in animal models, and the seizures fluctuate either between stage 1 and stage 5 or in between the stages of CS (stages 3 and 5). During continuous SE, the electrographic activity does not always correspond to the behavioral seizures. Furthermore, progression of NCS to CS is not always consistent in mice and rats. For example, during the transition from NCS to CS, we observed a pattern of HFT spikes on the EEG that had no behavioral correlation in both mice and rats (**Figures 1A,B**). During SE, a variety of epileptiform spiking activities were observed on the EEG, even though the animals were not exhibiting any behavioral seizures. These include spike trains containing isolated epileptiform spikes or spike clusters with <12-s duration (**Figures 2B–E**) (45). Since not every experiment will require telemetry, a video acquisition, in addition to direct observation, is useful to quantify the exact duration of convulsive SE in a given time. To precisely quantify the severity of SE, we considered the exact duration of CS (stage ≥3) that occurred between the first onset of CS following kainate injection and the time the DZP was administered. By RLD of kainate, we could achieve >30 min of continuous CS in 95% of the animals with <15% mortality rate in both mice (irrespective of strains) and rats. These results are consistent with the previous studies (2, 43, 44, 51, 53). Irrespective of the model, DZP at 10 mg/kg (i.p.) terminated behavioral seizures in the vast majority of animals, but had little or no impact on continuous seizure activity, i.e., epileptiform spiking activity in those animals that experienced severe seizures (45, 54–56). However, DZP reduced mortality rate in animals with severe SE to some extent (56–58), but completely suppressed epileptiform spikes in animals that had mild SE (45). It has been known that severe seizures cause either internalization or inactivation of $GABA_A$ receptors at the synaptic terminals that result in diminished response to the DZP treatment (8, 49, 54, 59, 60).

In summary, the length of the convulsive SE in animal models usually lasts for >30 min by the RLD method of kainate, in contrast to a SHD method. The severity of SE can be determined by quantifying the exact duration of different stages of CS (stages 3–5) from continuous video recording and/or by direct observation. Telemetry implanted animals require ~40% less kainate to induce convulsive SE. The epileptiform spike frequency can

be considered to determine the severity of SE in addition to behavioral seizures quantification. This approach will reduce variability in determining the initial severity of convulsive SE in disease-modifying experiments that require long-term video-EEG monitoring. In addition to the power spectral analysis, it may be useful to quantify stage-specific spike frequencies during SE to determine the severity of SE and to correlate with behavioral seizures where appropriate. The refined RLD method of kainate administration overcomes some of the shortcomings in generating convulsive SE models, reduces mortality rate, and the cost of experiments.

AUTHOR CONTRIBUTIONS

SS: performed the experiments, analyzed the data, reviewed the literature, wrote the manuscript, and prepared the tables and figures. SP: performed the experiments and analyzed the data; AK: contributed animals. TT: conceived the idea, designed the study, and wrote/edited the manuscript.

ACKNOWLEDGMENTS

We thank Sarah Mientka, Biological/Pre-Medical Illustrator for editing the images.

FUNDING

This research was supported by the start-up funds and Presidential Initiative on Interdisciplinary Research (Big Data Brain Initiative) fund to TT, Iowa State University, Iowa, USA, and the NIH funding (NS088206) and Eugene and Linda Lloyd Chair Endowment to AK.

REFERENCES

1. Park KM, Kim SE, Lee BI, Kim HC, Yoon DY, Song HK, et al. Top 100 cited articles on epilepsy and status epilepticus: a bibliometric analysis. *J Clin Neurosci* (2017) 42:12–8. doi:10.1016/j.jocn.2017.02.065
2. Tse K, Puttachary S, Beamer E, Sills GJ, Thippeswamy T. Advantages of repeated low dose against single high dose of Kainate in C57BL/6J mouse model of status epilepticus: behavioral and electroencephalographic studies. *PLoS One* (2014) 9. doi:10.1371/journal.pone.0096622
3. Lehmkuhle MJ, Thomson KE, Scheerlinck P, Pouliot W, Greger B, Dudek FE. A simple quantitative method for analyzing electrographic status epilepticus in rats. *J Neurophysiol* (2009) 101:1660–70. doi:10.1152/jn.91062.2008
4. Racine RJ. Modification of seizure activity by electrical stimulation: II. Motor seizure. *Electroencephalogr Clin Neurophysiol* (1972) 32:281–94. doi:10.1016/0013-4694(72)90177-0
5. Lüttjohann A, Fabene PF, Luijtelaar GV. A revised Racine's scale for PTZ-induced seizures in rats. *Physiol Behav* (2009) 98:579–86. doi:10.1016/j.physbeh.2009.09.005
6. Phelan KD, Shwe U, Williams DK, Greenfield LJ, Zheng F. Pilocarpine-induced status epilepticus in mice: a comparison of spectral analysis of electroencephalogram and behavioral grading using the Racine scale. *Epilepsy Res* (2015) 117:90–6. doi:10.1016/j.eplepsyres.2015.09.008
7. Kaplan PW. The EEG of status epilepticus. *J Clin Neurophysiol* (2006) 23:221–9. doi:10.1097/01.wnp.0000220837.99490.66
8. Fritsch B, Stott JJ, Donofrio JJ, Rogawski MA. Treatment of early and late kainic acid-induced status epilepticus with the noncompetitive AMPA receptor antagonist GYKI 52466. *Epilepsia* (2010) 51:108–17. doi:10.1111/j.1528-1167.2009.02205
9. Puttachary S, Sharma S, Verma S, Yang Y, Putra M, Thippeswamy A, et al. 1400W, a highly selective inducible nitric oxide synthase inhibitor is a potential disease modifier in the rat kainate model of temporal lobe epilepsy. *Neurobiol Dis* (2016) 93:184–200. doi:10.1016/j.nbd.2016.05.013
10. Puttachary S, Sharma S, Tse K, Beamer E, Sexton A, Crutison J, et al. Immediate epileptogenesis after kainate-induced status epilepticus in C57BL/6J mice: evidence from long term continuous video-EEG telemetry. *PLoS One* (2015) 10:e0131705. doi:10.1371/journal.pone.0131705
11. Seinfeld S, Goodkin HP, Shinnar S. Status epilepticus. *Cold Spring Harb Perspect Med* (2016) 6(3):a022830. doi:10.1101/cshperspect.a022830
12. Manno EM. Status epilepticus. *Neurohospitalist* (2011) 1:23–31. doi:10.1177/1941875210383176
13. Gastaut H. Classification of status epilepticus. *Adv Neurol* (1983) 34:15–35.
14. Dodson WE, DeLorenzo RJ, Pedley TA, Shinnar S, Treiman DM, Wannamaker BB. Treatment of convulsive status epilepticus. Recommendations of the Epilepsy Foundation of Americas Working Group on status epilepticus. *JAMA* (1993) 270:854–9. doi:10.1001/jama.270.7.854
15. Lowenstein DH, Bleck T, Macdonald RL. It's time to revise the definition of status epilepticus. *Epilepsia* (1999) 40:120–2. doi:10.1111/j.1528-1157.1999.tb02000.x
16. Shinnar S, Berg AT, Moshe SL, Shinnar R. How long do new-onset seizures in children last? *Ann Neurol* (2001) 49:659–64. doi:10.1002/ana.1018.abs
17. Trinka E, Cock H, Hesdorffer D, Rossetti AO, Scheffer IE, Shinnar S, et al. A definition and classification of status epilepticus – report of the ILAE task force on classification of status epilepticus. *Epilepsia* (2015) 56:1515–23. doi:10.1111/epi.13121
18. Furtado MDA, Lumley LA, Robison C, Tong LC, Lichtenstein S, Yourick DL. Spontaneous recurrent seizures after status epilepticus induced by soman in Sprague–Dawley rats. *Epilepsia* (2010) 51:1503–10. doi:10.1111/j.1528-1167.2009.02478.x
19. Castel-Branco MM, Alves GL, Figueiredo IV, Falcao AC, Caramona MM. The maximal electroshock seizure (MES) model in the preclinical assessment of potential new antiepileptic drugs. *Methods Find Exp Clin Pharmacol* (2009) 31:101–6. doi:10.1358/mf.2009.31.2.1338414
20. Loscher W, Fassbender CP, Nolting B. The role of technical, biological and pharmacological factors in the laboratory evaluation of anticonvulsant drugs. II. Maximal electroshock seizure models. *Epilepsy Res* (1991) 8:79–94. doi:10.1016/0920-1211(91)90075-Q
21. White HS, Johnson M, Wolf HH, Kupferberg HJ. The early identification of anticonvulsant activity: role of the maximal electroshock and subcutaneous pentylenetetrazol seizure models. *Ital J Neurol Sci* (1995) 16:73–7. doi:10.1007/BF02229077
22. Loscher W, Ferland RJ, Ferraro TN. The relevance of inter- and intrastrain differences in mice and rats and their implications for models of seizures and epilepsy. *Epilepsy Behav*. (2017) 73:214–35. doi:10.1016/j.yebeh.2017.05.040
23. Reddy DS, Kuruba R. Experimental models of status epilepticus and neuronal injury for evaluation of therapeutic interventions. *Int J Mol Sci* (2013) 14:18284–318. doi:10.3390/ijms140918284
24. Golden GT, Smith GG, Ferraro TN, Reyes PF. Rat strain and age differences in kainic acid induced seizures. *Epilepsy Res* (1995) 20:151–9. doi:10.1016/0920-1211(94)00079-C
25. Schauwecker PE. Strain differences in seizure-induced cell death following pilocarpine-induced status epilepticus. *Neurobiol Dis* (2012) 45:297–304. doi:10.1016/j.nbd.2011.08.013
26. Nairismagi J, Grohn OHJ, Kettunen MI, Nissinen J, Kauppinen RA, Pitkanen A. Progression of brain damage after status epilepticus and its association with epileptogenesis: a quantitative MRI study in a rat model of temporal lobe epilepsy. *Epilepsia* (2004) 45:1024–34. doi:10.1111/j.0013-9580.2004.08904.x
27. Nadler JV. Kainic acid as a tool for the study of temporal lobe epilepsy. *Life Sci* (1981) 29:2031–42. doi:10.1016/0024-3205(81)90659-7
28. Mikati M. Neuronal cell death in a rat model of mesial temporal lobe epilepsy is induced by the initial status epilepticus and not by later repeated spontaneous seizures. *Epilepsia* (2004) 45:296–296. doi:10.1111/j.0013-9580.2004.58503.x
29. Pitkänen A, Nissinen J, Nairismägi J, Lukasiuk K, Gröhn OH, Miettinen R, et al. Progression of neuronal damage after status epilepticus and during spontaneous seizures in a rat model of temporal lobe epilepsy. *Prog Brain Res* (2002) 135:67–83. doi:10.1016/s0079-6123(02)35008-8

30. Löscher W. Animal models of epilepsy for the development of antiepileptogenic and disease-modifying drugs. A comparison of the pharmacology of kindling and post-status epilepticus models of temporal lobe epilepsy. *Epilepsy Res* (2002) 50:105–23. doi:10.1016/s0920-1211(02)00073-6
31. White A, Williams PA, Hellier JL, Clark S, Dudek FE, Staley KJ. EEG spike activity precedes epilepsy after kainate-induced status epilepticus. *Epilepsia* (2010) 51:371–83. doi:10.1111/j.1528-1167.2009.02339.x
32. Buckmaster PS. Laboratory animal models of temporal lobe epilepsy. *Comp Med* (2004) 54:473–85.
33. Williams PA, White AM, Clark S, Ferraro DJ, Swiercz W, Staley KJ, et al. Development of spontaneous recurrent seizures after kainate-induced status epilepticus. *J Neurosci* (2009) 29:2103–12. doi:10.1523/jneurosci.0980-08.2009
34. Sutula TP. Mechanisms of epilepsy progression: current theories and perspectives from neuroplasticity in adulthood and development. *Epilepsy Res* (2004) 60:161–71. doi:10.1016/j.eplepsyres.2004.07.001
35. Rattka M, Brandt C, Löscher W. The intrahippocampal kainate model of temporal lobe epilepsy revisited: epileptogenesis, behavioral and cognitive alterations, pharmacological response, and hippoccampal damage in epileptic rats. *Epilepsy Res* (2013) 103:135–52. doi:10.1016/j.eplepsyres.2012.09.015
36. Robel S, Buckingham SC, Boni JL, Campbell SL, Danbolt NC, Riedemann T, et al. Reactive astrogliosis causes the development of spontaneous seizures. *J Neurosci* (2015) 35:3330–45. doi:10.1523/jneurosci.1574-14.2015
37. Puttachary S, Sharma S, Thippeswamy A, Thippeswamy T. Immediate epileptogenesis: impact on brain in C57BL/6J mouse kainate model. *Front Biosci (Elite Ed)* (2016) 8:390–411. doi:10.2741/e775
38. Ferraro TN, Golden GT, Smith GG, Berrettini WH. Differential susceptibility to seizures induced by systemic kainic acid treatment in mature DBA/2J and C57BLl6J mice. *Epilepsia* (1995) 36:301–7. doi:10.1111/j.1528-1157.1995.tb00999.x
39. Chaix Y, Ferraro TN, Lapouble E, Martin B. Chemoconvulsant-induced seizure susceptibility: toward a common genetic basis? *Epilepsia* (2007) 48:48–52. doi:10.1111/j.1528-1167.2007.01289.x
40. Müller CJ, Gröticke I, Hoffmann K, Schughart K, Löscher W. Differences in sensitivity to the convulsant pilocarpine in substrains and sublines of C57BL/6 mice. *Genes Brain Behav* (2009) 8:481–92. doi:10.1111/j.1601-183x.2009.00490.x
41. Bryant CD, Zhang NN, Sokoloff G, Fanselow MS, Ennes HS, Palmer AA, et al. Behavioral differences among C57BL/6 substrains: implications for transgenic and knockout studies. *J Neurogenet* (2008) 22:315–31. doi:10.1080/01677060802357388
42. Rao MS, Hattiangady B, Reddy DS, Shetty AK. Hippocampal neurodegeneration, spontaneous seizures, and mossy fiber sprouting in the F344 rat model of temporal lobe epilepsy. *J Neurosci Res* (2006) 83:1088–105. doi:10.1002/jnr.20802
43. Hellier JL, Patrylo PR, Buckmaster PS, Dudek F. Recurrent spontaneous motor seizures after repeated low-dose systemic treatment with kainate: assessment of a rat model of temporal lobe epilepsy. *Epilepsy Res* (1998) 31:73–84. doi:10.1016/s0920-1211(98)00017-5
44. Glien M, Brandt C, Potschka H, Voigt H, Ebert U, Löscher W. Repeated low-dose treatment of rats with pilocarpine: low mortality but high proportion of rats developing epilepsy. *Epilepsy Res* (2001) 46:111–9. doi:10.1016/s0920-1211(01)00272-8
45. Sharma S, Puttachary S, Thippeswamy T. Glial source of nitric oxide in epileptogenesis: a target for disease modification in epilepsy. *J Neurosci Res* (2017). doi:10.1002/jnr.24205
46. Beamer E, Otahal J, Sills GJ, Thippeswamy T. N(w)-propyl-L-arginine (L-NPA) reduces status epilepticus and early epileptogenic events in a mouse model of epilepsy: behavioural, EEG and immunohistochemical analyses. *Eur J Neurosci* (2012) 36:3194–203. doi:10.1111/j.1460-9568.2012.08234
47. Bortel A, Lévesque M, Biagini G, Gotman J, Avoli M. Convulsive status epilepticus duration as determinant for epileptogenesis and interictal discharge generation in the rat limbic system. *Neurobiol Dis* (2010) 40:478–89. doi:10.1016/j.nbd.2010.07.015
48. Klitgaard H, Matagne A, Vanneste-Goemaere J, Margineanu DG. Pilocarpine-induced epileptogenesis in the rat: impact of initial duration of status epilepticus on electrophysiological and neuropathological alterations. *Epilepsy Res* (2002) 51(1–2):93–107. doi:10.1016/S0920-1211(02)00099-2
49. Goodkin HP, Joshi S, Mtchedlishvili Z, Brar J, Kapur J. Subunit-specific trafficking of GABAA receptors during status epilepticus. *J Neurosci* (2008) 28:2527–38. doi:10.1523/jneurosci.3426-07.2008
50. Apland JP, Aroniadou-Anderjaska V, Figueiredo TH, Rossetti F, Miller SL, Braga MF. The limitations of diazepam as a treatment for nerve agent-induced seizures and neuropathology in rats: comparison with UBP302. *J Pharmacol Exp Ther* (2014) 351:359–72. doi:10.1124/jpet.114.217299
51. Hellier JL, Dudek FE. Chemoconvulsant model of chronic spontaneous seizures. *Curr Protoc Neurosci* (2005) Chapter 9:unit 9.19. doi:10.1002/0471142301.ns0919s31
52. Cavalheiro E, Riche D, Le Gal La SG. Long-term effects of intrahippocampal kainic acid injection in rats: a method for inducing spontaneous recurrent seizures. *Electroencephalogr Clin Neurophysiol* (1982) 53:581–9. doi:10.1016/0013-4694(82)90134-1
53. Lévesque M, Avoli M. The kainic acid model of temporal lobe epilepsy. *Neurosci Biobehav Rev* (2013) 37:2887–99. doi:10.1016/j.neubiorev.2013.10.011
54. Jones DM, Esmaeil N, Maren S, Macdonald RL. Characterization of pharmacoresistance to benzodiazepines in the rat Li-pilocarpine model of status epilepticus. *Epilepsy Res* (2002) 50:301–12. doi:10.1016/s0920-1211(02)00085-2
55. Qashu F, Figueiredo TH, Aroniadou-Anderjaska V, Apland JP, Braga MFM. Diazepam administration after prolonged status epilepticus reduces neurodegeneration in the amygdala but not in the hippocampus during epileptogenesis. *Amino Acids* (2009) 38:189–97. doi:10.1007/s00726-008-0227-2
56. Pitkänen A, Kharatishvili I, Narkilahti S, Lukasiuk K, Nissinen J. Administration of diazepam during status epilepticus reduces development and severity of epilepsy in rat. *Epilepsy Res* (2005) 63:27–42. doi:10.1016/j.eplepsyres.2004.10.003
57. Brandt C, Gastens A, Sun M, Hausknecht M, Loscher W. Treatment with valproate after status epilepticus: effect on neuronal damage, epileptogenesis, and behavioral alterations in rats. *Neuropharmacology* (2006) 51:789–804. doi:10.1016/j.neuropharm.2006.05.021
58. Goodman J. Experimental models of Status Epilepticus. In: Peterson SL, Albertson TE, editor. *Neuropharmacol Met Epilepsy Res*. Boca Raton, FL: CRC Press (1998). p. 96–118. doi:10.1201/9781420048889.ch5
59. Morimoto K, Fahnestock M, Racine RJ. Kindling and status epilepticus models of epilepsy: rewiring the brain. *Prog Neurobiol* (2004) 73:1–60. doi:10.1016/j.pneurobio.2004.03.009
60. Joshi S, Kapur J. $GABA_A$ receptor plasticity during Status Epilepticus. In: Noebels JL, Avoli M, Rogawski MA, editors. *Jaspers's Basic Mech Epilepsies*. Bethesda, MD: National Center for Biotechnology Information (2012). p. 545–54. doi:10.1093/med/9780199746545.003.0041

Conflict of Interest Statement: The authors declare that the research was conducted in the absence of any commercial or financial relationships that could be construed as a potential conflict of interest.

frontiers in Pharmacology

ORIGINAL RESEARCH
published: 22 September 2017
doi: 10.3389/fphar.2017.00676

Involvement of PPARγ in the Anticonvulsant Activity of EP-80317, a Ghrelin Receptor Antagonist

*Chiara Lucchi[1†], Anna M. Costa[1†], Carmela Giordano[1†], Giulia Curia[1], Marika Piat[1], Giuseppina Leo[1], Jonathan Vinet[1], Luc Brunel[2], Jean-Alain Fehrentz[2], Jean Martinez[2], Antonio Torsello[3] and Giuseppe Biagini[1,4]**

[1] Laboratory of Experimental Epileptology, Department of Biomedical, Metabolic and Neural Sciences, University of Modena and Reggio Emilia, Modena, Italy, [2] Centre National de la Recherche Scientifique, Max Mousseron Institute of Biomolecules, National School of Chemistry Montpellier, University of Montpellier, Montpellier, France, [3] School of Medicine and Surgery, University of Milano-Bicocca, Milan, Italy, [4] Center for Neuroscience and Neurotechnology, University of Modena and Reggio Emilia, Modena, Italy

Ghrelin, des-acyl ghrelin and other related peptides possess anticonvulsant activities. Although ghrelin and cognate peptides were shown to physiologically regulate only the ghrelin receptor, some of them were pharmacologically proved to activate the peroxisome proliferator-activated receptor gamma (PPARγ) through stimulation of the scavenger receptor CD36 in macrophages. In our study, we challenged the hypothesis that PPARγ could be involved in the anticonvulsant effects of EP-80317, a ghrelin receptor antagonist. For this purpose, we used the PPARγ antagonist GW9662 to evaluate the modulation of EP-80317 anticonvulsant properties in two different models. Firstly, the anticonvulsant effects of EP-80317 were studied in rats treated with pilocarpine to induce *status epilepticus* (SE). Secondly, the anticonvulsant activity of EP-80317 was ascertained in the repeated 6-Hz corneal stimulation model in mice. Behavioral and video electrocorticographic (ECoG) analyses were performed in both models. We also characterized levels of immunoreactivity for PPARγ in the hippocampus of 6-Hz corneally stimulated mice. EP-80317 predictably antagonized seizures in both models. Pretreatment with GW9662 counteracted almost all EP-80317 effects both in mice and rats. Only the effects of EP-80317 on power spectra of ECoGs recorded during repeated 6-Hz corneal stimulation were practically unaffected by GW9662 administration. Moreover, GW9662 alone produced a decrease in the latency of tonic-clonic seizures and accelerated the onset of SE in rats. Finally, in the hippocampus of mice treated with EP-80317 we found increased levels of PPARγ immunoreactivity. Overall, these results support the hypothesis that PPARγ is able to modulate seizures and mediates the anticonvulsant effects of EP-80317.

Keywords: 6-Hz corneal stimulation, EP-80317, ghrelin, peroxisome proliferator-activated receptor gamma, pilocarpine, status epilepticus, seizure

OPEN ACCESS

Edited by:
Batool F. Kirmani,
Texas A&M Health Science Center College of Medicine, United States

Reviewed by:
Wladyslaw-Lason, Institute of Pharmacology PAS in Krakow, Poland
Fengfei Wang, Texas A&M Health Science Center College of Medicine, United States

***Correspondence:**
Giuseppe Biagini
gbiagini@unimore.it

† These authors have contributed equally to this work.

Specialty section:
This article was submitted to Neuropharmacology, a section of the journal Frontiers in Pharmacology

Received: *14 June 2017*
Accepted: *08 September 2017*
Published: *22 September 2017*

Citation:
Lucchi C, Costa AM, Giordano C, Curia G, Piat M, Leo G, Vinet J, Brunel L, Fehrentz J -A, Martinez J, Torsello A and Biagini G (2017) Involvement of PPARγ in the Anticonvulsant Activity of EP-80317, a Ghrelin Receptor Antagonist. Front. Pharmacol. 8:676. doi: 10.3389/fphar.2017.00676

INTRODUCTION

Ghrelin and des-acyl ghrelin are neuroactive peptides prevalently produced in the stomach by X/A-like cells in rats, or P/D1 cells in humans (Rindi et al., 2002; Kojima, 2005; Chen et al., 2009). They regulate very important physiological functions, such as growth hormone secretion, food intake and metabolism by interacting with hypothalamic neurons (Nakazato et al., 2001). Ghrelin has also

been investigated for its possible role in regulating neuronal activity in other brain regions, since its receptor was found to be expressed out of the hypothalamus and especially in the hippocampus (Zigman et al., 2006). Interestingly, ghrelin was demonstrated to play an important role in learning and memory, cognitive functions in which the hippocampus is critically involved (Diano et al., 2006; Carlini et al., 2010; Li et al., 2013). Furthermore, ghrelin was also shown to modulate energy metabolism in areas other than the hypothalamus, as well as to be involved in the rewarding system of the brain (Egecioglu et al., 2010; Skibicka and Dickson, 2011; Skibicka et al., 2011; Perelló and Zigman, 2012). Overall, these evidences delineate a variety of physiological roles for ghrelin in the central nervous system (CNS).

Ghrelin has also been implicated in cerebral diseases. Specifically, it was shown to afford neuroprotection in models of cerebral ischemia (Spencer et al., 2013), Parkinson's disease (Bayliss and Andrews, 2013), and *status epilepticus* (SE) (Xu et al., 2009; Lucchi et al., 2013). Interestingly, this last neuroprotective effect occurred at a dosage unable to alter the epileptic activity. However, ghrelin was also found to modulate seizures induced by several, different approaches (Casillas-Espinosa et al., 2012; Portelli et al., 2012a; Kovac and Walker, 2013; Clynen et al., 2014; Curia et al., 2014; Dobolyi et al., 2014). Independent studies suggested an anticonvulsant activity of ghrelin in experimental paradigms by which seizures were induced using pentylenetetrazole (Obay et al., 2007), penicillin (Aslan et al., 2009), kainic acid (Lee et al., 2010), and pilocarpine (Portelli et al., 2012b). According to Lee et al. (2010), the anticonvulsant effects of ghrelin could be related to the interaction of this peptide with its established receptor. However, the ghrelin receptor was also demonstrated to possess a proconvulsant activity in basal condition, whereas the observed anticonvulsant properties of ghrelin ligands were explained by the induction of ghrelin receptor internalization (Portelli et al., 2012b).

Other than ghrelin, ghrelin receptor agonists such as hexarelin (Biagini et al., 2011), capromorelin (Portelli et al., 2012b), and JMV-1843 (Coppens et al., 2016), the inverse agonists A778193 and [D-Arg^{1}, D-Phe^{5}, D-Trp^{7,9}, Leu^{11}] substance P (Portelli et al., 2012b), as well as the antagonist EP-80317 (Biagini et al., 2011), were all proven to be anticonvulsants. These data may suggest that all ghrelin receptor ligands could be able to desensitize neurons expressing the ghrelin receptor, so to block its proconvulsant activity (Portelli et al., 2012b). However, this hypothesis could not be supported in the case of the ghrelin receptor antagonist JMV-2959, which did not alter the induction of SE by pilocarpine (Biagini et al., 2011). Alternatively, it could be hypothesized that the variety of ghrelin-related peptides able to induce anticonvulsant effects may interact with different receptors that share a common anticonvulsant activity. Indeed, the existence of multiple ghrelin receptors has been hypothesized immediately following the discovery of ghrelin receptor (Davenport et al., 2005; Müller et al., 2015). In particular, it was evident that the protective effects exerted by ghrelin, des-acyl ghrelin and other related peptides in presence of an inflammatory reaction, especially in the cardiovascular system, were independent of the ghrelin receptor (Bujold et al., 2009, 2013; Bulgarelli et al., 2009).

EP-80317 (Haic-D-Mrp-D-Lys-Trp-D-Phe-Lys-NH_2) is a hexapeptide with a primary structure similar to that of hexarelin, from which it differs for substitutions in the first and third amino acid residues causing the loss of the growth hormone (GH)-releasing properties possessed by the original peptide (Momany et al., 1981). EP-80317 is pharmacologically active on macrophages, and its activity on these cells was found to be dependent on activation of the peroxisome proliferator-activated receptor gamma (PPARγ). However, the ability to activate PPARγ is also common to ghrelin, des-acyl ghrelin and other ghrelin-related peptides, as all of them are able to interact with the CD36 scavenger receptor (Bujold et al., 2009, 2013). In the CNS, CD36 appears to be expressed prevalently although not exclusively in microglia (Glezer et al., 2009), whereas PPARγ is found in neurons of various cerebral regions, including those known to be involved in the generation and propagation of seizure activity, such as the hippocampus and the piriform cortex (Moreno et al., 2004; Warden et al., 2016). For this reason, we tried to elucidate whether PPARγ could be involved in the anticonvulsant effects of EP-80317. To this purpose, we designed experiments in which administration of EP-80317 was challenged by pretreatment with the PPARγ inhibitor GW9662 (Wong et al., 2015), in rodents exposed to seizure induction. Additionally, we characterized the expression of PPARγ in the hippocampus of mice treated with EP-80317.

MATERIALS AND METHODS

Animals and Treatments

A total of thirty-seven adult male Sprague-Dawley rats (Harlan, San Pietro al Natisone, Italy), ranging 260–270 g of body weight, and 66 4-week-old male CD-1 mice (Charles River, Calco, Italy) were used in this study. All animals were housed in a specific pathogen-free facility under controlled environment with *ad libitum* access to water and food.

EP-80317 was obtained through conventional solid phase synthesis, dissolved in a physiologic solution and administered through intraperitoneal (i.p.) injection (330 μg/kg). GW9662 and dimethyl sulfoxide (DMSO) were purchased from Sigma–Aldrich Chemicals (St. Louis, MO, United States). GW9662 was dissolved in DMSO and diluted with saline and then administered (2 mg/kg, i.p.) (Rani et al., 2016).

All experiments were in compliance with the European Directive 2010/63/EU and carried out according to the national guidelines on animal experimental research of the Italian Ministry of Health (DM 126/2011 – B and DM 92/2013). The University of Modena and Reggio Emilia Ethics Committee approved the study protocol. All efforts were made to refine procedures to improve the welfare and to reduce the number of animals that were used.

Experimental Design

For the pilocarpine model, we subdivided rats into four groups for behavior and video electrocorticographic (ECoG) recordings:

(i) 10 control rats received saline (1 ml/kg, i.p.), (ii) 10 rats received EP-80317 alone, (iii) seven rats received GW9662 alone, and (iv) 10 rats received GW9662 10 min prior to EP-80317.

For the repeated 6-Hz corneal stimulation model, we considered a number of mice ($n = 39$) for behavior and video-ECoG recordings, and the others ($n = 27$) for immunohistochemical and immunofluorescence analysis. In particular, for behavior and video-ECoG recordings, we subdivided mice into the following groups: (i) nine control mice received saline (1 ml/kg, i.p.), (ii) 12 mice received EP-80317 alone (330 μg/kg, i.p.), (iii) nine mice received GW9662 alone (2 mg/kg, i.p.), and (iv) nine mice received GW9662 10 min prior to EP-80317, both at the already indicated doses. For immunohistochemical analyses, four control mice were used to determine basal levels of the investigated marker and were neither treated nor stimulated. Still, they were handled and exposed to the same procedure as the others. Twelve were saline-treated mice, while the other 11 mice received an i.p. EP-80317 injection. Moreover, these animals were used for qualitative immunofluorescence experiments but, in this case, we used only three mice per treatment group.

Pilocarpine Protocol and Behavioral Analysis

Pilocarpine (Sigma–Aldrich, Milan, Italy) was injected i.p. (380 mg/kg) to induce SE. The pilocarpine injection was preceded by methylscopolamine (1 mg/kg, i.p.; Sigma–Aldrich) to prevent the peripheral effects of cholinergic stimulation (Curia et al., 2008). EP-80317, GW9662 alone, or saline were injected i.p. 20 min after methylscopolamine and 10 min before pilocarpine. In the group of rats treated with GW9662 and then with EP-80317, the first drug was administered 10 min prior to the second one. In all rats experiencing SE, diazepam (20 mg/kg, i.p.; Hospira Italia, Naples, Italy) was injected 10 min after the SE onset to guarantee survival. This procedure stops convulsive seizures, leaving non-convulsive SE unaltered for hours (Gualtieri et al., 2012).

Drug-induced responses in rats were observed directly and graded by blind to treatment expert raters. Seizures were graded according to a modification of the Racine's scale (Racine, 1972). In particular, we considered: (i) non-convulsive seizures, ranked as stage 1 to stage 3; (ii) convulsive seizures, ranked as stage 4 to stage 5; (iii) SE (stage 6), considered as the stage in which rats either did not recover normal behavior (i.e., exploration, grooming, or motor reaction to stimuli) between one seizure and the other, or in which they displayed continuous shaking for more than 5 min (Lowenstein, 1999). Rats were sacrificed 72 h after SE to assess the absence of cerebral lesions caused by electrode implant, and the presence of injuries developed during the SE.

Corneal Stimulation Protocol and Behavioral Analysis

Mice were stimulated once and allowed to recover for 72 h before being stimulated up to four sessions. Corneal stimulation was performed as previously described (Giordano et al., 2015, 2016). Briefly, a topical eye anesthetic (0.4% oxybuprocaine hydrochloride eye drops, Novesin, Novartis, Switzerland) was applied 10 min before stimulation. All mice received the injection of EP-80317, GW9662, or saline 10 min before each session of corneal stimulation. When GW9662 preceded EP-80317, it was administered 20 min before each session. Stimulation (fixed current intensity of 32 mA, pulse width of 0.2 ms, duration of 3 s, frequency of 6 Hz) was delivered via corneal electrodes connected to a stimulator (ECT Unit 5780; Ugo Basile, Comerio, Italy).

Seizure severity was ranked according to the following score: (i) stunned posture and eye blinking; (ii) head nodding, Straub tail and repetitive rhythmic movements (stereotypies) such as chewing; (iii) unilateral or alternating forelimb clonus; (iv) generalized tonic-clonic convulsions without loss of posture and rearings; (v) generalized tonic-clonic convulsions with loss of posture. Seizure scores were first recorded through direct observation, then reanalyzed on video recordings to quantify the duration of behavioral changes by an investigator unaware of the stimulation session. Recovery from seizures was defined as the reappearance of a normal exploratory behavior.

Electrodes Implantation for Electrocorticographic (ECoG) Recordings

For electrode implantation, anesthesia was induced with volatile isoflurane (4% induction and 1–2% maintenance) in rats, whereas mice were anesthetized with ketamine (150 μg/g, i.p.) + xylazine (10 μg/g, i.p.). After deep anesthesia was reached (assessed by deep breath, loss of tail and eye reflexes), the skin was shaved, disinfected with povidone-iodine 10% (Betadine® skin solution; Meda Pharma, Milano, Italy), cut and opened to expose the skull. Guiding holes were drilled and epidural electrodes (stainless steel Ø = 1 mm; PlasticsOne, Roanoke, VA, United States) were implanted in frontal (bregma 0 mm, 3.5 mm lateral from midline in rats and bregma 0 mm, 3 mm lateral from midline in mice) and occipital cortices (bregma −6.5 mm, 3.5 mm lateral from midline in rats and bregma −3.5 mm, 3 mm lateral from midline in mice) of both hemispheres. One electrode was implanted below the lambda on the midline in all animals and used as a reference. Electrodes were connected through steel wire to terminal gold pins (Bilaney Consultant GmbH, Düsseldorf, Germany) inserted in a plastic pedestal (PlasticsOne) cemented on heads. At the end of the surgery, gel containing 2.5 g lidocaine chloride, 0.5 g neomycin sulfate and 0.025 g fluocinolone acetonide (Neuflan® gel; Molteni Farmaceutici, Scandicci, FI, Italy) was applied to reduce acute pain and risk of infection. All animals were monitored until complete recovery from anesthesia, and were housed in single cages without grids or environmental enrichments to reduce risk of headset loss.

Video ECoG Recordings

For brain activity recording, animals were placed in cages with paper filter cover that allowed cable connection between headset and preamplifiers. Electrical brain activity was digitally filtered (0.3 Hz high-pass, 500 Hz low-pass), acquired at 1 kHz per channel, and stored on a personal computer after the mathematical subtraction of traces of recording electrodes

from trace of reference electrode, using a PowerLab8/30 amplifier connected to 4 BioAmp preamplifiers (ADInstruments; Dunedin, Otago, New Zealand). Videos were digitally captured through a camera connected to the computer and synchronized to the ECoG traces through LabChart 7 PRO internal trigger. Four days after electrode implantation, all animals were connected to the recording system and received the sequence of treatments described above. To facilitate handling and pharmacological manipulations, recordings were stopped, animals were temporarily disconnected while being injected and reconnected soon after. In particular, rats were recorded for 20 min after methylscopolamine administration, 10 min after EP-80317, GW9662 or saline injection, 10 min after SE onset and at least 2 h after diazepam administration. Rats that did not experience SE were recorded for at least 90 min after pilocarpine injection, until signs of normal behavior (exploring, grooming) reappeared. Mice were recorded after EP-80317, GW9662 or saline injection and 6-Hz corneal stimulation, until signs of normal behavior reappeared.

ECoG Analysis

Electrocorticographic traces were digitally filtered offline (band-pass: high 50 Hz, low 1 Hz) and manually analyzed using LabChart 7 PRO software (AD Instruments) by expert raters.

In rats, we measured the duration of each electrographic seizure, characterized as epileptiform ECoG patterns with trains of 150–250 ms long spikes with amplitudes at least twice as the previous 2 s baseline. Seizures occurring within 5 s of each other were defined as one epileptic event.

In mice, we quantified the ECoG signal of each seizure performing a power spectral analysis, that described the distribution of signal power over frequency (Dressler, 2004). In particular, the power spectrum was obtained by fast Fourier transformation of the ECoG waveforms (LabChart 7 PRO, ADInstruments) and used to obtain the mean power spectra for the experimental groups. The maximum value of power spectra (peak value) was considered for each mouse. Peak values of power, recorded from frontal and occipital electrodes, were evaluated to investigate whether modifications of ictal activity had occurred from the first to the fourth stimulation.

Immunohistochemistry

Control mice and mice receiving up to one or three sessions of 6-Hz corneal stimulation and treated with saline or EP-80317 were used for tissue analysis. Mice deeply anesthetized with isoflurane were transcardially perfused with phosphate buffered saline (PBS, pH 7.4) followed by Zamboni's fixative (pH 6.9), 14–17 h after the seizure. Brains were post-fixed at 4°C in the same fixative for 24 h, cryoprotected in 15 and 30% sucrose solutions (Vinet et al., 2016) and stored at −80°C until used. Horizontal sections of 50 μm were cut using a freezing sliding microtome (Leica SM2000 R; Leica, Nussloch, Germany). For immunostaining, sections were washed in Tris-buffered saline (TBS) and incubated in 3% H_2O_2 in TBS (30 min) to quench endogenous peroxidase activity. Following another washing step, sections were blocked 1 h in TBS containing 2% bovine serum albumin, 0.3% Triton X-100 (Tx) and 5% normal goat serum. Sections were then placed at 4°C with a polyclonal rabbit anti-PPARγ (Ab209350; Abcam, Cambridge, United Kingdom, dilution 1:2000, 48 h). After washing, sections were incubated for 1 h with a biotinylated anti-rabbit secondary antibody (Vector Laboratories, Burlingame, CA, United States; 1:200), and later with the avidin-biotin-peroxidase complex (Elite ABC Kit; Vector Laboratories, Burlingame, CA, United States). The immunostaining was performed in 0.05% 3,3-diaminobenzidine tetrahydrochloride for 5 min (DAB, Sigma–Aldrich, Milan, Italy) and developed by adding 0.03% H_2O_2. Finally, sections were washed again in TBS, mounted on gelatin-coated slides and cover slipped with Eukitt (Eukitt®, O. Kindler GmbH & Co., Freiburg, Germany).

Image Analysis

Immunostained sections related to bregma from −8.04 mm to −5.04 mm for hippocampal CA1 and CA3 regions, and hilus of the dentate gyrus (DH) were analyzed using an Axioskop microscope (Carl Zeiss Vision GmbH, Munchen, Germany) equipped with a 10X objective. Images were digitally captured by a Sony CCD-IRIS B–W video camera, along the ventrodorsal direction of the brain (approximately 6–7 serial horizontal sections separated by 0.5 mm). A mouse brain atlas-C57BL/6J horizontal was used to assess brain sections. The image analysis was carried out using the KS300 software (Carl Zeiss Vision GmbH), as previously described (Biagini et al., 2005; Curia et al., 2013; Giordano et al., 2015, 2016). PPARγ immunoreactivity was measured as field area values, corresponding to the addition of areas of the specific profiles obtained after discrimination from background staining. Background values in each section were obtained from areas devoid of specific immunostaining, such as the angular bundle. All measurements were taken bilaterally and the final values represent the left–right average.

Double Immunofluorescence

We performed a PPARγ/67-kDa glutamate decarboxylase (GAD67) qualitative double immunofluorescence to assess PPARγ expression in interneurons. PPARγ expression was further evaluated in different interneuron subsets by PPARγ/parvalbumin (PV), PPARγ/somatostatin-28 (SOM) or PPARγ/vasoactive intestinal peptide (VIP) qualitative double immunofluorescences. For PPARγ/GAD67 immunofluorescence, sections were washed in TBS at room temperature and unmasking in sodium citrate at 98°C and permeabilized for 1 h in TBS/0.02% Triton X-100 containing 5% normal goat serum. Concerning PPARγ/PV, PPARγ/SOM and PPARγ/VIP immunofluorescences, sections were washed in TBS at room temperature and permeabilized for 1 h in TBS/0.1% Triton X-100 containing 5% normal goat serum. Then, sections were incubated for 48 h with primary antibodies: rabbit anti-PPARγ (Ab209350; Abcam, Cambridge, United Kingdom, dilution 1:50), mouse anti-GAD67 (MAB5406; Chemicon International, Billerica, MA, United States, dilution 1:200), mouse anti-PPARγ (E-8, sc-7273; Santa Cruz Biotechnology, Santa Cruz, CA, United States, dilution 1/50), rabbit anti-PV (Ab11427; Abcam, Cambridge, MA, United States, dilution 1:2000), rabbit anti-SOM (20089; Immunostar, Hudson, WI,

United States, dilution 1/1000) and rabbit anti-VIP (20077; Immunostar, Hudson, WI, United States, dilution 1/500). Following a washing step in TBS, sections were incubated for 3 h at room temperature with secondary antibodies Alexa Fluor 488-labeled goat anti-mouse antibody (A-11001; Invitrogen, Carlsbad, CA, United States, dilution 1:500) and Alexa Fluor 594-labeled goat anti-rabbit (A-11012; Invitrogen, Carlsbad, CA, United States, dilution 1:500). After rinsing sections in TBS, brain sections were placed on gelatinized glass slides, dried, and mounted with Mowiol after incubation with DAPI. Images were acquired using a Leica TCS SP2 (Leica Laser Technik, Heidelberg, Germany) confocal microscope. All images were taken using a 40X magnification.

Statistics

Chi-Square test (χ^2) was used to compare the percentage (%) of rats experiencing SE in the various treatment groups. Pairwise comparisons with Fisher's exact test (using α correction) were used to establish differences among groups. Additionally, the time interval (min) required to develop seizures and SE in the various groups was analyzed by Kruskal–Wallis test. Dunn's test was used for multiple comparisons. One-way analysis of variance (ANOVA) was used to compare electrographic seizure duration (sec) in each treatment groups.

The χ^2 test was also used to compare mice experiencing seizures with loss of posture in the various treatment groups. Again, pairwise comparisons with Fisher's exact test (using α correction) were used to establish differences among groups. Electrocorticographic recordings, analyzed as peak values of power spectra, were compared using two-way ANOVA, considering treatments as the between-factor and sessions as the within-factor. The Holm-Šídák test was used for multiple comparisons. All statistical analyses were performed using Sigmaplot 11 (Systat Software, San Jose, CA, United States). Unless otherwise indicated, results are shown as mean ± standard error of the mean (SEM); p-values lower than 0.05 were considered as statistically significant.

RESULTS

EP-80317 Reduced the Percentage of Animals Developing SE after Pilocarpine Injection

Response to pilocarpine was assessed by expert raters who directly annotated the motor responses observed during seizure development according to the modified Racine's scale (Racine, 1972; Lucchi et al., 2013), and by offline analysis of video-EcoG recordings. Four ($n = 1$ saline group, $n = 2$ EP-80317 group, and $n = 1$ GW9662 group) animals died during continuous tonic-clonic seizures and were excluded from the analysis. Consistently with previous findings (Biagini et al., 2011), pilocarpine induced SE in 100% of saline-treated rats. Instead, only 50% of rats treated with EP-80317 developed SE ($p < 0.05$ vs. saline-treated rats, Fisher's exact test). Additionally, we also found that the percentages of rats developing SE after pilocarpine administration in groups treated with GW9662 or GW9662+EP-80317 (respectively, 83% and 80%) were not significantly different from that observed in saline-treated rats (**Table 1**).

GW9662 Accelerated the Development of Convulsive Seizure and SE in the Pilocarpine Model

We calculated the time interval required to develop the first stage 1-3 and stage 4-5 seizure after pilocarpine administration, as median and interquartile range (IRQ) values. Moreover, we calculated the time interval required to develop SE (**Table 2**). No significant differences were found when comparing the latency periods of the first stage 1-3 seizure in the various treatment groups. Instead, the latency periods for developing the first stage 4-5 seizure were significantly different in GW9662-treated or GW9662+EP-80317-treated rats compared to, respectively, saline-treated rats ($p < 0.05$ for both groups, Dunn's test) and the EP-80317 group of treatment ($p < 0.05$). In addition, the latency periods for developing SE after the first stage 4-5 seizure were significantly shorter in GW9662-treated and GW9662+EP-80317-treated rats compared to saline-treated rats ($p < 0.05$).

Drug Treatments Did Not Affect Seizure Duration in Pilocarpine-Treated Rats

We measured the average seizure duration in traces obtained from ECoG recordings (**Figure 1**) performed in the various groups of treatment. No differences were found for animals treated, respectively, with saline (65.32 ± 8.75 s) or GW9662 (67.15 ± 10.95 s). Although the EP-80317 group presented a lower seizure duration (45.75 ± 9.24 s), this difference did not reach a statistically significant level. Mean seizure duration was also lower (49.91 ± 12.64 s) in GW9662+EP-80317 but, again, not enough to be statistically relevant.

EP-80317 Transiently Reduced the Seizure Severity and Duration in the Repeated 6-Hz Corneal Stimulation Model

Experimenters first visually monitored seizures induced through 6-Hz corneal stimulation and their pharmacological modulations. The first seizure duration was significantly shorter in mice treated with EP-80317 compared to control mice ($p < 0.05$, Holm-Šídák test), thus confirming the anticonvulsant properties of this molecule (Biagini et al., 2011;

TABLE 1 | Percentage (%) of rats developing *status epilepticus* (SE) in the various treatment groups.

Treatments	Percentage (%) of rats developing SE
Saline ($n = 9$)	100%
EP-80317 (EP, $n = 8$)	50%*
GW9662 (GW, $n = 6$)	83%
GW+EP ($n = 10$)	80%

*$p < 0.05$, EP-80317 vs. saline; Fisher's exact test.

TABLE 2 | Median and interquartile range values of latency periods for developing seizure and *status epilepticus* (SE) in the various treatment groups.

Latency (min)	Saline	EP-80317 (EP)	GW9662 (GW)	GW+EP
From pilocarpine injection to first stage 1-3 seizure	2.00 (1.75–3.50)	4.00 (3.00–11.75)	3.00 (2.00–4.00)	3.00 (3.00–4.00)
From pilocarpine injection to first stage 4-5 seizure	9.00 (6.75–10.25)	18.00 (8.00–21.25)	3.00 (2.00–4.00)*§	3.00 (3.00–4.00)*§
From pilocarpine injection to SE	17.00 (16.00–18.50)	13.00 (10.75–25.00)	14.00 (11.00–14.50)	16.50 (14.50–21.75)
From first stage 4-5 seizure to SE	8.00 (8.00–10.50)	5.50 (2.75–6.75)	3.00 (2.50–4.50)#	3.50 (3.00–6.50)#

*$p < 0.05$, GW9662 vs. saline and GW9662+EP-80317 vs. saline; Dunn's test. §$p < 0.05$, GW9662 vs. EP-80317 and GW9662+EP-80317 vs. EP-80317. #$p < 0.05$, GW9662 vs. saline and GW9662+EP-80317.

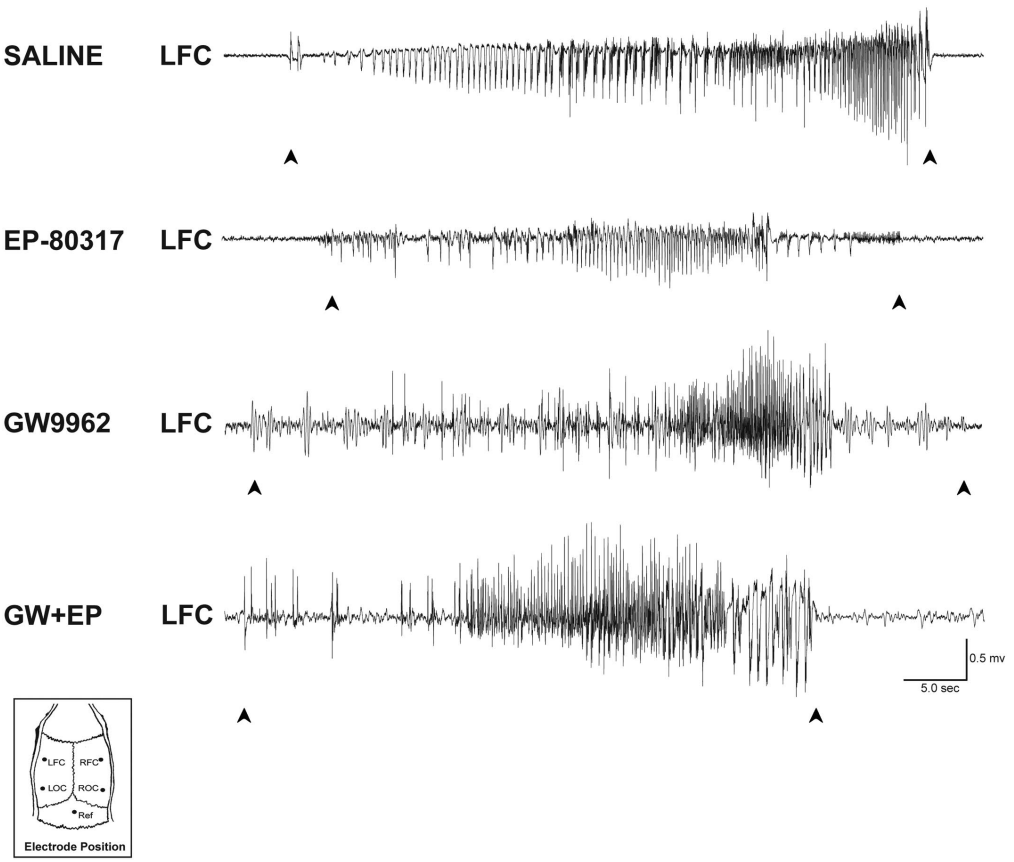

FIGURE 1 | ECoG analysis of seizure duration in the pilocarpine model. Representative epileptiform activity recorded from each treatment group is shown. In saline-treated and GW9662-treated rats, the seizure duration was similar to those of EP-80317 and GW9662+EP-80317 (GW+EP) groups. LFC, left frontal cortex; LOC, left occipital cortex; Ref, reference electrode; RFC, right frontal cortex; ROC, right occipital cortex.

Giordano et al., 2016). No differences were noticed by comparing controls to mice treated with GW9662 alone or prior to EP-80317 (**Figure 2A**). Similarly seizure severity, defined as the percentage of mice displaying loss of posture during seizures, was also less pronounced in the presence of EP-80317 ($p < 0.05$, EP-80317 vs. saline in the first session of stimulation; Fisher's exact test). No differences were observed by comparing the other groups with saline-treated mice (**Figure 2B**).

As expected (Giordano et al., 2015), seizures significantly shortened by repeating 6-Hz corneal stimulation ($p < 0.01$, sessions three and four vs. session one in saline-treated mice; Holm-Šídák test). Consequently, no differences between mice treated with saline and EP-80317 were observed from the second session onward (**Figure 2A**). Moreover, the severity of seizures progressed in all groups, including mice treated with EP-80317 (**Figure 2B**), which confirmed the appearance of resistance to the effects of EP-80317 (Giordano et al., 2016). Consistently, in the fourth session of 6-Hz corneal stimulation no differences were present within the various treatment groups.

EP-80317 Prevented the Increase in Power Spectra of Seizures Induced by Repeated 6-Hz Corneal Stimulation

Seizures induced by 6-Hz corneal stimulation and their pharmacological modulations were further monitored through

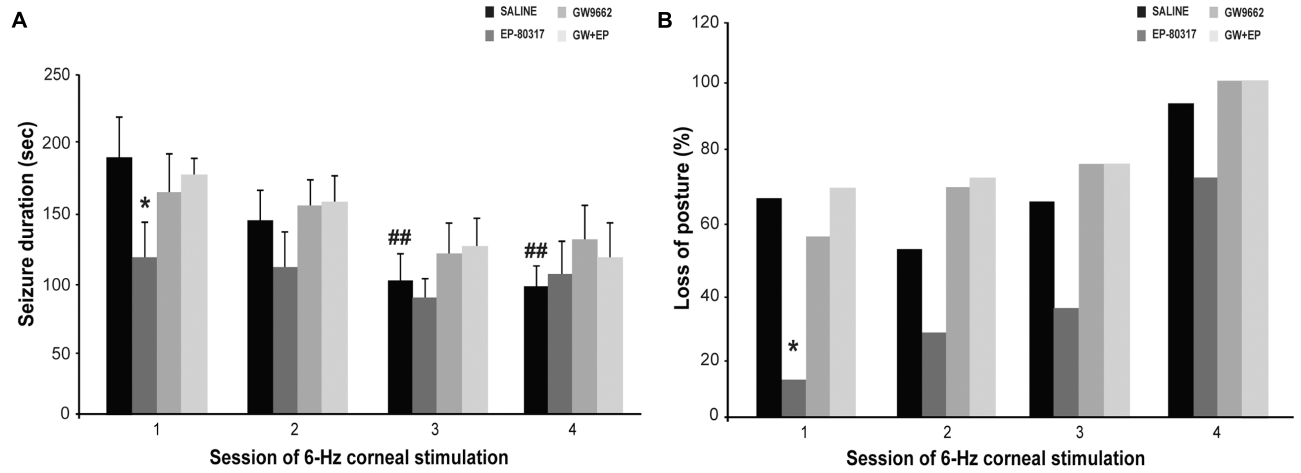

FIGURE 2 | Behavioral changes observed during repeated 6-Hz corneal stimulation. Seizure duration and severity are respectively illustrated in **(A,B)** for the various treatment groups. **(A)** The PPARγ activator EP-80317 significantly reduced the duration of seizures induced by the first 6-Hz corneal stimulation (*$p < 0.05$, EP-80317 vs. saline in the first session of stimulation; Holm-Šídák test). Administering GW9662, a PPARγ blocker, counteracted this effect (GW+EP group). Note also that seizure duration significantly decreased in control mice at the third and fourth sessions ($^{\#\#}p < 0.01$, sessions three or four vs. session one in saline-treated mice; Holm-Šídák test). **(B)** The seizure severity, evaluated as the percentage of animals displaying postural loss during convulsions, was also significantly affected by EP-80317 (*$p < 0.05$, EP-80317 vs. saline in the first session of stimulation; Fisher's exact test).

video ECoG recordings. In particular, we compared power spectra of seizures recorded from frontal (not shown) and occipital electrodes (**Figure 3A**). As previously reported (Giordano et al., 2015), power peaks did not change for ictal events recorded through frontal cortex electrodes, in all groups, whereas in the occipital recording we noticed the presence of an epileptogenic process. In particular, we found a significant increase in power peaks recorded from occipital electrodes in the fourth session, both in saline-treated and GW9662-treated mice ($p < 0.01$ for saline-treated mice; $p < 0.05$ for GW9662-treated mice, session four vs. session one; Holm-Šídák test; **Figure 3B**). Conversely, power peaks in mice treated with EP-80317 did not change from the first to the fourth session of 6-Hz corneal stimulation, suggesting an antiepileptogenic effect. This effect was not completely prevented by administering GW9662 prior to EP-80317, although a trend was present ($p = 0.09$). Interestingly, significantly lower values were found in the fourth session of mice treated with EP-80317 compared to saline-treated mice ($p < 0.05$; **Figure 3B**).

EP-80317 Significantly Increased PPARγ Immunoreactivity in the Hippocampus of Mice Exposed to the First 6-Hz Corneal Stimulation

We evaluated the effects of repeated exposure to 6-Hz corneal stimulation on PPARγ immunoreactivity in the *stratum pyramidalis* of CA1 (**Figure 4**), in both *stratum pyramidalis* and *stratum radiatum/lacunosum-moleculare* of CA3 (**Figure 5**), and finally in the DH (**Figure 6**). First, we quantified the changes occurring after the first and third session of seizure induction in pyramidal cells of the hippocampus and in mossy cells of the DH. PPARγ levels were scantily detectable in all sampled regions of unstimulated control mice. PPARγ immunoreactivity was not significantly changed in regions of interest of saline-treated mice. Notably, in animals treated with EP-80317 we observed a prominent increase in PPARγ levels after the first 6-Hz corneal stimulation, reaching a statistically significant level in all the considered regions ($p < 0.05$ vs. controls, in CA1; $p < 0.001$ vs. controls and saline-treated mice, in CA3 and DH; Holm-Šídák test; **Figures 4–6**). After the third seizure induction, PPARγ immunoreactivity returned to basal levels in all hippocampal regions.

To evaluate the response in interneurons, we analyzed the changes occurring in the *stratum radiatum/lacunosum-moleculare* of the CA3 (**Table 3**). Again, PPARγ levels were barely detectable in unstimulated control mice and saline-treated mice, but a significant increase in PPARγ levels was found in mice treated with EP-80317 after the first 6-Hz corneal stimulation ($p < 0.01$ vs. controls; $p < 0.05$ vs. saline-treated mice, Holm-Šídák test; **Table 3**). Consistently, PPARγ levels returned to basal levels after the third seizure induction.

PPARγ Is Expressed in Different Subsets of Interneurons

To confirm that PPARγ was expressed in interneurons, we performed a double immunofluorescence experiment with PPARγ and GAD67 antibodies. We found that not all interneurons coexpressed GAD67 and PPARγ immunoreactivity (**Figure 7**, top panels). Thus, to assess the subset of interneurons expressing PPARγ immunoreactivity, we evaluated PPARγ/PV, PPARγ/SOM and PPARγ/VIP colabeling. PPARγ-positive cells were frequently observed within PV interneurons (**Figure 7**, in which arrows indicate colabeling), and less frequently identified

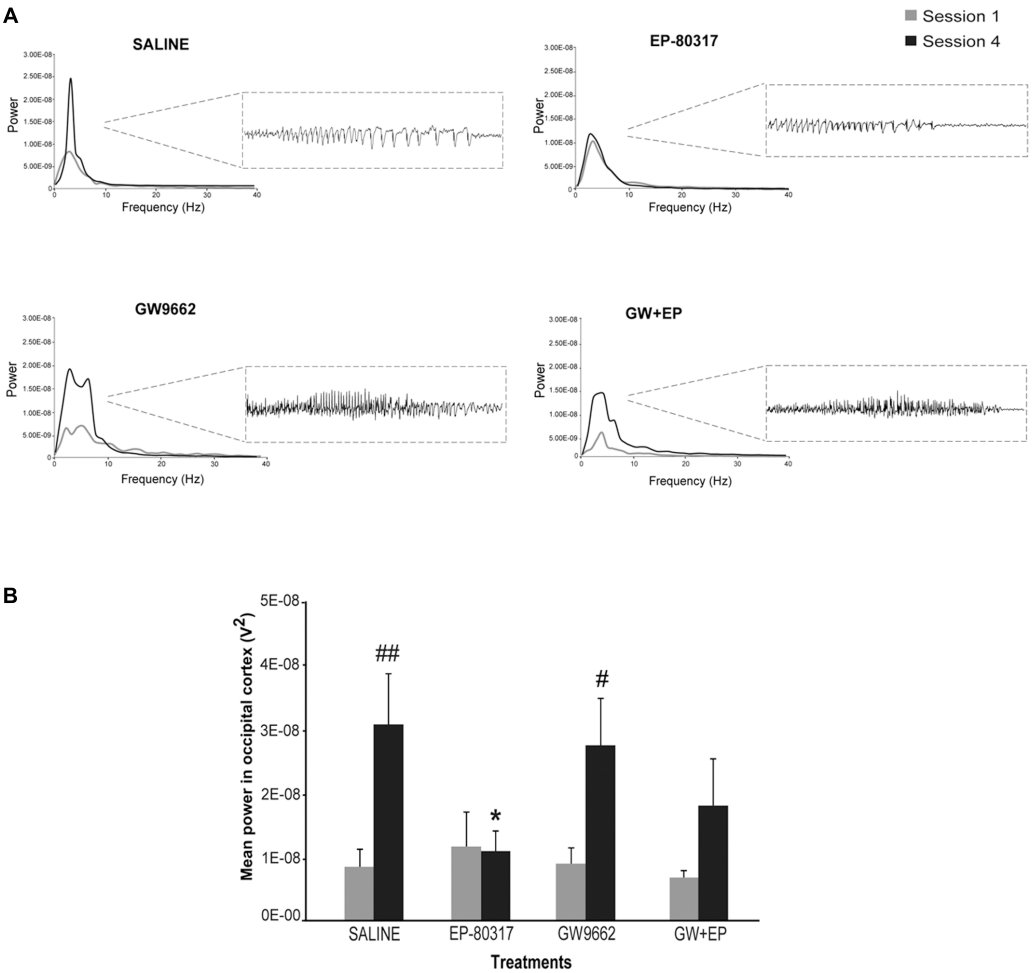

FIGURE 3 | Electrographic changes observed during repeated 6-Hz corneal stimulation. **(A)** Representative power spectra obtained at session one and four are illustrated for each treatment group. Note that powers of ictal activity did not significantly change going from first to fourth stimulation in mice treated with EP-80317, whereas clear alterations were present in all other groups. The inset on the right shows electrographic traces corresponding to power spectra of traces recorded by the occipital electrodes, after the fourth seizure induction. The gray color is for the first session; the black color is for the fourth session. **(B)** Mean power spectra of ictal events obtained through one or four separated 6-Hz corneal stimulation sessions. Histograms show that the power peak of ictal events significantly increased at the fourth session in saline-treated mice ($^{\#\#}p < 0.01$, session 4 vs. session 1; Holm-Šídák test) and in mice treated with GW9662 ($^{\#}p < 0.05$, session 4 vs. session 1), but not in mice treated with EP-80317 alone or in combination with GW9662 (GW+EP). Note also that the mean power peak of animals treated with EP-80317 was significantly lower than that of saline-treated mice, at the fourth stimulation ($^{*}p < 0.05$, EP-80317 vs. saline in the fourth session of stimulation).

within SOM interneurons. In contrast, PPARγ never colocalized with VIP in interneurons (**Figure 7**, in which arrowheads indicate lack of colabeling).

DISCUSSION

In the present investigation we confirmed that EP-80317 displays anticonvulsant effects in the pilocarpine model and in the repeated 6-Hz corneal stimulation model. As major findings of our investigation, we also demonstrated that GW9662, an inhibitor of PPARγ activity, is able to counteract the anticonvulsant effects of EP-80317 in both the animal models, with the notable exception of the antiepileptogenic properties disclosed by analyzing the ECoG power spectrum in mice. We also observed a proconvulsant activity of GW9662 when analyzing the latency period of stage 4-5 seizures, and the latency period of SE onset after the first stage 4-5 seizure in the pilocarpine model. Interestingly, PPARγ immunoreactivity was transiently increased in pyramidal cells and interneurons belonging to PV and SOM subclasses, in coincidence with the anticonvulsant effects of EP-80317 in 6-Hz corneally stimulated mice.

We previously established that the ghrelin receptor antagonist EP-80317 is an anticonvulsant in the pilocarpine model (Biagini et al., 2011), as well as in the repeated 6-Hz corneal stimulation model (Giordano et al., 2016). We also hypothesized that its anticonvulsant activity could not be explained by an involvement of the ghrelin receptor, as we did not observe any anticonvulsant activity of either the ghrelin receptor

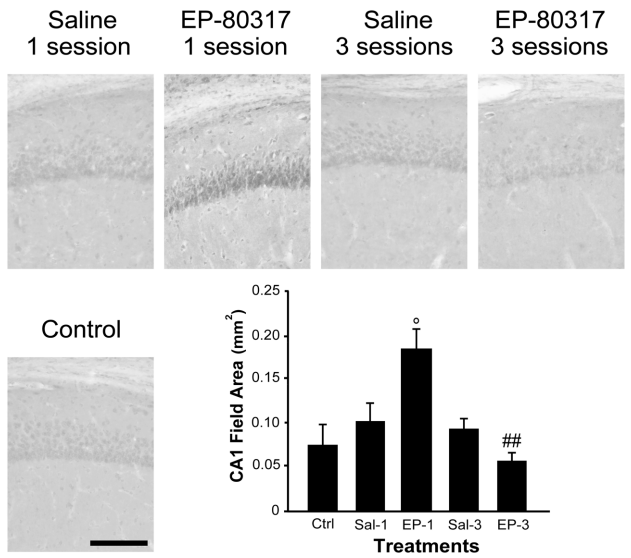

FIGURE 4 | PPARγ immunoreactivity in the hippocampal CA1 region of mice treated with saline or EP-80317 and exposed to different sessions of 6-Hz corneal stimulation. PPARγ immunoreactivity is illustrated in a representative unstimulated control (Ctrl) mouse and in mice treated with saline (Sal) or EP-80317 (EP) and respectively exposed to one (Sal-1, EP-1) or three (Sal-3, EP-3) different sessions of 6-Hz corneal stimulation. Note that PPARγ levels were significantly increased after the first session in EP-80317 mice only ($^{\circ}p < 0.05$, EP-1 vs. Ctrl; Holm-Šídák test). Note also that PPARγ levels were significantly reduced in the third session of EP-80317 mice ($^{\#\#}p < 0.01$, EP-3 vs. EP-1). Scale bar: 100 μm.

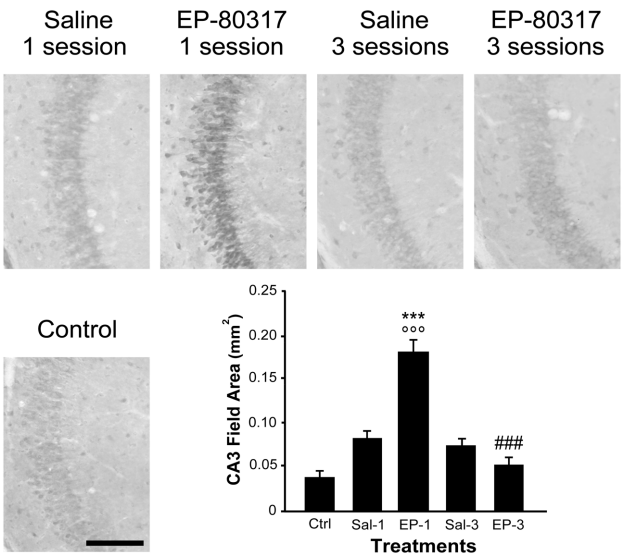

FIGURE 5 | PPARγ immunoreactivity in the hippocampal CA3 region of mice treated with saline or EP-80317 and exposed to different sessions of 6-Hz corneal stimulation. PPARγ immunoreactivity is illustrated in a representative unstimulated control (Ctrl) mouse and in mice treated with saline (Sal) or EP-80317 (EP) and respectively exposed to one (Sal-1, EP-1) or three (Sal-3, EP-3) different sessions of 6-Hz corneal stimulation. Note that PPARγ levels were significantly increased after the first session in EP-80317 mice only ($^{\circ\circ\circ}p < 0.001$, EP-1 vs. Ctrl; Holm-Šídák test). In EP-80317 mice, PPARγ levels were also significantly different from saline-treated mice ($^{***}p < 0.001$, EP-1 vs. Sal-1 in CA3). Note also that PPARγ levels were significantly reduced in the third session of EP-80317 mice ($^{\#\#\#}p < 0.001$, EP-3 vs. EP-1). Scale bar: 100 μm.

antagonist JMV-2959 (Biagini et al., 2011), nor of ghrelin, and of the ghrelin receptor agonist JMV-1843 (Biagini et al., 2011; Lucchi et al., 2013), all administered i.p. 10 min before injecting pilocarpine. At odds with our data, however, other investigators consistently showed that ghrelin produces some anticonvulsant effects in different seizure models (Portelli et al., 2012a,b). Furthermore, JMV-1843 also was found to be an anticonvulsant when used at high doses (Coppens et al., 2016). So, technical reasons, such as the more direct intracerebroventricular route of ghrelin administration in some cases (Portelli et al., 2012b), the earlier timing of ghrelin injection in others (Obay et al., 2007; Lee et al., 2010; Portelli et al., 2012b), and the different doses of the tested ghrelin receptor agonist (Coppens et al., 2016) may help in understanding why ghrelin receptor agonists in our hands did not display anticonvulsant properties (Biagini et al., 2011; Lucchi et al., 2013). Alternatively, it could be proposed that different receptors are involved in the anticonvulsant effects of ghrelin and its related peptides.

EP-80317 was found to activate PPARγ, as well as its cascade in apolipoprotein E-deficient mice (Bujold et al., 2009, 2013; Bulgarelli et al., 2009). Although PPARγ was mainly localized in the liver and in adipocytes, in which it was characterized for its role in metabolism regulation (Demers et al., 2008; Li et al., 2014; Gorga et al., 2017), it was also found that PPARγ agonists such as rosiglitazone or pioglitazone display antiseizure effects (Adabi Mohazab et al., 2012; Hong et al., 2013). It has also been proposed that PPARγ plays a key role in the antiseizure effects of cannabinoid agonists (Payandemehr et al., 2015), as well as in the anticonvulsant effects of the ketogenic diet (Jeong et al., 2011; Simeone et al., 2017). In agreement with these suggestions, our data support the involvement of PPARγ in the anticonvulsant effects of EP-80317. Consistently, by inhibiting PPARγ with the antagonist GW9662, the effects of rosiglitazone on seizure-like activity induced by Mg^{2+}-free medium in hippocampal slices were partially prevented (Wong et al., 2015). In line with these *in vitro* studies, the effects of EP-80317 were counteracted by GW9662 in our *in vivo* experiments and, additionally, we have identified a proconvulsant effect of GW9662 in the pilocarpine model. Indeed, as GW9662 produced a decrease in the latency period of tonic-clonic seizures and accelerated the onset of SE, a question arises on whether the GW9662 and EP-80317 combination resulted in the simple summation of their independent pro/anticonvulsant effects or not, at least in the pilocarpine model.

The suggested ability to modulate seizures of PPARγ could be explained by the fact that this nuclear receptor is also expressed in peripheral immune cells, microglia, and neurons (Moreno et al., 2004; Bujold et al., 2009; Warden et al., 2016). Especially by acting on immune cells, PPARγ exerts a negative modulation of macrophages and microglia reactivity (Moreno et al., 2004;

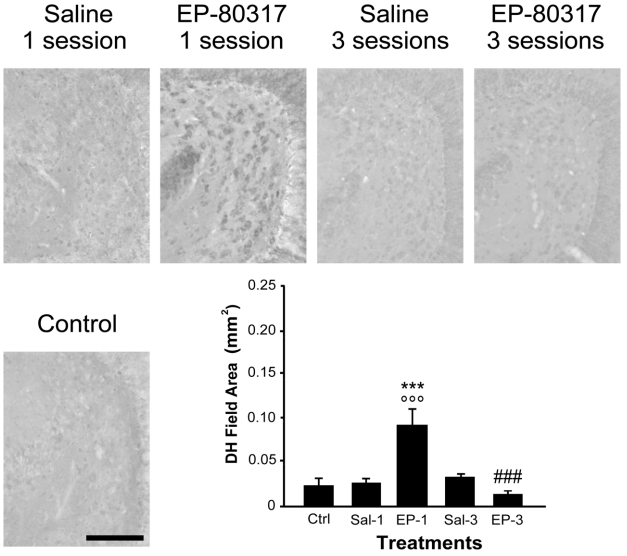

FIGURE 6 | PPARγ immunoreactivity in the hilus of dentate gyrus (DH) of mice treated with saline or EP-80317 and exposed to different sessions of 6-Hz corneal stimulation. PPARγ immunoreactivity is illustrated in a representative unstimulated control (Ctrl) mouse and in mice treated with saline (Sal) or EP-80317 (EP) and respectively exposed to one (Sal-1, EP-1) or three (Sal-3, EP-3) different sessions of 6-Hz corneal stimulation. Note that PPARγ levels were significantly increased after the first session in EP-80317 mice only ($^{\circ\circ\circ}p < 0.001$, EP-1 vs. Ctrl; Holm-Šídák test). PPARγ levels were also significantly different from saline-treated mice ($^{***}p < 0.001$, EP-1 vs. Sal-1). Note also that PPARγ levels were significantly reduced in the third session of EP-80317 mice ($^{\#\#\#}p < 0.001$, EP-3 vs. EP-1). Scale bar: 100 μm.

TABLE 3 | EP-80317 (EP) significantly increased PPARγ immunoreactivity in interneurons within the CA3 *stratum radiatum/lacunosum-moleculare* of mice exposed to the first 6-Hz corneal stimulation (EP-1), but not in mice exposed to the third stimulation (EP-3), compared to saline-treated mice (Sal) and controls (Ctrl).

Treatment groups	Field area (mm^2) mean values	SEM
Ctrl ($n = 4$)	0.016	0.0016
Sal-1 ($n = 5$)	0.020	0.0021
EP-1 ($n = 5$)	$0.035^{\circ\circ *}$	0.0055
Sal-3 ($n = 7$)	0.018	0.0009
EP-3 ($n = 6$)	$0.010^{\#\#\#}$	0.0018

$^{*}p < 0.05$, EP-1 vs. Sal-1; Holm-Šídák test; $^{\circ\circ}p < 0.01$, EP-1 vs. Ctrl; $^{\#\#\#}p < 0.001$, EP-3 vs. EP-1.

Bujold et al., 2009; Warden et al., 2016), resulting in an anti-inflammatory action in the nervous tissue (Jeong et al., 2011). This effect may be important as several lines of evidence suggest that leukocytes and microglia are critical in establishing the onset of SE in the pilocarpine model (Fabene et al., 2008; Vezzani et al., 2015; Vinet et al., 2016). In particular, treatment with antibodies against leukocyte α_4 integrin, which is involved in inflammation, successfully prevented the onset of SE in pilocarpine-treated mice (Fabene et al., 2008). Additional evidences indicate that inflammation is required to establish the SE in pilocarpine-treated rodents (Marchi et al., 2009; Vezzani et al., 2015). Overall, these findings suggest that EP-80317 activation of the PPARγ pathway in immune cells (Bujold et al., 2009, 2013; Bulgarelli et al., 2009) may have contributed to prevent the SE in pilocarpine-treated rats. However, we cannot rule out the possibility that other ghrelin analogs could share the same mechanism found for EP-80317. Indeed, further experiments are required to establish if PPARγ may mediate the anticonvulsant effects of other ghrelin receptor agonists or antagonists.

The effects of EP-80317 on PPARγ could be dependent on a direct modulation of the neuronal activity. As a matter of fact, EP-80317 markedly increased PPARγ immunoreactivity in hippocampal pyramidal neurons and also in interneurons of 6-Hz corneally stimulated mice. It is interesting to notice that we have identified PPARγ in interneurons and described its expression in different interneuron subpopulations for the first time. Recently, the role of interneurons in seizure initiation and propagation has become more controversial (de Curtis and Avoli, 2016). In particular, the different interneuron subclasses were suggested to play specific roles in modulating seizures (Khoshkhoo et al., 2017). Here, we found that PV and SOM but not VIP interneurons expressed PPARγ and, thus, were probably involved in the anticonvulsant effects of EP-80317. Interestingly, optogenetic inhibition of VIP interneurons affected both the seizure threshold and duration, whereas PV and SOM interneuron inhibition apparently reduced only the seizure duration (Khoshkhoo et al., 2017). According to these data, it is possible that the effects on seizure duration observed with EP-80317 in 6-Hz stimulated mice could be partly mediated by modulation of PV and SOM interneurons. It could also be of interest to evaluate other PPARγ modulators, such as rosiglitazone or pioglitazone, in the pilocarpine model and, especially, in the repeated 6-Hz corneal stimulation model to examine their effects in exactly the same experimental conditions in which we characterized EP-80317.

Although all the EP-80317 anticonvulsant effects were counteracted by GW9662, a notable exception was found by analyzing the ECoG power spectra of 6-Hz corneally stimulated mice. In particular, we observed that the power of ECoG recordings increased significantly in saline-treated and GW9662-treated mice, but not in mice receiving EP-80317 or GW9662+EP-80317. These findings suggest that the already proposed antiepileptogenic activity of EP-80317 (Giordano et al., 2016) may be independent of PPARγ activation. This hypothesis is in line with the time course of PPARγ induction in the hippocampus, which has been characterized by a transient increase at the first session of seizure induction returning to basal levels at the third session. So, PPARγ was presumably restored at basal levels when the effect of EP-80317 on the power of ECoG recordings was still present. Although we could not establish if this last finding was related to antagonism at the ghrelin receptor, it was certainly worth to further investigate this pharmacological activity of EP-80317 in view of the well-recognized need of antiepileptogenic drugs to prevent the appearance of epilepsy in subjects exposed to this risk, as in the case of patients which develop SE and, for this reason (Santamarina et al., 2015), may become affected by epilepsy.

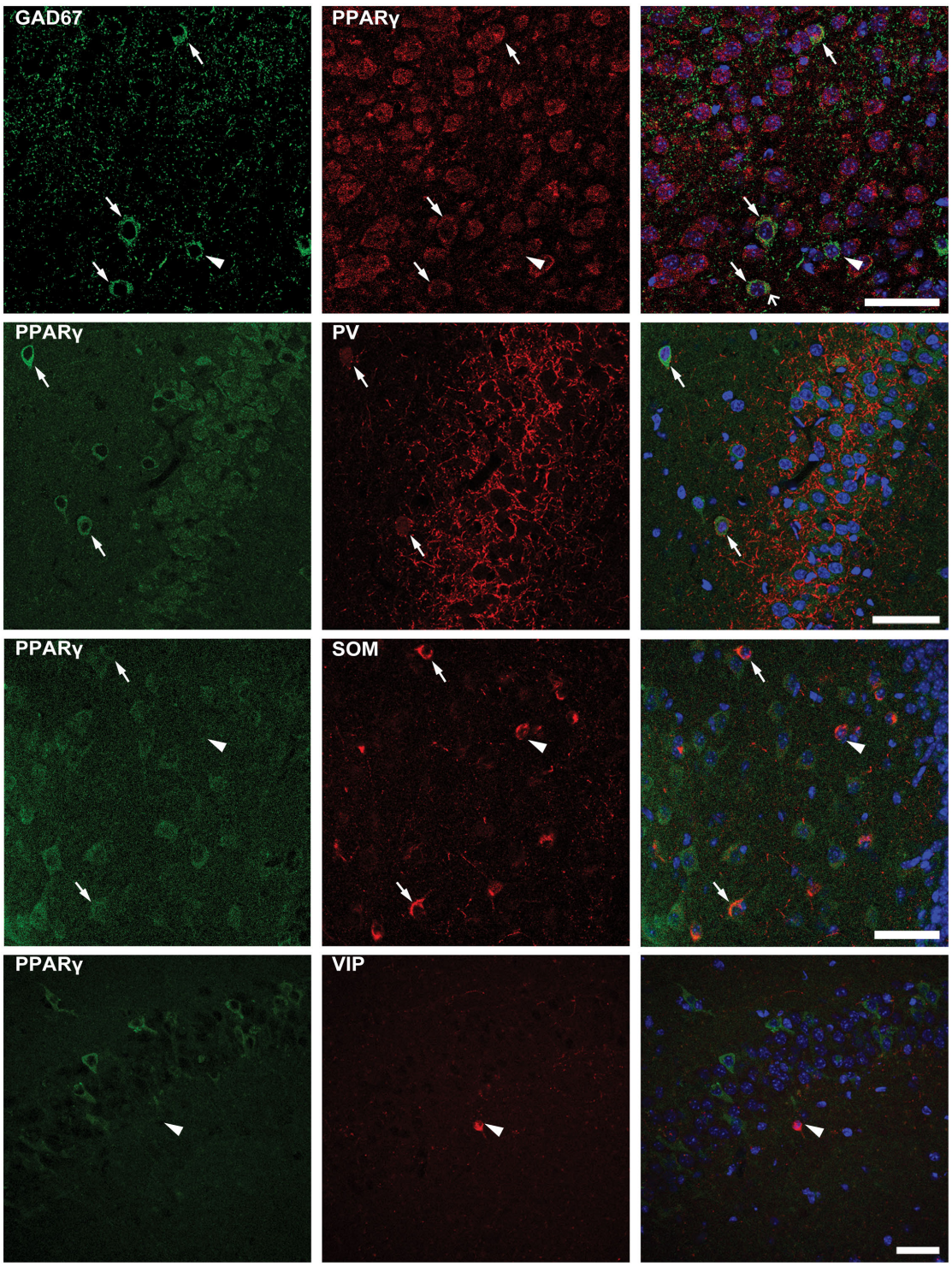

FIGURE 7 | Double immunofluorescence of interneurons expressing PPARγ. Photomicrographs illustrating co-labeling with glutamate decarboxylase 67 (GAD67, green) and PPARγ (red) in CA1 of a representative mouse are shown in top panels. Double immunofluorescence revealed the co-expression of GAD67 and PPARγ in some (arrows), but not all interneurons (arrowhead point to a PPARγ negative interneuron). Scale bar: 50 μm. Photomicrographs illustrating co-labeling of PPARγ (green) and parvalbumin (PV, red), somatostatin (SOM, red), or vasoactive intestinal peptide (VIP, red) in the hippocampus of mice exposed to repeated 6-Hz corneal stimulation are sequentially shown from the second row to bottom. Note that double immunofluorescence revealed the co-labeling of PPARγ/PV in CA3, PPARγ/SOM in the hilus of dentate gyrus (DH) (arrows), but not PPARγ/VIP in CA1 (arrowhead). Scale bar: 50 μm.

AUTHOR CONTRIBUTIONS

GB is responsible for the experimental design, contributed to the acquisition, analysis and interpretation of all the experiments, drafted and revised the work. CL, AC, and CG performed the experiments and contributed to acquisition and analysis of most of the results and revised the work. GC, MP, GL, and JV performed part of the experiments and revised the work. AT, LB, J-AF, and JM provided the anticonvulsant, contributed to data interpretation and revised the work.

FUNDING

This study was supported by the Italian Ministry of Health (grant RF-2010-2309921 to GB).

ACKNOWLEDGMENT

JV is fellow of the Umberto Veronesi Foundation (https://www.fondazioneveronesi.it/).

REFERENCES

Adabi Mohazab, R., Javadi-Paydar, M., Delfan, B., and Dehpour, A. R. (2012). Possible involvement of PPAR-gamma receptor and nitric oxide pathway in the anticonvulsant effect of acute pioglitazone on pentylenetetrazole-induced seizures in mice. *Epilepsy Res.* 101, 28–35. doi: 10.1016/j.eplepsyres.2012.02.015

Aslan, A., Yildirim, M., Ayyildiz, M., Güven, A., and Agar, E. (2009). The role of nitric oxide in the inhibitory effect of ghrelin against penicillin-induced epileptiform activity in rat. *Neuropeptides* 43, 295–302. doi: 10.1016/j.npep.2009.05.005

Bayliss, J. A., and Andrews, Z. B. (2013). Ghrelin is neuroprotective in Parkinson's disease: molecular mechanisms of metabolic neuroprotection. *Ther. Adv. Endocrinol. Metab.* 4, 25–36. doi: 10.1177/2042018813479645

Biagini, G., D'Arcangelo, G., Baldelli, E., D'Antuono, M., Tancredi, V., and Avoli, M. (2005). Impaired activation of CA3 pyramidal neurons in the epileptic hippocampus. *Neuromol. Med.* 7, 325–342. doi: 10.1385/NMM:7:4:325

Biagini, G., Torsello, A., Marinelli, C., Gualtieri, F., Vezzali, R., Coco, S., et al. (2011). Beneficial effects of desacyl-ghrelin, hexarelin and EP-80317 in models of status epilepticus. *Eur. J. Pharmacol.* 670, 130–136. doi: 10.1016/j.ejphar.2011.08.020

Bujold, K., Mellal, K., Zoccal, K. F., Rhainds, D., Brissette, L., Febbraio, M., et al. (2013). EP 80317, a CD36 selective ligand, promotes reverse cholesterol transport in apolipoprotein E-deficient mice. *Atherosclerosis* 229, 408–414. doi: 10.1016/j.atherosclerosis.2013.05.031

Bujold, K., Rhainds, D., Jossart, C., Febbraio, M., Marleau, S., and Ong, H. (2009). CD36-mediated cholesterol efflux is associated with PPARgamma activation via a MAPK-dependent COX-2 pathway in macrophages. *Cardiovasc. Res.* 83, 457–464. doi: 10.1093/cvr/cvp118

Bulgarelli, I., Tamiazzo, L., Bresciani, E., Rapetti, D., Caporali, S., Lattuada, D., et al. (2009). Desacyl-ghrelin and synthetic GH-secretagogues modulate the production of inflammatory cytokines in mouse microglia cells stimulated by β-amyloid fibrils. *J. Neurosci. Res.* 87, 2718–2727. doi: 10.1002/jnr.22088

Carlini, V. P., Ghersi, M., Schiöth, H. B., and de Barioglio, S. R. (2010). Ghrelin and memory: differential effects on acquisition and retrieval. *Peptides* 31, 1190–1193. doi: 10.1016/j.peptides.2010.02.021

Casillas-Espinosa, P. M., Powell, K. L., and O'Brien, T. J. (2012). Regulators of synaptic transmission: roles in the pathogenesis and treatment of epilepsy: regulators of synaptic transmission. *Epilepsia* 53, 41–58. doi: 10.1111/epi.12034

Chen, C.-Y., Asakawa, A., Fujimiya, M., Lee, S.-D., and Inui, A. (2009). Ghrelin gene products and the regulation of food intake and gut motility. *Pharmacol. Rev.* 61, 430–481. doi: 10.1124/pr.109.001958

Clynen, E., Swijsen, A., Raijmakers, M., Hoogland, G., and Rigo, J.-M. (2014). Neuropeptides as targets for the development of anticonvulsant drugs. *Mol. Neurobiol.* 50, 626–646. doi: 10.1007/s12035-014-8669-x

Coppens, J., Aourz, N., Walrave, L., Fehrentz, J.-A., Martinez, J., De Bundel, D., et al. (2016). Anticonvulsant effect of a ghrelin receptor agonist in 6Hz corneally kindled mice. *Epilepsia* 57, e195–e199. doi: 10.1111/epi.13463

Curia, G., Gualtieri, F., Bartolomeo, R., Vezzali, R., and Biagini, G. (2013). Resilience to audiogenic seizures is associated with p-ERK1/2 dephosphorylation in the subiculum of Fmr1 knockout mice. *Front. Cell. Neurosci.* 7:46. doi: 10.3389/fncel.2013.00046

Curia, G., Longo, D., Biagini, G., Jones, R. S. G., and Avoli, M. (2008). The pilocarpine model of temporal lobe epilepsy. *J. Neurosci. Methods* 172, 143–157. doi: 10.1016/j.jneumeth.2008.04.019

Curia, G., Lucchi, C., Vinet, J., Gualtieri, F., Marinelli, C., Torsello, A., et al. (2014). Pathophysiogenesis of mesial temporal lobe epilepsy: is prevention of damage antiepileptogenic? *Curr. Med. Chem.* 21, 663–688. doi: 10.2174/09298673206613119152201

Davenport, A. P., Bonner, T. I., Foord, S. M., Harmar, A. J., Neubig, R. R., Pin, J.-P., et al. (2005). International Union of Pharmacology. LVI. Ghrelin receptor nomenclature, distribution, and function. *Pharmacol. Rev.* 57, 541–546. doi: 10.1124/pr.57.4.1

de Curtis, M., and Avoli, M. (2016). GABAergic networks jump-start focal seizures. *Epilepsia* 57, 679–687. doi: 10.1111/epi.13370

Demers, A., Rodrigue-Way, A., and Tremblay, A. (2008). Hexarelin signaling to PPAR γ in metabolic diseases. *PPAR Res.* 2008, 1–9. doi: 10.1155/2008/364784

Diano, S., Farr, S. A., Benoit, S. C., McNay, E. C., da Silva, I., Horvath, B., et al. (2006). Ghrelin controls hippocampal spine synapse density and memory performance. *Nat. Neurosci.* 9, 381–388. doi: 10.1038/nn1656

Dobolyi, A., Kékesi, K. A., Juhász, G., Székely, A. D., Lovas, G., and Kovács, Z. (2014). Receptors of peptides as therapeutic targets in epilepsy research. *Curr. Med. Chem.* 21, 764–787. doi: 10.2174/09298673206613119154018

Dressler, O. (2004). Awareness and the EEG power spectrum: analysis of frequencies. *Br. J. Anaesth.* 93, 806–809. doi: 10.1093/bja/aeh270

Egecioglu, E., Jerlhag, E., Salomé, N., Skibicka, K. P., Haage, D., Bohlooly-Y, M., et al. (2010). Ghrelin increases intake of rewarding food in rodents: ghrelin and food reward. *Addict. Biol.* 15, 304–311. doi: 10.1111/j.1369-1600.2010.00216.x

Fabene, P. F., Mora, G. N., Martinello, M., Rossi, B., Merigo, F., Ottoboni, L., et al. (2008). A role for leukocyte-endothelial adhesion mechanisms in epilepsy. *Nat. Med.* 14, 1377–1383. doi: 10.1038/nm.1878

Giordano, C., Costa, A. M., Lucchi, C., Leo, G., Brunel, L., Fehrentz, J.-A., et al. (2016). Progressive seizure aggravation in the repeated 6-Hz corneal stimulation model is accompanied by marked increase in hippocampal p-ERK1/2 immunoreactivity in neurons. *Front. Cell. Neurosci.* 10:281. doi: 10.3389/fncel.2016.00281

Giordano, C., Vinet, J., Curia, G., and Biagini, G. (2015). Repeated 6-Hz corneal stimulation progressively increases FosB/ΔFosB levels in the lateral amygdala and induces seizure generalization to the hippocampus. *PLOS ONE* 10:e0141221. doi: 10.1371/journal.pone.0141221

Glezer, I., Bittencourt, J. C., and Rivest, S. (2009). Neuronal expression of Cd36, Cd44, and Cd83 antigen transcripts maps to distinct and specific murine brain circuits. *J. Comp. Neurol.* 517, 906–924. doi: 10.1002/cne.22185

Gorga, A., Rindone, G. M., Regueira, M., Pellizzari, E. H., Camberos, M. C., Cigorraga, S. B., et al. (2017). PPARγ activation regulates lipid droplet formation and lactate production in rat Sertoli cells. *Cell Tissue Res.* doi: 10.1007/s00441-017-2615-y [Epub ahead of print].

Gualtieri, F., Curia, G., Marinelli, C., and Biagini, G. (2012). Increased perivascular laminin predicts damage to astrocytes in CA3 and piriform cortex following chemoconvulsive treatments. *Neuroscience* 218, 278–294. doi: 10.1016/j.neuroscience.2012.05.018

Hong, S., Xin, Y., HaiQin, W., GuiLian, Z., Ru, Z., ShuQin, Z., et al. (2013). The PPARγ agonist rosiglitazone prevents neuronal loss and attenuates development of spontaneous recurrent seizures through BDNF/TrkB signaling following pilocarpine-induced status epilepticus. *Neurochem. Int.* 63, 405–412. doi: 10.1016/j.neuint.2013.07.010

Jeong, E. A., Jeon, B. T., Shin, H. J., Kim, N., Lee, D. H., Kim, H. J., et al. (2011). Ketogenic diet-induced peroxisome proliferator-activated receptor-γ activation

decreases neuroinflammation in the mouse hippocampus after kainic acid-induced seizures. *Exp. Neurol.* 232, 195–202. doi: 10.1016/j.expneurol.2011.09.001

Khoshkhoo, S., Vogt, D., and Sohal, V. S. (2017). Dynamic, cell-type-specific roles for GABAergic interneurons in a mouse model of optogenetically inducible seizures. *Neuron* 93, 291–298. doi: 10.1016/j.neuron.2016.11.043

Kojima, M. (2005). Ghrelin: structure and function. *Physiol. Rev.* 85, 495–522. doi: 10.1152/physrev.00012.2004

Kovac, S., and Walker, M. C. (2013). Neuropeptides in epilepsy. *Neuropeptides* 47, 467–475. doi: 10.1016/j.npep.2013.10.015

Lee, J., Lim, E., Kim, Y., Li, E., and Park, S. (2010). Ghrelin attenuates kainic acid-induced neuronal cell death in the mouse hippocampus. *J. Endocrinol.* 205, 263–270. doi: 10.1677/JOE-10-0040

Li, E., Chung, H., Kim, Y., Kim, D. H., Ryu, J. H., Sato, T., et al. (2013). Ghrelin directly stimulates adult hippocampal neurogenesis: implications for learning and memory. *Endocr. J.* 60, 781–789. doi: 10.1507/endocrj.EJ13-0008

Li, Z., Xu, G., Qin, Y., Zhang, C., Tang, H., Yin, Y., et al. (2014). Ghrelin promotes hepatic lipogenesis by activation of mTOR-PPAR signaling pathway. *Proc. Natl. Acad. Sci. U.S.A.* 111, 13163–13168. doi: 10.1073/pnas.1411571111

Lowenstein, D. H. (1999). Status epilepticus: an overview of the clinical problem. *Epilepsia* 40, S3–S8. doi: 10.1111/j.1528-1157.1999.tb00872.x

Lucchi, C., Curia, G., Vinet, J., Gualtieri, F., Bresciani, E., Locatelli, V., et al. (2013). Protective but not anticonvulsant effects of ghrelin and JMV-1843 in the pilocarpine model of status epilepticus. *PLOS ONE* 8:e72716. doi: 10.1371/journal.pone.0072716

Marchi, N., Fan, Q., Ghosh, C., Fazio, V., Bertolini, F., Betto, G., et al. (2009). Antagonism of peripheral inflammation reduces the severity of status epilepticus. *Neurobiol. Dis.* 33, 171–181. doi: 10.1016/j.nbd.2008.10.002

Momany, F. A., Bowers, C. Y., Reynolds, G. A., Chang, D., Hong, A., and Newlander, K. (1981). Design, synthesis, and biological activity of peptides which release growth hormone in vitro*. *Endocrinology* 108, 31–39. doi: 10.1210/endo-108-1-31

Moreno, S., Farioli-Vecchioli, S., and Cerù, M. P. (2004). Immunolocalization of peroxisome proliferator-activated receptors and retinoid X receptors in the adult rat CNS. *Neuroscience* 123, 131–145. doi: 10.1016/j.neuroscience.2003.08.064

Müller, T. D., Nogueiras, R., Andermann, M. L., Andrews, Z. B., Anker, S. D., Argente, J., et al. (2015). Ghrelin. *Mol. Metab.* 4, 437–460. doi: 10.1016/j.molmet.2015.03.005

Nakazato, M., Murakami, N., Date, Y., Kojima, M., Matsuo, H., Kangawa, K., et al. (2001). A role for ghrelin in the central regulation of feeding. *Nature* 409, 194–198. doi: 10.1038/35051587

Obay, B. D., Tasdemir, E., Tümer, C., Bilgin, H. M., and Sermet, A. (2007). Antiepileptic effects of ghrelin on pentylenetetrazole-induced seizures in rats. *Peptides* 28, 1214–1219. doi: 10.1016/j.peptides.2007.04.003

Payandemehr, B., Ebrahimi, A., Gholizadeh, R., Rahimian, R., Varastehmoradi, B., Gooshe, M., et al. (2015). Involvement of PPAR receptors in the anticonvulsant effects of a cannabinoid agonist, WIN 55,212-2. *Prog. Neuropsychopharmacol. Biol. Psychiatry* 57, 140–145. doi: 10.1016/j.pnpbp.2014.11.005

Perelló, M., and Zigman, J. M. (2012). The role of ghrelin in reward-based eating. *Biol. Psychiatry* 72, 347–353. doi: 10.1016/j.biopsych.2012.02.016

Portelli, J., Michotte, Y., and Smolders, I. (2012a). Ghrelin: an emerging new anticonvulsant neuropeptide. *Epilepsia* 53, 585–595. doi: 10.1111/j.1528-1167.2012.03423.x

Portelli, J., Thielemans, L., Ver Donck, L., Loyens, E., Coppens, J., Aourz, N., et al. (2012b). Inactivation of the constitutively active ghrelin receptor attenuates limbic seizure activity in rodents. *Neurotherapeutics* 9, 658–672. doi: 10.1007/s13311-012-0125-x

Racine, R. J. (1972). Modification of seizure activity by electrical stimulation. II. Motor seizure. *Electroencephalogr. Clin. Neurophysiol.* 32, 281–294. doi: 10.1016/0013-4694(72)90177-0

Rani, N., Bharti, S., Bhatia, J., Nag, T. C., Ray, R., and Arya, D. S. (2016). Chrysin, a PPAR-γ agonist improves myocardial injury in diabetic rats through inhibiting AGE-RAGE mediated oxidative stress and inflammation. *Chem. Biol. Interact.* 250, 59–67. doi: 10.1016/j.cbi.2016.03.015

Rindi, G., Necchi, V., Savio, A., Torsello, A., Zoli, M., Locatelli, V., et al. (2002). Characterisation of gastric ghrelin cells in man and other mammals: studies in adult and fetal tissues. *Histochem. Cell Biol.* 117, 511–519. doi: 10.1007/s00418-002-0415-1

Santamarina, E., Gonzalez, M., Toledo, M., Sueiras, M., Guzman, L., Rodríguez, N., et al. (2015). Prognosis of status epilepticus (SE): relationship between SE duration and subsequent development of epilepsy. *Epilepsy Behav.* 49, 138–140. doi: 10.1016/j.yebeh.2015.04.059

Simeone, T. A., Matthews, S. A., Samson, K. K., and Simeone, K. A. (2017). Regulation of brain PPARgamma2 contributes to ketogenic diet anti-seizure efficacy. *Exp. Neurol.* 287, 54–64. doi: 10.1016/j.expneurol.2016.08.006

Skibicka, K. P., and Dickson, S. L. (2011). Ghrelin and food reward: the story of potential underlying substrates. *Peptides* 32, 2265–2273. doi: 10.1016/j.peptides.2011.05.016

Skibicka, K. P., Hansson, C., Alvarez-Crespo, M., Friberg, P. A., and Dickson, S. L. (2011). Ghrelin directly targets the ventral tegmental area to increase food motivation. *Neuroscience* 180, 129–137. doi: 10.1016/j.neuroscience.2011.02.016

Spencer, S., Miller, A., and Andrews, Z. (2013). The role of ghrelin in neuroprotection after ischemic brain injury. *Brain Sci.* 3, 344–359. doi: 10.3390/brainsci3010344

Vezzani, A., Dingledine, R., and Rossetti, A. O. (2015). Immunity and inflammation in status epilepticus and its sequelae: possibilities for therapeutic application. *Expert Rev. Neurother.* 15, 1081–1092. doi: 10.1586/14737175.2015.1079130

Vinet, J., Vainchtein, I. D., Spano, C., Giordano, C., Bordini, D., Curia, G., et al. (2016). Microglia are less pro-inflammatory than myeloid infiltrates in the hippocampus of mice exposed to status epilepticus. *Glia* 64, 1350–1362. doi: 10.1002/glia.23008

Warden, A., Truitt, J., Merriman, M., Ponomareva, O., Jameson, K., Ferguson, L. B., et al. (2016). Localization of PPAR isotypes in the adult mouse and human brain. *Sci. Rep.* 6:27618. doi: 10.1038/srep27618

Wong, S.-B., Cheng, S.-J., Hung, W.-C., Lee, W.-T., and Min, M.-Y. (2015). Rosiglitazone suppresses *in vitro* seizures in hippocampal slice by inhibiting presynaptic glutamate release in a model of temporal lobe epilepsy. *PLOS ONE* 10:e0144806. doi: 10.1371/journal.pone.0144806

Xu, J., Wang, S., Lin, Y., Cao, L., Wang, R., and Chi, Z. (2009). Ghrelin protects against cell death of hippocampal neurons in pilocarpine-induced seizures in rats. *Neurosci. Lett.* 453, 58–61. doi: 10.1016/j.neulet.2009.01.067

Zigman, J. M., Jones, J. E., Lee, C. E., Saper, C. B., and Elmquist, J. K. (2006). Expression of ghrelin receptor mRNA in the rat and the mouse brain. *J. Comp. Neurol.* 494, 528–548. doi: 10.1002/cne.20823

Conflict of Interest Statement: AT, GB, and other inventors share a patent on the possible therapeutic use of growth hormone secretagogues for epileptic disorders (patent 0001399610 – 2013; http://www.uibm.gov.it/uibm/dati/Avanzata.aspx?load=info_list_uno&id=1800628&table=Invention&#ancoraSearch).

The other authors declare that the research was conducted in the absence of any commercial or financial relationships that could be construed as a potential conflict of interest.

The reviewer FW and handling Editor declared their shared affiliation.

Advantages of publishing in Frontiers

OPEN ACCESS
Articles are free to read for greatest visibility and readership

FAST PUBLICATION
Around 90 days from submission to decision

HIGH QUALITY PEER-REVIEW
Rigorous, collaborative, and constructive peer-review

TRANSPARENT PEER-REVIEW
Editors and reviewers acknowledged by name on published articles

Frontiers
Avenue du Tribunal-Fédéral 34
1005 Lausanne | Switzerland

Visit us: www.frontiersin.org
Contact us: info@frontiersin.org | +41 21 510 17 00

REPRODUCIBILITY OF RESEARCH
Support open data and methods to enhance research reproducibility

DIGITAL PUBLISHING
Articles designed for optimal readership across devices

FOLLOW US
@frontiersin

IMPACT METRICS
Advanced article metrics track visibility across digital media

EXTENSIVE PROMOTION
Marketing and promotion of impactful research

LOOP RESEARCH NETWORK
Our network increases your article's readership